ISSN 2186-3644 Online ISSN 2186-361X

IRDR

Intractable & Rare Diseases Research

Volume 6, Number 4
November, 2017

IRCA BSSA

IACMHR

www.irdrjournal.com

IRDR
Intractable & Rare Diseases Research

ISSN: 2186-3644
Online ISSN: 2186-361X
CODEN: IRDRA3
Issues/Year: 4
Language: English
Publisher: IACMHR Co., Ltd.

Intractable & Rare Diseases Research is one of a series of peer-reviewed journals of the International Research and Cooperation Association for Bio & Socio-Sciences Advancement (IRCA-BSSA) Group and is published quarterly by the International Advancement Center for Medicine & Health Research Co., Ltd. (IACMHR Co., Ltd.) and supported by the IRCA-BSSA, Shandong Academy of Medical Sciences, and Shandong Rare Disease Association.

Intractable & Rare Diseases Research devotes to publishing the latest and most significant research in intractable and rare diseases. Articles cover all aspects of intractable and rare diseases research such as molecular biology, genetics, clinical diagnosis, prevention and treatment, epidemiology, health economics, health management, medical care system, and social science in order to encourage cooperation and exchange among scientists and clinical researchers.

Intractable & Rare Diseases Research publishes Original Articles, Brief Reports, Reviews, Policy Forum articles, Case Reports, News, and Letters on all aspects of the field of intractable and rare diseases research. All contributions should seek to promote international collaboration.

IRCA-BSSA Group Journals

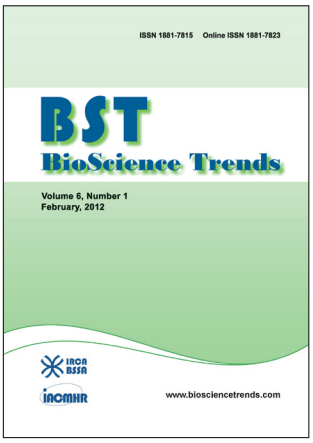

ISSN: 1881-7815
Online ISSN: 1881-7823
CODEN: BTIRCZ
Issues/Year: 6
Language: English
Publisher: IACMHR Co., Ltd.
www.biosciencetrends.com

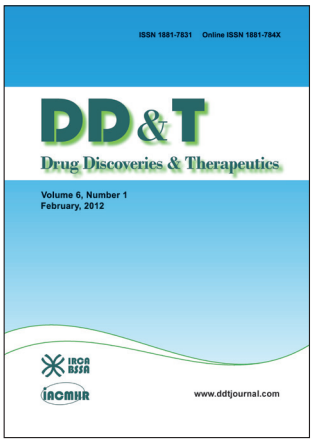

ISSN: 1881-7831
Online ISSN: 1881-784X
CODEN: DDTRBX
Issues/Year: 6
Language: English
Publisher: IACMHR Co., Ltd.
www.ddtjournal.com

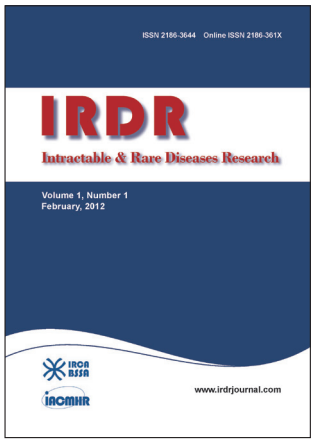

ISSN: 2186-3644
Online ISSN: 2186-361X
CODEN: IRDRA3
Issues/Year: 4
Language: English
Publisher: IACMHR Co., Ltd.
www.irdrjournal.com

Intractable & Rare Diseases Research

Editorial and Head Office

Pearl City Koishikawa 603, 2-4-5 Kasuga, Bunkyo-ku,
Tokyo 112-0003, Japan

Tel: +81-3-5840-9968, Fax: +81-3-5840-9969
E-mail: office@irdrjournal.com
URL: www.irdrjournal.com

Editorial Board

CONTENTS

Volume 6, Number 4, 2017

Reviews

234 - 241 **The paradoxical role of tumor-infiltrating immune cells in lung cancer.**
Xiaodan Zheng, Yuhai Hu, Chengfang Yao

242 - 248 **Fibrodysplasia ossificans progressiva: Basic understanding and experimental models.**
Zijuan Qi, Jing Luan, Xiaoyan Zhou, Yazhou Cui, Jinxiang Han

249 - 255 **Epidemiology, diagnosis, and treatment of Wilson's disease.**
Jing Liu, Jing Luan, Xiaoyan Zhou, Yazhou Cui, Jinxiang Han

256 - 261 **SInfection after total knee arthroplasty and its gold standard surgical treatment: Spacers used in two-stage revision arthroplasty.**
Junren Lu, Jing Han, Chi Zhang, Yi Yang, Zhenjun Yao

Original Articles

262- 268 **Microglia express ABI3 in the brains of Alzheimer's disease and Nasu-Hakola disease.**
Jun-ichi Satoh, Yoshihiro Kino, Motoaki Yanaizu, Youhei Tosaki, Kenji Sakai, Tsuyoshi Ishida, Yuko Saito

269 - 273 **Estradiol and proinflammatory cytokines stimulate ISG20 expression in synovial fibroblasts of patients with osteoarthritis.**
Zhiwei Zheng, Lin Wang, Jihong Pan

274 - 280 **The expression profile of IFITM family gene in rats.**
Yanqin Lu, Qingli Zuo, Yao Zhang, Yanzhou Wang, Tianyou Li, Jinxiang Han

281 - 290 **Differences of basic and induced autophagic activity between K562 and K562/ADM cells.**
Feifei Wang, Jing Chen, Zhewen Zhang, Juan Yi, Minmin Yuan, Mingyan Wang, Na Zhang, Xuemin Qiu, Hulai Wei, Ling Wang

Brief Reports

291 - 294 ***In vivo* quantification of amyloid burden in TTR-related cardiac amyloidosis.**
Alexander Marco Kollikowski, Florian Kahles, Svetlana Kintsler, Sandra Hamada, Sebastian Reith, Ruth Knüchel, Christoph Röcken, Felix Manuel Mottaghy, Nikolaus Marx, Mathias Burgmaier

295 - 298 **MTHFR promoter hypermethylation may lead to congenital heart defects in Down syndrome.**
Ambreen Asim, Sarita Agarwal, Inusha Panigrahi, Nazia Saiyed, Sonal Bakshi

CONTENTS (*Continued*)

299 - 303 **Steroid-resistant nephrotic syndrome caused by co-inheritance of mutations at *NPHS1* and *ADCK4* genes in two Chinese siblings.**
Hongwen Zhang, Fang Wang, Xiaoyu Liu, Xuhui Zhong, Yong Yao, Huijie Xiao

Case Reports

304 - 309 **Inflammatory fibroid polyp of the gastric antrum presenting as hypovolemic shock: Case report and literature review.**
Kyle D. Klingbeil, Alexandra Balaban, Raymond M. Fertig, A. Caresse Gamret, Yuna Gong, Carolyn Torres, Shevonne S. Satahoo

310 - 313 **Disseminated mucormycosis: A sinister cause of neutropenic fever syndrome.**
Ghazal Tansir, Neha Rastogi, Prashant Ramteke, Prabhat Kumar, Manish Soneja, Ashutosh Biswas, Sanchit Kumar, Pankaj Jorwal, Upendra Baitha

314 - 318 **Expanded dengue syndrome in secondary dengue infection: A case of biopsy proven rhabdomyolysis induced acute kidney injury with intracranial and intraorbital bleeds.**
Ghazal Tansir, Chhavi Gupta, Shubham Mehta, Prabhat Kumar, Manish Soneja, Ashutosh Biswas

Communication

319 - 321 **An up-date on epigenetic and molecular markers in testicular germ cell tumors.**
Paolo Chieffi

Guide for Authors

Copyright

(*This journal was partially supported by a Grant-in-Aid for Scientific Research from Japan Society for the Promotion of Science.*)

Review

DOI: 10.5582/irdr.2017.01059

The paradoxical role of tumor-infiltrating immune cells in lung cancer

Xiaodan Zheng[1], Yuhai Hu[1], Chengfang Yao[2,*]

[1] *Clinical Laboratory, Wuhan Hankou Hospital, Wuhan, China;*
[2] *Key Laboratory for Tumor Immunology and Traditional Chinese Medicine Immunology, Institute of Basic Medicine, Shandong Academy of Medical Sciences, Ji'nan, China.*

Summary **Lung cancer remains one of the leading causes of death worldwide, and lung cancers have often already metastasized when diagnosed. Numerous studies have noted the infiltration of immune cells in the lung cancer microenvironment, but these cells play a dualistic role, *i.e.* they suppress and/or promote tumor development and growth based on tumor progression and different cytokines in the microenvironment. These tumor-infiltrating immune cells create different microenvironments depending on their type and interaction. Chemokines act as a bridge in this process by recruiting immune cells to the tumor site and they regulate the phenotypes and functions of those cells. The current review summarizes current knowledge about the tumor-infiltrating immune cells in lung cancer as well as the mechanisms involved in suppression and promotion of tumor development and growth.**

Keywords: Lung cancer, tumor microenvironment, infiltrating immune cells, chemokine

1. Introduction

Lung carcinoma is a major cause of death throughout the world; more than 1.82 million people are diagnosed with lung carcinoma annually (13% of all cancers) and lung carcinoma causes 1.59 million deaths (19.4% of all cancers) (*1,2*). By the time the tumor is diagnosed, it has often already metastasized (*3*). Despite advances, treatments such as surgery, radiotherapy, chemotherapy, and multimodal therapies can rarely control metastatic disease and they are seldom curative. Patients with lung cancer have a limited long-term survival (*4*) because treated lung tumors will ultimately relapse since a number of tumor clones or "cancer-initiating cells" have escaped the initial treatment. These escaped cells will be more resistant to therapeutic modalities. Therefore, an adjuvant therapy that could effectively destroy these remaining tumor cells would have a substantial impact on tumor treatment.

Released online in J-STAGE as advance publication November 15, 2017.

**Address correspondence to:*
Dr. Chengfang Yao, Institute of Basic Medicine, Shandong Academy of Medical Sciences, No. 18877 Jingshi Road, Ji'nan 250062, Shandong, China.
E-mail: xyz27315@sina.com

Immunotherapy has a demonstrable efficacy in patients with cancer (*5*). These cells or cytokines can infiltrate the tumor site by activating the host immune cells, thus inducing a specific antitumor immune response. Therefore, the effect of the treatment depends, to a great extent, on the tumor microenvironment. Tumor-infiltrating immune cells play critical roles in the tumor microenvironment by promoting or suppressing tumor development and progression depending on their type and functional interactions (*6*).

There is an obvious infiltration of different types of immune cells in lung cancer. These immune cells typically include natural killer (NK) cells, T lymphocytes, macrophages, dendritic cells (DC), myeloid-derived suppressor cells (MDSCs), and B cells (*7*). These cells serve different functions and combine or cancel out each other, thus creating the microenvironment for lung cancer. Cancer progression and survival are significantly associated with these cell types and functions and their localization in tissue.

2. Diagnostic subtypes of lung cancer

Lung carcinoma is a solid tumor with low antigenicity and a heterogenic phenotype that evades the host's immune defense. Lung cancers usually arise from basal epithelial cells and have two main histological

types: non-small-cell lung cancer (NSCLC) and small-cell lung cancer (SCLC). NSCLC accounts for approximately 85% of lung cancer cases. Since their cells differ in appearance, NSCLCs are classified into 3 major groups (squamous, adenocarcinomas, and large cell cancers) depending on the origin of their cells and their pathological characteristics. Adenocarcinoma is the most frequent type, accounting for 40% of all NSCLCs while squamous cancer accounts for 30% of NSCLCs. The remaining NSCLCs (5-10%) are large cell carcinoma. The other type of lung cancer, SCLCs, consists of smaller than normal undifferentiated cells (*1*).

3. The role of T-lymphocytes in lung cancer

In a variety of human solid tumors, tumor-infiltrating T-lymphocytes (TILs) are considered to play important roles in immunosurveillance in a tumor-bearing host. $CD4^+$ and $CD8^+$ T cells are the two main subsets of T-lymphocytes and have different effects on tumor immunity within the tumor microenvironment (*8*).

3.1. *$CD8^+$ T lymphocytes*

Most $CD8^+$ T cells are cytotoxic T lymphocytes. Cytotoxic T cells are a major subset of T cells that constructively mediates an effective antitumor response: these cells can recognize particular tumor-associated antigens (TAA) presenting on major histocompatibility complex (MHC) class I molecules on the surface of cancer cells and they have the ability to kill cancer cells directly (*9*). Tumor-infiltrating $CD8^+$ T cells can be classified into two groups by their location: $CD8^+$ T cells within cancer stroma adjacent to cancer cell nests, or $CD8^+$ T cells within the cancer cell nests themselves (*9*). Naito and colleagues (*10*) found that the presence of large numbers of $CD8^+$ T cells in cancer cell nests was a favorable independent prognostic factor in colorectal carcinomas. A similar result was noted in breast cancer (*11*). Moreover, studies have indicated the prognostic significance of infiltrating $CD8^+$ T cells in breast cancer (*12*), melanoma (*13*), anal squamous cell carcinoma (*14*), and oropharyngeal squamous carcinoma (*15*). However, the role of TILs in the survival of patients with an NSCLC is still debated. Wakabayashi and colleagues (*16*) contended that $CD4^+$ T cells in the cancer stroma, and not $CD8^+$ T cells in cancer cell nests, are associated with a favorable prognosis in human NSCLC. Another study indicated that neither $CD8^+$ T cells within cancer cell nests nor those in the cancer stroma had a significant impact on patient survival (*9*). That study found that infiltrating $CD8^+$ T cells and $CD4^+$ T cells in NSCLC may cooperate to suppress cancer progression and their presence together appears to be an independent favorable prognostic factor for this disease.

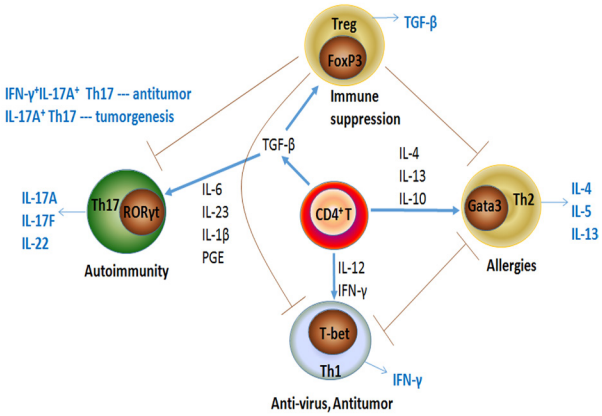

Figure 1. Interaction among $CD4^+$ T-cell subsets. When stimulated with different cytokines, naive $CD4^+$ T cells become polarized toward four different cell subsets: Th1, Th2, Th17, and Treg cells. Each of these $CD4^+$ T-cell subsets serves a different biological role in antitumor immunity by secreting identical cytokines. Th1 and Th2 cells play an important role in the tumor microenvironment and Th17 and Treg cells play an important role in immune homeostasis. The grey arrows indicate the effector functions of the various $CD4^+$ T cell subsets.

3.2. *$CD4^+$ helper T cells*

Various studies have indicated that $CD4^+$ helper T cells are present in the lungs of patients with NSCLC, but their role in antitumor activity is dualistic: some $CD4^+$ T cells seemingly hinder the function of $CD8^+$ T cells and therefore indirectly promote tumor growth, whereas others might help with the activation of $CD8^+$ T cells (*17*), which are key to removing cancerous tissue or cells. $CD4^+$ helper T cells can be functionally classified into Th1, Th2, Th17, and regulatory T cells (Tregs) based on the secretion of cytokines, and each cell subset has its own unique function (*18*). As shown in Figure 1, these $CD4^+$ T cell subsets play different biological functions in antitumor immunity and tumor immune evasion. Th1 and Th2 play an important role in the tumor microenvironment and Th17 and Tregs play an important role in immune homeostasis (*19*).

3.3. *Th1/Th2/Th17/Treg paradigm*

When stimulated with different cytokines, different transcription factors select precursor T cells in response to various cytokines or other mediators and differentiate into different subtypes of $CD4^+$ T cells. Th1 cells differentiate when stimulated with interleukin (IL)-12 and interferon-gamma (IFN-γ) through the transcription factor T-bet. Activated Th1 cells release other cytokines like IL-2, IFN-γ, and tumor necrosis factor alpha (TNF-α), which can activate some effector cells such as macrophages, NK cells, and cytotoxic T-lymphocytes (CTLs). These effector cells effectively eliminate tumor cells. The GATA3 transcription factor becomes active and Th2 cells become polarized towards this phenotype

in response to IL-4 and IL-6. Activated Th2 cells, which produce IL-4, IL-5, IL-6, IL-10, and IL-13, are key to allergic responses and protection against infection by helminthic parasites (*20,21*). It is widely believed that cytokines that are secreted by Th1 cells can facilitate CTLs generation, whereas a Th2 cytokine profile might favor antibody response and be detrimental to the induction of CTLs (*22,23*). A study (*24*) examined the expression of Th1 and Th2 cells in lung cancer and found that the proportion of Th2 cells was significantly lower than that of Th1 cells, indicating that Th1 cells are dominant tumor infiltrators.

Th17 cells become activated through the transcription factor retinoid-related orphan receptor gamma t (RORγT) when stimulated with transforming growth factor β (TGF-β), IL-6, IL-23, IL-1β (in humans), and prostaglandin E (PGE) (*25,26*). Th17 cells have been found to play a contradictory role in tumorigenesis. Numerous studies have identified the tumor-promoting effects of Th17 cells. However, IL-17A$^+$IFN-γ$^+$ Th17 cells have tumor-protective characteristics in tumor immunity (*27*). The varying functions of the Th17 subset in tumor immunity are largely due to the cytokines they secrete, such as IL-17A, IL-17F, IL-21, IL-22, IFN-γ, and granulocyte-macrophage colony-stimulating factor (GM-CSF) (*28*). In addition, the antitumor functions of Th17 cells are related to effector lymphocytes, including Th1, Tc1, and NK cells (*29*).

Treg cells are formed as a result of the transcription factor forkhead box P3 (Foxp3), which is the dominant transcription factor of Treg cells. Developmental pathways of Th17 and Treg cells are closely related. TGF-β alone induces expression of FoxP3 (*30,31*) and RORγT (*31*) in TCR-stimulated naive CD4$^+$ T cells. Thus TGF-β is a critical factor for Th17 and Treg cells and is essential for inducing both RORγT and Foxp3. Despite the induction of these transcription factors, TGF-β is unable to initiate Th17 differentiation *in vitro* unless pro-inflammatory cytokines, such as IL-6 or IL-21, are present. When these cytokines are present, the TGF-β-induced Foxp3 expression is down-regulated and RORγT expression is up-regulated (*30,32*). In the absence of significant inflammation, TGF-β promotes the differentiation of Treg cells, which maintain immune tolerance. This is because of Foxp3-mediated inhibition of the activity of RORγT, resulting in silencing of IL-17 and IL-23 expression (*33*).

Th17 and Treg cells have opposite roles in the development of autoimmune and inflammatory diseases. Th17 cells promote autoimmunity while Treg cells seem to control it and therefore play an important role in autoimmune pathogenesis by maintaining self-tolerance and by controlling the growth and activation of autoreactive CD4$^+$ effector T cells (*34*). Tregs inhibit the recruitment of CD8$^+$ T lymphocytes in tumors and their effector functions are critical to inhibiting lung tumor growth (*35*). Tregs inhibit the immune system partly by utilizing membrane TGF-β and are thought to be key to downregulating Th1, Th2, and Th17 cells, possibly preventing autoimmunity (*36*). Thus, the abundance of Tregs are within lung tumor tissue is not surprising (*37*).

Accordingly, the Th1/Th2/Th17/Treg paradigm is essential for maintaining immune homeostasis based on cytokine production, and the cytokine environment they create determines the fate of the host's antitumor immunity.

4. The role of MDSCs in lung cancer

4.1. *Functional and molecular characterization of MDSCs*

MDSCs were first identified as immunosuppressive CD11b$^+$ Gr-1$^+$ myeloid cells in cancer patients in the 1980s (*38*). MDSCs represent a heterogenic population of immature myeloid cells that consists of myeloid progenitors and precursors of macrophages, granulocytes, and DCs they are characterized by a potent ability to suppress various T cell functions (*39*).

In mice, MDSCs are cells that simultaneously express the two markers CD11b and Gr-1 (*38*). Gr-1 includes the macrophage and neutrophil markers Ly6C and Ly6G, while CD11b is characteristic of macrophages (*40*). More recently, MDSCs have been subdivided into different subtypes based on their expression of Ly6C and Ly6G. CD11b$^+$Ly6G$^+$Ly6Clo cells with a granulocytic-like morphology and multilobed nuclei are called granulocytic MDSCs, whereas CD11b$^+$Ly6G$^-$Ly6C^{hi} cells with a monocytic-like morphology are referred to as monocytic MDSCs (*41*). In cancer patients, MDSCs are defined as cells that express the common myeloid marker CD33 but that lack expression of markers of mature myeloid and lymphoid cells (*42*). MDSCs are typically CD11b$^+$CD33$^+$CD34$^+$CD14$^-$ cells that vary in the expression of CD15, CD124, CD66, and MHC-II, along with that of other markers (*43*).

4.2. *Cellular and molecular mechanisms of MDSC-mediated immune suppression*

Lung cancer escapes the host's immune surveillance by dysregulating inflammation. Tumors and their surrounding stroma can produce growth factors, cytokines, and chemokines that recruit, expand, and activate MDSCs. Teixeira and colleagues (*44*) noted an increased number of MDSCs infiltrating lung cancer in mice. Another study confirmed the hypothesis that activating immune cells through disruption of MDSC-mediated immune suppression would promote antitumor immunity in a murine model of lung cancer (*45*). MDSCs can suppress immune responses to newly displayed tumor antigens and promote tumor progression; they may even contribute to the metastasis

of the tumor. There are several mechanisms by which MDSCs suppress antitumor responses. MDSCs restrain T cell functions in tumor tissues and draining lymph nodes by using two enzymes involved in L-arginine metabolism: arginase-1(ARG-1), which depletes the milieu of L-arginine, and induced nitric oxide synthase 2 (iNOS2), which generates nitric oxide (NO) (*46,47*).

Reactive oxygen species (ROS) are physiologically produced by activated neutrophils and macrophages as mediators of innate immunity. In chronic inflammation, ROS can weaken T cell responses by affecting CD3-ζ expression. H_2O_2 produced either by tumor-associated macrophages or by neutrophils isolated from the synovial fluid of patients with rheumatoid arthritis has been found to substantially decrease T cell proliferation *in vitro* (*48,49*). ROS can also affect the affinity of Ag-specific TCR, which may explain the specificity of the tolerance induced by Gr-1$^+$CD11b$^+$ MDSCs. In addition to the effect of ARG-1 and ROS, MDSCs may affect CD8$^+$ T cells via the inhibitory molecules B7-H1 and B7-H4 (*50*). In addition, MDSCs can enhance immune suppression by directly inducing Tregs through the production of IL-10 and TGF-β or ARG (*51,52*). Tregs actively down-regulate the activation and expansion of antitumor-reactive T cells (*53*) and NK cells (*54*). Cysteine, another essential amino acid for T-cell activation, is depleted by MDSCs (*55*).

5. The role of macrophages in lung cancer

Macrophages are among the most abundant normal cells in the tumor microenvironment and play a central role in tissue repair and remodeling during homeostasis and stress response. They are the first line of defense against pathogens. These cells originate from bone marrow precursors and extravasate into normal tissues, where they acquire distinct morphological and functional properties directed by local tissue and the immunological microenvironment (*56*).

Tumor-associated macrophages (TAMs) have complex dual functions in their interaction with neoplastic cells, and evidence suggests that they are part of inflammatory circuits that promote tumor progression (*57*). This is evidence that macrophages, rather than being tumoricidal as suggested after their activation *in vitro* (*58*), have a pro-tumoral phenotype *in vivo* both at the primary site and at metastases (*59*). Indeed, macrophages are polarized into a pro-tumoral phenotype when lung cancer develops (*60*).

Macrophages are exceptionally diverse in their functions, reflecting their different origins, differing local environments, and different responses to challenges (*61*). Given the function of macrophages in immunity, two classes of macrophages have been proposed: *i*) activated macrophages responding to IFN-γ, TNF-a, and Toll-like receptor 4 (TLR4) activation are involved in Th1-type responses since Th1 cells are capable of killing pathogens via mechanisms just like iNOS, and *ii*) alternatively activated macrophages that differentiate in response to IL-4 and IL-13 are involved in Th2-type responses, including humoral immunity and wound healing (*62*). Mills and colleagues called these states M1 (activated) and M2 (alternatively activated). M1 activity inhibits cell proliferation and causes tissue damage, while M2 activity promotes cell proliferation and tissue repair (*63*). These descriptions suggest that TAMs could either suppress (M1) or promote (M2) tumor development and progression (*64*). However, such definitions are limited and may not be applicable to the complex tumor microenvironment (*65*). In contrast to this dualistic M1/M2 definition, TAMs include several distinct populations that often share characteristics of both types but with greater overall similarity to macrophages involved in developmental processes (*66,67*).

6. The role of NK cells in lung cancer

NK cells can mediate several effector functions: *i*) direct cytotoxicity, including exocytosis of cytotoxic granules containing perforin and granzyme B, *ii*) up-regulation of death receptor ligand expression and the engagement of cognate death receptors on target cells, which can lead to apoptosis of target cells, *iii*) NK cells produce an array of immune-active cytokines, including IFN-γ, TNF-α, and GM-CSF (*68*), which places them at the crossroads of innate and adaptive immunity. They also augment monoclonal antibody activity through antibody-mediated cellular cytotoxicity and can be transfected with chimeric antigen receptors (*69*), and *iv*) NK cells can release other soluble mediators, such as PGE2, that shape the responses of the immune system. A clear correlation between NK cell activity in the lungs and tumor cell clearance from the lungs has been reported in both mouse and human studies (*70*). Manuela and colleagues found that depletion of NK cells resulted in an increase in the number of tumor nodes in lung cancer, suggesting that NK cells are key to the control of the growth of lung cancer. A study has found that the activity of NK cells is key to the development or rejection of MHC-I-deficient lymphomas (*71*) while another study found that depletion of NK cells promoted the growth of fibrosarcomas (*72*). In addition, a recent study found that the development of lung cancer depends on the function of NK cells. Kreisel and colleagues found that depletion of NK cells promoted urethane-induced lung tumor growth in a mouse strain that is normally not susceptible to lung cancer (*73*).

7. The role of dendritic cells in lung cancer

Antigen-presenting cells can deliver TAA and prime TAA-specific T cells. DCs are professional antigen-presenting cells and can express MHC-I and MHC-II molecules and costimulatory molecules on their

cell surface, all of which assist in T-cell activation (*74*). There are several cell types capable of antigen presentation in the lung, including resident DCs (*75*).

Evidence indicates that DCs play a significant role in induction of antitumour immunity (*76*). Immunotherapy with DCs co-cultured with cytokine-induced killer cells (DC-CIK) has been widely studied and might be a new strategy for treatment of NSCLC. Studies have indicated the efficacy and the safety of DC-CIK immunotherapy (*77*). When immature in peripheral tissue, DCs express different chemokine receptors, such as CC chemokine receptor 1 (CCR1), CCR2, CCR4, CCR5, CCR6, CCR8, and CXC chemokine receptor 4 (CXCR4) (*76*). When they encounter exogenous and endogenous antigens including tumor cell-derived antigens around a tumor, DCs can capture those antigens and they can mature in response to inflammatory stimuli such as toll-like receptor-mediated signals. Mature DCs start to express chemokine receptors such as CCR7 and CXCR4. Guided by chemokines, DCs enter the T-cell areas of regional lymph nodes (*78*).

8. The important role of chemokines in lung carcinoma

When considering the role of tumor-infiltrating immune cells in the lung cancer microenvironment, one cannot ignore the importance of chemokines, which recruit immune cells to the tumor and also regulate their phenotypes and functions. Relatively recent studies have revealed that chemokines regulate the movement of a wide variety of immune cells including lymphocytes, NK cells, and DCs in both physiological and pathological conditions (*79*). These features mean that chemokines play crucial roles in immune responses. Chemokines function biologically by linking to their corresponding receptors, which are 7-transmembrane G protein-coupled receptors (GPCR) (*80*). Chemokines are structurally divided into 4 subgroups: CXC, CC, CX3C, and C (*81*).

TAMs are derived mostly from circulating monocytes that are attracted to tumor sites by locally produced chemotactic factors, such as CCL2, CCL5, CCL7, CCL8, and CXCL12, and macrophage colony stimulating factor (M-CSF). CCL2 is presumed to play an important role in TAM recruitment (*82*). MDSCs can be recruited by CCL2 in several types of mouse cancers, such as Lewis lung cancer, meth A sarcoma, melanoma, and lymphoma (*83*). MDSCs express CXCR2 and are detected in abundance in NSCLC (84). CXCR2 ligands, including CXCL1, CXCL2, and CXCL5, are abundant in lung cancer tissue and tumorigenesis can be markedly inhibited by a deficiency in CXCR2 as a result of inhibiting infiltration of MDSCs (Figure 2). NK cells migrate to lymph nodes mainly by utilizing CXCR3, while their migration to inflamed tissues, including tumor sites, involves CCR1, CCR2, CCR5, CXCR3, and CX3CR1 (*85*). Thus, the ligands for these receptors

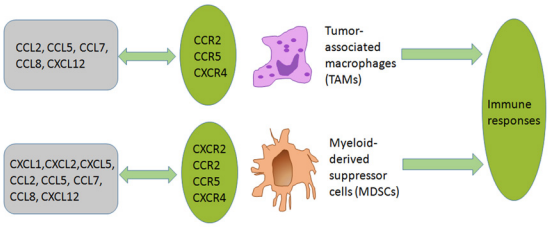

Figure 2. Effects of chemokines on TAMs and MDSCs. TAMs are derived mostly from circulating monocytes which are attracted to tumor sites by locally produced chemotactic factors including CCL2, CCL5, CCL7, CCL8, and CXCL12. MDSCs express CXCR2 and can be recruited to a tumor site by CXCR2 ligands like CXCL1, CXCL2, and CXCL5. MDSCs can also be recruited by CCL2, CCL5, CCL7, CCL7, CCL8, and CXCL12 in lung cancer.

can regulate the migration of NK cells and may enhance their functions. Treg cells express CCR4, and its ligand, CCL22, regulates intratumoral infiltration of Tregs in various tumors (*86*).

Lung stroma cells can produce abundant chemokines, such as CXCL1, CXCL2, CXCL5, CXCL9, CXCL10, and CXCL11. CXCL10 is an important chemokine responsible for the recruitment and localization of inflammatory cells to sites of tissue damage or infection. It is bound by CXCR3, a receptor shared with CXCL4. CXCL9 and CXCL11, which are expressed on $CD4^+$ T cells, $CD8^+$ T cells, NK cells, B cells, and DCs (*87,88*), are responsible for their recruitment and localization to the lungs.

9. Conclusion

Studies have indicated the importance of tumor-infiltrating immune cells in tumor development and control and studies have sought to characterize the infiltration of a tumor by those immune cells, providing insight into the effects of tumor-infiltrating immune cells on tumor behavior. Different tumors have different immune profiles, and the current review has focused on lung cancer. There is an obvious infiltration of different types of immune cells, including NK cells, T lymphocytes, macrophages, DCs, MDSCs, and B cells, in lung cancer. A distinctive lung cancer microenvironment is created by immune cells with various functions and interactions, and this microenvironment can ultimately affect tumor progression and survival. In this process, chemokines act as a bridge since they can recruit immune cells to a tumor and they can also regulate the phenotypes and functions of those cells. Although the role of lung cancer-infiltrated immune cells has been reviewed here, the paradoxical role of tumor-infiltrating cells in lung carcinoma still needs to be studied further.

Acknowledgements

This work was supported by grants from the Natural

Science Foundation of China (No. 81573728) and the Natural Science Foundation of Shandong Province (No. ZR2015HM007).

References

1. Mendes F, Antunes C, Abrantes AM, Gonçalves AC, Nobre-Gois I, Sarmento AB, Botelho MF, Rosa MS. Lung cancer: The immune system and radiation. Br J Biomed Sci. 2015; 72:78-84.
2. Chapman AM, Sun KY, Ruestow P, Cowan DM, Madl AK. Lung cancer mutation profile of EGFR, ALK, and KRAS: Meta-analysis and comparison of never and ever smokers. Lung Cancer. 2016; 102:122-134.
3. Tyl M, Domagała-Kulawik J. Lung cancer and COPD - Growing clinical problem. Pol Merkur Lekarski. 2017; 43:5-9.
4. Skowronek J. Brachytherapy in the treatment of lung cancer - A valuable solution. J Contemp Brachytherapy. 2015; 7:297-311.
5. Bustamante Alvarez JG, González-Cao M, Karachaliou N, Santarpia M, Viteri S, Teixidó C, Rosell R. Advances in immunotherapy for treatment of lung cancer. Cancer Biol Med. 2015; 12:209-222.
6. Ohue Y, Kurose K, Nozawa R, Isobe M, Nishio Y, Tanaka T, Doki Y, Hori T, Fukuoka J, Oka M, Nakayama E. Survival of lung adenocarcinoma patients predicted from expression of PD-L1, galectin-9, and XAGE1 (GAGED2a) on tumor cells and tumor-infiltrating T cells. Cancer Immunol Res. 2016; 4:1049-1060.
7. Domingues P, González-Tablas M, Otero Á, Pascual D, Miranda D, Ruiz L, Sousa P, Ciudad J, Gonçalves JM, Lopes MC, Orfao A, Tabernero MD. Tumor infiltrating immune cells in gliomas and meningiomas. Brain Behav Immun. 2016; 53:1-15.
8. Geng Y, Shao Y, He W, Hu W, Xu Y, Chen J, Wu C, Jiang J. Prognostic role of tumor-infiltrating lymphocytes in lung cancer: A meta-analysis. Cell Physiol Biochem. 2015; 37:1560-1571.
9. Hiraoka K, Miyamoto M, Cho Y, Suzuoki M, Oshikiri T, Nakakubo Y, Itoh T, Ohbuchi T, Kondo S, Katoh H. Concurrent infiltration by CD8+ T cells and CD4+ T cells is a favourable prognostic factor in non-small-cell lung carcinoma. Br J Cancer. 2006; 94:275-280.
10. Naito Y, Saito K, Shiiba K, Ohuchi A, Saigenji K, Nagura H, Ohtani H. CD8+ T cells infiltrated within cancer cell nests as a prognostic factor in human colorectal cancer. Cancer Res. 1998; 58:3491-3494.
11. Ibrahim EM, Al-Foheidi ME, Al-Mansour MM, Kazkaz GA. The prognostic value of tumor-infiltrating lymphocytes in triple-negative breast cancer: A meta-analysis. Breast Cancer Res Treat. 2014; 148:467-476.
12. Rathore AS, Kumar S, Konwar R, Makker A, Negi MP, Goel MM. CD3+, CD4+ & CD8+ tumour infiltrating lymphocytes (TILs) are predictors of favourable survival outcome in infiltrating ductal carcinoma of breast. Indian J Med Res. 2014; 140:361-369.
13. Rahbar M, Naraghi ZS, Mardanpour M, Mardanpour N. Tumor-infiltrating CD8+ lymphocytes effect on clinical outcome of muco-cutaneous melanoma. Indian J Dermatol. 2015; 60:212.
14. Hu WH, Miyai K, Cajas-Monson LC, Luo L, Liu L, Ramamoorthy SL. Tumor-infiltrating $CD8^+$ T lymphocytes associated with clinical outcome in anal squamous cell carcinoma. J Surg Oncol. 2015; 112:421-426.
15. Oguejiofor K, Hall J, Slater C, Betts G, Hall G, Slevin N, Dovedi S, Stern PL, West CM. Stromal infiltration of CD8 T cells is associated with improved clinical outcome in HPV-positive oropharyngeal squamous carcinoma. Br J Cancer. 2015; 113:886-893.
16. Sznurkowski JJ, Zawrocki A, Emerich J, Biernat W. Prognostic significance of $CD4^+$ and $CD8^+$ T cell infiltration within cancer cell nests in vulvar squamous cell carcinoma. Int J Gynecol Cancer. 2011; 21:717-721.
17. Wang L, Song Y, Men X. Variance of TNFAIP8 expression between tumor tissues and tumor-infiltrating CD4+ and CD8+ T cells in non-small cell lung cancer. Tumour Biol. 2014; 35:2319-2325.
18. Weaver CT, Hatton RD. Interplay between the T_H17 and T_{Reg} cell lineages: A (co-)evolutionary perspective. Nat Rev Immunol. 2009; 9:883-889.
19. Sallusto F, Lanzavecchia A. Heterogeneity of CD4+ memory T cells: Functional modules for tailored immunity. Eur J Immunol. 2009; 39:2076-2082.
20. Meng M, Li C, Yang F, Chen H, Li X, Yang Y, Chen D. Novel immunostimulators with a thiazolidin-4-one ring promote the immunostimulatory effect of human iNKT cells on the stimulation of Th2-like immune responsiveness via GATA3 activation *in vitro*. Int Immunopharmacol. 2016; 39:353-358.
21. Bredo G, Storie J, Shrestha Palikhe N, Davidson C, Adams A, Vliagoftis H, Cameron L. Interleukin-25 initiates Th2 differentiation of human $CD4^+$ T cells and influences expression of its own receptor. Immun Inflamm Dis. 2015; 3:455-468.
22. Sadeghi S, Sanati MH, Taghizadeh M, Mansouri P, Jadali Z. Study of Th1/Th2 balance in peripheral blood mononuclear cells of patients with alopecia areata. Acta Microbiol Immunol Hung. 2015; 62:275-285.
23. Guo L, Huang Y, Chen X, Hu-Li J, Urban JF Jr, Paul WE. Innate immunological function of TH2 cells *in vivo*. Nat Immunol. 2015; 16:1051-1059.
24. Ito N, Nakamura H, Tanaka Y, Ohgi S. Lung carcinoma: analysis of T helper type 1 and 2 cells and T cytotoxic type 1 and 2 cells by intracellular cytokine detection with flow cytometry. Cancer. 1999; 85:2359-2367.
25. Quintana FJ. Old dog, new tricks: IL-6 cluster signaling promotes pathogenic TH17 cell differentiation. Nat Immunol. 2016; 18:8-10.
26. Peters A, Fowler KD, Chalmin F, Merkler D, Kuchroo VK, Pot C. IL-27 induces Th17 differentiation in the absence of STAT1 signaling. J Immunol. 2015; 195:4144-4153.
27. Martin-Orozco N, Muranski P, Chung Y, Yang XO, Yamazaki T, Lu S, Hwu P, Restifo NP, Overwijk WW, Dong C. T helper 17 cells promote cytotoxic T cell activation in tumor immunity. Immunity. 2009; 31:787-798.
28. Llosa NJ, Geis AL, Thiele Orberg E, Housseau F. Interleukin-17 and type 17 helper T cells in cancer management and research. Immunotargets Ther. 2014; 3:39-54.
29. Jones SA, Sutton CE, Cua D, Mills KH. Therapeutic potential of targeting IL-17. Nat Immunol. 2012; 13:1022-1025.
30. Li S, Fan Q, He S, Tang T, Liao Y, Xie J. MicroRNA-21 negatively regulates Treg cells through a TGF-β1/Smad-independent pathway in patients with coronary heart

disease. Cell Physiol Biochem. 2015; 37:866-878.
31. Lee YJ, Hyung KE, Yoo JS, Jang YW, Kim SJ, Lee DI, Lee SJ, Park SY, Jeong JH, Hwang KW. Effects of exposure to extremely low-frequency electromagnetic fields on the differentiation of Th17 T cells and regulatory T cells. Gen Physiol Biophys. 2016; 35:487-495.
32. Zhou L, Ivanov II, Spolski R, Min R, Shenderov K, Egawa T, Levy DE, Leonard WJ, Littman DR. IL-6 programs T(H)-17 cell differentiation by promoting sequential engagement of the IL-21 and IL-23 pathways. Nat Immunol. 2007; 8:967-974.
33. Zhou L, Lopes JE, Chong MM, Ivanov II, Min R, Victora GD, Shen Y, Du J, Rubtsov YP, Rudensky AY, Ziegler SF, Littman DR. TGF-beta-induced Foxp3 inhibits T(H)17 cell differentiation by antagonizing RORgammat function. Nature. 2008; 453:236-240.
34. Noack M, Miossec P. Th17 and regulatory T cell balance in autoimmune and inflammatory diseases. Autoimmun Rev. 2014; 13:668-677.
35. Ganesan AP, Johansson M, Ruffell B, Yagui-Beltrán A, Lau J, Jablons DM, Coussens LM. Tumor-infiltrating regulatory T cells inhibit endogenous cytotoxic T cell responses to lung adenocarcinoma. J Immunol. 2013; 191:2009-2017.
36. Arellano B, Graber DJ, Sentman CL. Regulatory T cell-based therapies for autoimmunity. Discov Med. 2016; 22:73-80.
37. Wei T, Zhang J, Qin Y, Wu Y, Zhu L, Lu L, Tang G, Shen Q. Increased expression of immunosuppressive molecules on intratumoral and circulating regulatory T cells in non-small-cell lung cancer patients. Am J Cancer Res. 2015; 5:2190-2201.
38. Atretkhany KN, Drutskaya MS. Myeloid-derived suppressor cells and proinflammatory cytokines as targets for cancer therapy. Biochemistry (Mosc). 2016; 81:1274-1283.
39. Ballbach M, Hall T, Brand A, Neri D, Singh A, Schaefer I, Herrmann E, Hansmann S, Handgretinger R, Kuemmerle-Deschner J, Hartl D, Rieber N. Induction of myeloid-derived suppressor cells in cryopyrin-associated periodic syndromes. J Innate Immun. 2016; 8:493-506.
40. Srivastava MK, Andersson Å, Zhu L, Harris-White M, Lee JM, Dubinett S, Sharma S. Myeloid suppressor cells and immune modulation in lung cancer. Immunotherapy. 2012; 4:291-304.
41. Condamine T, Gabrilovich DI. Molecular mechanisms regulating myeloid-derived suppressor cell differentiation and function. Trends Immunol. 2011; 32:19-25.
42. Qu P, Wang LZ, Lin PC. Expansion and functions of myeloid-derived suppressor cells in the tumor microenvironment. Cancer Lett. 2016; 380:253-256.
43. Meirow Y, Kanterman J, Baniyash M. Paving the road to tumor development and spreading: Myeloid-derived suppressor cells are ruling the fate. Front Immunol. 2015; 6:523.
44. Teixeira D, Almeida JS, Visniauskas B, Gomes GN, Hirata AE, Bueno V. Myeloid-derived suppressor cells and associated events in urethane-induced lung cancer. Clinics (Sao Paulo). 2013; 68:858-864.
45. Srivastava MK, Zhu L, Harris-White M, Kar UK, Huang M, Johnson MF, Lee JM, Elashoff D, Strieter R, Dubinett S, Sharma S. Myeloid suppressor cell depletion augments antitumor activity in lung cancer. PLoS One. 2012; 7:e40677.
46. Gato-Cañas M, Martinez de Morentin X, Blanco-Luquin I, Fernandez-Irigoyen J, Zudaire I, Liechtenstein T, Arasanz H, Lozano T, Casares N, Chaikuad A, Knapp S, Guerrero-Setas D, Escors D, Kochan G, Santamaría E. A core of kinase-regulated interactomes defines the neoplastic MDSC lineage. Oncotarget. 2015; 6:27160-27175.
47. Otsubo D, Yamashita K, Fujita M, Nishi M, Kimura Y, Hasegawa H, Suzuki S, Kakeji Y. Early-phase treatment by low-dose 5-fluorouracil or primary tumor resection inhibits MDSC-mediated lung metastasis formation. Anticancer Res. 2015; 35:4425-4431.
48. Otsuji M, Kimura Y, Aoe T, Okamoto Y, Saito T. Oxidative stress by tumor-derived macrophages suppresses the expression of CD3 zeta chain of T-cell receptor complex and antigen-specific T-cell responses. Proc Natl Acad Sci U S A. 1996; 93:13119-13124.
49. Liu YK, Yang HW, Wang MH, Wang W, Liu F, Yang HL. N-acetylcysteine attenuates cobalt nanoparticle-induced cytotoxic effects through Inhibition of cell death, reactive oxygen species-related signaling and cytokines expression. Orthop Surg. 2016; 8:496-502.
50. Chou HS, Hsieh CC, Charles R, Wang L, Wagner T, Fung JJ, Qian S, Lu LL. Myeloid-derived suppressor cells protect islet transplants by B7-H1 mediated enhancement of T regulatory cells. Transplantation. 2012; 93:272-282.
51. Rastad JL, Green WR. Myeloid-derived suppressor cells in murine AIDS inhibit B-cell responses in part via soluble mediators including reactive oxygen and nitrogen species, and TGF-β. Virology. 2016; 499:9-22.
52. Gabrilovich DI, Ostrand-Rosenberg S, Bronte V. Coordinated regulation of myeloid cells by tumours. Nat Rev Immunol. 2012; 12:253-268.
53. Enokida T, Nishikawa H. Regulatory T cells, as a target in anticancer immunotherapy. Immunotherapy. 2017; 9:623-627.
54. Fan R, Xiang Y, Yang L, Liu Y, Chen P, Wang L, Feng W, Yin K, Fu M, Xu Y, Wu J. Impaired NK cells' activity and increased numbers of CD4 + CD25+ regulatory T cells in multidrug-resistant Mycobacterium tuberculosis patients. Tuberculosis (Edinb). 2016; 98:13-20.
55. Edgington-Mitchell LE, Rautela J, Duivenvoorden HM, Jayatilleke KM, van der Linden WA, Verdoes M, Bogyo M, Parker BS. Cysteine cathepsin activity suppresses osteoclastogenesis of myeloid-derived suppressor cells in breast cancer. Oncotarget. 2015; 6:27008-27022.
56. Panni RZ, Linehan DC, DeNardo DG. Targeting tumor-infiltrating macrophages to combat cancer. Immunotherapy. 2013; 5:1075-1087.
57. Liu Y, Cao X. The origin and function of tumor-associated macrophages. Cell Mol Immunol. 2015; 12:1-4.
58. Fidler IJ. Macrophage therapy of cancer metastasis. Ciba Found Symp. 1988; 141:211-222.
59. Biswas SK, Allavena P, Mantovani A. Tumor-associated macrophages: Functional diversity, clinical significance, and open questions. Semin Immunopathol. 2013; 35:585-600.
60. Huang WC, Chan ML, Chen MJ, Tsai TH, Chen YJ. Modulation of macrophage polarization and lung cancer cell stemness by MUC1 and development of a related small-molecule inhibitor pterostilbene. Oncotarget. 2016; 7:39363-39375.
61. Wynn TA, Chawla A, Pollard JW. Macrophage biology in development, homeostasis and disease. Nature. 2013; 496:445-455.
62. Roy S, Schmeier S, Arner E, et al. Redefining the transcriptional regulatory dynamics of classically and

alternatively activated macrophages by deepCAGE transcriptomics. Nucleic Acids Res. 2015; 43:6969-6982.
63. Mills CD. M1 and M2 macrophages: Oracles of health and disease. Crit Rev Immunol. 2012; 32:463-488.
64. Almendros I, Gileles-Hillel A, Khalyfa A, Wang Y, Zhang SX, Carreras A, Farré R, Gozal D. Adipose tissue macrophage polarization by intermittent hypoxia in a mouse model of OSA: Effect of tumor microenvironment. Cancer Lett. 2015; 361:233-239.
65. Qian BZ, Pollard JW. Macrophage diversity enhances tumor progression and metastasis. Cell. 2010; 141:39-51.
66. Zhang ZM, Yang Z, Zhang Z. Distribution and characterization of tumor-associated macrophages/microglia in rat C6 glioma. Oncol Lett. 2015; 10:2442-2446.
67. Zhang J, Yao H, Song G, Liao X, Xian Y, Li W. Regulation of epithelial-mesenchymal transition by tumor-associated macrophages in cancer. Am J Transl Res. 2015; 7:1699-1711.
68. Li J, Dong X, Zhao L, Wang X, Wang Y, Yang X, Wang H, Zhao W. Natural killer cells regulate Th1/Treg and Th17/Treg balance in chlamydial lung infection. J Cell Mol Med. 2016; 20:1339-1351.
69. Klingemann HG. Cellular therapy of cancer with natural killer cells-Where do we stand? Cytotherapy. 2013; 15:1185-1194.
70. Al Omar SY, Marshall E, Middleton D, Christmas SE. Increased killer immunoglobulin-like receptor expression and functional defects in natural killer cells in lung cancer. Immunology. 2011; 133:94-104.
71. Kärre K, Ljunggren HG, Piontek G, Kiessling R. Selective rejection of H-2-deficient lymphoma variants suggests alternative immune defence strategy. J Immunol. 2005; 174:6566-6569.
72. Smyth MJ, Crowe NY, Godfrey DI. NK cells and NKT cells collaborate in host protection from methylcholanthrene-induced fibrosarcoma. Int Immunol. 2001; 13:459-463.
73. Kreisel D, Gelman AE, Higashikubo R, Lin X, Vikis HG, White JM, Toth KA, Deshpande C, Carreno BM, You M, Taffner SM, Yokoyama WM, Bui JD, Schreiber RD, Krupnick AS. Strain-specific variation in murine natural killer gene complex contributes to differences in immunosurveillance for urethane-induced lung cancer. Cancer Res. 2012; 72:4311-4317.
74. Sabado RL, Balan S, Bhardwaj N. Dendritic cell-based immunotherapy. Cell Res. 2017; 27:74-95.
75. Desch AN, Henson PM, Jakubzick CV. Pulmonary dendritic cell development and antigen acquisition. Immunol Res. 2013; 55:178-186.
76. Palucka K, Banchereau J. Cancer immunotherapy via dendritic cells. Nat Rev Cancer. 2012; 12:265-277.
77. Wang S, Wang Z. Efficacy and safety of dendritic cells co-cultured with cytokine-induced killer cells immunotherapy for non-small-cell lung cancer. Int Immunopharmacol. 2015; 28:22-28.
78. Sozzani S. Dendritic cell trafficking: more than just chemokines. Cytokine Growth Factor Rev. 2005; 16:581-592.
79. Liu J, Li F, Ping Y, Wang L, Chen X, Wang D, Cao L, Zhao S, Li B, Kalinski P, Thorne SH, Zhang B, Zhang Y. Local production of the chemokines CCL5 and CXCL10 attracts CD8+ T lymphocytes into esophageal squamous cell carcinoma. Oncotarget. 2015; 6:24978-24989.
80. Moser B, Wolf M, Walz A, Loetscher P. Chemokines: Multiple levels of leukocyte migration control. Trends Immunol. 2004; 25:75-84.
81. Zlotnik A, Yoshie O. The chemokine superfamily revisited. Immunity. 2012; 36:705-716.
82. Sica A, Allavena P, Mantovani A. Cancer related inflammation: The macrophage connection. Cancer Lett. 2008; 267:204-215.
83. Lazennec G, Richmond A. Chemokines and chemokine receptors: New insights into cancer-related inflammation. Trends Mol Med. 2010; 16:133-144.
84. Spaks A. Role of CXC group chemokines in lung cancer development and progression. J Thorac Dis. 2017; 9:S164-S171.
85. Walzer T, Vivier E. G-protein-coupled receptors in control of natural killer cell migration. Trends Immunol. 2011; 32:486-492.
86. Smyth MJ, Ngiow SF, Teng MW. Targeting regulatory T cells in tumor immunotherapy. Immunol Cell Biol. 2014; 92:473-474.
87. Kohrgruber N, Gröger M, Meraner P, Kriehuber E, Petzelbauer P, Brandt S, Stingl G, Rot A, Maurer D. Plasmacytoid dendritic cell recruitment by immobilized CXCR3 ligands. J Immunol. 2004; 173:6592-6602.
88. Basset L, Chevalier S, Danger Y, Arshad MI, Piquet-Pellorce C, Gascan H, Samson M. Interleukin-27 and IFNγ regulate the expression of CXCL9, CXCL10, and CXCL11 in hepatitis. J Mol Med (Berl). 2015; 93:1355-1367.

(Received September 1, 2017; Revised October 17, 2017; Accepted October 24, 2017)

Review

DOI: 10.5582/irdr.2017.01055

Fibrodysplasia ossificans progressiva: Basic understanding and experimental models

Zijuan Qi[1,2], Jing Luan[2], Xiaoyan Zhou[2], Yazhou Cui[2], Jinxiang Han[2,*]

[1] *School of Medicine and Life Sciences, University of Jinan-Shandong Academy of Medical Science, Ji'nan, China;*
[2] *Key Laboratory for Rare Disease Research of Shandong Province, Key Laboratory for Biotech Drugs of the Ministry of Health, Shandong Medical Biotechnological Center, Shandong Academy of Medical Sciences, Ji'nan, China.*

Summary **Fibrodysplasia ossificans progressive (FOP) is an extremely rare autosomal dominant disorder characterized by congenital malformations of the great toes and progressive heterotopic ossification that can induce a disabling second skeleton. Spontaneously occurring flare-ups can cause inflammatory soft tissue to swell, followed by progressive and disabling heterotopic endochondral ossification. FOP is very rare, with an estimated incidence of one case per two million individuals. There is no definitive treatment for FOP, but the longevity of patients with FOP can be extended by early diagnosis and appropriate prevention of flares-up. Some promising treatment strategies and targets have recently been reported. The current review describes the classical phenotype and genotype of FOP, useful methods of diagnosing the condition, therapeutic approaches and commonly used drugs, and experimental models used to study this disease.**

Keywords: Fibrodysplasia ossificans progressive, phenotype and genotype, disease modeling, induced pluripotent stem cells

1. Introduction

Fibrodysplasia ossificans progressive (FOP), also known as myositis ossificans (*1*), is a rare autosomal dominant disorder with an incidence of one in two million births with no sexual, racial, or regional predisposition (*2*). Most patients are scattered around the world except in instances of familial inheritance (*3*). The earliest reports of FOP by Patin (1692) and Freke (1739) describe its symptoms (*4*). Later, Stonham, Burton-Fanning, and other physicians reported patients of different genders, ages, and even entire families with FOP and their phenotypes (*5*).

Abnormal ossification of the joints and soft tissues such as skeletal muscles, tendons, and ligaments (without myocardium and smooth muscle) and congenital hallux valgus are two typical symptoms of FOP (*6*). Heterotopic ossification (HO) is often associated with disability, such as skeletal deformities (trunk, limb, and facial deformity), chronic pain, growth defects, and stiffness. FOP seriously affects the quality of life and the mental health of patients. The average life expectancy of patients with FOP is no more than 40 years (*7*). The specific pathogenesis of FOP is not yet clear, and the early phenotype of the disease is easily confused with other diseases, including tumors, fibromas, and bursitis, resulting in its misdiagnosis (*8*). Moreover, there is no effective treatment for the disease (*9*).

Here, epidemiological studies on FOP and some common mutations are summarized. Clinically treating the condition is difficult, but diagnosis and treatment of the conditions are making progress. Moreover, experimental models are being used to identify the mechanism of onset of FOP. Greater understanding of the prevalence and symptoms of FOP would facilitate a definitive diagnosis and identify effective precautionary measures. Every step would help to prolong the life-span and improve the quality of life for patients.

2. Prevalence of FOP

FOP is an extremely rare, autosomal dominant disease

**Address correspondence to:*
Dr. Jinxiang Han, Key Laboratory for Rare Disease Research of Shandong Province, Key Laboratory for Biotech Drugs of the Ministry of Health, Shandong Medical Biotechnological Center, Shandong Academy of Medical Sciences, Ji'nan, Shandong 250062, China.
E-mail: jxhan9888@aliyun.com

with a prevalence of 1/2,000,000 (*2*). Ninety-five percent of patients manifest HO before the age of 15, and the latest report of the oldest patient with HO involves a patient who was 56 years of age (*10,11*). According to the CEMARA and PMSI databases, the average age of patients with FOP was 25.5 years, the average age of onset was 7.1 years, and the average age at diagnosis was 10.2 years (*11*).

Statistics for Europe indicate that 30 cases have been confirmed in the UK among about 49 million residents, with a prevalence of 0.61 per million. Spain is estimated to have an incidence of 0.36 per million (*12*), and French data indicate a prevalence of 1.36 per million. These figures are roughly similar to the international prevalence of the condition (*11*).

At present, most patients reported are in the United States, accounting for about 25.6% of all registered patients. This is followed by China, which accounts for about 10.8% of registered patients. Patients with FOP in Brazil account for about 8.4%. Compared to European and American patients, Asian patients are younger (*3*). Despite the extremely low incidence of FOP, there are still a large number of patients with FOP in China due to its huge population. Although definite figures for China are still unclear, the prevalence of FOP can be used to estimate the number of patients. Based on the incidence of FOP, there are at least 650 patients with FOP in China (*7*). For various reasons such as the level of medical research into the condition, however, only about 70 cases are reported, accounting for no more than 12% of all such patients in China. Understanding of the symptoms and mutations of FOP needs to be increased and the condition needs to be better diagnosed.

3. Mutations and diagnosis

The types of mutations of FOP in China are the same as those in other countries and regions (*7*). According to that study, 92% patients have the "classic" clinical presentation of FOP with a mutation of the *ACVR1/ALK2* gene (R260H,c.617G>A), while the remaining 8% have atypical symptoms with mutations at other sites of *ACVR1/ALK2* or other bases of R260H.

So far, 13 missense mutations and a 3-base deletion mutation have been found in FOP, and the detailed types and phenotypes of common mutations are shown in Table 1 (*2,7,10,13,14*).

The "classic" clinical presentation of FOP with a mutation of the *ACVR1/ALK2* gene (R260H, c.617G>A) induces structural changes in the GS domain. Eighty percent of patients with this mutation may have a congenital big toe (hallux valgus deformity), and some may exhibit soft tissue swelling leading to the formation of abnormal bone in the first decade of life (*15*). More than 90% of "classic" patients have a tumor in the tibia and more than 80% have a vertebral deformity (*16*). However, 1.5% of patients with this mutation also have a thumb deformity just like those with G356D (G328 R/W/E) mutations, and some patients with R260H will have cataracts, delayed growth, or other atypical symptoms (*14*).

In the early stages, 80% of patients with FOP often only have an obvious phenotype-malformations of the great toes - but trauma and infection may lead to abnormal bone formation from soft tissue swelling (*8*). Trauma, surgery, intramuscular injections, and immune injections cause swelling of soft tissue, and the occurrence of flare-ups is believed to signal the onset of HO (*17*). Inflammation of soft tissue can gradually infect skeletal muscles, tendons, ligaments, fascia, and aponeuroses, causing abnormal bone formation in these areas, and abnormal bone formation ultimately affects the patient's ability to move as well as the patient's lifespan. Though bone formation is episodic,

Table 1. Common mutations of FOP

Codon	Nucleotide	Domain	Features
R206H	605G>T 617G>A	GS	*i*) Characteristic malformations of great toe, *ii*) HO, *iii*) Tibialosteochondromas, *iv*) Spine malformations, *v*)Broad femoral necks
Q207E	c.619C>G	GS	*i*) Characteristic malformations of great toe, *ii*)HO, *iii*) Tibialosteochondromas, *iv*) Spine malformations, *v*) Broad femoral necks
R202I	605G>T	GS	*i*) HO, *ii*)One short great toe
G325A	974G>C	PK	*i*) Characteristic malformations of great toe, *ii*) Late-onset HO
G328W G328E G328R	c.982G>A c.982G>T c.983G>A	PK	*i*) HO, *ii*) Short broad femoral necks, *iii*) Thumb malformations
G356D	1067G>A	PK	*i*) HO, *ii*) Spine malformations, *iii*) Medial tibialosteochondromas
R258S R258G	774G>C 774G>T	PK	*i*) HO, *ii*) Cognitive impairment, *iii*) Diffuse scalp hair thinning
R375P	c.1124G>C	PK	*i*) HO, *ii*) Normal or minimal changes in great toes

FOP, fibrodysplasia ossificans progressiva; GS, glycine-serine-rich domain; HO, heterotopic ossification; PK, protein kinase domain.

disability is cumulative (*17*). Loss of mobility or even chewing ability can be caused by severe osteogenesis abnormalities, so most patients have to rely on wheelchairs to move around by the third decade of life (*18*). Death due to FOP is caused by the complications of thoracic insufficiency syndrome. Deformities of the joints, limbs, and face also place the patient under enormous psychological strain.

Since there is no effective treatment for FOP, diagnosis of the disease needs to be improved and prevention action needs to be taken to delay its progression. Early diagnosis has become the key to extending the life of patients with FOP. However, 90% of patients with FOP are misdiagnosed in the early stages of the disease. Since there are no diagnostic indicators of FOP, doctors and patients lack understanding of FOP and the early symptoms are not taken seriously, causing a delay in treatment. In specific terms, about 90% of patients with FOP worldwide have been misdiagnosed, and 67% of patients have received incorrect or unnecessary treatment. Treatment or diagnostic techniques such as removing excess bone and a biopsy can cause iatrogenic injury that accelerate HO (*13*). Improper treatment has caused irreparable damage or permanent disability to more than 50% of patients (*17*). Differentiating FOP from tumors, fibromas, and bursitis is essential to diagnosis. A typical mutation of R206H, which accounts for the highest proportion of patients overall, causes flare-ups in the first decades of life (*16*). Therefore, pediatricians and parents must be alert to congenital deformities of the great toes and soft tissue swelling in children consider the likelihood of FOP (*19*).

Before HO develops, routine physical examinations, including a radiographic skeletal survey, will not provide sufficient evidence to definitively diagnose FOP. The most authoritative indicator is the detection of the *ACVR1/ALK2* gene. Kaplan *et al*. obtained genomic DNA from 7 children suspected of having FOP after venipuncture (*19*). A genetic analysis confirmed that the 7 patients had an *ACVR1/ALK2* (R206H, c.617G>A) mutation. Single gene detection allows rapid and accurate diagnosis of patients with FOP before the onset of HO. Without a clear goal or obvious disease phenotype, whole genome sequencing or whole-exome sequencing (WES) is an effective means of reducing the trauma caused by a biopsy, improving the accuracy of diagnosis, avoiding a tedious physical examination, and it also equally helps to identify other rare diseases like FOP (*20,21*).

After HO develops, progressive extra-skeletal ossifications become typical deformities of FOP. In addition to clinical manifestations, imaging analysis (CT and MRI) is an important method of diagnosis. CT clearly reveals typical HO (*8*). MRI is also an important tool for diagnosis of FOP because it can reveal pre-osseous lesions, usually appearing as soft tissue swelling, and skeletal malformations. After HO occurs, plain X-rays can reveal abnormal osteogenesis. FOP cannot be diagnosed prenatally (*22*).

Although there is no effective treatment for FOP, prompt diagnosis can allow disease progression to be delayed, because patient can avoid intramuscular injections, tooth modifications which can cause wound (*23,24,25*). Prevention of trauma and infection is crucial before flare-ups occur (*26*). Patients should not enter dangerous areas or participate in strenuous activities. Living arrangements need to be improved and protective devices such as helmets need to be worn. Special attention should be paid to avoiding surgical procedures because trauma resulting from surgery can cause massive HO (*11*).

4. Existing and potential treatments

Patients with FOP are generally normal except for congenital great toe deformities in infancy. Fifty percent of flare-ups are caused by trauma, viral infection, intramuscular injections, muscle strain, and excessive fatigue in the first decade, resulting in swelling of the soft tissue and abnormal ossification of the muscles and ligaments (*20,25*). There is no effective treatment for FOP, but some drugs can be used to relieve initial symptoms.

When flare-ups begin, a brief 4-day course of high-dose corticosteroids such as prednisone can be used to relieve inflammation and tissue edema, but corticosteroids only can be used to relieve inflammation in areas such as the mandibular joint (*27*). The frequent use of corticosteroids to treat swelling in the trunk and neck is not recommended due to the difficulty in assessing the onset of flare-ups (*8*).

When corticosteroids are discontinued, mast cell inhibitors, aminobisphosphonates, non-steroidal anti-inflammatory drugs, and COX-2 inhibitors could be used to treat later flare-ups. A small dose of a muscle relaxant may help to relieve muscle spasms (*27,28*). Non-steroidal anti-inflammatory drugs inhibit the synthesis of prostaglandin, which induces resistant HO in animal models. Clinically, steroids, non-steroids, and anti-inflammatory drugs can mitigate inflammation and pain, but they cannot reduce the frequency of HO. Aminobisphosphonates affect the function and survival of osteoclasts, thus influencing bone formation, but the efficacy and safety of these drugs have not been established (*29*).

At present, effective drugs are a key area of study. The *ACVR1/ALK2* mutation causes partial deletion of the *ACVR1/ALK2* inhibitory protein FKBP12, so *ACVR1/ALK2* remains weakly activated in the absence of stimulation by BMP signals, causing HO (*30*). Therefore, one potential strategy would be to inhibit the activity of pathways related to the *ACVR1/ALK2* gene to inhibit abnormal bone formation (*31*). As an example, LDN-193189, optimized by dorsomorphin,

is a ALK2 protein inhibitor that repairs and maintains abnormal FOP-iPSc cells *in vitro*, and there is evidence of the therapeutic value of this drug in treating FOP (*32*). The other strategy would be to inhibit inflammation or to inhibit of osteoblastic progenitor cell activity (the RAR gamma agonist palovarotene) (*33*). Hindering the microenvironment for HO is a possible strategy. As an example, imatinib has a positive effect on multiple FOP related targets, and a clinical trial has demonstrated that it inhibits *ACVR1/ALK2* signaling, inflammatory triggers, pre-osseous fibro proliferative cells, and stimulatory mast cells. Kaplan *et al*. proved that imatinib significantly reduced the incidence of flare-ups (*9*).

New drug targets have been discovered with the increasing understanding of the pathogenesis of FOP. Many drugs, such as imatinib, are in clinical trials, and appropriate drugs may be available in the near future because of better understanding of the mechanism of onset of FOP.

5. Cells models of FOP

Studies on FOP are mainly focused on the specific mechanism of onset of HO and drug screening (*8,12,34*). The nature of FOP is particularly problematic because of the difficulty in acquiring living tissue to study the mechanisms of the disease. Minor trauma or an infection may cause tissue swelling followed by development of HO in the ligaments and connective tissue (*15*). At present, the main models used to study the pathogenesis of FOP are mouse cells, knockout mice, and induced pluripotent stem cells (*25*).

The cells most often used to model FOP are mouse cells (*35*). When studying the abnormal expression mechanism of pathogenic *ACVR1/ALK2*, different researchers have chosen different cell models, and their results differ. Vectors containing mutated *ACVR1/ALK2* have been transfected into cells such as U-2OS (*36*), MC3T3-E1 (*37*), and C2C12 (*38*), but levels of Smad1/5/8 expression differed. In addition to the transfection process (expression and transfection efficiency), the cell type may account for differences in expression (*39,40*). Patients FOP have endochondral ossification, so many studies have focused on cells related to chondrocytes. The differentiation of mouse embryonic fibroblasts into chondrocytes demonstrates that *ACVR1/ALK2* is a key factor in chondrogenesis. Embryonic fibroblasts, the origin of mouse mesenchymal cells, can be obtained from the head and limbs of mouse embryos. A rat chondrocyte cell line (ATDC5) expressing BMP-responsive luciferase has been used in high throughput drug screening. The cells can differentiate into mature chondrocytes when cultured in differentiation medium, and drugs that down-regulate the *ACVR1/ALK2* gene could be distinguished based on the intensity of the fluorescence signal, providing a basic model for drug screening and retesting of existing drugs (*25*).

ACVR1/ALK2 gene knockout mice are commonly used (*41*). Most knockout mice have the FOP phenotype. Murine cells and mice as models of FOP have indeed made great progress, but mice and murine cells cannot meet more detailed experimental needs. There are certain interspecies differences between mice and humans. For example, some knockout mice die during the perinatal period, so more appropriate models are urgently needed (*42*). Dermal fibroblasts obtained from patients with FOP are more suitable. A 3-mm thick piece of skin is removed from a patient with FOP and then macerated and cultured. Mineralization is then induced to study the role of TGF in osteogenic differentiation. Since trauma can easy trigger flare-ups in patients with FOP, sampling must be performed very carefully and skillfully to avoid trauma or infection (*43*).

In 2006, Takahashiand Yamanaka induced somatic cell reprogramming with a recombinant factor, thus obtaining induced pluripotent stem cells (iPSc) (*44*). This new technique has opened up new avenues and methods of studying the biological characteristics of many diseases (*45*). iPSc have several advantages. First, iPSc have a potent capacity for self-renewal and grow rapidly. *In vitro* experiments have been able to provide large quantities of needed cells, avoiding the tedious process of obtaining primary cells. Second, their potential for differentiation enables iPSc to differentiate into specific cells, providing cells at different stages of differentiation (*46*). iPSc can be obtained from somatic cells without causing ethical issues. With individual specificity, iPSc can carry disease-related pathogenic genes and an individual's specific genetic background (*47*). The induction of iPSc *in vitro* rapidly and effectively indicates the phenotype of disease in an individual specific background. A variety of somatic cells can be

Table 2. Induced pluripotent stem cell models of FOP

Sample	Types	Somatic cell	Vector	*Ref.*
4 patients	R206H and G356D	Skin fibroblasts	Sendai virus	(*32*)
2 patients	R206H	Urine Cell	Episomal vectors	(*48*)
purchased	R206H	Human dermal fibroblasts	Episomal vectors	(*49*)
2 patients	R206H	Urine	Sendai virus vector	(*50*)
5 patients	R206H	Primary human dermal fibroblasts	Retroviruses and integration-free episomal plasmid	(*51*)
5 patients	R260H	Primary human dermal fibroblasts	Retroviruses and integration-free episomal plasmid	(*40,52,53*)
4 patients	R206H	Fibroblasts	Retrovirus or episomal plasmids	(*54*)

FOP, fibrodysplasia ossificans progressiva.

reprogrammed into stem cells, including skin fibroblasts (*32*) and kidney epithelial cells (*48*), and Sendai virus and non-integration vector can be used as programming tools (*49*).

iPSc have been obtained by somatically reprogramming cells from patients with FOP. This provides a new, more accurate and appropriate cell model for the study of the pathogenesis of FOP. Hamasaki *et al*. used incompletely reprogrammed FOP-iPSc as an alternative tool to screen new drugs (*32*). Hino *et al*. induced chondrogenic differentiation of MSC cells from FOP-iPSc and concluded that BMP signals were activated by actinA (*50*). Relevant studies are listed in Table 2.

Surgery is not generally appropriate for patients with FOP, so future studies should focus on drug screening and noninvasive treatment. Intramuscular injections remain a potential risk, so safer dosing schedules should be considered. FOP-iPSc, a strong operational and theoretical basis for elucidation of the pathogenesis of FOP and drug screening, should be the main *in vitro* model used in future experiments. Effective therapies and drugs to treat FOP should be available in the near future.

Acknowledgement

This work was supported by the Innovation Project of the Shandong Academy of Medical Sciences.

References

1. Nilsson OS. Heterotopic ossification. Acta Orthop Scand. 1998; 69:103-106.
2. Miao J, Zhang C, Wu S, Peng Z, Tania M. Genetic abnormalities in fibrodysplasia ossificans progressiva. Genes Genet Syst. 2012; 87:213-219.
3. Pignolo R J, Bedford-Gay C, Liljesthröm M, Durbin-Johnson B P, Shore E M, Rocke DM, Kaplan FS. The natural history of flare-ups in fibrodysplasia ossificans progressiva (FOP): A comprehensive global assessmen. J Bone Miner Res. 2016; 31:650-656.
4. Shore EM, Gannon FH, Kaplan FS. Fibrodysplasia ossificans progressiva: Why do some people have two skeletons? Rev Rhum Engl Ed. 1997; 64(Suppl 6):92S-97S.
5. Shore EM, Xu M, Feldman GJ, *et al*. A recurrent mutation in the BMP type I receptor ACVR1 causes inherited and sporadic fibrodysplasia ossificans progressiva.Nat Genet. 2006; 38:525-527.
6. Hildebrand L, Gaber T, Kühnen P, Morhart R, Unterbörsch H, Schomburg L, Seemann P. Trace element and cytokine concentrations in patients with Fibrodysplasia Ossificans Progressiva (FOP): A case control study. J Trace Elem Med Biol, 2017; 39:186-192.
7. Zhang W, Zhang K, Song L, Pang J, Ma H, Shore EM, Kaplan FS, Wang P. The phenotype and genotype of fibrodysplasia ossificans progressiva in China: A report of 72 cases. Bone. 2013; 57:386-391.
8. Kitterman JA, Kantanie S, Rocke DM, Kaplan FS. Iatrogenic harm caused by diagnostic errors in fibrodysplasia ossificans progressiva. Pediatrics. 2005; 116:e654-e661.
9. Kaplan FS, Andolina JR, Adamson PC, Teachey DT, Finklestein JZ, Ebb DH, Whitehead B, Jacobs B, Siegel DM, Keen R, Hsiao E, Pignolo RJ. Early clinical observations on the use of imatinib mesylate in FOP: A report of seven cases. Bone. 2017; pii: S8756-3282(17)30245-4. doi: 10.1016/j.bone.2017.07.019.
10. Whyte MP, Wenkert D, Demertzis JL, DiCarlo EF, Westenberg E, Mumm S. Fibrodysplasia ossificans progressiva: Middle-age onset of heterotopic ossification from a unique missense mutation (c.974G>C, p.G325A) in ACVR1. J Bone Miner Res. 2012; 27:729-737.
11. Baujat G, Choquet R, Bouée S, Jeanbat V, Courouve L, Ruel A, Michot C, Le Quan Sang KH, Lapidus D, Messiaen C, Landais P, Cormier-Daire V. Prevalence of fibrodysplasia ossificans progressiva (FOP) in France: An estimate based on a record linkage of two national databases. Orphanet J Rare Dis. 2017; 12:123.
12. Morales-Piga A, Bachiller-Corral J, Trujillo-Tiebas MJ, Villaverde-Hueso A, Gamir-Gamir ML, Alonso-Ferreira V, Vázquez-Díaz M, Posada de la Paz M, Ayuso-García C. Fibrodysplasia ossificans progressiva in Spain: Epidemiological, clinical, and genetic aspects. Bone. 2012; 51:748-755.
13. Ratbi I, Borcciadi R, Regragui A, Ravazzolo R, Sefiani A. Rarely occurring mutation of ACVR1 gene in Moroccan patient with fibrodysplasia ossificans progressiva. Clin Rheumatol. 2010; 29:119-121.
14. Kaplan F S, Xu M, Seemann P, *et al*. Classic and atypical fibrodysplasia ossificans progressiva (FOP) phenotypes are caused by mutations in the bone morphogenetic protein (BMP) type I receptor ACVR1. Hum Mutat. 2009; 30:379-390.
15. Pacifici M, Shore E M. Common mutations in ALK2/ACVR1, a multi-faceted receptor, have roles in distinct pediatric musculoskeletal and neural orphan disorders. Cytokine Growth Factor Rev.2016; 27:93-104.
16. Deirmengian GK, Hebela NM, O'Connell M, Glaser DL, Shore EM, Kaplan FS. Proximal tibial osteochondromas in patients with fibrodysplasia ossificans progressiva. J Bone Joint Surg Am. 2008; 90:366-374.
17. Pignolo R J, Shore E M, Kaplan F S. Fibrodysplasia ossificans progressiva: Clinical and genetic aspects. Orphanet J Rare Dis.2011; 6:80.
18. Kaplan FS, Pignolo RJ, Shore EM. From mysteries to medicines: Drug development for fibrodysplasia ossificans progressive. Expert Opin Orphan Drugs. 2013;1:637-649
19. Kaplan FS, Xu M, Glaser DL, Collins F, Connor M, Kitterman J, Sillence D, Zackai E, Ravitsky V, Zasloff M, Ganguly A, Shore EM. Early diagnosis of fibrodysplasia ossificans progressiva. Pediatrics. 2008; 121:e1295-1300.
20. Liu H, Sawyer SL, Gos M, Grynspan D, Issa K, Ramphal R, Rotaru C; FORGE Canada Consortium, Majewski J, Boycott KM, Graham G, Bromwich M. Atypical fibrodysplasia ossificans progressiva diagnosed by whole-exome sequencing. Am J Med Genet A. 2015; 167:1337-1341.
21. Rafati M, Mohamadhashem F, Hoseini A, Hoseininasab F, Ghaffari SR. A novel ACVR1 mutation detected by whole exome sequencing in a family with an unusual skeletal dysplasia.Eur J Med Genet. 2016; 59:330-336.
22. Lin FY, Lin CH, Shu G, Chen CK. Fibrodysplasia

ossificans progressiva: Initial presentation with a preosseous lesion of the scalp and its MRI appearance. Skeletal Radiol. 2016; 45:991-996.
23. Luchetti W, Cohen RB, Hahn GV, Rocke DM, Helpin M, Zasloff M, Kaplan FS. Severe restriction in jaw movement after routine injection of local anesthetic in patients who have fibrodysplasia ossificans progressiva. Oral Surg Oral Med Oral Pathol Oral Radiol Endod. 1996, 81:21-25.
24. Glaser D L, Kaplan F S. Treatment considerations for the management of fibrodysplasia ossificans progressiva. Clin Rev Bone Miner Metab. 2005; 3:243-250.
25. Glaser D L, Rocke D M, Kaplan F S. Catastrophic falls in patients who have fibrodysplasia ossificans progressiva. Clin Orthop Relat Res. 1998; 346:110-116.
26. Cappato S, Tonachini L, Giacopelli F, Tirone M, Galietta LJ, Sormani M, Giovenzana A, Spinelli AE, Canciani B, Brunelli S, Ravazzolo R, Bocciardi R. High-throughput screening for modulators of ACVR1 transcription: discovery of potential therapeutics for fibrodysplasia ossificans progressiva. Dis Model Mech.2016; 9:685-696.
27. FS Kaplan, EM Shore, DL Glaser, S Emerson, JM Connor. The medical management of fibrodysplasia ossificans progressiva: Current treatment considerations .China Forestry Publishing House, China. 2003; 64:359-363.
28. Simmons DL, Botting RM, Hla T. Cyclooxygenase isozymes: The biology of prostaglandin synthesis and inhibition. Pharmacol Rev. 2004; 56:387-437.
29. Schuetz P, Mueller B, Christ-Crain M, Dick W, Haas H. Amino-bisphosphonates in heterotopic ossification: First experience in five consecutive cases. Spinal Cord. 2005; 43:604-610.
30. Chaikuad A, Alfano I, Kerr G, Sanvitale CE, Boergermann JH, Triffitt JT, von Delft F, Knapp S, Knaus P, Bullock AN. Structure of the bone morphogenetic protein receptor ALK2 and implications for fibrodysplasia ossificans progressiva. J Biol Chem. 2012; 287:36990-36998.
31. Dey D, Bagarova J, Hatsell S J, *et al*. Two tissue-resident progenitor lineages drive distinct phenotypes of heterotopic ossification. Sci Transl Med. 2016; 8:366ra163.
32. Hamasaki M, Hashizume Y, Yamada Y, Katayama T, Hohjoh H, Fusaki N, Nakashima Y, Furuya H, Haga N, Takami Y, Era T. Pathogenic mutation of ALK2 inhibits induced pluripotent stem cell reprogramming and maintenance: Mechanisms of reprogramming and strategy for drug identification. Stem Cells. 2012; 30:2437-2749.
33. Kaplan F S, Pignolo R J, Mukaddam M M A, *et al*. Hard targets for a second skeleton: Therapeutic horizons for fibrodysplasia ossificans progressiva (FOP). Expert Opin Orphan Drugs. 2017; 5:291-294.
34. Shore E M, Xu M, Feldman G J, *et al*. A recurrent mutation in the BMP type I receptor ACVR1 causes inherited and sporadic fibrodysplasia ossificans progressiva. Nat Genet. 2006; 38:525-527.
35. Chakkalakal SA, Zhang D, Culbert AL, Convente MR, Caron RJ, Wright AC, Maidment AD, Kaplan FS, Shore EM. An ACVR1 R206H knock-in mouse has fibrodysplasia ossificans progressiva. J Bone Miner Res. 2012; 27:1746-1756.
36. Yano M, Kawao N, Tamura Y, Okada K, Kaji H. A novel factor, Tmem176b, induced by activin-like kinase 2 signal promotes the differentiation of myoblasts into osteoblasts. Exp Clin Endocrinol Diabetes. 2014; 122:7-14.
37. Ohte S, Shin M, Sasanuma H, *et al*. A novel mutation of ALK2, L196P, found in the most benign case of fibrodysplasia ossificans progressiva activates BMP-specific intracellular signaling equivalent to a typical mutation, R206H. Biochem Biophys Res Commun. 2011; 407:213-218.
38. van Dinther M, Visser N, de Gorter DJ, Doorn J, Goumans MJ, de Boer J, ten Dijke P. ALK2 R206H mutation linked to fibrodysplasia ossificans progressiva confers constitutive activity to the BMP type I receptor and sensitizes mesenchymal cells to BMP-induced osteoblast differentiation and bone formation. J Bone Miner Res. 2010; 25:1208-1215.
39. Shen Q, Little SC, Xu M, Haupt J, Ast C, Katagiri T, Mundlos S, Seemann P, Kaplan FS, Mullins MC, Shore EM. The fibrodysplasia ossificans progressiva R206H ACVR1 mutation activates BMP-independent chondrogenesis and zebrafish embryo ventralization. J Clin Invest. 2009; 119:3462-3472.
40. Matsumoto Y, Ikeya M, Hino K, Horigome K, Fukuta M1, Watanabe M, Nagata S, Yamamoto T, Otsuka T, Toguchida J. New protocol to optimize ips cells for genome analysis of fibrodysplasia ossificans progressiva. Stem Cells. 2015; 33:1730-1742.
41. Chakkalakal SA, Uchibe K, Convente MR, Zhang D, Economides AN, Kaplan FS, Pacifici M, Iwamoto M, Shore EM. Palovarotene inhibits heterotopic ossification and maintains limb mobility and growth in mice with the human ACVR1 (R206H) fibrodysplasia ossificans progressiva (FOP) mutation. J Bone Miner Res. 2016; 31:1666-1675.
42. Hatsell S J, Idone V, Wolken D M, *et al*. ACVR1 R206H receptor mutation causes fibrodysplasia ossificans progressiva by imparting responsiveness to activin A. Sci Transl Med. 2015; 7:303ra137.
43. Micha D, Voermans E, Eekhoff ME, van Essen HW, Zandieh-Doulabi B, Netelenbos C, Rustemeyer T, Sistermans EA, Pals G, Bravenboer N. Inhibition of TGFβ signaling decreases osteogenic differentiation of fibrodysplasia ossificans progressiva fibroblasts in a novel *in vitro* model of the disease. Bone. 2016; 84:169-180.
44. Takahashi K, Yamanaka S. Induction of pluripotent stem cells from mouse embryonic and adult fibroblast cultures by defined factors. Cell. 2006; 126:663-676.
45. Dimos JT1, Rodolfa KT, Niakan KK, Weisenthal LM, Mitsumoto H, Chung W, Croft GF, Saphier G, Leibel R, Goland R, Wichterle H, Henderson CE, Eggan K. Induced pluripotent stem cells generated from patients with ALS can be differentiated into motor neurons. Science. 2008; 321:1218-1221.
46. Barruet E, Hsiao EC. Using human induced pluripotent stem cells to model skeletal diseases. Methods Mol Biol.2016; 1353:101-118.
47. Cyranoski D. Stem-cell pioneer banks on future therapies. Nature. 2012; 488:139.
48. Cai J, Orlova VV, Cai X, Eekhoff EMW, Zhang K, Pei D, Pan G, Mummery CL, Ten Dijke P. Induced pluripotent stem cells to model human fibrodysplasia ossificans progressiva. Stem Cell Reports. 2015; 5:963-970.
49. Kim BY, Jeong S, Lee SY, Lee SM, Gweon EJ, Ahn H, Kim J, Chung SK. Concurrent progress of reprogramming and gene correction to overcome therapeutic limitation of mutant ALK2-iPSC. Exp Mol Med; 2016; 48:e237.
50. Hildebrand L, Rossbach B, Kühnen P, Gossen M, Kurtz

A, Reinke P1, Seemann P, Stachelscheid H. Generation of integration free induced pluripotent stem cells from fibrodysplasia ossificans progressiva (FOP) patients from urine samples. Stem Cell Res. 2016; 16:54-58.
51. Hino K, Ikeya M, Horigome K, Matsumoto Y, Ebise H, Nishio M, Sekiguchi K, Shibata M, Nagata S, Matsuda S, Toguchida J. Neofunction of ACVR1 in fibrodysplasia ossificans progressiva. Proc Natl Acad Sci U S A. 2015; 112:15438-15443.
52. Matsumoto Y, Hayashi Y, Schlieve CR, Ikeya M, Kim H, Nguyen TD, Sami S, Baba S, Barruet E, Nasu A, Asaka I, Otsuka T, Yamanaka S, Conklin BR, Toguchida J, Hsiao EC. Induced pluripotent stem cells from patients with human fibrodysplasia ossificans progressiva show increased mineralization and cartilage formation. Orphanet J Rare Dis. 2013, 8:190.
53. Barruet E, Morales BM, Lwin W, White MP, Theodoris CV, Kim H1, Urrutia A, Wong SA, Srivastava D, Hsiao EC. The ACVR1 R206H mutation found in fibrodysplasia ossificans progressiva increases human induced pluripotent stem cell-derived endothelial cell formation and collagen production through BMP-mediated SMAD1/5/8 signaling. Stem Cell Res Ther. 2016; 7:115.
54. Hayashi Y, Hsiao EC, Sami S, *et al*. BMP-SMAD-ID promotes reprogramming to pluripotency by inhibiting p16/INK4A-dependent senescence. Proc Natl Acad Sci U S A. 2016; 113:13057-13062.

(Received August 17, 2017; Revised November 16, 2017; Accepted November 24, 2017)

Review

DOI: 10.5582/irdr.2017.01057

Epidemiology, diagnosis, and treatment of Wilson's disease

Jing Liu[1,2], Jing Luan[2], Xiaoyan Zhou[2], Yazhou Cui[2], Jinxiang Han[2,*]

[1] *School of Medicine and Life Sciences, University of Jinan-Shandong Academy of Medical Science, Ji'nan, China;*
[2] *Key Laboratory for Rare Disease Research of Shandong Province, Key Laboratory for Biotech Drugs of the Ministry of Health, Shandong Medical Biotechnological Center, Shandong Academy of Medical Sciences, Ji'nan, China.*

Summary **Wilson's disease (WD) is an autosomal recessive disease caused by a mutation of the *ATP7B* gene, resulting in abnormal copper metabolism. The major clinical features of WD include liver disease, neurological disorders, K-F rings, and osteoporosis. The prevalence of WD in China is higher than that in Western countries. Early diagnosis and lifelong treatment will lead to better outcomes. Drugs such as sodium dimercaptosuccinate (Na-DMPS), Zn, and Gandou Decoction can be used to treat WD. Some studies have shown that the combination of traditional Chinese medicine and Western medicine is the best approach to treating WD. In order to identify better treatments, this article describes the specific clinical symptoms of Wilson's disease, its diagnosis, and treatment options.**

Keywords: Wilson's disease, Kayser-Fleischer rings, D-PCA

1. Introduction

Wilson's disease (WD), also named hepatolenticular degeneration, is an autosomal recessive disorder of copper (Cu) metabolism caused by an *ATP7B* gene mutation (*1*). WD was first identified by Wilson in 1912 (*2*). Cheng reported the first two cases of WD in China (*3*). Research on WD began to surge after the 1950s, and the number of reported cases had gradually caught up to that in Western countries.

The gene that causes WD is located on chromosome 13q14-21 (*4*). This gene, *ATP7B*, encodes a P-type ATPase that participates in ceruloplasmin synthesis and excretion of copper. Pathogenic mutations in *ATP7B* disrupt the normal structure or function of enzymes and lead to copper deposition in multiple organs, leading to different clinical manifestations. In the light of its various manifestations, misdiagnosis is not uncommon (*5*). Many researchers have focused on determining the relationship between the genotype and phenotype of WD (*6*). From 2004 to 2015, Dong *et al*. identified 58 new mutations and determined the first Chinese *ATP7B* pathogenic mutation spectrum (*7*). D-penicillamine (D-PCA) is recommended for most patients with WD (*8*). However, D-PCA is not suitable for patients with severe spasms, deformities, or dysphonia and patients who are allergic to D-PCA. Dimercaptosuccinic acid (DMSA) is first drug used to treat WD in China (*9*). DMSA is recommended as an alternative for patients with severe neurological symptoms. In addition, monozygous therapy is suitable for asymptomatic WD, as well as maintenance therapy after the use of copper chelating agents (*10*). WD is a genetic disorder that can be alleviated, so most patients have a favorable prognosis. The prevalence of WD in China is higher than that in Western countries, but there are few clinical trials in China and treatment is often based on the experience of experts and evidence from other countries. Therefore, appropriate treatments need to be studied and developed specifically for Chinese patients with WD (*5*). This article describes the clinical features of WD and treatment options.

**Address correspondence to:*
Dr. Jinxiang Han, Key Laboratory for Rare Disease Research of Shandong Province, Key Laboratory for Biotech Drugs of the Ministry of Health, Shandong Medical Biotechnological Center, Shandong Academy of Medical Sciences, Ji'nan, Shandong 250062, China.
E-mail: jxhan9888@aliyun.com

2. Epidemiology

2.1. *WD in Western countries*

Sternlieb and Scheinberg first estimated the incidence of WD to be 5/1,000,000 in 1968 (*11*). From 1949-1977, Bachman *et al*. studied WD in Leipzig, Germany and calculated that the prevalence of WD to be 29/1,000,000

births (*12*). In 1981, Saito reported that the prevalence of WD was 33/1,000,000 births (*13*). In 1991, Park *et al*. attempted to determine the prevalence of WD in Scotland by examining computerized hospital records, survey results, and death certificates (*14*). They identified 21 patients with WD in a population 5,090,700, for a prevalence of 4/1,000,000. In 1993, Reilly *et al*. used a similar methodological approach to determine the prevalence of WD in the Republic of Ireland, and they identified 26 cases over a 19-year period (*15*). Patients in 5 of those cases died before being formally diagnosed. Between 1950 and 1969, the adjusted birth rate of individuals with WD was 17/1,000,000, which was equivalent to a gene frequency of 0.41% and the incidence of heterozygotes was 0.82% (*16*). In order to account for the highest level of kinship, the gene frequency was modified to 0.36% and the incidence of heterozygotes was modified to 0.72% to provide a minimum disease estimate.

Sequencing of *ATP7B* in 1,000 control participants in the UK allowed the frequency of an individual carrying two mutant *ATP7B* alleles to be estimated at 1/7,026 (*17*). The most common mutation in Europe and North America is p.H1069Q (*1*).

2.2. *WD in Asia*

The WHO estimates that the global prevalence of WD is 1/10,000 to 1/30,000. The prevalence of WD is higher in China than in the West (*18*). Since the first estimate of WD in 1968, considerable progress has been made in China. Cheng *et al*. conducted two consecutive surveys in three counties of Anhui province (Jinzhai, Hanshan, and Lixin counties) (*19*). A total of 153,370 individuals were examined and 9 individuals with WD were identified. Three of these individuals had neurological symptoms, 1 had hepatic symptoms, 1 had both hepatic and neurological symptoms, and the remaining 4 individuals had other symptoms. Of 8 individuals in whom genetic mutations were detected, 7 had mutations in the *ATP7B* gene. The other individual did not have an *ATP7B* mutation but her copper biochemical test results met the diagnostic criteria for WD. The incidence of WD was 1.96/100,000 and the prevalence was 5.87/100,000. In all of the identified cases, diagnosis was based on clinical features, biochemical parameters, and the presence of Kayser-Fleischer (K-F) rings. Given that K-F rings may be absent, patients may be asymptomatic but have other common biochemical abnormalities, the technical limitations of screening levels, and differences in expertise among physicians, the actual prevalence of WD may be underestimated (*5*). According to a haplotype analysis of 660 participants in Hong Kong, the incidence of WD among Chinese was estimated to be 1/5,400 (*20*), which indicates that the average mortality rate of Chinese patients with WD is higher than that in the American or European population (*5*).

In a survey of 500 healthy Korean participants, the prevalence of WD was lower than 1/3,000 and the frequency of carriers was 1/27 (*21*). The molecular epidemiology of *ATP7B* in these populations has also been confirmed by the fact that WD is more prevalent in Asians than Caucasians (*5*). While the most common mutation in Europe and North America is p.H1069Q, the most common mutation in Asia is p.Arg778L (*1*).

3. Clinical features

3.1. *Nerve damage*

In 1932, Cheng described the clinical history of two patients who are 24 years of age (*3*). The two patients clinically presented with impaired motor movements, involuntary movements (including tremors), cone dystrophy, peristalsis, and "dancing" movements (repetitive, complex, and well-coordinated but involuntary movements). In the 1950s, Zhang summarized recent studies on WD and concluded that the major clinical manifestation of WD was neuropathy, and especially damage to the extrapyramidal system (*22*). Neurological manifestations include involuntary movements, stiffness, tremors, and oropharyngeal dysfunction such as expectoration and dysphonia (*23*). As a patient with WD reaches the age of 20 or 30, the patient's condition may deteriorate and trembling may be evident. Muscle stiffness will develop during movement, fine movement will deteriorate, and the patient is then likely to exhibit "dancing" movements (*23*). Speech difficulties and drooling are the most common manifestations of WD (*23*), and they will appear in the early stages. Other symptoms, including dystonia, dysfunction, gait abnormalities, ataxia, autonomic dysfunction, and memory deterioration (*5*) are also common in Chinese patients with WD. Psychotic symptoms are usually nonspecific, such as depression, mania, personality changes, and mental retardation (*23*).

3.2. *Neurological symptoms*

A review of the medical records of patients with WD at Shengjing Hospital from 1993-2001 indicated that 20.3% (27/133) had neurological symptoms at diagnosis and 69.9% (93/133) had hepatic symptoms at diagnosis (*24*). Hepatic symptoms are mainly liver dysfunction, including acute or chronic hepatitis, cirrhosis, hepatic encephalopathy, and fulminant hepatitis. However, patients without neurological manifestations are likely to be misdiagnosed. According to one figure, only 33.1% (44/133) of patients were correctly diagnosed when initially seen (*5*).

3.3. *K-F rings*

K-F rings are a common ophthalmological sign and

the easiest way to identify WD. The transparent tissue of the eye provides a unique opportunity to observe the deposition of copper in tissue (*23*). A red or green ring forms around the corneal limbus, and copper deposition is greater in the upper portion and lower in the lower portion. Copper is deposited on the surface of Descemet's membrane and the surface of endothelial cells (*25*). At least 50% of patients have this symptom and it is always present when the central nervous system is fatigued (*23*). In a non-randomized case series, K-F rings were found in 23.1% (12/52) of patients with liver disease and a neurological disorder was found in 100% (11/11) (*26*). If patients have overt neurological symptoms, the absence of K-F rings cannot be used to rule out WD (*5*). Bile excretion is the main way that the body reduces the copper concentration and K-F rings are caused by the deposition of copper, so those rings are also found in patients with chronic cholestasis (*27*). Li *et al*. found that patients with K-F rings developed symptoms at maturity and that if the first doctor is poorly informed about WD, then WD may not be identified, possibly delaying diagnosis (*2*). In addition, patients with K-F rings had higher levels of 24 h urinary copper and lower levels of alanine aminotransferase (ALT) (*28*).

3.4. *Osseous findings*

Patients with WD have a lower bone mineral density and are prone to osteoporosis and fractures (*29*). Osteoarthritis is one of the manifestations of WD. Osseous findings include osteoporosis (the most common), facet joint inflammation, osteomalacia, juvenile osteoarthritis, spinal osteochondritis, fractures, and heterotopic ossification. Patients with hypercalciuria had a statistically significant lower bone mineral content (BMC) and bone mineral density (BMD) than those without hypercalciuria (*30-33*).

4. Diagnosis

4.1. *Molecular diagnosis*

The methods of identifying WD include molecular diagnosis (laboratory diagnosis), diagnostic imaging (*2*), and genetic analysis. Molecular diagnosis has increased in use. The clinical manifestations of WD include liver disease, brain and nervous system damage, osteoporosis, and K-F rings (*34*). Liver damage may not be identified. Routine liver function tests are not diagnostic. Tremors can be a clue to the diagnosis of WD affecting the nervous system (*35*). Patients with neurological or psychiatric symptoms tend to be more often identified as having WD. The presence of K-F rings at the edge of the cornea is also diagnostic (*23*). The study of copper metabolism is most important. The loss of more than 200 ug of copper within 24 hours is very serious. The loss of large amounts of proteins can occur in WD and chronic liver diseases characterized by biliary obstruction and biliary cirrhosis, but primary liver disease differs from WD. In WD, the concentration of copper in plasma increases proportional to that in urine (*35*). In 1954, Earl found that copper ion concentration can be detected in urine. In 1996, Ravlin found that a low level or undetectable plasma ceruloplasmin could be a rough indicator of WD. A high level of urinary copper excretion in the absence of proteinuria and in association with a low or low-normal plasma copper level will also confirm the diagnosis. The level of plasma ceruloplasmin that can be determined by laboratory screening is the first step in diagnosing WD, followed by the level of copper ions (*35*).

4.2. *Imaging studies*

Nuclear magnetic resonance imaging (MRI) of the brains of patients with WD revealed abnormalities, and the basal ganglia were the areas most often affected (*36*). The main signs of WD are hypointensity on T1-weighted images and hyperintensity on T2-weighted images in the caudate nucleus, thalamus, midbrain, pons, and cerebellum, although in some rare cases there is hyperintensity on T1-weighted images and hypointensity on T2-weighted images (*5*). Concurrent signal changes are more common in the basal ganglia, thalamus, and brainstem (*2*). Patients with WD have varying degrees of atrophy of the frontal cortex, enlargement of the ventricles, and hydrocephalus. The brain abnormalities identified on MRI can subside after successful treatment (*2*), so MRI is a useful way to monitor the effectiveness of treatment (*5*).

4.3. *Genetic analysis*

Genetic analysis has also become routine. WD is caused by mutations in the *ATP7B* gene. At present, direct sequence analysis is the most accurate way to identify *ATP7B* mutations. The most common mutations are point mutations, but other types of mutations have also been identified, such as small deletions or insertions, total deletions, and splice site mutations. Previous studies have indicated that WD in China seems to have been caused by a number of relatively common mutations and a number of rare mutations (*37*). New *ATP7B* mutations have been reported very frequently. Li *et al*. identified 62 cases of WD, 14 of which involved new mutations (*15*). Dong *et al*. concluded a long-term study of 632 samples of *ATP7B* variants from patients with WD in China between 2004 and 2005, and they detected 173 variants, 58 of which were new types of *ATP7B* (*5*). Common mutations include p.R778L with a frequency of 1.7%, p.P992L with a frequency of 2.6%, p.T935M with a frequency of 1.6%, and p.A874V with a frequency of 3.8% (*23*). The three most prevalent alleles were *p.R778L*, *p.P992L*, and *p.T935M*. A study

Table1. The treatment of WD in Chinese medicine and Western medicine

Items	Medication	Advantages and disadvantages	Suitable patients	*Ref.*
Western medicine	D-PCA	Orally administered; Promotes copper excretion; Causes serious adverse reactions.	Not suitable for the treatment of patients with liver disease, patients with severe neurological disorders, patients with advanced WD, and patients with an allergy to D-PCA.	(*39-40*)
	DMSA	Orally administered; Promotes copper excretion.	Suitable for mild and moderate neurological symptoms and psychiatric symptoms and PCA intolerance.	(*41-43*)
	Na-DMPS	Injected; Low toxicity.	Suitable for mild and moderate neurological symptoms and psychiatric symptoms and D-PCA intolerance.	(*42*)
	TETA	Easily absorbed; Causes mild adverse reactions.	Patients who cannot tolerate D- PCA.	(*40-43*)
	Tetrathiomolybdate (TM)	Promotes copper excretion; Causes mild adverse reactions. Not suitable for long-term use.	Suitable for neurological symptoms, not suitable for long-term treatment.	(*44-46*)
	Zn	Promotes copper excretion.	Treatment of asymptomatic disease and maintenance therapy after the use of copper chelating agents.	(*41*)
Chinese medicine	Gandou Decoction Shugan; Lidan Paidu Decoction	Adjuvant therapy; Not as effective as D-PCA and Na-DMPS; Causes mild adverse reactions; Can be used concomitantly with Western medicine.	Mild and moderate patients.	(*41,47-52*)

DMSA, dimercaptosuccinic acid; D-PCA, D-penicillamine; Na-DMPS, sodium dimercaptosuccinate; TETA, triethylene tetramine; TM, tetrathiomolybdate; WD, Wilson's disease.

has suggested that multiple allele-specific PCR be used to screen for WD (*5*).

5. Treatment

5.1. *D-PCA*

Early and lifelong treatment is the key to the treatment of WD (*5*). WD is mainly treated with Western medicine, surgery, hemodialysis, gene therapy, or cell transplantation (Table 1). Patients with WD have copper deposits and copper is mainly taken in through food, so a low copper diet (such as rice, wheat flour, corn, milk, eggs, white radish, poultry, beef, and rabbit) is second-line treatment after first-line treatment (*38*). Foods high in copper like shellfish, nuts, beans, chocolate, and whole grains should be avoided (*23*). A high protein diet should be consumed because the increased excretion of amino acids can increase urinary excretion, thereby reducing the deposition of copper. Drug therapy is mainly excessive copper chelation (*5*).

D-PCA is the drug of choice for treatment of WD since it can chelate copper *in vivo*, promote its excretion, and effectively reduce the severity of disease. D-PCA has the advantage of inducing a high level of urinary copper excretion, but copper is excreted slowly. Therefore, D-PCA is not suitable for patients with severe or advanced WD. If D-PCA is administered over a prolonged period, adverse reactions are not uncommon, including neurological deterioration, early symptoms of gastrointestinal diseases and allergic reactions, leukopenia, thrombocytopenia, hemolytic anemia, and autoimmune diseases (*39*). When D-PCA is administered to mice, levels of both hydroxyl radicals and free copper in the striatum increase, which may lead to deterioration of the nervous system, so D-PCA should be used with caution. D-PCA is contraindicated for patients with severe neurological symptoms, and especially patients with muscle stiffening. The most serious adverse reaction is anaphylaxis, which is evident as a fever and rash over the first few days. Use of PCA should immediately be halted when a serious adverse reaction occurs (*5*). Similarly, D-PCA should not be administered to patients with liver disease since it will increase the burden on the liver, which may lead to temporary signs of early treatment. Given the impact of adverse reactions and neurological deficits during initial treatment, 20-50% patients may be affected, though those impacts are sometimes irreversible. Some experts contend that PCA should not be the drug of choice for treatment of WD (*40*). In China, however, D-PCA is still the drug of choice because of its effectiveness, prevalence, and low price (*5*).

5.2. *Dimercaptosuccinic acid (DMSA) and sodium dimercaptosuccinate (Na-DMPS)*

DMSA is a broad-spectrum metal antidote and an alternative to maintenance therapy. DMSA was the first drug used to treat WD in China (*5*). Dimercaptopropanol results in a lower level of urinary copper and causes more severe adverse effects than other drugs, so its use

has been discontinued (*41*). Na-DMPS is low in toxicity, but it is ill-suited for patients with advanced WD and critically ill patients. Calcium disodium edetate ($CaNa_2$-EDTA) has a low toxicity, but zinc and iron are easier to chelate than copper, so $CaNa_2$-EDTA causes excretion of a small amount of copper in urine (*4*). DMSA and Na-DMPS are recommended for patients with neurological and psychiatric symptoms, mild to moderate hepatic symptoms, and patients who cannot tolerate D-PCA. Use of DMSA and Na-DMPS is particular to China. Because these drugs are not mentioned in studies of liver disease published by the American Society for Liver Disease Research (*42*) and the European Research Association (*14*). Hu *et al*. conducted a clinical study using several heavy metal poisoning antidotes (GSH, DMS, EDTA, DMPS, PCA, and DMSA) to treat WD (*43*). PCA was the most effective oral preparation, followed by DMSA, while DMPS was the most effective injection, followed by DMS and $CaNa_2$-EDTA (glutathione (GSH) was only mildly effective).

5.3. *Tetrathiomolybdate*

Tetrabromomolybdate (TM) can bind to free copper in serum and food (*4*). The use of PCA can aggravate neurological symptoms in patients with severe symptoms (*44*). However, TM rarely causes further or irreversible nerve damage. Brewer *et al*. treated 55 patients with WD in the brain (*45*), and only two had worsening neurological symptoms. As a result, some experts recommend using TM without PCA to treat WD, and TM is considered to be a fast drug that causes relatively mild adverse reactions. However, excessive amounts of molybdenum are toxic, and therefore TM is not used in long-term maintenance therapy (*46*).

5.4. *Zinc*

Zn has been recognized as an effective adjuvant to reduce copper absorption in patients with WD. Yang used oral zinc sulfate or zinc gluconate to treat patients with WD and found that urinary copper excretion increased significantly (*41*). When patients used zinc sulfate as part of maintenance therapy, their clinical symptoms improved significantly in the third year of follow-up. A study in the US indicated that Zn has good clinical efficacy in asymptomatic patients and preclinical patients and in the maintenance phase after the use of copper chelators (*10*).

5.5. *Traditional Chinese medicine*

As adjuvant therapy, Chinese medicine can promote copper excretion in bile, feces, and urine (*4*). Suitable Chinese medicines include Gandou Decoction (*41*), Shugan Lidan Paidu Decoction (*47*), Xiaoyao Powder (*48*), Chaihuang Gandou Powder (*49*), Bushen Jianpi Decoction (*50*), and Gandou De-Copper Pills (*51*). Xue *et al*. found that DMPS and Gaudou Decoction can improve liver function and delay the progression of liver fibrosis by indirectly enhancing the degradation of metalloproteinase-1 in the extracellular matrix. A systematic review of nine randomized controlled trials indicated that Gaudou Decoction appears to be effective, safe, and well-tolerated as a single therapy or adjuvant therapy (*52*).

5.6. *Surgery*

Surgery mainly involves a splenectomy and orthotopic liver transplantation (OLT). The former can treat patients with WD who have severe spleen hyperactivity (*53*). OLT is suitable for decompensated liver disease or "refractory" disease that cannot be alleviated by medication alone. OLT is the only viable option for patients with WD and fulminant liver disease (FHF) or abdominal problems. However, OLT is not suitable for patients with neurological symptoms alone because long-term neurological damage cannot be alleviated by transplantation (*40*). Although OLT is an effective treatment, surgery is a risk and immunosuppression is painful. Although OLT results in greater long-term excretion of copper, it is extremely costly (*4*).

5.7. *Cell transplantation*

Cell transplantation mainly includes hepatocyte transplantation and stem cell transplantation. Hepatocyte transplantation has become the treatment of choice for abnormal liver metabolism and genetic disorders in recent years. "*In vitro*" gene therapy involves transferring a gene from a donor into the body of a recipient. Compared to "*in vivo*" gene therapy, "*in vitro*" gene therapy has the advantages of little risk and ease. However, mature hepatocytes are highly differentiated somatic cells. Their proliferation capacity is limited and *in vitro* proliferation is particularly difficult. In addition, immune rejection is a possibility (*4*). However, stem cell transplantation can solve this problem. In stem cell transplantation, hepatocytes and bile duct cells can be obtained from bone marrow cells. Stem cells can be obtained from donor bone marrow or peripheral blood and they have greater ability to proliferate than hepatocytes. In addition, stem cells can also differentiate into neurons and other cells, so they may have a therapeutic effect on the neurological symptoms of WD. An animal study has indicated that gene therapy and cell transplantation can eventually restore copper homeostasis and reverse liver disease (*54*), suggesting that cell transplantation is the preferable option.

5.8. *Hemodialysis*

Hemodialysis can reduce the level of copper in patients

with WD in a short period of time and it can also remove other toxic substances. It can be used in patients with severe or end-stage WD (*4*).

5.9. *Genetic counseling*

Genetic counseling is also important. Although heterozygous carriers of defective genes are asymptomatic, they will pass a defective gene to their offspring if they marry someone who has similar symptoms. Twenty-five percent of children of heterozygous carriers are normal, 50% are asymptomatic, and 25% develop WD (*23*).

Symptomatic treatment and rehabilitation training are also indispensable. A daily change in symptoms can also enable patients to actively participate in social activities.

6. Conclusion

At present, the prevalence of WD is higher in China than in other countries, and research has made less progress than it has abroad. Early identification, diagnosis, and preemptive treatment of WD are critical to improving patient outcomes (*1*). A combination of traditional Chinese medicine and Western medicine is the best way to treat WD. An individualized treatment program has been put into practice to study the relationship between the genotype and phenotype of WD, but this is far from enough (*5*). Therefore, appropriate treatments need to be studied and developed specifically for Chinese patients with WD.

Acknowledgements

This work was supported by the Innovation Project of the Shandong Academy of Medical Sciences.

References

1. Hahn SH. Population screening for Wilson's disease. Ann N Y Acad Sci. 2014; 1315:64-69.
2. Bandmann O, Weiss KH, Kaler SG. Wilson's disease and other neurological copper disorders. Lancet Neurol. 2015; 14:103-113.
3. Cheng YL. Hepatolenticular degeneration (pseudosclerosis, progressive lenticular degeneration and torsion spasm) review of literature and report of two cases. Chin Med J. 1932; 46:347-364.
4. Li WJ, Wang JF, Wang XP. Wilson's disease: Update on integrated Chinese and Western medicine. Chin J Integr Med. 2013; 19:233-240.
5. Xie JJ, Wu ZY. Wilson's Disease in China. Neurosci Bull. 2017; 33:323-330.
6. Hedera P. Update on the clinical management of Wilson's disease. Appl Clin Genet. 2017; 10:9-19.
7. Dong Y, Ni W, Chen WJ, Wan B, Zhao GX, Shi ZQ, Zhang Y, Wang N, Yu L, Xu JF, Wu ZY. Spectrum and classification of *ATP7B* variants in a large cohort of Chinese patients with Wilson's disease guides genetic diagnosis. Theranostics. 2016; 6:638-649.
8. Roberts EA, Schilsky ML, American Association for Study of Liver Diseases (AASLD). Diagnosis and treatment of Wilson disease: An update. Hepatology. 2008; 47:2089-2111.
9. Zhang YD, Yang RM. Therapeutic assessment of dimercaptosuccinic acid capsule in the treatment of hepatolenticular degeneration. New Drugs Clin Rem. 1990; 9:73-76.
10. Brewer GJ, Dick RD, Johnson VD, Brunberg JA, Kluin KJ, Fink JK. Treatment of Wilson's disease with zinc: XV longterm follow-up studies. J Lab Clin Med. 1998; 132:264-278.
11. Sternlieb I, Scheinberg IH. Prevention of Wilson's disease in asymptomatic patients. N Engl J Med. 1968; 278:352-359.
12. Bachmann H, Lössner J, Gruss B, Ruchholtz U. The epidemiology of Wilson's disease in the German Democratic Republic and current problems from the viewpoint of population genetics. Psychiatr Neurol Med Psychol (Leipz). 1979; 31:393-400.
13. Saito T. An assessment of efficiency in potential screening for Wilson's disease. J Epidemiol Community Health. 1981; 35:274-280.
14. Park RH, McCabe P, Fell GS, Russell RI. Wilson's disease in Scotland. Gut. 1991; 32:1541-1545.
15. Reilly M, Daly L, Hutchinson M. An epidemiological study of Wilson's disease in the Republic of Ireland. J Neurol Neurosurg Psychiatry. 1993; 56:298-300.
16. Lo C, Bandmann O. Epidemiology and introduction to the clinical presentation of Wilson disease. Handb Clin Neurol. 2017; 142:7-17.
17. Coffey AJ, Durkie M, Hague S, *et al*. A genetic study of Wilson's disease in the United Kingdom. Brain. 2013 May; 136(Pt 5):1476-1487.
18. Coffey AJ, Durkie M, Hague S, *et al*. A genetic study of Wilson's disease in the United Kingdom. Brain. 2013; 136(Pt 5):1476-1487.
19. Cheng N, Wang K, Hu W, Sun D, Wang X, Hu J, Yang R, Han Y. Wilson disease in the South chinese han population. Can J Neurol Sci. 2014; 41:363-367.
20. Mak CM, Lam CW, Tam S, *et al.* Mutational analysis of 65 Wilson disease patients in Hong Kong Chinese: Identification of 17 novel mutations and its genetic heterogeneity. J Hum Genet. 2008; 53:55-63.
21. Park HD, Ki CS, Lee SY, Kim JW. Carrier frequency of the R778L, A874V, and N1270S mutations in the *ATP7B* gene in a Korean population. Clin Genet. 2009; 75:405-407.
22. Zhang YC. Research on hepatolenticular degeneration over the past 10 years. Zhonghua Shen Jing Jing Shen Ke Za Zhi. 1959; 5:326-327. (in Chinese)
23. Veharanta T, Immonen P. Hepatolenticular degeneration, Wilson's disease. Duodecim. 1981; 97:743-745.
24. Lin LJ, Wang DX, Ding NN, Lin Y, Jin Y, Zheng CQ. Comprehensive analysis on clinical features of Wilson's disease: An experience over 28 years with 133 cases. Neurol Res. 2014; 36:157-163.
25. Cope-Yokoyama S, Finegold MJ, Sturniolo GC, Kim K, Mescoli C, Rugge M, Medici V. Wilson disease: histopathological correlations with treatment on follow-up liver biopsies. World J Gastroenterol. 2010; 16:1487-1494.
26. Huo LJ, Liao RD, Chen XM. Ophthalmic manifestations of Wilson's disease. Zhonghua Yan Ke Za Zhi. 2008;

44:128-130. (in Chinese)
27. European Association for Study of Liver. EASL clinical practice guidelines: Wilson's disease. J Hepatol. 2012; 56:671-685.
28. Li XH, Lu Y, Ling Y, Fu QC, Xu J, Zang GQ, Zhou F, De-Min Y, Han Y, Zhang DH, Gong QM, Lu ZM, Kong XF, Wang JS, Zhang XX. Clinical and molecular characterization of Wilson's disease in China: Identification of 14 novel mutations. BMC Med Genet. 2011; 12: 6.
29. Quemeneur AS, Trocello JM, Ea HK, Ostertag A, Leyendecker A, Duclos-Vallée JC, de Vernejoul MC, Woimant F, Lioté F. Bone status and fractures in 85 adults with Wilson's disease. Osteoporos Int. 2014; 25:2573-2580.
30. Rodriguez Nieva N, Febrer Rotger A, Meléndez Plumed M, Vernet Bori A. Osteoarthropathy in three siblings with Wilson's disease. An Pediatr (Barc). 2004; 61:181-184. (in Spanish)
31. Golding DN, Walshe JM. Proceedings: The musculoskeletal features of Wilson's disease: A clinical, radiological, and serological survey. Ann Rheum Dis. 1975; 34:201.
32. Hegedus D, Ferencz V, Lakatos PL, Meszaros S, Lakatos P, Horvath C, Szalay F. Decreased bone density, elevated serum osteoprotegerin, and beta-cross-laps in Wilson disease. J Bone Miner Res. 2002; 17:1961-1967.
33. Xie YZ, Zhang XZ, Xu XH, Zhang ZX, Feng YK. Radiologic study of 42 cases of Wilson disease. Skelet Radiol. 1985; 13:114-119.
34. Filippi C, Dhawan A. Current status of human hepatocyte transplantation and its potential for Wilson's disease. Ann N Y Acad Sci. 2014; 1315:50-55.
35. Walshe JM. Particularization degeneration (Wilson's disease). Br Med Bull. 1957; 13:132-135.
36. Bembenek JP, Kurczych K, Członkowska A. TMS-induced motor evoked potentials in Wilson's disease: A systematic literature review. Bioelectromagnetics. 2015; 36:255-266.
37. Huang F, Liang X, Xu P, Lin Z, Zhou X, Wang Y, Hou G, Cheng G. Using fluorescence PCR analysis for early diagnosis and carriers detection of Chinese Wilson's disease. Zhonghua Yi Xue Yi Chuan Xue Za Zhi. 2001; 18:17-20. (in Chinese)
38. Zhao YZ, Zhao LH, Wu B. Treatment of Wilson disease integrated traditional Chinese and Western medicine. Chin J Birth Health Heredity. 2006; 14:95-96. (in Chinese)
39. Yang RM. Treatment of hepatolenticular degeneration with integrated traditional Chinese and Western medicine. Chin J Integr Tradit West Med. 2007; 27:773-775. (in Chinese)
40. Ala A, Walker AP, Ashkan K, Dooley JS, Schilsky ML. Wilson's disease. Lancet. 2007; 369:397-408.
41. Wang XP, Zhang WF, Huang HY, Preter M. Neurology in the People's Republic of China – An update. Eur Neurol. 2010; 64:320-324.
42. Roberts EA, Schilsky ML. A practice guideline on Wilson disease. Hepatology. 2003; 37:1475-1492.
43. Hu JY, Yang RM, Han YZ, Hong MF, Wang X, Li K, Wenbin HU. The clinical study of six antidotes against heavy metal poisoning in Wilson's disease. Anhui Med J. 2004; 25:361-365. (in Chinese)
44. Medici V, Trevisan CP, D'Incà R, Barollo M, Zancan L, Fagiuoli S, Martines D, Irato P, Sturniolo GC. Diagnosis and management of Wilson's disease: Results of a single center experience. J Clin Gastroenterol. 2006; 40:936-941.
45. Brewer GJ. Neurologically presenting Wilson's disease: Epidemiology, pathophysiology and treatment. CNS Drugs. 2005; 19:185-192.
46. Brewer GJ. Tetrathiomolybdate anticopper therapy for Wilson's disease inhibits angiogenesis, fibrosis and inflammation. J Cell Mol Med. 2003; 7:11-20.
47. Wang DH, Chen JL, Yuan XS. Clinical observation on the effect of Shugan Lidan Paidu Decoction on 38 patients with Wilson disease. J Tradit Chin Med. 2009; 50:142-144. (in Chinese)
48. Li XF, Zhang R, Li WH. Thirty cases of Wilson disease treated by modified Xiaoyao Powder combined with acupuncture and penicillamine. Hebei J Tradit Chin Med. 2011; 33:205-206. (in Chinese)
49. Chen JL, Wang DH. Clinical observation on the effect of Chaihuang Gandou Powder on 59 patients with Wilson disease. J Sichuan Tradit Chin Med. 2010; 28:72-74. (in Chinese)
50. Tan ZH, Cheng JM. Thirty-two cases of Wilson Disease treated by Bushen Jianpi Decoction. J Hubei Tradit Chin Med. 2008; 30:44-45. (in Chinese)
51. Xu JP, Li YL, Zhang ZP. Study of the curative effect of Gandou De-Copper Pills in the treatment of Wilson disease. Practical J Integr Tradit West Med. 1997; 10:1242-1243. (in Chinese)
52. Xue BC, Yang RM, Hu JY. Effect of Gandou Decoction IV combined with short-term decoppering therapy with sodium dimercapto-sulphonate on serum indexes of hepatic fibrosis in patients with Wilson's disease. Zhongguo Zhong Xi Yi Jie He Za Zhi. 2007; 27:785-788. (in Chinese)
53. Huang F, Yu ZG, Liang XL. Treatment of Wilson's disease and splenosis: Analysis of splenectomy specimens from 16 cases. Chin J Nervous Mental Dis. 2000; 26: 6-8. (in Chinese with English abstract)
54. Merle U, Encke J, Tuma S, Volkmann M, Naldini L, Stremmel W. Lentiviral gene transfer ameliorates disease progression in Long-Evans cinnamon rats: An animal model for Wilson disease. Scand J Gastroenterol. 2006; 41:974-982.

(Received August 17, 2017; Revised November 18, 2017; Accepted November 24, 2017)

Mini-Review

DOI: 10.5582/irdr.2017.01049

Infection after total knee arthroplasty and its gold standard surgical treatment: Spacers used in two-stage revision arthroplasty

Junren Lu, Jing Han, Chi Zhang*, Yi Yang, Zhenjun Yao

Orthopedic Surgery, Zhongshan Hospital affiliated with Fudan University, Shanghai, China.

Summary **Periprosthetic joint infection (PJI) is one of the most devastating postoperative complications of total knee arthroplasty (TKA). Treatment varies depending on the type of infection, but two-stage revision arthroplasty using an antibiotic spacer is considered to be the gold standard of treatment. Several types of spacers are available at the moment, each with different benefits and indications, and these spacers may be improved in the future. The primary goals of selecting a given spacer are to locally deliver antibiotics and to preserve soft tissue. Use of an appropriate spacer subsequently decreases the difficulty of the second revision, the operating time, and ultimately the risk of postoperative complications.**

Keywords: Total knee arthroplasty (TKA), infection, diagnosis, treatment, spacer

1. Introduction

Total knee arthroplasty (TKA), also known as total knee replacement (TKR), is one of the more common and successful orthopedic joint surgeries performed to treat degenerative diseases of the knee (*1-3*). The procedure is commonly performed on patients with severe osteoarthritis, rheumatoid arthritis, or pigmented villonodular synovitis with the main aim of relieving pain and joint dysfunction. Degenerative changes in the knee commonly occur in the elderly, though those changes are increasingly prevalent in younger patients due to changes in lifestyle. The procedure itself involves significant postoperative pain and involves a period of rigorous postoperative rehabilitation. Rehabilitation takes around 6 weeks and involves the use of mobility aids such as a walker, crutches, or a cane to compensate for the diminished weight-bearing capacity of the treated limb (*4*).

Several postoperative complications can occur after TKA, including deep vein thrombosis, fractures of the femoral shaft or periprosthetic fractures, loss of limb motion, knee instability, and postoperative infection, and these complications all affect the overall success of TKA in different ways (*5*). Postsurgical prosthesis-related infections are rare but nonetheless one of the most devastating postoperative complications (*6*). Numerous factors contribute to the rate of infection; despite the development of infection control, rates of infection are still as high as 3% (*6-8*).

2. Diagnosis

At present, there are no optimal criteria for diagnosis of a periprosthetic joint infection (PJI) after TKA (*9*). An accepted definition of PJI is based on the fulfilment of one of two major criteria: two positive periprosthetic cultures with phenotypically identical organisms and/or the presence of a sinus tract communicating with the prosthesis. PJI is also diagnosed if three of six minor criteria are fulfilled (Table 1): an elevated level of serum C-reactive protein (CRP) and an increased erythrocyte sedimentation rate (ESR), an elevated synovial fluid white blood cell count (WBC), changes on a leukocyte esterase test strip, an increased percentage of synovial fluid polymorphonuclear neutrophils (PMN%), or a single positive result from histological analysis of periprosthetic tissue (*9*).

PJI after TKA primarily presents as symptoms and signs of infection (*6-7,10-11*). These include pain in the affected knee joint, swelling, erythema, effusion, signs of inflammation, and persistent drainage after TKA.

Released online in J-STAGE as advance publication October 24, 2017.

**Address correspondence to:*
Dr. Chi Zhang, Department of Orthopaedic Surgery, Zhongshan Hospital of Fudan University, 180 Fenglin Road, Xuhui District, Shanghai 200032, China.
E-mail: zhang.chi@zs-hospital.sh.cn

Table 1. Threshold values for the minor criteria used to diagnose acute and chronic PJI, as proposed by the International Consensus Group on Periprosthetic Joint Infection (*10*).

Criterion	Acute PJI (< 90 days)	Chronic PJI (> 90 days)
C-Reactive Protein (CRP, mm/hr)	No definite threshold was determined	30
Erythrocyte Sedimentation Rate (ESR, mm/hr)	100	10
Synovium White Blood Cell (WBC) Count (cells/μL)	10,000	3,000
Synovium Fluid Polymorphonuclear Neutrophils (PMN%)	90	80
Leukocyte Esterase	+ or ++	+ or ++
Histological Analysis of Tissue	> 5 neutrophils per high power field in 5 high-power fields (×400)	> 5 neutrophils per high-power field in 5 high-power fields (×400)

These symptoms are accompanied by a limited range of motion (ROM) beyond what is normally expected after primary TKA. Symptoms of pain and a limited ROM differ from regular postoperative pain or lingering pain and are indications of infection.

Radiological findings may also aid in diagnosing PJI (*6-7*). Late-stage findings such as periosteal bone formation, scattered foci of osteolysis, and subchondral bone formation suggest the presence of a postoperative infection. The presence of a radiolucent zone around the prosthesis is not usually present in acute infections but is present in chronic infections (*6-7*). This particularly aids in assessing the stability of the implant and ultimately determining the method of treatment. Nuclear imaging is particularly useful in the diagnosis of PJI as its results are not affected by the metallic prosthesis. An example of an imaging technique is the triple-phase technetium-99 bone scan (TBPS), which is widely used to identify bone remodelling around the prosthesis (*6*). A major disadvantage of TBPS is that it is unable to distinguish between a septic knee and aseptic loosening of the implant. Fluro-deoxyglucose positron emission tomography (FDG-PET) is another nuclear modality used to diagnose PJI (*6*). Inflammatory cells express a high amount of glucose transporters, causing an excess of deoxyglucose that cannot be metabolized by cells and that can be identified by a scanner (*12*). Although expensive, FDG-PET has been reported to have a sensitivity of 91% and a specificity of 72% in the diagnosis of PJI, and results can be obtained relatively soon after the examination is finished (*13*).

Numerous treatment options are available for the management of PJI, but revision surgery is regarded as the best method of treatment (*6-7,10-11*). Revision can be performed either in one or two stages. Two-stage revision arthroplasty is regarded as the gold standard for treatment of PJI of the knee (*10*). Unlike one-stage revision, two-stage revision requires the patient to undergo surgical treatment in two stages and the usage of an interim spacer. Numerous studies have reported that two-stage revision is more successful at controlling infection (*14-19*).

At present, several versions of antibiotic spacers are available. These spacers fall into three categories: (*i*) a spacer made of antibiotic-loaded bone cement over an endoskeleton or a standard prosthesis (*ii*), a spacer made from cement molded intraoperatively (*iii*), and prefabricated commercial spacers. These spacers are divided into articulating spacers (spacers allowing a degree of limb motion in between revision surgeries) and static spacers (spacers that immobilize the lower limb in between the two revision surgeries). In two-stage knee revision, the articulating interface can be cement-on-cement, cement-on-polyethylene, or cement-on-metal (*7-8*).

3. Procedure

Two-stage revision surgery is regarded as the golden standard for the treatment for PJI. This procedure can involve the use of static or articulating spacers. Numerous studies have reported that two-stage revision surgery and articulating spacers can result in a rate of infection control as high as 95% in patients with PJI (*6-7,10-11*). Hart *et al*. reported that using this procedure has a success rate of 87.5% even when including patients who have undergone multiple surgeries (*20-21*).

The first stage of the revision involves a complete debridement of all lingering sources of infection in the affected joint cavity. This includes the prosthesis used in the primary TKA, cement, and inflamed tissue within the joint cavity. An antibiotic-loaded cement is chosen over regular bone cement to provide high doses of antibiotics, usually both vancomycin and gentamycin or tobramycin, that are locally eluted within the joint cavity. This cement is used in accordance with postsurgical intravenous antibiotics that are tailored to the pathogen causing the infection. The duration of antibiotic administration is continued for at least six to eight weeks until the infection is eradicated according to routine blood test results and radiological findings. Then patients are eligible to undergo the second surgery.

Other methods of surgical treatment have their own indications and rate of infection control. Debridement and irrigation is reported to have a success rate varying from 16-80%, but this particular procedure is limited to acute infections, in which the infected prosthesis is not removed (*22-24*). One-stage revision surgery is reported to have a success rate varying from 73-100% (*24-25*). However, one-stage revision surgery has a specific indication: it is performed on patients who

are unable to withstand the physical stress of multiple surgeries and on those with an infection that is caused by a single, non-resistant, non-virulent pathogen (*6-7,10*). Arthrodesis and amputation of the affected knee is usually the last result for patients who have an uncontrolled infection, life-threatening sepsis, and/or significant bone loss that cannot be corrected surgically. Arthrodesis and amputation is not usually chosen and results in an overall decrease in the patient's quality of life (*6-7,10*).

4. Types of spacers

4.1. *Static spacers*

Use of a static spacer involves the immobilization of the affected leg knee during revision surgeries. This proves to be its main disadvantage but a static spacer is particularly suitable in situations where patients present with a severe infection with obvious swelling of the soft tissues (*27-28*). The local delivery of antibiotics provides a stable localized concentration of the antibiotics used in the bone cement. Preservation of the joint space and infection control are required for future revision treatment.

As mentioned earlier, static spacers are used when patients present with a severe uncontrolled infection or when patients have ligamentous instability, insufficient extensor mechanisms, a compromised soft tissue layer over the joint, or severe bone loss after removal of the prosthesis implanted during primary TKA.

A study has reported that the main advantages of static spacers are that they provide better relief for patients with infected and congested tissues and that they cost significantly less than articulating spacers (*28*). However, other studies have reported that static spacers yield poor postoperative limb mobility compared to articulating spacers (*6,27-28*). A study by Emerson *et al*. compared patients who underwent revision surgery using a static spacer to those who underwent that surgery using articulating spacers (*29*), and the study found no marked differences in infection control for static spacers (7.7%, 2 out of 26 knees) and articulating spacers (9.1%, 2 out of 22 knees) (P = 0.8). However, the study did find marked difference in limb mobility outcomes after the second revision: static spacers resulted in an ROM of 93.7° and articulating spacers resulted in an ROM of 107.8°. A systematic review by Voleti *et al*. compared the results of using static and articulating spacers in revision treatment and it noted similar results (*30*). Voleti *et al*. analyzed a combination of level III and level IV studies that involved a total 1,526 patients. Static spacers were used to treat 654 patients and articulating spacers were used to treat 857. None of the reviewed studies noted any marked difference in infection control (12% for static spacers and 8% for articulating spacers), but they did note significant differences in the postoperative ROM (91° for static spacers and 101° for articulating spacers).

4.2. *Articulating spacers*

The main advantage of articulating spacers is that they allow motion of the affected knee in between revision surgeries. This further facilitates recovery of limb function, as patients can continue to move the affected knee even when an interim spacer is used. As with static spacers, articulating spacers also maintain the joint space and provide a local effusion of antibiotics.

There are no apparent contraindications to the usage of articulating spacers. A review by Mazzucchelli *et al*. reported that articulating spacers may not be used in cases where patients are found to have inadequate soft tissue cover over the knee since it may lead to problems with wound healing (*28*). Numerous studies have also reported that spacer fractures are a common postoperative complication of using articulating spacers (*31-32*). Prefabricated commercial spacers may prove to be problematic in cases of severe bone loss after removal of the primary prosthesis. In such cases, static spacers should be chosen.

Articulating spacers have been found to result in a greater postoperative ROM with the same rate of infection control (*28*). These are several factors for this better outcome, though the main one is the preservation of the length and elasticity of extensor mechanisms. Ambulation in between revision surgeries also prevents tissue scarring around the knee, quadriceps shortening, and capsular thickening and contracture (*28,33*). This subsequently facilitates future revision surgeries by reducing surgical exposure and the overall difficulty of revision (*34-35*). Several versions of articulating spacer interfaces are presently available: cement-on-cement, cement-on-polyethylene, and metal-on-polyethylene.

4.2.1. *Articulating spacers with a cement-on-cement interface*

An antibiotic-loaded acrylic cement is used to fabricate both the femoral and tibial components. Cement-on-cement spacers are basically fabricated by a surgeon or prefabricated. The spacers typically consist of antibiotic-loaded bone cement, and vancomycin and tobramycin or gentamycin are usually added. Molds of different sizes are used to form the femoral and tibial components with the antibiotic mixture serving as the base. Antibiotics are added without exceeding 10% of the total weight of the bone cement to keep from compromising the structural integrity of the spacer (*36-37*).

In a study of 24 patients, Durbhakula *et al*. used custom molds to fabricate both the femoral and tibial components (*38*). Durbhakula *et al*. used antibiotic spacers loaded with 2.4 g of tobramycin and 1.0 g of vancomycin. Postoperative follow-up was conducted for up to 33 months. Postoperative ROM was found

to be 104°. A study of similar hand-made spacers by Villanueva-Martínez *et al*. reported that ROM was an average of 80° and that there were reinfections at 5 years (*31*).

An example of a commercial prefabricated spacer is the Interspace Knee temporary knee spacer (Exatech, Gainesville, FL. USA, sold as the Spacer-K (Tecres, Verona, Italy) in Europe). This spacer has been approved by the US Food and Drug Administration (FDA) for use in the treatment of PJI in two-stage revision surgeries (*27*). However, the antibiotic component of the Interspace Knee spacer has proven to be a major disadvantage (*39*). The spacer is available in three sizes with gentamycin dosages ranging from 0.8 g to 1.7 g, which is significantly lower than the suggested dosage of 3.6 g antibiotic per 40 g of bone cement. Another prefabricated gentamycin/vancomycin-loaded cement spacer (Spacer-K® or Vancogenx-Space Knee®, Tecres, Sommacampagna, Italy) is also available. This spacer is available in four sizes: small, medium, large, and extra-large (60-, 70-, 80- and 90-mm tibial plateau dimensions, respectively). These spacers are also pre-loaded with antibiotics by the manufacturer.

A variation on this type of spacer involves the addition of a prosthetic stem into both the tibial and femoral intramedullary canals. The prosthetic stem is fabricated using 3 mm K-wires that are then coated with an antibiotic cement mixture. Only the proximal part of the stem and the prosthesis component are fixed onto the bone surface.

4.2.2. *Articulating spacers with a cement-on-polyethylene interface*

In a study of 28 patients, Evans *et al*. used 40 g of Palacos R cement (Zimmer) along with 4.8 g of tobramycin and 4.0 g of vancomycin to fabricate articulating cement spacers (*40*). The cement spacer was either hand-made or prepared using a disposable mold. A stemmed, posterior-stabilized, polyethylene femoral component was coated with the prepared cement mixture and implanted as an interim spacer. Evans *et al*. obtained a success rate of up to 75% in the knees that were operated on. Few studies have described the use of this type of spacer, and the overall feasibility of this type of spacer needs to be studied further.

A possible benefit of this type of spacer is the omission of the tibial component, thus reducing operating time and surgical difficulty. A shorter operating time increases the overall success of this method of treatment.

4.2.3. *Articulating spacers with a metal-on-polyethylene interface*

The earliest record of a procedure using these spacers is a review by Hofmann *et al.* in 1995 (*41*). A study of 26 patients with PJI performed two-revision arthroplasty using a spacer with a cement-on-polyethylene interface. An articulating spacer is fabricated by autoclaving the removed component. The re-sterilized femoral component is reinserted during the same surgery. The femoral component articulates with a new polyethylene-tibial component instead of a tibial component made of regular cement. A polyethylene patellar component with pegs removed is used in 40% of the patients. The antibiotic cement used was Simplex-P cement (Howmedica, Rutherford, NJ) along with tobramycin, mixed at a ratio of 4.8 g of tobramycin to 40 g of cement. This method of cement preparation is used to fabricate the femoral, patellar, and polyethylene inserts for the tibial component.

In a study of 26 patients by Hoffman *et al*. (*41*), reimplantation was successful in all but one patient who died of non-spacer related complications. The overall follow-up for those patients was 31 months (range: 12-70 months). None of the patients had poor results, and 72% of the patients had excellent results. Postoperative ROM increased an average of 30° in terms of the arc of motion. No problems with wound healing, deep vein thrombosis, or pulmonary emboli were noted.

PROSTALAC® (prosthesis with antibiotic-loaded acrylic cement, DePuy Synthes, Warsaw, IN) is a commercial prefabricated spacer with a metal-on-polyethylene interface that has been available since 1987. The spacer consists of tibial and femoral components, both consisting of antibiotic-loaded cement, along with a bicondylar metal shell on the femoral component and a complementary polyethylene insert on the tibial component. The spacer is available in different sizes and thicknesses (*42*).

5. Conclusion

Numerous versions of arthroplasty spacers are available for clinical use. At present, there is no clear consensus on the best way to select a spacer. There are no apparent differences in infection control by static and articulating spacers, but numerous studies have found that articulating spacers yield a greater postoperative ROM. Numerous aspects must be considered to determine which type of articulating spacer will be appropriate. Patient age, severity of infection, and even cost must be included in that determination. In general, the main purpose of using a spacer in revision TKA is for effective infection control.

References

1. Van M, Nace J, Mont MA. Management of primary knee osteoarthritis and indications for total knee arthroplasty for general practitioners. J Am Osteopath Assoc. 2012; 112:709-715.
2. Pagnamo MW, Clarke HD, Jacofsky DJ, Amendola A, Repicci JA. Surgical treatment of the middle-aged patient

with arthritic knees. Instr Course Lect, 2005; 54:251-259.
3. Ringdahl E, Pandit S. Treatment of knee osteoarthritis. Am Fam Physician. 2011; 83:1287-1292.
4. Leopold SS. Minimally invasive total knee arthroplasty for osteoarthritis. N Engl J Med. 2009; 360:1749-1758.
5. Tayton ER, Frampton C, Hooper GJ, Young SW. The impact of patient and surgical factors on the rate of infection after primary total knee arthroplasty: An analysis of 64,566 joints from the New Zealand Joint Registry. Bone Joint J. 2016; 98-B:334-340.
6. Kalore NV, Gioe TJ, Singh JA. Diagnosis and management of infected total knee arthroplasty. Open Orthop J. 2011; 5:86-91.
7. Martínez-Pastor JC, Maculé-Beneyto F, Suso-Vergara S. Acute infection in total knee arthroplasty: Diagnosis and treatment. Open Orthop J. 2013; 7:(Suppl 2:M5)197-204.
8. Cury RP, Cinagawa EH, Camarga OP, Honda EK, Klautau GB, Salles MJ. Treatment of infection after total knee arthroplasty. Acta Ortop Bras. 2015; 23:239-243.
9. Della Valle C, Parvizi J, Bauer TW, DiCesare PE, Evans RP, Segreti J, Spangehl M, Watters WC 3rd, Keith M, Turkelson CM, Wies JL, Sluka P, Hitchcock K; American Academy of Orthopaedic Surgeons. American Academy of Orthopaedic Surgeons clinical practice guideline on: The diagnosis of periprosthetic joint infections of the hip and knee. J Bone Joint Surg Am. 2011; 93:1355-1357.
10. Chun KC, Kim KM, Chun CH. Infection following total knee arthroplasty. Knee Surg Relat Res. 2013; 25:93-99.
11. de Carvalho LH, Tempon EF, Badet R. Infection after total knee replacement: Diagnosis and treatment. Rev Bras Ortop. 2013; 24:389-396.
12. Zhuang H, Duarte PS, Pourdehnad M, Maes A, Van Acker F, Shnier D, Garino JP, Fitzgerald RH, Alavi A. The promising role of 18F-FDG PET in detecting infected lower limb prosthesis implants. J Nucl Med. 2001;42:44-48.
13. Reinartz P. FDG-PET in patients with painful hip and knee arthroplasty: Technical breakthrough or just more of the same. Q J Nucl Med Mol Imaging. 2009; 53:41-50.
14. Sayeed Z, Anoushiravani AA, El-Othmani MM, Chambers MC, Mihalko WM, Jiranek WA, Paprosky WG, Saleh JK. Two-stage revision total knee arthroplasty in the setting of periprosthetic knee infection. Instr Course Lect. 2017; 66:249-262.
15. Claassen L, Plaass C, Daniilidis K, Calliess T, von Lewinski G. Two-stage revision total knee arthroplasty in cases of periprosthetic joint infection: An analysis of 50 cases. Open Orthop J. 2015; 9:49-56.
16. Silvestre A, Almeida F, Renovell P, Morante E, López R. Revision of infected total knee arthroplasty: Two-stage reimplantation using an antibiotic-impregnated static spacer. Clin Orthop Surg. 2013; 5:180-187.
17. Kini SG, Gabr A, Das R, Sukeik M, Haddad FS. Two-stage revision for periprosthetic hip and knee joint infections. Open Orthop J. 2016; 10:579-588.
18. Petrie J, Sassoon A, Haidukewych G. Two-stage revision for the infected total knee arthroplasty: The gold standard. Sem Arthroplasty. 2013; 24:149-151.
19. Brunnekreef J, Hannink G, Malefijt MW. Recovery of knee mobility after a static or mobile spacer in total knee infection. Acta Orthop Belg. 2013; 79:83-89.
20. Hart WJ, Jones RS. Two-stage revision of infected total knee replacements using articulating cement spacers and short-term antibiotic therapy. J Bone Joint Surg (Br). 2006; 88:1011-1015.
21. Durbhakula SM, Czajka J, Fuchs MD, Uhl RL. Antibiotic-loaded articulating cement spacer in the 2-stage exchange of infected total knee arthroplasty. J Arthroplasty. 2004; 19:768-774.
22. Bradbury T, Fehring TK, Taunton M, Hanssen A, Azzam K, Parvizi J, Odum SM. The fate of acute methicillin-resistant Staphylococcus aureus periprosthetic knee infections treated by open debridement and retention of component. J Arthroplasty. 2009; 24(6 suppl):101-104.
23. Hartman MB, Fehring TK, Jordan L, Norton HJ. Periprosthetic knee sepsis: The role of irrigation and debridement. Clin Orthop Relat Res. 1991; 273:113-118.
24. Silva M, Tharani R, Schmalzried TP. Results of direct exchange or debridement of the infected total knee arthroplasty. Clin Orthop Relat Res. 2002; 404:125-131.
25. Buechel FF, Femino FP, D'Alessio J. Primary exchange revision arthroplasty for infected total knee replacement: A long-term study. Am J Orthop (Belle Mead NJ). 2004; 33:190-198.
26. Jamsen E, Stogiannidis I, Malmivaara A, Pajamki J, Puolakka T, Konttinen YT. Outcome of prosthesis exchange for infected knee arthroplasty: The effect of treatment approach. Acta Orthop. 2009; 80:67-77.
27. Jacobs C, Christian CP, Berend ME. Static and mobile antibiotic-impregnated cement spacers for the management of prosthetic joint infection. J Am Acad Orthop Surg. 2009; 17:356-368.
28. Mazzucchelli L, Rosso F, Marmotti A, Bonasia DE, Bruzzone M, Rossi R. The use of spacers (static and mobile) in infection knee arthroplasty. Curr Rev Musculoskelet Med. 2015; 8:373-382.
29. Emerson RH Jr., Muncie M, Tarbox TR, Higgins LL. Comparison of a static with a mobile spacer in total knee infection. Clin Orthop Relat Res. 2002; 404:132-138.
30. Voleti PB, Baldwin KD, Lee GC. Use of static or articulating spacers for infection following total knee arthroplasty: A systematic literature review. J Bone Joint Surg Am. 2013; 95:1594-1599.
31. Villanueva-Martínez M, Ríos-Luna A, Pereiro J, Fahandez-Saddi H, Villamor A. Hand-made articulating spacers in two-stage revision for infected total knee arthroplasty: Good outcome in 30 patients. Acta Orthop. 2008; 79:674-682.
32. Cui Q, Mihalko WM, Shields JS, Ries M, Saleh KJ. Antibiotic-impregnated cement spacers for the treatment of infection associated with total hip or knee arthroplasty. J Bone Joint Surg Am. 2007; 89:871-882.
33. Thabe H, Schill S. Two-stage reimplantation with an application spacer and combined with delivery of antibiotics in the management of prosthetic joint infection. Oper Orthop Traumatol. 2007; 19:78-100.
34. Hsu YC Cheng HC, Ng TP, Chiu KY. Antibiotic-loaded cement articulating spacer for 2-stage reimplantation in infected total knee arthroplasty: A simple and economic method. J Arthroplasty. 2007; 22:1060-1066.
35. Choi HR Malchau H, Bedair H. Are prosthetic spacers safe to use in 2-stage treatment for infected total knee arthroplasty? J Arthroplasty. 2012; 27:1474-1479. e1.
36. Masri BA, Duncan CP, Beauchamp CP. Long-term elution of antibiotics from bone-cement: An *in vivo* study using the prosthesis of antibiotic-loaded acrylic cement (PROSTALAC) system. J Arthoplasty. 1998; 13:331-338.
37. Koo KH, Yang JW, Cho SH, Song HR, Park HB, Ha YC, Chang JD, Kim SY, Kim YH. Impregnation of

vancomycin, gentamycin, and cefotaxime in a cement spacer for two-stage cementless reconstruction in infected total hip arthroplasty. J Arthroplasty. 2001; 16:882-892.
38. Durbhakula SM, Czajka J, Fuchs MD, Uhl RL. Antibiotic-loaded articulating cement spacer in the 2-stage exchange of infected total knee arthroplasty. J Arthroplasty. 2004; 19:768-774.
39. Jiranek WA, Hannsenn AD, Greenwald AS. Antibiotic-loaded bone cement in aseptic total joint replacement: Whys, wherefores & caveats. Presented at the 71st Annual Meeting of the American academy of Orthopaedic Surgeons, Washington, DC, February 23-27, 2005. Available online at: *http://orl-inc.com/wp-content/uploads/2016/03/ALBC-Committee-2005.pdf* (accessed August 30, 2017).
40. Evans RP. Successful treatment of total hip and knee infection with articulating antibiotic components: A modified treatment method. Clin Orthop Relat Res. 2004; 427:37-46.
41. Hofmann AA, Kane KR, Tkach TK, Plaster RL, Camargo MP. Treatment of infected total knee arthroplasty using an articulating spacer. Clin Orthop Relat Res. 1995; 321:45-52.
42. Haddad FS, Masri BA, Campbell D, McGraw RW, Beauchamp CP, Duncan CP. The PROSTALAC functional spacer in two-stage revision for infected knee replacements: Prosthesis of antibiotic-loaded acrylic cement. J Bone Joint Surg Br. 2000; 82:807-812.

(Received August 8, 2017; Revised September 25, 2017; Accepted September 28, 2017)

Original Article

DOI: 10.5582/irdr.2017.01073

Microglia express ABI3 in the brains of Alzheimer's disease and Nasu-Hakola disease

Jun-ichi Satoh[1,*], Yoshihiro Kino[1], Motoaki Yanaizu[1], Youhei Tosaki[1], Kenji Sakai[1], Tsuyoshi Ishida[2], Yuko Saito[3]

[1] *Department of Bioinformatics and Molecular Neuropathology, Meiji Pharmaceutical University, Tokyo, Japan;*
[2] *Department of Pathology and Laboratory Medicine, Kohnodai Hospital, NCGM, Chiba, Japan;*
[3] *Department of Laboratory Medicine, National Center Hospital, NCNP, Tokyo, Japan.*

Summary **Nasu-Hakola disease (NHD) is a rare autosomal recessive leukoencephalopathy caused by a loss-of-function mutation of either *TYROBP* (*DAP12*) or *TREM2* expressed in microglia. A rare variant of the *TREM2* gene encoding p.Arg47His causes a 3-fold increase in the risk for late-onset Alzheimer's disease (LOAD). A recent study demonstrated that a rare coding variant p.Ser209Phe in the ABI family member 3 (*ABI3*) gene, a regulator of actin cytoskeleton organization, confers risk of developing of LOAD, although the pattern of ABI3 expression in AD and NHD brains with relevance to microglial pathology remains to be characterized. We investigated the cell type-specific expression of ABI3 in the brains derived from four non-neurological controls (NC), ten AD and five NHD cases by immunohistochemistry. We identified an intense ABI3 immunoreactivity chiefly on a subset of microglia with ramified or amoeboid morphology located in the grey matter and the white matter of the frontal cortex and the hippocampus of NC, AD, and NHD cases. The immunolabeled area of ABI3-positive microglia was not significantly different among NC, AD, and NHD cases due to great variability from case to case. The clusters of ABI3-immunoreactive microglia were found exclusively in AD brains and they were associated with amyloid plaques. Although these observations do not actively support the view that ABI3-immunoreactive microglia play a central role in the development of leukoencephalopathy in NHD brains and the neurodegeneration in AD brains, the intense expression of ABI3 on microglia might regulate their migration under conditions of health and disease in the central nervous system (CNS).**

Keywords: ABI3, Alzheimer's disease, leukoencephalopathy, microglia, Nasu-Hakola disease

1. Introduction

Nasu-Hakola disease (NHD), also designated polycystic lipomembranous osteodysplasia with sclerosing leukoencephalopathy (PLOSL; OMIM 221770), is a rare autosomal recessive disorder, characterized by progressive presenile dementia and formation of multifocal bone cysts, caused by genetic mutations of either *TYROBP*(*DAP12*) or *TREM2* (*1*). Clinically, the patients with NHD show recurrent bone fractures during the third decade of life, and a frontal lobe syndrome during the fourth decade of life, and progressive dementia and death until the fifth decade of life (*2*). Pathologically, the brains of NHD patients exhibit extensive demyelination designated leukoencephalopathy, astrogliosis, accumulation of axonal spheroids, and remarkable activation of microglia predominantly in the white matter of frontal and temporal lobes and the basal ganglia (*3*). Although NHD patients are clustered in Japan and Finland, approximately 200 NHD cases are presently reported worldwide. TREM2 and DAP12 constitute a receptor/adaptor signaling complex expressed exclusively on osteoclasts, dendritic cells, macrophages, and microglia (*4*). It is generally supposed that a complete loss of function of the TREM2-DAP12 signaling pathway in microglia

Released online in J-STAGE as advance publication November 21, 2017.

**Address correspondence to:*
Dr. Jun-ichi Satoh, Department of Bioinformatics and Molecular Neuropathology, Meiji Pharmaceutical University, 2-522-1 Noshio, Kiyose, Tokyo, Japan.
E-mail: satoj@my-pharm.ac.jp

induces leukoencephalopathy in NHD. Thus, NHD is a primary disease of microglia termed "microgliopathy" (*5*), although the mechanisms how functionally aberrant microglia evoke leukoencephalopathy remain unknown.

Alzheimer's disease (AD) is characterized by the hallmark pathology comprised of widespread amyloid-β (Aβ) deposition, neurofibrillary tangle (NFT) formation, extensive neurodegeneration, and profound activation of microglia in the brain (*6*). The complex interaction between multiple genetic and environmental factors affecting various molecular pathways plays a key role in AD, although the precise molecular mechanism underlying AD remains largely unknown.

Microglia, resident myeloid cells in the central nervous system (CNS), play a pivotal role in maintenance of brain homeostasis, along with progression of neurodegenerative diseases (*7*). Microglia originate from erythromyeloid progenitors in the yolk sac and populate the CNS during early embryonic development (*8*). Microglia actively survey the surrounding microenvironment with dynamic processes. A battery of the genes, such as *TREM2*, *BIN1*, *ABCA7*, *PICALM*, *CASS4*, *HLA-DRB1*, *MS4A6A*, *ZCWPW1*, *INPP5D* and *CD33*, whose polymorphic variants modulate the risk of late-onset AD (LOAD), are expressed abundantly in microglia (*9*). The most notable example is a significant association between an approximately 3-fold increase in the risk for LOAD and a rare variant of the *TREM2* gene encoding p.Arg47His located in the ligand binding domain of TREM2 (*10*). These observations suggest that a partial loss of function of the TREM2-DAP12 signaling pathway in microglia causes amyloid pathology, tau pathology, and neurodegeneration in AD.

Recently, by genotyping using a whole-exome microarray followed by *de novo* genotyping and analysis of imputed genotypes, a three-stage case-control study of 85,133 subjects identified rare coding missense variants associated with LOAD (*11*). They are composed of a protective variant of p.Pro522Arg in *PLCG2*, a risk variant of p.Ser209Phe in *ABI3*, and a risk variant of p.Arg62His in *TREM2*. Among them, the Phe209 allele of *ABI3* showed consistent evidence for increasing the LOAD risk with a minor allele frequency (MAF) of 0.011 in cases and 0.008 in controls. However, the pattern of expression of ABI3 in the brains of AD, along with NHD with relevance to microglial pathology remains unknown. In the present study, for the first time, we attempt to clarify the cell type-specific expression of ABI3 in the brains of AD and NHD by immunohistochemistry.

2. Materials and Methods

2.1. *Human brain tissues*

The brain autopsies were performed at the National Center Hospital, National Center of Neurology and Psychiatry (NCNP), Japan, Kohnodai Hospital, National Center for Global Health and Medicine (NCGM), Japan, and affiliated hospitals of Research Resource Network (RRN), Japan. The comprehensive examination by established neuropathologists (YS and TI) validated the pathological diagnosis. In all cases, written informed consent was obtained. The Ethics Committee of the NCNP for the Human Brain Research, the Ethics Committee of the NCGM on the Research Use of Human Samples, and the Human Research Ethics Committee (HREC) of the Meiji Pharmaceutical University (MPU) approved the present study.

For immunohistochemical studies, serial sections of the frontal cortex and the hippocampus were prepared from four subjects who died of non-neurological causes (NC), composed of a 63-year-old man who died of prostate cancer and acute myocardial infarction (NC1), a 67-year-old man who died of dissecting aortic aneurysm (NC2), a 57-year-old man who died of alcoholic liver cirrhosis (NC3), and a 61-year-old man who died of rheumatoid arthritis with interstitial pneumonia (NC4), ten AD patients, composed of a 68-year-old woman (AD1), a 70-year-old woman (AD2), a 68-year-old woman (AD3), a 56-year-old man (AD4), a 59-year-old man (AD5), an 81-year-old man (AD6), a 68-year-old woman (AD7), an 80-year-old man (AD8), a 72 year-old man (AD9), and a 77-year-old woman (AD11), and five NHD patients, composed of a 42-year-old man (NHD1), a 48-year-old woman (NHD2), a 44-year-old man (NHD3), a 32-year-old woman (NHD4), and a 38-year-old man (NHD5). The homozygous mutation of a single base deletion of 141G (c.141delG) in exon 3 of DAP12 was identified in NHD1, NHD2, and NHD5, while the genetic analysis was not performed in NHD3 or NHD4. All AD cases were satisfied with the Consortium to Establish a Registry for Alzheimer's Disease (CERAD) criteria for diagnosis of definite AD (*12*). They were categorized into the stage C of amyloid deposition and the stage VI of neurofibrillary degeneration, following the Braak's staging (*13*).

2.2. *Immunohistochemistry*

After deparaffination, tissue sections were heated in 10 mM citrate sodium buffer, pH 6.0 by autoclave at 110℃ for 15 min in a temperature-controlled pressure chamber (Biocare Medical, Pacheco, CA, USA). They were treated at room temperature (RT) for 15 min with 3% hydrogen peroxide-containing methanol to block the endogenous peroxidase activity. They were then incubated with phosphate-buffered saline (PBS) containing 10% normal goat serum at RT for 15 min to block non-specific staining, followed by incubation in a moist chamber at 4℃ overnight with rabbit polyclonal anti-ABI3 antibody (HPA017345; Atlas Antibodies,

Bromma, Sweden) or rabbit polyclonal anti-Iba1 antibody (Wako Pure Chemical, Tokyo, Japan) for a marker specific for microglia. The specificity of anti-ABI3 antibody was validated by western blot analysis of recombinant human ABI3 protein expressed in HEK293 cells, which were transfected with the pcDNA4/HisMax TOPO vector (Thermo Fisher Scientific, Carlsbad, CA, USA) containing the full-length ABI3 sequence. After washing with PBS, tissue sections were incubated at RT for 30 min with horseradish peroxidase (HRP)-conjugated secondary antibody (Nichirei, Tokyo, Japan), followed by incubation with diaminobenzidine tetrahydrochloride (DAB) substrate (Vector, Burlingame, CA, USA), and DAB enhancing solution (Vector) for detection of ABI3 immunolabeling. They were processed for a counterstain with hematoxylin. Negative controls underwent all the steps except for exposure to primary antibody. In limited experiments, double immunolabeling was performed using rabbit anti-ABI3 antibody and mouse monoclonal antibodies against glial fibrillary acidic protein (GFAP) (GA5; Nichirei, Tokyo, Japan), neuronal nuclei antigen (NeuN) (1B7; Abcam, Cambridge, UK), 2',3'-cyclic nucleotide 3'-phosphodiesterase (CNPase) (11-5B; Sigma, St. Louis, MO, USA), gp91phox (Abcam), or amyloid-β peptide (12B2; Immunobiological Laboratories, Gunma, Japan), followed by incubation with HRP-conjugated or alkaline phosphatase-conjugated anti-rabbit or anti-mouse secondary antibody and exposure to DAB substrate and Warp Red chromogen (Biocare Medical).

2.3. *Quantification of ABI3 immunoreactivity*

To quantify immunolabeled areas, the images derived from three fields of the white matter or the grey matter per each section were captured at a 200× magnification on the Olympus BX51 universal microscope. They were then processed for quantification by using ImageJ software (National Institute of Health, Bethesda, MD, USA). The ABI3-immunolabeled area was calibrated by the Iba1-immunolabeled area. The differences in the ABI3/Iba1 ratio among NC, AD, and NHD subjects were evaluated statistically by one-way analysis of variance (ANOVA) followed by post-hoc Tukey's test.

2.4. *Quantitative RT-PCR analysis*

To investigate the effects of inflammatory mediators on ABI3 expression, v-*myc*-immortalized human microglial cells named HMO6 (*14*), incubated in 10% fetal bovine serum (FBS)-containing Dulbecco's Modified Eagle's Medium (DMEM), were exposed for 24 hours to 1 μg/mL lipopolysaccharide (LPS; Sigma), recombinant human IFNγ, IL-4, IL-13 or TGFβ1 (50 ng/mL each; Peprotech, London, UK), followed by extraction of total cellular RNA. For quantitative RT-PCR (qPCR) analysis, cDNA was amplified by PCR on LightCycler 96 (Roche Diagnostics, Tokyo, Japan) with SYBR Green I and a primer set composed of 5'catgcatatggagaaggtggcc3' and 5'tgcctgttcttgacagctgcgt3' for detection of a 200 bp product of the *ABI3* gene (NM_016428.2). The expression levels of ABI3 were standardized against the levels of glyceraldehyde-3-phosphate dehydrogenase (G3PDH) detected in the corresponding cDNA samples. All the assays were performed in triplicate.

3. Results

First of all, we validated the specificity of anti-ABI3 antibody HPA017345 by western blot analysis of Xpress-tagged recombinant human ABI3 protein expressed in HEK293 cells (Figure 1, panels a, b). Then, by immunohistochemistry using HPA017345, we identified an intense expression of ABI3 immunoreactivity chiefly on a subset of microglia with ramified or amoeboid morphology located in the grey matter and the white matter of the frontal cortex and the hippocampus derived from NC, AD, and NHD subjects (Figures 2-4, panels a-d). ABI3 immunoreactivity was found to be located in the cytoplasm. We occasionally found inconsistent staining of capillary walls, and perivascular and intravascular macrophages/monocytes. In AD brains, some of ABI3-immunoreactive microglia formed the clusters and they were often closely associated with amyloid deposition (Figure 3, panels c, d). In contrast, the clusters of ABI3-expressing microglia were almost undetectable in both NC and NHD brains. By double immunolabeling, the expression pattern of ABI3 overlapped with that of gp91phox, a marker of microglia (*15*) (Figure 5, panel a), whereas GFAP-positive astrocytes, CNPase-positive oligodendrocytes, and NeuN-positive neurons did not express ABI3 (Figure 5, panels b-d), suggesting that astrocytes, oligodendrocytes and neurons do not express discernible levels of ABI3

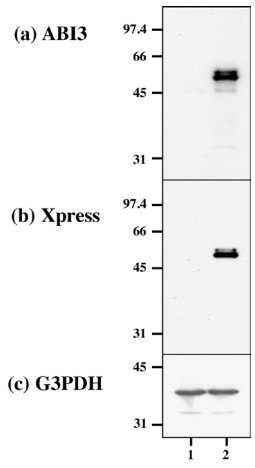

Figure 1. The specificity of ABI3 antibody. Western blot of non-transfected HEK293 cells (**lane 1**) and the cells transfected with the vector containing the full-length ABI3 sequence (**lane 2**). **(a)** ABI3, **(b)** Xpress tag, and **(c)** G3PDH as a loading control.

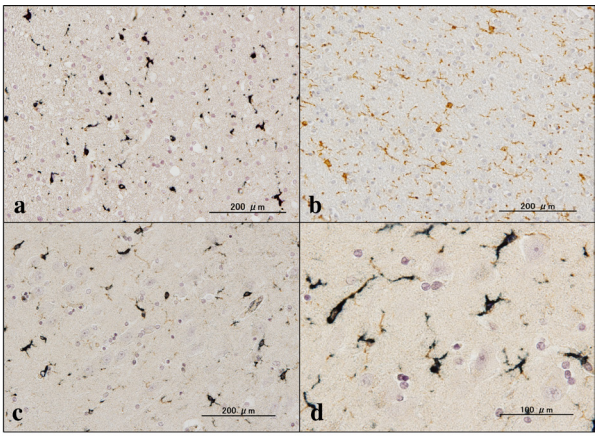

Figure 2. Expression of ABI3 in NC brains. (a) the frontal lobe white matter, ABI3, **(b)** the same area of **(a)**, Iba1, **(c)** the CA1 region of the hippocampus, ABI3, and **(d)** the same area of **(c)**, ABI3.

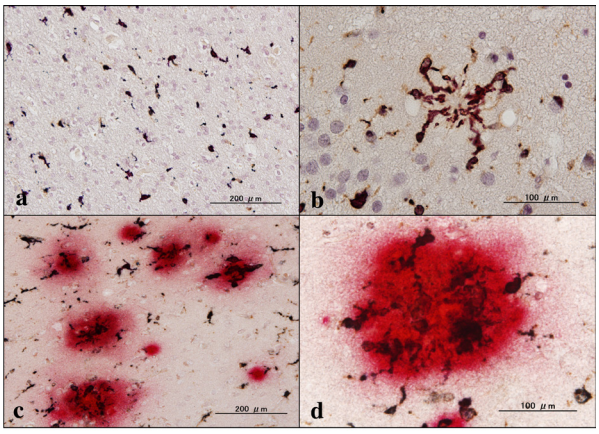

Figure 3. Expression of ABI3 in AD brains. (a) the frontal lobe white matter, ABI3, **(b)** the granular cell layer of the dentate gyrus of the hippocampus, ABI3, **(c)** the frontal cortex, ABI3 (dark brown), amyloid-β (red), and **(d)** the same area of **(c)**, ABI3 (dark brown), amyloid-β (red).

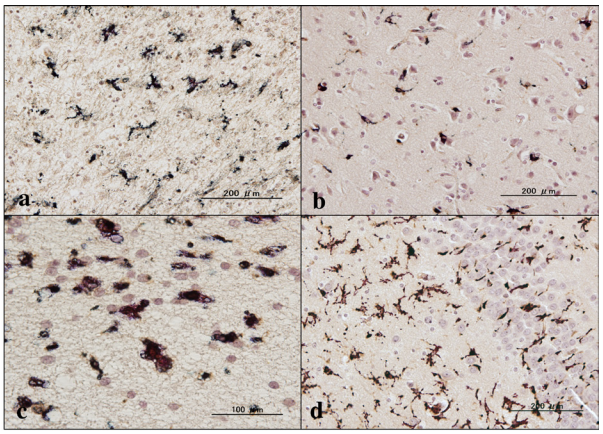

Figure 4. Expression of ABI3 in NHD brains. (a) the frontal lobe white matter, ABI3, **(b)** the frontal cortex, ABI3, **(c)** the frontal lobe white matter, ABI3, and **(d)** the granular cell layer of dentate gyrus of the hippocampus, ABI3.

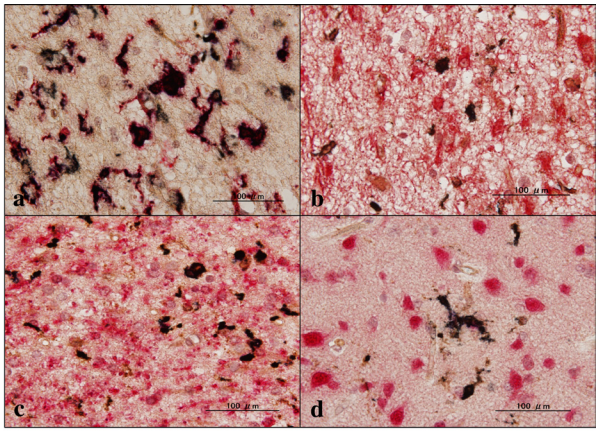

Figure 5. Expression of ABI3 in AD brains. (a) the periventricular white matter of the the hippocampus, ABI3 (dark brown), gp91phox (red), **(b)** the periventricular white matter of the hippocampus, ABI3 (dark brown), GFAP (red), **(c)** the temporal lobe white matter, ABI3 (dark brown), CNPase (red), and **(d)** the frontal cortex, ABI3 (dark brown), NeuN (red)

in the human brain. By quantitative analysis, the immunolabeled area of ABI3-positive microglia was not significantly different among NC, AD, and NHD cases in the grey matter (p = 0.8689) and the white matter (p = 0.8237) due to great variability in the area of ABI3-immunolabeled microglia from case to case (Figure 6). These observations do not actively support the view that ABI3-immunoreactive microglia play a central role in the development of leukoencephalopathy in NHD brains and the neurodegeneration in AD brains. In HMO6 cells, a culture model of human microglia, the treatment with TGFβ1 but not with LPS, IFNγ, IL-4 or IL-13 significantly elevated ABI3 mRNA expression levels (p = 0.0001) (Figure 7).

4. Discussion

A recent study identified p.Ser209Phe in the *ABI3* gene as a risk variant for LOAD, although the expression of ABI3 in the human brain tissues remains to be determined (*11*). NHD is regarded as microgliopathy due to the complete loss of function of the TREM2-DAP12 signaling pathway in microglia, while AD is characterized by the partial loss of function of this pathway. Therefore, we attempted to investigate the pattern of ABI3 expression with relevance to microglial pathology in both AD and NHD brains. As a result, we identified an intense ABI3 immunoreactivity almost exclusively on a subset of microglia in NC, AD, and NHD brains.

ABI3 belongs to the Abelson-interactor (ABI) family of proteins, including ABI1, ABI2 and ABI3, which serve as a class of cytoplasmic molecular adaptors. Both ABI1 and ABI2 were originally identified as a binding partner for the c-ABL kinase, a non-receptor tyrosine kinase, whose activation induces cell growth,

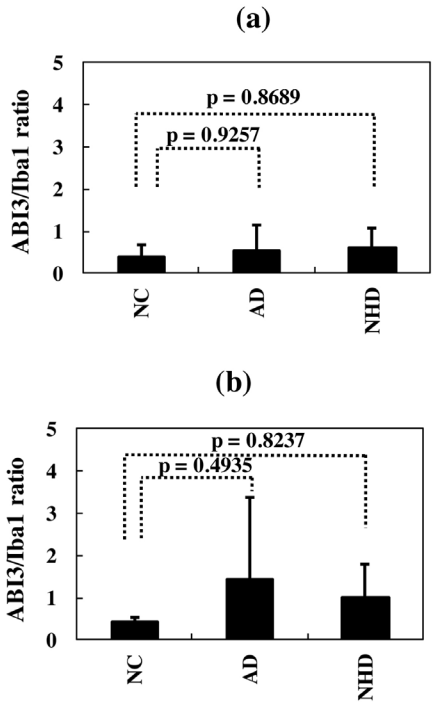

Figure 6. Quantitative analysis of ABI3 expression on microglia in NC, AD, and NHD brains. (a) The ABI3-immunolabeled area/Iba1-immunolabelled area ratio, the grey matter of the frontal cortex, and **(b)** The ABI3-immunolabeled area/Iba1-immunolabeled area ratio, the white matter of the frontal cortex.

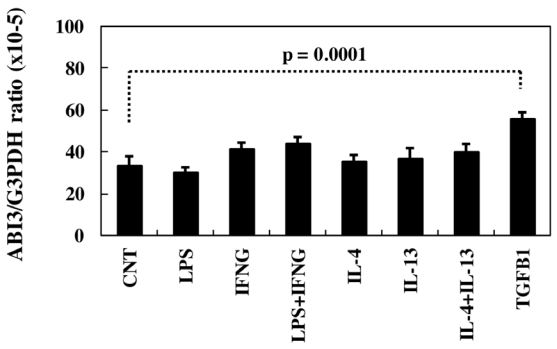

Figure 7. Quantitative RT-PCR analysis of ABI3 expression in HMO6 microglia in culture. HMO6 cells were exposed for 24 hours to 1 μg/ml lipopolysaccharide (LPS), recombinant human IFNγ, IL-4, IL-13 or TGFβ1 (50 ng/mL each), followed by extraction of total cellular RNA that is processed for qRT-PCR. The expression levels of ABI3 were standardized against the levels of G3PDH.

transformation, and cytoskeletal organization. ABI3 was initially cloned as a new molecule including Src-homology 3 (SH3) domain (NESH) (*16*). Members of ABI family encode a protein containing an amino-terminal homeodomain homologous region (HHR), a proline-rich (PR) region, and a carboxy-terminal SH3 domain. They constitute the WAVE regulatory complex (WRC) that regulates actin cytoskeleton organization (*17,18*). WRC is a macromolecular complex, composed of five-subunit proteins that include ABI (ABI1, ABI2 or ABI3), WAVE (WAVE1, WAVE2 or WAVE3), Nap1, PIR121/Sra1, and HSPC300 (*19*). WRC regulates Arp2/3-mediated actin filament nucleation and actin network assembly in response to the Rac GTPase. WRC containing ABI3 is functionally distinct from that containing ABI1 (*17,18*). Both ABI1 and ABI2 but not ABI3 promote the c-ABL-mediated phosphorylation of WAVE2, since ABI3 does not directly interact with c-ABL (*17,18*). WAVE2 phosphorylation by c-ABL activates WRC, leading to formation of lamellipodial membrane protrusions. A linker region between the PR region and the SH3 domain of ABI1 is crucial for its interaction with c-ABL (*18*).

At present, the precise biological function of ABI3 in microglia remains unknown. ABI3 expression is often lost in invasive cancer cells (*20*). This is attributable to transcriptional silencing by methylation of specific CpG sites located within the ABI3 promoter (*21*). Forced expression of ABI3 in v-*src*-transformed NIH3T3 (SRD) cells, thyroid cancer cells, or colon cancer cells inhibits cell growth, invasiveness and migration, and enhances cellular senescence *in vitro* and reduces the tumor growth and metastasis *in vivo*, indicating that ABI3 acts as a tumor suppressor gene (*20,22*). In contrast, treatment of SRD cells overexpressing ABI3 with a tyrosine kinase inhibitor imatinib mesylate markedly promotes formation of invadopodia, actin-rich ventral membrane protrusions with extracellular matrix-degrading activity, and enhances the metastatic potential (*18,23*). Microglia, along with macrophages, are capable of producing podosomes, a matrix-degrading ventral cell surface structure similar to invadopodia (*24*). These observations suggest that ABI3 expressed on microglia in NC, AD, and NHD brains might positively regulate their motility and migration capacity *via* formation of podosomes, particularly when the activity of c-ABL tyrosine kinase is suppressed. In contrast, ABI3 mRNA expression is upregulated in TREM2-deficient microglia that exhibit a reduction in chemotaxis and migration (*25*).

Forced expression of ABI3 suppresses proliferation of thyroid and colon cancer cells (*22*). ABI3 expression in these cells increases the percentage of cells located in G0/G1 phase by upregulating the cell cycle inhibitor $p21^{WAF1}$ and downregulating ERK phosphorylation and E2F1 expression. Therefore, the possibility exists that an intense expression of ABI3 on microglia in NC, AD, and NHD brains might negatively regulate cell proliferation. The SH3 domain of ABI3 interacts with p21-activated kinase (PAK), whose activation positively regulates cell motility. The SRD cells overexpressing ABI3 show a significant decrease in PAK2 phosphorylation at Thr402 (*20*). Forced expression of ABI3 in thyroid cancer cells substantially reduced the phosphorylation of AKT at both Thr308 and Ser473 and GSK3β at Ser9 (*26*). ABI3 is phosphorylated at Ser342 by signaling through the PI3K/AKT pathway. Non-phosphorylated form of

ABI3 is preferentially incorporated in WRC, while the phosphorylated form represents an inactive protein not included in the complex. ABI3 serves as a downstream mediator of the PI3K/AKT pathway that disrupts WRC *via* phosphorylation of ABI3 (*26*).

Microglia adopt two distinct activation phenotypes, composed of a proinflammatory and neurotoxic "classical" activation (M1) phenotype by exposure to LPS and IFNγ and an anti-inflammatory and neuroprotective "alternative" activation (M2) phenotype following treatment with IL-4 and IL-13 (*27*). We found upregulation of ABI3 mRNA expression in HMO6 microglial cells by exposure to TGFβ1 but not by LPS, IFNγ, IL4 or IL-13. TGFβ1 plays a pivotal role in development and maintenance of microglia both *in vitro* and *in vivo* (*28*). Microglia is lost in the CNS-specific TGFβ1 deficient mice that exhibit progressive motor paralysis and death by 23-25 weeks of age, indicating that TGFβ1 acts as a major differentiation and survival factor for microglia (*28*). TGFβ1-treated microglia show a quiescent phenotype that resembles M0 cells (*29*). Importantly, TGFβ1 promotes microglial clearance of amyloid-β (*30*). We identified an intense ABI3 immunoreactivity on the microglia associated with amyloid plaques in AD, possibly related to their migration onto amyloid plaques.

In conclusions, we found that ABI3 is expressed almost exclusively on a subset of microglia in NC, AD, and NHD brains. The pattern of ABI3 expression was similar among the cases, although the clusters of ABI3-immunoreactive microglia were found predominantly in AD brains, associated with amyloid plaques. The biological implications of an intense expression of ABI3 on microglia in AD and NHD brains remain to be clarified.

Acknowledgements

The authors thank Drs. Kenji Jinnai, Nobutaka Arai, Kiyotaka Nakamagoe, Nobutaka Motohashi, and Saburo Yagishita for providing us brain samples. This work was supported by grants from the Research on Intractable Diseases, entitled "Clinicopathological and genetic studies of Nasu-Hakola disease" (H21-Nanchi-Ippan-201; H22-Nanchi-Ippan-136), the Ministry of Health, Labour and Welfare of Japan, and grants from the JSPS KAKENHI (C25430054 and 16K07043) and the Dementia Drug Development Research Center (DRC) project (S1511016), the Ministry of Education, Culture, Sports, Science and Technology (MEXT), Japan.

References

1. Klünemann HH, Ridha BH, Magy L, Wherrett JR, Hemelsoet DM, Keen RW, De Bleecker JL, Rossor MN, Marienhagen J, Klein HE, Peltonen L, Paloneva J. The genetic causes of basal ganglia calcification, dementia, and bone cysts: DAP12 and TREM2. Neurology. 2005; 64:1502-1507.
2. Bianchin MM, Capella HM, Chaves DL, Steindel M, Grisard EC, Ganev GG, da Silva Júnior JP, Neto Evaldo S, Poffo MA, Walz R, Carlotti Júnior CG, Sakamoto AC. Nasu-Hakola disease (polycystic lipomembranous osteodysplasia with sclerosing leukoencephalopathy - PLOSL): A dementia associated with bone cystic lesions. From clinical to genetic and molecular aspects. Cell Mol Neurobiol. 2004; 24:1-24.
3. Satoh J, Tabunoki H, Ishida T, Yagishita S, Jinnai K, Futamura N, Kobayashi M, Toyoshima I, Yoshioka T, Enomoto K, Arai N, Arima K. Immunohistochemical characterization of microglia in Nasu-Hakola disease brains. Neuropathology. 2011; 31:363-375.
4. Xing J, Titus AR, Humphrey MB. The TREM2-DAP12 signaling pathway in Nasu-Hakola disease: A molecular genetics perspective. Res Rep Biochem. 2015; 5:89-100.
5. Satoh J. Possible role of microgliopathy in the pathogenesis of Nasu-Hakola disease. Clin Exp Neuroimmunol. 2013; 4 Suppl 1:17-26.
6. Sarlus H, Heneka MT. Microglia in Alzheimer's disease. J Clin Invest. 2017; 127:3240-3249.
7. Colonna M, Butovsky O. Microglia function in the central nervous system during health and neurodegeneration. Annu Rev Immunol. 2017; 35:441-468.
8. Ginhoux F, Prinz M. Origin of microglia: Current concepts and past controversies. Cold Spring Harb Perspect Biol. 2015; 7:a020537.
9. Yeh FL, Hansen DV, Sheng M. TREM2, microglia, and neurodegenerative diseases. Trends Mol Med. 2017; 23:512-533.
10. Jonsson T, Stefansson H, Steinberg S, et al. Variant of TREM2 associated with the risk of Alzheimer's disease. N Engl J Med. 2013; 368:107-116.
11. Sims R, van der Lee SJ, Naj AC, et al. Rare coding variants in PLCG2, ABI3, and TREM2 implicate microglial-mediated innate immunity in Alzheimer's disease. Nat Genet. 2017; 49:1373-1384.
12. Mirra SS, Heyman A, McKeel D, Sumi SM, Crain BJ, Brownlee LM, Vogel FS, Hughes JP, van Belle G, Berg L. The Consortium to Establish a Registry for Alzheimer's Disease (CERAD). Part II. Standardization of the neuropathologic assessment of Alzheimer's disease. Neurology. 1991; 41:479-486.
13. Braak H, Alafuzoff I, Arzberger T, Kretzschmar H, Del Tredici K. Staging of Alzheimer disease-associated neurofibrillary pathology using paraffin sections and immunocytochemistry. Acta Neuropathol. 2006; 112:389-404.
14. Nagai A, Nakagawa E, Hatori K, Choi HB, McLarnon JG, Lee MA, Kim SU. Generation and characterization of immortalized human microglial cell lines: Expression of cytokines and chemokines. Neurobiol Dis. 2001; 8:1057-1068.
15. Satoh JI, Kino Y, Yanaizu M, Tosaki Y, Sakai K, Ishida T, Saito Y. Expression of gp91phox and p22phox, catalytic subunits of NADPH oxidase, on microglia in Nasu-Hakola disease brains. Intractable Rare Dis Res. 2016; 5:275-279.
16. Miyazaki K, Matsuda S, Ichigotani Y, Takenouchi Y, Hayashi K, Fukuda Y, Nimura Y, Hamaguchi M. Isolation and characterization of a novel human gene (NESH) which encodes a putative signaling molecule similar to e3B1 protein. Biochim Biophys Acta. 2000; 1493:237-241.

17. Hirao N, Sato S, Gotoh T, Maruoka M, Suzuki J, Matsuda S, Shishido T, Tani K. NESH (Abi-3) is present in the Abi/WAVE complex but does not promote c-Abl-mediated phosphorylation. FEBS Lett. 2006; 580:6464-6470.
18. Sekino S, Kashiwagi Y, Kanazawa H, Takada K, Baba T, Sato S, Inoue H, Kojima M, Tani K. The NESH/Abi-3-based WAVE2 complex is functionally distinct from the Abi-1-based WAVE2 complex. Cell Commun Signal. 2015; 13:41.
19. Chen B, Brinkmann K, Chen Z, Pak CW, Liao Y, Shi S, Henry L, Grishin NV, Bogdan S, Rosen MK. The WAVE regulatory complex links diverse receptors to the actin cytoskeleton. Cell. 2014; 156:195-207.
20. Ichigotani Y, Yokozaki S, Fukuda Y, Hamaguchi M, Matsuda S. Forced expression of NESH suppresses motility and metastatic dissemination of malignant cells. Cancer Res. 2002; 62:2215-2219.
21. Moraes L, Galrão AL, Rubió I, Cerutti JM. Transcriptional regulation of the potential tumor suppressor *ABI3* gene in thyroid carcinomas: Interplay between methylation and NKX2-1 availability. Oncotarget. 2016; 7:25960-25970.
22. Latini FR, Hemerly JP, Freitas BC, Oler G, Riggins GJ, Cerutti JM. ABI3 ectopic expression reduces *in vitro* and *in vivo* cell growth properties while inducing senescence. BMC Cancer. 2011; 11:11.
23. Matsuda S, Ichigotani Y, Okumura N, Yoshida H, Kajiya Y, Kitagishi Y, Shirafuji N. NESH protein expression switches to the adverse effect of imatinib mesylate. Mol Oncol. 2008; 2:16-19.
24. Vincent C, Siddiqui TA, Schlichter LC. Podosomes in migrating microglia: Components and matrix degradation. J Neuroinflammation. 2012; 9:190.
25. Mazaheri F, Snaidero N, Kleinberger G, et al. TREM2 deficiency impairs chemotaxis and microglial responses to neuronal injury. EMBO Rep. 2017; 18:1186-1198.
26. Moraes L, Zanchin NIT, Cerutti JM. ABI3, a component of the WAVE2 complex, is potentially regulated by PI3K/AKT pathway. Oncotarget. 2017; 8:67769-67781.
27. Tang Y, Le W. Differential roles of M1 and M2 microglia in neurodegenerative diseases. Mol Neurobiol. 2016; 53:1181-1194.
28. Butovsky O, Jedrychowski MP, Moore CS, *et al*. Identification of a unique TGF-β-dependent molecular and functional signature in microglia. Nat Neurosci. 2014; 17:131-143.
29. Abutbul S, Shapiro J, Szaingurten-Solodkin I, Levy N, Carmy Y, Baron R, Jung S, Monsonego A. TGF-β signaling through SMAD2/3 induces the quiescent microglial phenotype within the CNS environment. Glia. 2012; 60:1160-1171.
30. Wyss-Coray T, Lin C, Yan F, Yu GQ, Rohde M, McConlogue L, Masliah E, Mucke L. TGF-β1 promotes microglial amyloid-β clearance and reduces plaque burden in transgenic mice. Nat Med. 2001; 7:612-618.

(Received November 1, 2017; Revised November 14, 2017; Accepted November 16, 2017)

Original Article

DOI: 10.5582/irdr.2017.01062

Estradiol and proinflammatory cytokines stimulate ISG20 expression in synovial fibroblasts of patients with osteoarthritis

Zhiwei Zheng[1,2,3,4], Lin Wang[2,3,4], Jihong Pan[2,3,4,*]

[1] *School of Medicine and Life Sciences, University of Jinan-Shandong Academy of Medical Sciences, Ji'nan, China;*
[2] *Shandong Medicinal Biotechnology Center, Ji'nan, China;*
[3] *Key Laboratory for Rare & Uncommon Diseases of Shandong Province, Ji'nan, China;*
[4] *Key Laboratory for Biotech-drugs of the Ministry of Health, Ji'nan, China.*

Summary **Interferon stimulated gene 20-kDa (ISG20) has been implicated in the pathology of osteoarthritis (OA) and it has been separately found to be responsive to estrogen stimulation. OA disproportionately affects women, and especially older women, suggesting some role of reproductive hormones in its pathology. The current study characterized the expression of ISG20 following stimulation with estradiol (E2) and proinflammatory cytokines in OA synovial fibroblasts (OASFs). E2 and the proinflammatory cytokines interleukin-6 (IL-6), lipopolysaccharide (LPS), and tumor necrosis factor α (TNF-α) were used to stimulate OASFs *in vitro*. The expression of ISG20 before and after stimulation was detected using quantitative real-time polymerase chain reaction (RT-qPCR) and Western blotting. E2 and proinflammatory cytokine (IL-6, LPS and TNF-α) stimulation significantly induced the expression of ISG20 both at the messenger RNA (mRNA) and protein level. Moreover, the induction was time- and dose-dependent. Small interfering RNA (siRNA) was transfected into OASFs, and expression of the inflammatory factors interleukin-1α (IL-1α), IL-6, and interleukin-10 (IL-10) was detected using RT-qPCR. Silencing ISG20 with siRNA inhibited the expression of IL-1α, IL-6, and IL-10. Thus, expression of ISG20 was regulated by estradiol and proinflammatory factors, while ISG20 in turn regulated the expression of other inflammatory factors. These data support the contention that ISG20 plays a role in the inflammatory process of OA.**

Keywords: Osteoarthritis, ISG20, Estradiol, proinflammatory factor, inflammation

1. Introduction

Osteoarthritis (OA) is a severe, chronic, progressive inflammatory disease of the joints, and particularly the knee. Affected joints are painful and have restricted function, which could lead to long-term disability (*1*). The pathogenesis of OA has yet to be fully understood, but is thought to be associated with sex, increasing age, trauma, wound healing, cartilage metabolic abnormalities, and immune abnormalities (*2,3*). Indeed, OA disproportionately affects women, and its prevalence is higher among older individuals. Women over the age of 50 years have a higher incidence of OA, so the menopause-related changes in hormone levels are hypothesized to contribute to arthritis (*4*). As the global population continues to age, understanding the pathogenesis of OA will become increasingly important.

Interferons (IFNs) comprise a family of secretory proteins chiefly characterized by their ability to induce cellular antiviral proteins (*5*). The interferon-stimulated genes (ISGs) produce proteins that act as antiviral effectors. One of these, interferon stimulated gene 20-kDa (ISG20), is an RNA exonuclease, and its expression can be induced by IFN types I (IFNα and IFNβ) and II (IFNγ) in various cell lines. ISG20 can cleave single-stranded RNA and DNA and it plays a key role in mediating the antiviral activity of IFN (*6-*

Released online in J-STAGE as advance publication November 2, 2017.

**Address correspondence to:*
Dr. Jihong Pan, Shandong Medicinal and Biotechnology Center, Shandong Academy of Medical Sciences, 18877 Jingshi Road, Ji'nan, Shandong 250062, China.
E-mail: pjh933@sohu.com

9). Expression of ISG20, also called HEM45 (HeLa estrogen-modulated, band 45), in human cervical cancer cells increases when stimulated with estrogen (*10*). Thus, ISG20 appears to be responsive to hormonal signals.

Recent evidence has also implicated ISG20 in the pathology of OA. Indeed, the messenger RNA (mRNA) level of ISG20 is lower in the synovial tissues of patients with OA than that in patients with rheumatoid arthritis (RA) (*11*). A recent study by the current authors found that inflammatory mediators such as lipopolysaccharide (LPS), interleukin-6 (IL-6), and tumor necrosis factor α (TNF-α) can stimulate ISG20 production in OA synovial fibroblasts (OASFs), indicating that ISG20 may act as a "sensor" in OASFs to exacerbate inflammation. However, the mechanism responsible for this function has yet to be identified. In order to determine how ISG20 contributes to the inflammation of OASFs, the current study characterized the expression and pathogenic signaling pathway of ISG20 in RASFs during inflammation. Since estradiol (E2) and proinflammatory factors play important roles in OA, this study also assessed the expression of ISG20 in response to stimulation with E2 and proinflammatory cytokines. These findings should identify the role of ISG20 in the pathogenesis of OA.

2. Materials and Methods

2.1. *Synovial tissues*

Synovial tissues (STs) were provided by Shandong Provincial Hospital. Tissues were collected during knee replacement surgery from patients with OA. All participants provided written informed consent to participate in this study, and the study plan was approved by the ethics committee of the Shandong Academy of Medical Sciences.

2.2. *Cell culture and treatment*

Synovial tissue was macerated and incubated with type II collagenase (1 mg/mL, Sigma-Aldrich) in Dulbecco's modified Eagle medium (DMEM, HyClone, Thermo Scientific) for 6 h at 37°C in 5% CO_2 (Thermo Scientific). The tissue was treated with 0.25% trypsin (Solabio) diluted in a phosphate-buffered saline (PBS) solution at a volume equivalent to the DMEM. Cells were filtered and cultured overnight in DMEM, supplemented with 10% fetal bovine serum (FBS, HyClone, Thermo Scientific), penicillin (100 IU/mL), and streptomycin (100 μg/mL, Gibco) for three passages. OASFs from passages 4-6 that tested negative for CD14, CD3, CD19, and CD56 expression according to flow cytometry were used is this study.

OASFs were cultured for 18 h at a density of 2-4 × 10^4/well in DMEM supplemented with 2% FBS. Then cells were cultured in the presence of E2, IL-6, LPS, or TNF-α. In order to avoid inclusion of other substances, E2 was diluted with certified charcoal-stripped FBS (BI, 04-201-1A) and serum without phenol red (MACGENE, CM15020).

2.3. *Inhibition of ISG20 expression with small interfering RNA (siRNA)*

Cultured OASFs were transfected with siRNA at 200 nmol/L using a HiPerFect transfection reagent (QIAGEN, Germany) according to the manufacturer's protocol. The cells were harvested for analysis 24 h after transfection. The sequence of siISG20 was 5'-GGCTACACAATCTACGACA-3'; a scrambled siRNA (5'-GGCTACACAATCTACGACA-3') was used as the negative control.

2.4. *Quantitative real-time PCR (RT-qPCR)*

Total RNA was extracted from cultured cells and human tissues using a TRIzol Reagent (Invitrogen) according to the manufacturers' protocol. RNA was reverse-transcribed using a ReverTra Ace qPCR RT Kit (Toyobo). RT-qPCR was conducted using a LightCycler 480 (Roche) with the following amplification protocol: denaturation at 95°C for 10 min, 40 cycles of denaturation at 95°C for 10 s, annealing at 60°C for 1 min, and extension at 72°C for 1s. Primers for RT-qPCR were also designed in accordance with the consensus sequence. GAPDH was used as an internal loading control. The sequences of primers were as follows: GAPDH 5'-GCACCGTCAAGGCTGAGAAC-3' (forward) and 5'-TGGTGAAGACGCCAGTGGA-3' (reverse); ISG20 5′- TGTTCTGGATGCTCTTGTGC-3′ (forward) and 5′- GCACTGAAAGAGGACATGAGC-3′ (reverse); ESR1 5′- GTCGCCTCTAACCTCGGG-3′ (forward) and 5′- GCTTTGGTGTGGAGGGTCAT -3′ (reverse). All primers were synthesized by BioSune (Shanghai, China). Relative messenger RNA (mRNA) levels were measured using the $2^{-\Delta \text{cycle threshold}}$ ($2^{-\Delta CT}$) method.

2.5. *Western blotting*

Whole cell lysates were separated using SDS-polyacrylamide gel electrophoresis (SDS-PAGE) and transferred onto a polyvinylidene difluoride membrane (Amersham Biosciences, Little Chalfont, UK). Western blotting was performed using anti-ISG20 (1:1000, ABCAM, ab154393). Tubulin (1:1000, ABCAM, ab7291) was used as a loading control for nuclear and cytoplasmic proteins.

2.6. Statistical analysis

Statistical analysis was performed using the Statistical Package for Social Sciences, version 17.0 (SPSS, USA). Data from cytological experiments were analyzed with the Student's *t*-test or chi-square test. $P < 0.05$ was

considered statistically significant in all calculations.

3. Results

3.1. *E2 can stimulate the expression of ISG20 in OASFs*

Women over the age of 50 have a higher incidence of OA, which suggests that changes in reproductive hormone levels may promote arthritis. In particular, E2 secretion decreases at menopause (*12*). To investigate whether ISG20 is responsive to E2, RT-qPCR and Western blotting were used to examine the expression of ISG20 in OASFs after stimulation with estradiol (E2). *ISG20* expression increased significantly after stimulation with 10^{-8} mol/L of E2 for 6 h ($p < 0.01$) (Figure 1A and 1B). Western blotting (Figure 1C) verified that the protein product was consistent with increased *ISG20* expression according to RT-qPCR.

3.2. *ISG20 is sensitive to extra-cellular stimulation with IL-6, TNF-α, and LPS*

To understand the pathological role of ISG20 in OA inflammation, the current study first investigated whether ISG20 expression is responsive to various inflammatory factors implicated in OA. Indeed, IL-6 (I), LPS (II), and TNF-α (III) treatments induced *ISG20* expression in OASFs to varying degrees (Figure 2A, 2B, and 2C). Moreover, the expression of *ISG20* increased in a dose-dependent manner in response to stimulation.

3.3. *The role of ISG20 in regulating inflammatory factors in OASFs*

Since the expression of ISG20 increased significantly after stimulating OASFs with E2 and pro-inflammatory cytokines, the current authors hypothesized that ISG20 may participate in inflammatory processes in OA. To test this hypothesis, siRNA was used to knock down expression of *ISG20*. After verifying the efficiency of the knockdown, RT-qPCR was used to detect its effect on expression of inflammatory factors interleukin-1α (IL-1α), IL-6, and interleukin-10 (IL-10), which play an important role in the inflammatory phenomenon of osteoarthritis (*12*). Results indicated that transfection of 200 nmol/L of siRNA-ISG20 for 24 hours significantly down-regulated the level of *ISG20* mRNA expression compared to the control group (Figure 3A, $p < 0.05$). Moreover, RT-qPCR results indicated that knockdown of *ISG20* in OASFs promoted lower levels of IL-1α, IL-6, and IL-10 expression (Figure 3B and 3C).

4. Discussion

The incidence of OA in women increases abruptly after menopause and is accompanied by a decrease in E2 secretion (*13*). E2 is the main estrogen in women who are premenopausal and postmenopausal. The estrogen level in joint fluid correlates with the level in blood, and E2 levels in joint fluid are similarly correlated with estrogen levels in serum from women with OA (*14*). These findings suggest that levels of hormones such as E2 change, increasing the incidence of OA. The current study found that an appropriate concentration of E2 can stimulate ISG20 expression in OASFs. This is consistent with results of studies indicating that E2 stimulation upregulates ISG20 expression in human cervical cancer cells and BD5, MDA-L3, MCF-7, and HepG2 cells (*10*).

Nonetheless, the function of E2 in OA-related

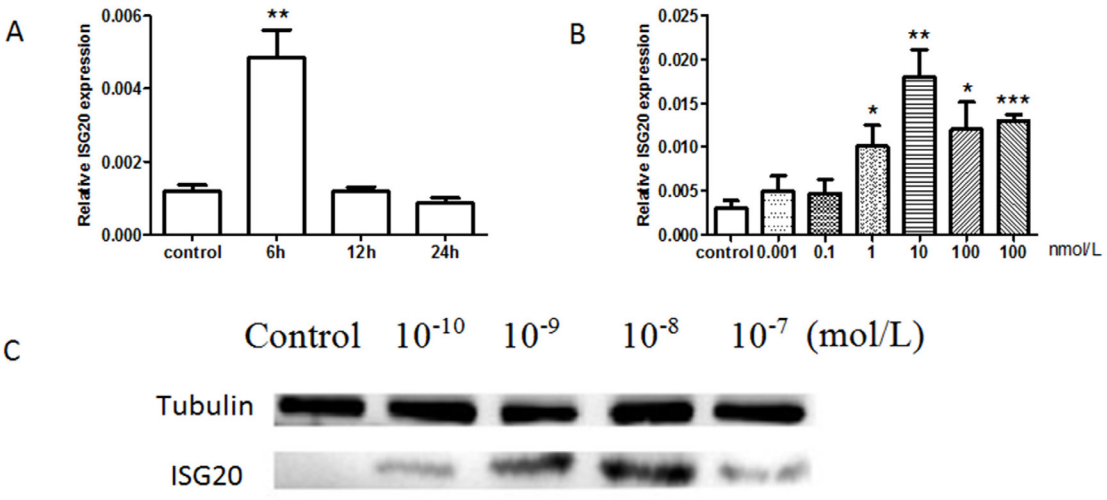

Figure 1. Effect of E2 on ISG20 in OASFs. (A) RT-qPCR was used to detect the effect of 10^{-8} mol/L of E2 on ISG20 in OASFs at different times; **(B)** RT-qPCR was used to detect ISG20 after OASFs were stimulated with E2 at serial concentrations for 6 h. The *p* value in A and B represents each of the times/doses compared to the control. $^{*}p < 0.05$, $^{**}p < 0.01$, $^{***}p < 0.001$; **(C)** Western blotting and RT-qPCR were used to detect ISG20 after OASFs were stimulated 2with E2 at serial concentrations for 6 h.

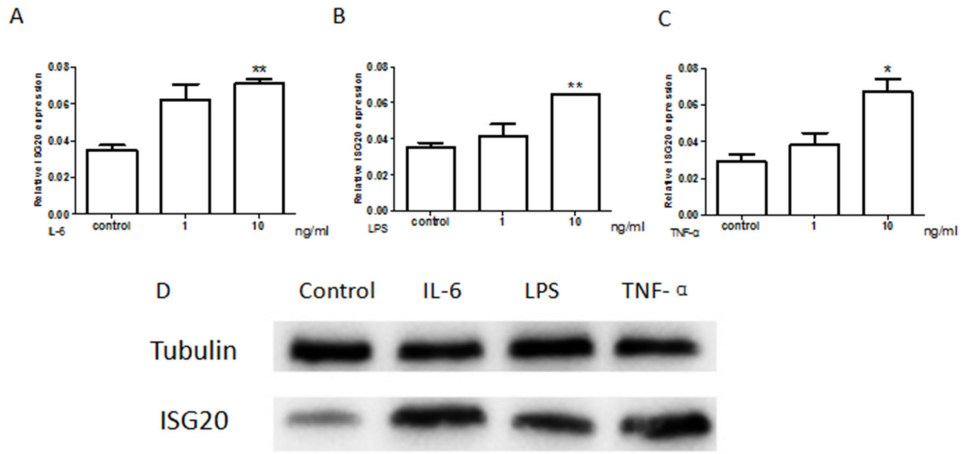

Figure 2. Proinflammatory factors can stimulate ISG20 in OASFs. OASFs were treated with10 ng/mL of IL-6 **(A)**, TNF-α **(B)**, or LPS **(C)** for 24 h in the presence or absence of a vehicle control. The expression of ISG20 was detected with RT-qPCR and Western blotting **(D)**. The *p* value in **A**, **B**, and **C** represents each of the doses compared to the control. All results are presented as the mean ± s.e.m. of three independent experiments performed in triplicate.$^{*}p < 0.05$, $^{**}p < 0.01$.

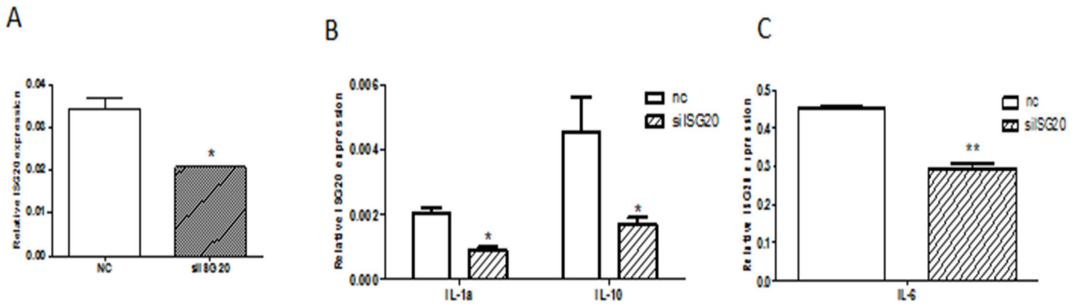

Figure 3. ISG20 is required for the production of inflammatory factors in OASFs. RT-qPCR was used to detect the efficiency of siRNA ISG20 **(A)** and the expression of inflammatory factorsIL-1α, IL-10, and IL-6 after the interference **(B** and **C)**. $^{*}p < 0.05$, $^{**}p < 0.01$.

inflammation is still debated. Martín-Millán and Castaneda hypothesize that estrogen plays a dual role as both an anti-inflammatory and a pro-inflammatory agent in the pathogenesis of OA (*15*). In contrast, de Klerk *et al*. suggest that there is no convincing evidence of a link between estrogen and OA (*16*). However, the current finding that ISG20 expression could be induced in OASFs by E2 and OA-related proinflammatory factors supports previous contentions that E2 may be pro-inflammatory in OA.

Inflammation is a common symptom of OA and is characterized by the presence of immune cells and the secretion of cytokines. Inflammatory factors are highly expressed in OA synovial tissue compared to normal synovial tissue (*3*). The current findings indicate that inflammatory factors IL-6, LPS, and TNF-α can promote *ISG20* mRNA expression. At the same time, knocked down expression of ISG20 with specifically targeted siRNA promotes the down-regulation of inflammatory cytokines such as IL-6, IL-1α, and IL-10. Thus, ISG20 may play a role in promoting inflammation in OASFs.

In summary, the current study found that ISG20 can be regulated by estradiol and proinflammatory factors such as IL-6, LPS, and TNF-α, and that, in turn, ISG20 can regulate the expression of the inflammatory cytokines IL-6, IL-1α, and IL-10 in OASFs. These findings help to understand the pathogenesis of OA, and particularly that among older women, and may lead to new therapeutic targets.

Acknowledgements

This work was supported by grants from the National Natural Science Foundation of China (Grant No. 81671624), the Natural Science Foundation of Shandong Province (Grant No. ZR2015YL029), the Shandong Health Science and Technology Research Program (Grant No.2014WS0054), Key Projects of Shandong Province (2017GSF218082), and the

Innovation Project of the Shandong Academy of Medical Sciences.

References

1. Ying B, Maimaiti AK, Song D, Zhu S. Myrtol ameliorates cartilage lesions in an osteoarthritis rat model. Int J Clin Exp Pathol. 2015; 8:1435-1442.
2. Anderson DD, Chubinskaya S, Guilak F, Martin JA, Oegema TR, Olson SA, Buckwalter JA. Post-traumatic osteoarthritis: Improved understanding and opportunities for early intervention. J Orthop Res. 2011; 29:802-809.
3. de Lange-Brokaar BJ, Ioan-Facsinay A, van Osch GJ, Zuurmond AM, Schoones J, Toes RE, Huizinga TW, Kloppenburg M. Synovial inflammation, immune cells and their cytokines in osteoarthritis: A review. Osteoarthritis Cartilage. 2012; 20:1484-1499.
4. Sniekers YH, Weinans H, Bierma-Zeinstra SM, van Leeuwen JP, van Osch GJ. Animal models for osteoarthritis: The effect of ovariectomy and estrogen treatment – A systematic approach. Osteoarthritis Cartilage. 2008; 16:533-541.
5. Horio T, Murai M, Inoue T, Hamasaki T, Tanaka T, Ohgi T. Crystal structure of human ISG20, an interferon-induced antiviral ribonuclease. FEBS Lett. 2004; 577:111-116.
6. Gongora C, David G, Pintard L, Tissot C, Hua TD, Dejean A, Mechti N. Molecular cloning of a new interferon-induced PML nuclear body-associated protein. J Biol Chem. 1997; 272:19457-19463.
7. Zheng Z, Wang L, Pan J. Interferon stimulated gene 20-kDa protein (ISG20) in infection and disease: Review and outlook. Intractable Rare Dis Res. 2017; 6:35-40.
8. Degols G, Eldin P, Mechti N. ISG20, an actor of the innate immune response. Biochimie. 2007; 89:831-835.
9. Nguyen LH, Espert L, Mechti N, Wilson DM. The human interferon-and estrogen-regulated ISG20/HEM45 gene product degrades single-stranded RNA and DNA *in vitro*. Biochemistry. 2001; 40:7174-7179.
10. Pentecost BT. Expression and estrogen regulation of the HEM45 mRNA in human tumor lines and in the rat uterus. J Steroid Biochem Mol Biol. 1998; 64:25-33.
11. Chang X, Yue L, Liu W, Wang Y, Wang L, Xu B, Wang Y, Pan J, Yan X. CD38 and E2F transcription factor 2 have uniquely increased expression in rheumatoid arthritis synovial tissues. Clin Exp Immunol. 2014; 176:222-231.
12. Cai H, Sun HJ, Wang YH, Zhang Z. Relationships of common polymorphisms in IL-6, IL-1A, and IL-1B genes with susceptibility to osteoarthritis: A meta-analysis. Clin Rheumatol. 2015; 34:1443-1453.
13. Sniekers YH, van Osch GJ, Ederveen AG, Inzunza J, Gustafsson JA, van Leeuwen JP, Weinans H. Development of osteoarthritic features in estrogen receptor knockout mice. Osteoarthritis Cartilage. 2009; 17:1356-1361.
14. Richette P, Laborde K, Boutron C, Bardin T, Corvol MT, Savouret JF. Correlation between serum and synovial fluid estrogen concentrations: Comment on the article by Sowers *et al*. Arthritis Rheum. 2007; 56:698-699.
15. Martín-Millán M, Castañeda S. Estrogens, osteoarthritis and inflammation. Joint Bone Spine. 2013; 80:368-373.
16. de Klerk BM, Schiphof D, Groeneveld FP, Koes BW, van Osch GJ, van Meurs JB, Bierma-Zeinstra SM. No clear association between female hormonal aspects and osteoarthritis of the hand, hip and knee: A systematic review. Rheumatology (Oxford). 2009; 48:1160-1165.

(Received September 13, 2017; Revised October 16, 2017; Accepted October 24, 2017)

Original Article

DOI: 10.5582/irdr.2017.01066

The expression profile of IFITM family gene in rats

Yanqin Lu[1,2,§], Qingli Zuo[1,2,§], Yao Zhang[1,2], Yanzhou Wang[3], Tianyou Li[3], Jinxiang Han[1,2,*]

[1] *Key Laboratory for Rare & Uncommon Diseases of Shandong Province, Shandong Medicinal Biotechnology Centre, Shandong Academy of Medical Sciences, Ji'nan, China;*
[2] *School of Medicine and Life Sciences, University of Ji'nan-Shandong Academy of Medical Sciences, Ji'nan, China;*
[3] *Department of Paediatric Surgery, Shandong Provincial Hospital, Ji'nan, China.*

Summary **The interferon-inducible transmembrane proteins (IFITMs) are a family of small transmembrane proteins belonging to the interferon (IFN)-stimulated gene (ISG) superfamily and strongly induced by IFNs. In this paper, we studied the expression profile of IFITMs in 32 organ tissues. The IFITM mRNA expression profile showed that IFITM1, IFITM2 and IFITM3 were expressed in each tissue, especially, in spermatophore, spermaduct, testicle and epididymis. The expression of IFITM1, IFITM2 and IFITM3 showed a trend from high to low. Except for IFITM3 and IFITM6, the others IFITMs were highly expressed in the bone marrow, and the expression level of them was higher in the tibia than that in other parts of the long bones. In liver, the relative expression of IFITM1 and IFITM3 was higher than that of other members. The expression level of IFITM5 was the highest in bone marrow, successively in pancreas, and it was low in skin, smooth muscle and fat. Interestingly, the expression profile of IFITM2 and IFITM7 in tissues was similar to IFITM5. The expression of IFITM2, IFITM5 and IFITM10 were higher in smooth muscle than that in skeletal muscle. IFITM2, IFITM5, IFITM7 and IFITM10 were both highly expressed in esophagus and trachea. In addition, the expression of IFITM6 in eyes was high, and also in pancreas, gallbladder and bone. In the present study, we systematically analyzed the mRNA expression profile of IFITMs in 32 organ tissues, providing the foundation for the study of the function of the IFITMs.**

Keywords: Rat, IFITMs, gene expression

1. Introduction

Interferons (IFNs), a group of low molecular glycoproteins synthesized by host cells, was discovered by Isaacs, who studied the interference factor about influenza virus in chick embryo chorioallantoic membrane (*1*). The following interferons are classified as type I, including IFN-α and IFN-β, and type II including IFN-γ only (*2*). INFs are a family of proteins that are released by a variety of cells in response to infections caused by viruses. A high level of antiviral protection is achieved by IFN-α, IFN-β and IFN-γ. Antiviral activity of interferons is based on the induction and regulation of innate and acquired immune mechanisms. By binding to transmembrane receptors, INFs interact with target cells activating the JAK/STAT pathways, but also other signaling pathways (*3*). This leads to induction and activation of many antiviral agents, such as protein kinase RNA-activated (PKR), the expression of interferon inducible transmembrane proteins (ISGs), ribonuclease 2-5A pathway, and Mx proteins, as well as numerous apoptotic pathways. As a result of the protective effect of interferons, virus binding to cells is stopped. Interferon inducible transmembrane protein (IFITM) is a key class of proteins in the ISGs-regulated expression products (*4*). The IFITM family has different functions, including the control of cell proliferation, promotion of homotypic adhesion, prevention of viral infection, maturation of bone matrix mineralization, regulation of germ cell development, *etc* (*5-7*).

Released online in J-STAGE as advance publication November 14, 2017.

[§]These authors contributed equally to this work.

**Address correspondence to:*
Dr. Jinxiang Han, Shandong Academy of Medical Sciences, 18877 Jingshi Road, 250062 Ji'nan, China.
E-mail: samshjx@sina.com

The human IFITM family consists of 5 members, namely IFITM1, IFITM2, IFITM3, IFITM5 and IFITM10, located on chromosome 11. Differently, the mice IFITM family includes IFITM1, IFITM2, IFITM3, IFITM5, IFITM6, IFITM7 and IFITM10. Except for IFITM7 located in chromosome 16, other genes in mice are located on chromosome 7. IFITM1, expressed in leukocytes and endothelial cells, has anti-proliferation functions and promotes homotypic adhesion (*5,8,9*). In many cell lines, IFITM2 could cause the cell cycle to stagnate and p53-dependent apoptosis (*10*). IFITM3 can inhibit the proliferation of cells (*11-13*). As a host immune barrier, IFITM1, IFITM2 and IFITM3 play an important role in the process of defense against respiratory virus invasion (*14-17*). Recently, they also have been reported as biomarkers of several tumors (*11,18-20*). IFITM5 is a IFITM-like protein, only expressed in human and mouse bone, especially in osteogenesis cells (*21*). The point mutation of IFITM5 causes osteogenesis imperfecta type V (*22*), and the overexpression of the mutant gene could promote Saos2 cell line apoptosis (*23*). IFITM6 was strongly expressed in spleen macrophages of tumor bearing mice. The IFITM10 sub-family is divided into two groups: aquatic and terrestrial types, suggesting that IFITM10 might be associated with adaptation to the aquatic environment. In addition, IFITM10 with CTSD can be used as a molecular marker for breast cancer (*24*). So far, no one has reported the function of IFITM7.

In the present study, we analyzed the expression pattern of IFITMs in different tissues of rats, providing a theoretical foundation for further research on their function.

2. Materials and Methods

2.1. *Rat tissue collection*

Rats (Wistar rats, male, 6-week-old) were purchased from the Animal Experimental Center of Shandong University. The study tissues compromised 32 organ tissues, including lung, heart, spleen, stomach, pancreas, liver, gallbladder, kidney, small intestine, large intestine, esophagus, trachea, cartilage, humerus, ulna, thighbone, tibia, eye, ear, skin, hair, spermatophore, spermaduct, epididymis, testis, skeletal muscle, smooth muscle, fat, brain, bone marrow and blood, *etc*. Each portion was frozen in liquid nitrogen and stored at -80°C until RNA was extracted. Total RNA was isolated with Trizol reagent (Invitrogen) according to the manufacturer's instructions.

2.2. *Primer design*

According to the IFITM family gene sequence on GenBank, primers were designed using *https://lifescience.roche.com*. Three pairs of primers were designed for each IFITM gene, according to the Ct value and the peak melting curve.

2.3. *Reverse transcription (RT)-PCR analysis*

Total RNA was isolated with Trizol reagent (Invitrogen) according to the manufacturer's instructions. RNAs from organ tissues were reverse-transcribed using PrimeScript™ RT Master Mix (Perfect Real Time) (Takara Biotechnology (Dalian) Co. Ltd.), and cDNAs of IFITMs were amplified by PCR using mice IFITMs specific primers. RT of RNA was performed in a final volume of 20 μL containing Random Primer (100 pmol/μL) of 1 μL, dNTP (10 mM) of 1 μL, 4 μg total RNA and diethyl pyrocarbonate (DEPC)-treated water. After incubation at 65°C for 5 min, 4 μL 5×PrimerScript Buffer, 0.5 μL RNase Inhibitor (40 U/μL) and 1 μL RNase (200 U/μL) were added, then the reaction was incubated at 30°C for 10 min, 42°C for 60 min, 75°C for 15 min and 4°C for 20 min. Quantitative PCR was performed using LightCycler 480 (Roche). Quantitative PCR was performed using LightCycler 480 (Roche). PCR was performed in a final volume of 40 μL containing 10 μL SYBR Green Master I (Roche), 1 μL upstream primers (10 mol/μL) and 1 μL downstream primers (10 mol/μL), 0.4 μL cDNA and 7.6 μL DEPC-treated water. PCR was performed for 40 cycles (denaturation at 94°C for 5 s, annealing at 55°C for 15s and extension at 72°C for 15 s). The IFITMs mRNA copy numbers in organ tissues were normalized to mRNA copy numbers of the house keeping gene, β-actin to give a value ΔCt. Other samples were then normalized to the lung sample giving ΔΔCt and finally the amount of IFITMs in organ samples relative to the lung sample was expressed as $2^{-\Delta\Delta Ct}$. This final value was used to determine the expression profile in 32 organ samples.

3. Results

3.1. *RT-qPCR primer design and screening*

The primers used for beta-actin (control) were 5'-CCAGAGCAAGAGAGGTAT-3' (forward) and 5'-CTGTGGTGGTGAAGCTGTAG-3' (reverse). The primer sequences of IFITMs are listed in supplementary Table S1. According to the Ct value and the peak melting curve, the best pairs we obtained are listed in Table 1 and used in our study.

3.2. *mRNA expression profiles of IFITMs in different tissues*

According to the RT-PCR, we obtained a result that the IFITM1, IFITM2 and IFITM3 genes of the rat were expressed in all 32 organ tissues examined (Figure 1). In bone marrow, the relative expression levels of IFITM1 and IFITM2 were higher, whereas

Table 1 Ct value of IFITM genes by RT-QPCR

Name	Mean Ct	SD
IFITM1-1	33.90	0.211974841
IFITM1-2	33.96	0.424617475
IFITM1-3	34.76	0.21007935
IFITM2-1	33.66	0.140118997
IFITM2-2	33.00	0.146401275
IFITM2-3	33.01	0.321299445
IFITM3-1	32.92	0.130128142
IFITM3-2	33.11	0.31214313
IFITM3-3	36.37	0.482942371
IFITM5-1	37.91	0.160934769
IFITM5-2	37.74	0.972950838
IFITM5-3	37.92	0.077674535
IFITM6-1	32.71	0.176729549
IFITM6-2	37.29	0.362261416
IFITM6-3	33.53	0.167431578
IFITM7-1	30.92	0.102632029
IFITM7-2	32.11	0.317647603
IFITM7-3	31.79	0.060277138
IFITM10-1	40	0
IFITM10-2	40.00	0
IFITM10-3	31.53	0.17691806
β-Actin	26.61	0.060827625

Note: the marked primer was chosen to use in our study.

IFITM3 was lower. In spleen, stomach, pancreas, liver, gallbladder and kidney, the relative expression levels of IFITM1 and IFITM3 were higher. Except for IFITM1, the expression levels of IFITM2 and IFITM3 were strong in skin and fat, while the relative expression levels of IFITM2 and IFITM3 were higher in skeletal muscle than in smooth muscle. In addition, the relative expression levels of IFITM1, IFITM2 and IFITM3 in bone were lower, however those in spermatophore were highest and in epididymis were lowest in tissues of the reproductive system.

The relative expression levels of IFITM5 and IFITM10 in the bone marrow were highest, and IFITM5 and IFITM10 were highly expressed only in esophagus, trachea, skull, bone, eye, ear, hair and skin, whereas they were expressed at a lower level in large intestine, small intestine, brain, blood and the tissues of the reproductive system. In smooth muscle, IFITM5 and IFITM10 expression was significantly higher than that in skeletal muscle. The relative expression level of IFITM5 was higher in pancreas and IFITM5 was also expressed in fat (Figure 2).

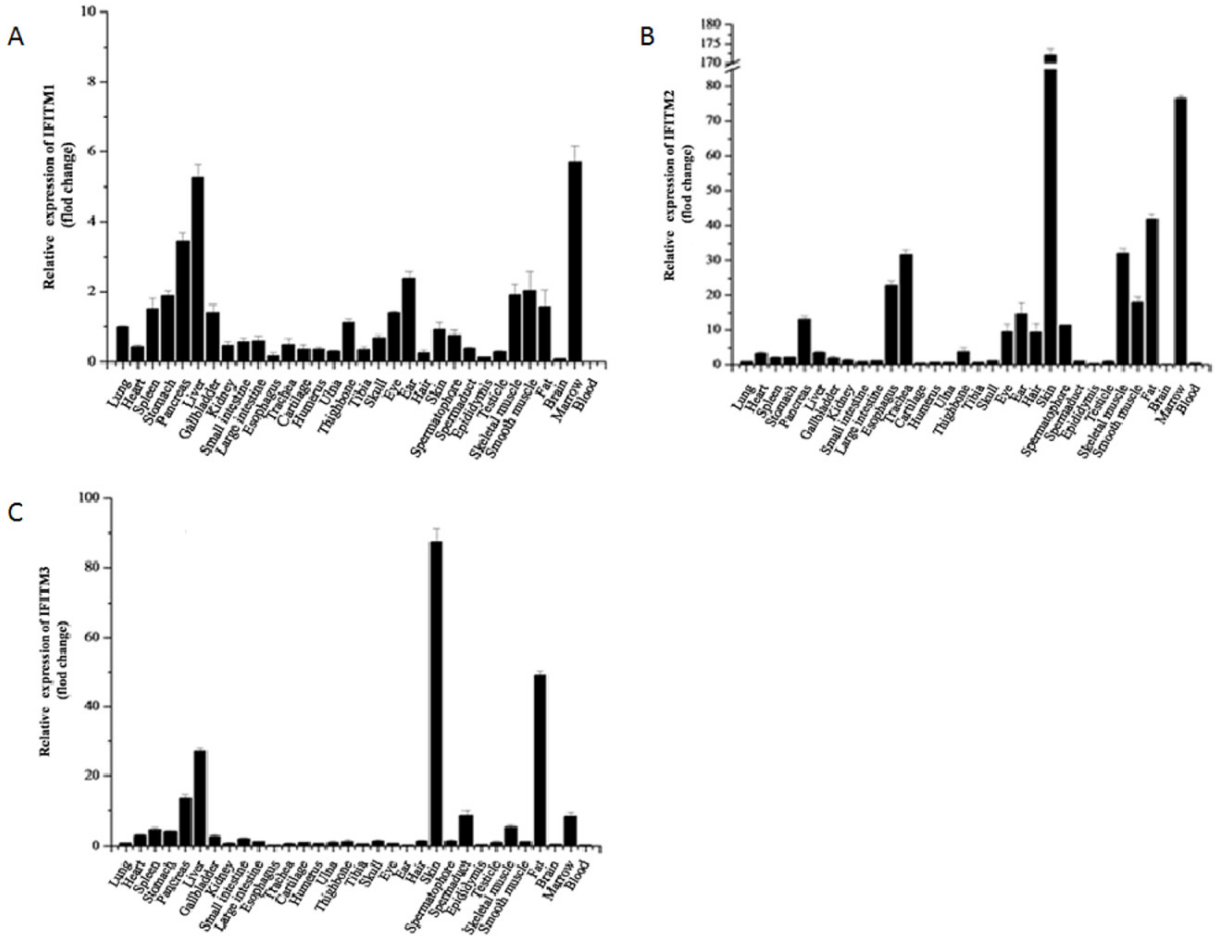

Figure 1. The relative expression of IFITM1(1A), IFITM2(1B) and IFITM3(1C) in different rat tissues.

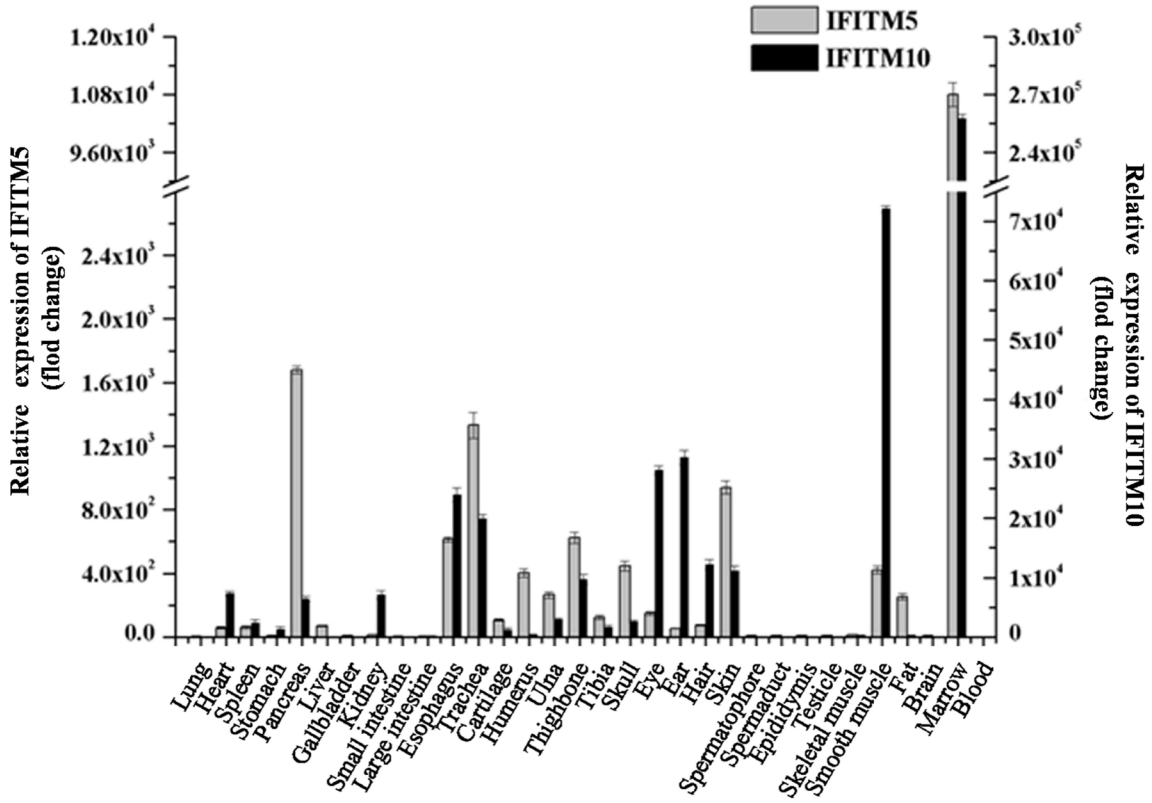

Figure 2. The relative expression of IFITM5 and IFITM10 in different rat tissues.

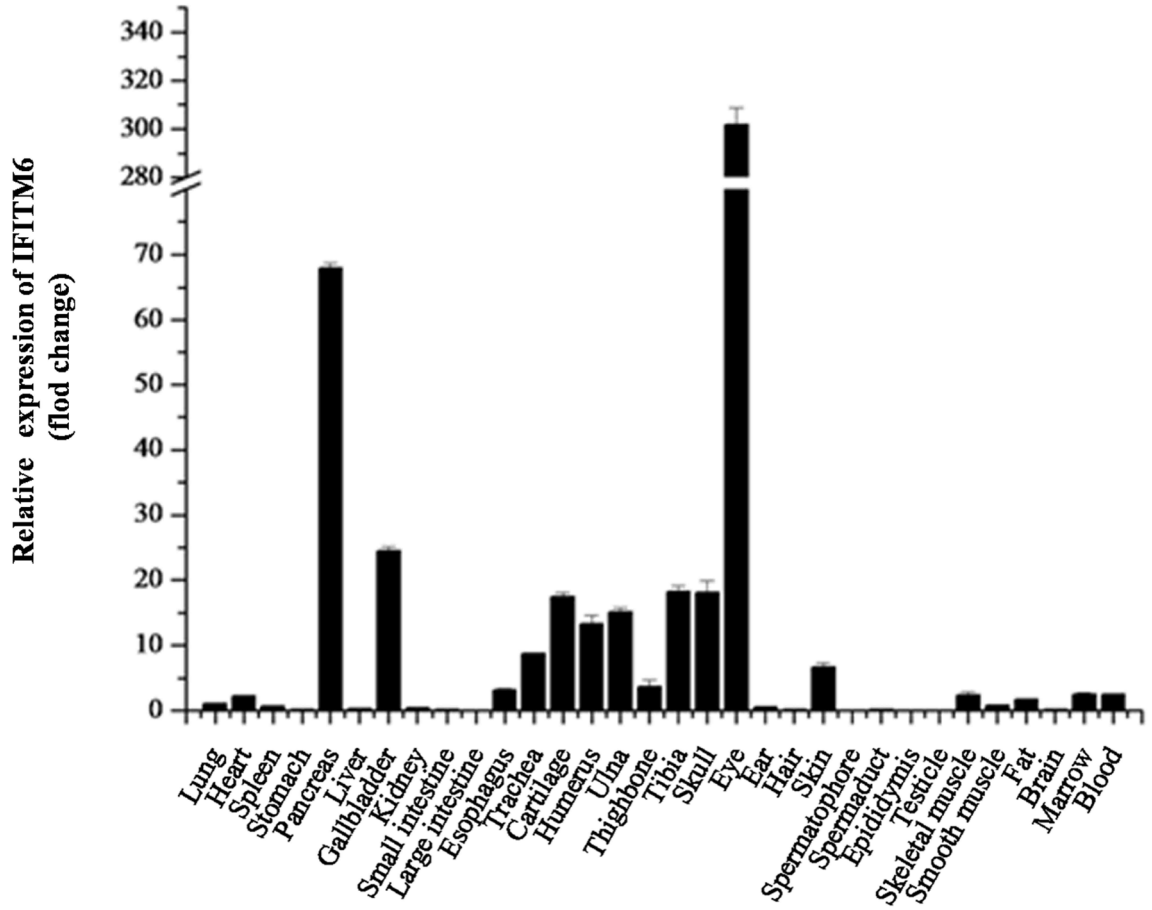

Figure 3. The relative expression of IFITM6 in different rat tissues.

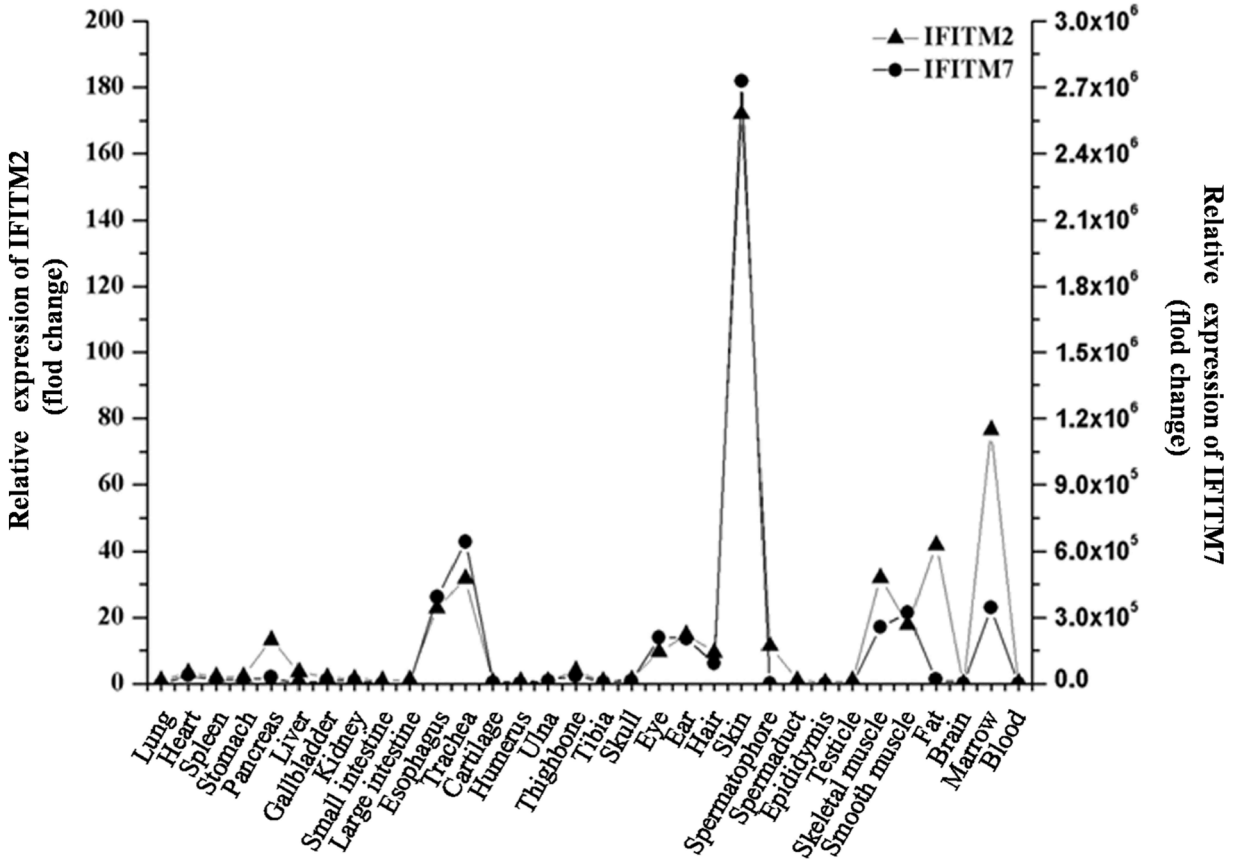

Figure 4. The relative expression trends of IFITM2 and IFITM7 in different rat tissues.

The expression level of IFITM6 was the highest in eye, higher in pancreas, gallbladder and bone, and very low in spleen, intestine, brain and the tissues of the reproductive system (Figure 3). The expression level of IFITM7 was similar to IFITM2, with the highest in skin, higher in the esophagus, eye, ear, hair, skeletal muscle, smooth muscle and bone marrow, and lower in other tissues (Figure 4).

4. Discussion

Interferon inducible transmembrane (IFITM) proteins, playing an important role in cell proliferation, adhesion and immune system regulation, are a recently discovered family of cellular anti-viral proteins that restrict the replication of a number of enveloped and non-enveloped viruses. IFITM proteins are located in the plasma membrane and endosomal membranes, the main portals of entry for many viruses. The interferon-inducible transmembrane proteins (IFITMs) are a family of small transmembrane proteins belonging to the ISG superfamily and strongly induced by IFNs (*25*). The IFITM proteins are the distinct restriction factors known to block viral entry, including restriction of virus fusion with the late endosomal or lysosomal compartments and penetration into the cytoplasm (*4,26*). It has been shown that gene cluster IFTIM1, 2, and 3, the immune-related genes, are critically involved in immune defense against a broad variety of viruses, including influenza virus, dengue virus, filoviruses, coronavirus, hepatitis C virus, lyssaviruses, and West Nile virus (*14,27-29*). Bailey showed that IFITM3 was expressed in the epithelial cells of the airway and visceral pleura, while IFITM1 and IFITM2 had low expression in other parts of the body (*30*). In our study, they were expressed in lung and trachea, but also expressed in other tissues. These findings are consistent with previous research that IFITM1, IFITM2 and IFITM3 were widely expressed in the human body (*4*), and had a differential expression profile in the development of primordial germ cells (*13*). The relative expression levels of IFITM2 and IFITM3 in skin were significantly higher than those in other tissues, suggesting that IFITM2 and IFITM3 may be related to antiviral defense. In testis and epididymis, spermatophore and spermaduct, IFITM1, IFITM2 and IFITM3 expression showed a trend from high to low, while IFITM5, IFITM6, IFITM7 and IFITM10 expression is very low. IFITM7 expression is similar to that of IFITM2, indicating that they have a similar function. Moffatt reported that IFITM5 is related to calcium deposition in bone (*21*). We found that IFITM5 was not only expressed in bone, but also expressed in bone marrow, skin, pancreas and smooth muscle,

and this is inconsistent with previous studies that IFITM5 was only expressed in bone. The reason for this difference may be that the specific expression of IFITM5 in bone is only in certain mammals (*21*). In the zebrafish model, IFITM5 was expressed in brain, muscle and liver tissues with no expression in bone; in the chicken model, its expression was high in muscle and liver, low in brain and ovary, but none in bone (*31*). Therefore, the expression level of IFITM5 in bone is different in various species, indicating that the IFITM5 gene may have other functions other than bone mineralization.

In addition, IFITM10 was highly expressed in the bone marrow; in smooth muscle, its expression was significantly higher than that in skeletal muscle; in the tissues of the intestinal and reproductive systems, it was unexpressed. Thus, the expression profile of IFITM10 is similar to that of IFITM5. Their distribution may be related to their gene homology (*31*), suggesting that IFITM10 and IFITM5 have similar functions. It is reported that IFITM10 was expressed in the brain and spleen of mice, whereas not expressed in bone (*31*). The expression level of IFITM10 in chicken was decreased with the continuous development of embryonic germ cells (*32*). IFITM10 had been reported in spleen tissues, and we found that IFITM10 was also expressed in esophagus, trachea, bone and muscle. IFITM6 was highly expression in macrophages (*7*), however, our results showed that IFITM6 was highly expressed in eye but not in spleen. There are still a few studies on IFITM6, IFITM7 and IFITM10. Currently, researchers pay more attention to the mechanism of their resistance to virus invasion and their relationship with tumors (*30,33*). In the present study, mRNA expression profile of IFITMs in different tissues was systematically compared and analyzed in rats, providing a favorable reference for revealing the functions of IFITMs. Next, we will analyze the protein expression profile of the IFITM family members.

Acknowledgements

This work was supported by a grant from the State Major Infectious Disease Research Program (China Central Government, 2017ZX10103004-007), Shandong Provincial Natural Science Foundation of China (2015ZRC03171) and Major Major Scientific and Technological Program of Shandong Province (2016ZDJS07A10)

References

1. Isaacs A, Lindenmann J. Pillars Article: Virus interference. I. The interferon. Proc R Soc Lond B Biol Sci. 1957; 147:258-267.
2. Pestka S, Krause CD, Walter MR. Interferons, interferon-like cytokines, and their receptors. Immunol Rev. 2004; 202:8-32.
3. Honda K, Yanai H, Takaoka A, Taniguchi T. Regulation of the type I IFN induction: A current view. Int Immunol. 2005; 17:1367-1378.
4. Diamond MS, Farzan M. The broad-spectrum antiviral functions of IFIT and IFITM proteins. Nat Rev Immunol. 2013; 13:46-57.
5. Evans SS, Collea RP, Leasure JA, Lee DB. IFN-alpha induces homotypic adhesion and Leu-13 expression in human B lymphoid cells. J Immunol. 1993; 150:736-747.
6. Lange UC, Saitou M, Western PS, Barton SC, Surani MA. The fragilis interferon-inducible gene family of transmembrane proteins is associated with germ cell specification in mice. BMC Dev Biol. 2003; 3:1.
7. Smith RA, Young J, Weis JJ, Weis JH. Expression of the mouse fragilis gene products in immune cells and association with receptor signaling complexes. Genes Immun. 2006; 7:113-121.
8. Deblandre GA, Marinx OP, Evans SS, Majjaj S, Leo O, Caput D, Huez GA, Wathelet MG. Expression cloning of an interferon-inducible 17-kDa membrane protein implicated in the control of cell growth. J Biol Chem. 1995; 270:23860-23866.
9. Evans SS, Lee DB, Han T, Tomasi TB, Evans RL. Monoclonal antibody to the interferon-inducible protein Leu-13 triggers aggregation and inhibits proliferation of leukemic B cells. Blood. 1990; 76:2583-2593.
10. Brem R, Oraszlan-Szovik K, Foser S, Bohrmann B, Certa U. Inhibition of proliferation by 1-8U in interferon-alpha-responsive and non-responsive cell lines. Cell Mol Life Sci. 2003; 60:1235-1248.
11. Tirosh B, Daniel-Carmi V, Carmon L, Paz A, Lugassy G, Vadai E, Machlenkin A, Bar-Haim E, Do MS, Ahn IS, Fridkin M, Tzehoval E, Eisenbach L. '1-8 interferon inducible gene family': putative colon carcinoma-associated antigens. Br J Cancer. 2007; 97:1655-1663.
12. Joung I, Angeletti PC, Engler JA. Functional implications in apoptosis by interferon inducible gene product 1-8D, the binding protein to adenovirus preterminal protein. J Microbiol. 2003; 41:295-299.
13. Tanaka SS, Matsui Y. Developmentally regulated expression of mil-1 and mil-2, mouse interferon-induced transmembrane protein like genes, during formation and differentiation of primordial germ cells. Mech Dev. 2002; 119:S261-S267.
14. Brass AL, Huang IC, Benita Y, John SP, Krishnan MN, Feeley EM, Ryan BJ, Weyer JL, van der Weyden L, Fikrig E, Adams DJ, Xavier RJ, Farzan M, Elledge SJ. The IFITM proteins mediate cellular resistance to influenza A H1N1 virus, West Nile virus, and dengue virus. Cell. 2009; 139:1243-1254.
15. Savidis G, Perreira JM, Portmann JM, Meraner P, Guo Z, Green S, Brass AL. The IFITMs inhibit Zika virus replication. Cell Rep. 2016; 15:2323-2330.
16. Muñoz-Moreno R, Cuesta-Geijo MÁ, Martinez-Romero C, Barrado-Gil L, Galindo I, Garcia-Sastre A, Alonso C. Antiviral role of IFITM proteins in african swine fever virus infection. PloS One. 2016; 11:e0154366.
17. Cui K, Wang H, Zai S, Feng Y. Expression of IFITM3 in colorectal carcinoma and its clinical significance. Zhonghua Zhong Liu Za Zhi. 2015; 37:352-355. (in Chinese)
18. Yang G, Xu Y, Chen X, Hu G. IFITM1 plays an essential role in the antiproliferative action of interferon-gamma. Oncogene. 2007; 26:594-603.

19. Fumoto S, Shimokuni T, Tanimoto K, Hiyama K, Otani K, Ohtaki M, Hihara J, Yoshida K, Hiyama E, Noguchi T, Nishiyama M. Selection of a novel drug-response predictor in esophageal cancer: A novel screening method using microarray and identification of IFITM1 as a potent marker gene of CDDP response. Int J Oncol. 2008; 32:413-423.
20. Li D, Peng Z, Tang H, Wei P, Kong X, Yan D, Huang F, Li Q, Le X, Li Q, Xie K. KLF4-mediated negative regulation of IFITM3 expression plays a critical role in colon cancer pathogenesis. Clin Cancer Res. 2011; 17:3558-3568.
21. Moffatt P, Gaumond MH, Salois P, Sellin K, Bessette MC, Godin E, de Oliveira PT, Atkins GJ, Nanci A, Thomas G. Bril: A novel bone-specific modulator of mineralization. J Bone Miner Res. 2008; 23:1497-1508.
22. Semler O, Garbes L, Keupp K, Swan D, Zimmermann K, Becker J, Iden S, Wirth B, Eysel P, Koerber F, Schoenau E, Bohlander SK, Wollnik B, Netzer C. A mutation in the 5'-UTR of IFITM5 creates an in-frame start codon and causes autosomal-dominant osteogenesis imperfecta type V with hyperplastic callus. Am J Hum Genet. 2012; 91:349-357.
23. Liu BY, Lu YQ, Han F, Wang Y, Mo XK, Han JX. Effects of the overexpression of IFITM5 and IFITM5 c.-14C>T mutation on human osteosarcoma cells. Oncol Lett. 2017; 13:111-118.
24. Zhang Z, Liu J, Li M, Yang H, Zhang C. Evolutionary dynamics of the interferon-induced transmembrane gene family in vertebrates. Plos One. 2012; 7:e49265.
25. Perreira JM, Chin CR, Feeley EM, Brass AL. IFITMs restrict the replication of multiple pathogenic viruses. J Mol Biol. 2013; 425:4937-4955.
26. Li K, Markosyan RM, Zheng YM, Golfetto O, Bungart B, Li M, Ding S, He Y, Liang C, Lee JC, Gratton E, Cohen FS, Liu SL. IFITM proteins restrict viral membrane hemifusion. PLoS Pathog. 2013; 9:e1003124.
27. Huang IC, Bailey CC, Weyer JL, *et al*. Distinct patterns of IFITM-mediated restriction of filoviruses, SARS coronavirus, and influenza A virus. PLoS Pathog. 2011; 7:e1001258.
28. Lu J, Pan Q, Rong L, He W, Liu SL, Liang C. The IFITM proteins inhibit HIV-1 infection. J Virol. 2011; 85:2126-2137.
29. Smith SE, Gibson MS, Wash RS, Ferrara F, Wright E, Temperton N, Kellam P, Fife M. Chicken interferon-inducible transmembrane protein 3 restricts influenza viruses and lyssaviruses in vitro. J Virol. 2013; 87:12957-12966.
30. Yu F, Ng SS, Chow BK, Sze J, Lu G, Poon WS, Kung HF, Lin MC. Knockdown of interferon-induced transmembrane protein 1 (IFITM1) inhibits proliferation, migration, and invasion of glioma cells. J Neurooncol. 2011; 103:187-195.
31. Hickford D, Frankenberg S, Shaw G, Renfree MB. Evolution of vertebrate interferon inducible transmembrane proteins. BMC Genomics. 2012; 13:155.
32. Okuzaki Y, Kidani S, Kaneoka H, Iijima S, Nishijima KI. Characterization of chicken interferon-inducible transmembrane protein-10. Biosci Biotechnol Biochem. 2017; 81:914-921.
33. He J, Li J, Feng W, Chen L, Yang K. Prognostic significance of INF-induced transmembrane protein 1 in colorectal cancer. Int J Clin Exp Pathol. 2015; 8:16007-16013.

(Received October 1, 2017; Revised October 25, 2017; Accepted October 31, 2017)

Supplemental Data

Supplementary Table S1. the IFITM primer sequence of rat

Gene name	Upstream primer sequence (5'-3')	Downstream primer sequence (5'-3')
IFITM1-1	TGAGATCTCCACGCCTGAC	CCACCATCTTCCTGTCCCTA
IFITM1-2	GCTGAGATCTCCACGCCTG	ACCATCTTCCTGTCCCTAGA
IFITM1-3	CGACAACCACCACAATCAAC	CCATCTTCCTGTCCCTAGACTTC
IFITM2-1	CTGGTCCCTGTTCAATACGC	CATCTTCCTGTCCCTGGACTT
IFITM2-2	GGTCTGGTCCCTGTTCAATA	CACCATCTTCCTGTCCCTGGA
IFITM2-3	CGGTAGTCTTTCAGTCGCTTTC	TGTGGACAGATATACGAAGGT
IFITM3-1	CTGGTCCCTGTTCAATACGC	ACCATCTTCCGATCCCTAGAC
IFITM3-2	GTCTGGTCCCTGTTCAATAC	CCACCATCTTCCGATCCCTAG
IFITM3-3	TCAACATGCCCAGAGAGGT	CCATCTTCCGATCCCTAGACT
IFITM5-1	ATCTGTGCTGCCTTGGTTTC	GCTTTGGAGCCATACTGCTT
IFITM5-2	CTGTGCTGCCTTGGTTTCCT	TTTGGAGCCATACTGCTTTG
IFITM5-3	GCTGGTCCACTCTGTCAAGG	GTCCCAGGAGCAGCAATG
IFITM6-1	CTGGTCCACATTCAGCACA	CATCTTCCTGTCCCTGGACTT
IFITM6-2	TGTGGTTTACATCAACAGTGACA	CATCTTCCTGTCCCTGGACTT
IFITM6-3	GGGTTTCATTGCCTATGTCTACTC	TGATAAGTATGATGAAGCAGACGAC
IFITM7-1	GTGTTCAACGTGCCCAGAG	ATTGAACAGGGACCAGACCA
IFITM7-2	ACGCTCTTCATGAACTTCTGC	TCTGCCGATCCCTACACTTC
IFITM7-3	TGGTCTGGTCCCTGTTCAAT	TCTGCCGATCCCTACACTTC
IFITM10-1	GACACCACAGAGGTGAACGA	GCTTCTTGTCCCGAACTTTG
IFITM10-2	AGTAGGTGAGCGGTACTGGTG	GCCTGGGAATCCAGAAGG
IFITM10-3	TGGGAACAAAGTGGAGTGCT	CAGCCAGAGCCTGACTCAC
β-Actin	GGCAATGAGCGGTTCCGAT	TGCCTGGGTACATGGTGGT

Original Article

DOI: 10.5582/irdr.2017.01069

Differences of basic and induced autophagic activity between K562 and K562/ADM cells

Feifei Wang[1,2,3,4], Jing Chen[5], Zhewen Zhang[5], Juan Yi[5], Minmin Yuan[1,2,3,4], Mingyan Wang[1,2,3,4], Na Zhang[1,2,3,4], Xuemin Qiu[1,2,3,4], Hulai Wei[5,*], Ling Wang[1,2,3,4,*]

[1] *Obstetrics and Gynecology Hospital, Fudan University, Shanghai, China;*
[2] *The Academy of Integrative Medicine of Fudan University, Shanghai, China;*
[3] *Laboratory for Reproductive Immunology, Hospital & Institute of Obstetrics and Gynecology, Fudan University Shanghai Medical College, Shanghai, China;*
[4] *Shanghai Key Laboratory of Female Reproductive Endocrine Related Diseases, Shanghai, China;*
[5] *Key Laboratory of Preclinical Study for New Drugs of Gansu Province, School of Basic Medical Sciences, Lanzhou University, Lanzhou, Gansu Province, China.*

Summary **Patients with acute myeloid leukemia (AML) often have a poor prognosis due to drug resistance, which is regarded as a tough problem during the period of clinical therapeutics. It has been reported that autophagy, an important event in various cellular processes, plays a crucial role in mediating drug-resistance to cancer cells. Our study attempts to comparatively investigate the differences of basic and induced autophagic activity between drug-sensitive and multidrug-resistant AML cells. The level of basic autophagy in K562/ADM cells was higher than that in K562 cells, which could be characterized by more cytosolic contents-packaged autophagic vacuoles in K562/ADM cells when compared to that in K562 cells. The observation of MDC staining showed that the fluorescent intensity of autophagosomes in K562/ADM cells was stronger than that in K562 cells. The expression of Beclin1 and the ratio of LC3-II to LC3-I were distinctly higher in K562/ADM cells, however, P62 protein was relatively lower in K562/ADM cells. Furthermore, we found that nutrient depletion could induce autophagic activity of both cell lines. However, autophagic activity of K562/ADM cells was always maintained at a higher level in contrast with K562 cells. ADM (Adriamycin) was also capable of inducing autophagic activity of K562 and K562/ADM cells, but the autophagic alteration in K562 cells appeared earlier. Taken together, our findings suggest that autophagy exerts an important effect on formation and maintenance of drug-resistance in AML cells.**

Keywords: Autophagic activity, drug-resistance, acute myeloid leukemia

1. Introduction

Acute myeloid leukemia (AML) is a highly malignant hematological neoplasm, which is characterized by high morbidity, poor prognosis and high cost of treatment, leading it to be a malignant neoplasm with one of the highest mortality rates (*1*). Plenty of therapeutic drugs have been used to treat patients with AML and good efficacy has been achieved (*2*). However, among those refractory patients, both drug resistance and poor prognosis appeared (*3*). Therefore, it is urgent to investigate the differences between drug-resistant and -sensitive AML cells, which may contribute to dissection of mechanisms in drug resistance.

Autophagy is an important cellular process associated with lysosome-mediated self-degradation in eukaryotic cells (*4*). According to different manners of substrate

Released online in J-STAGE as advance publication November 14, 2017.

**Address correspondence to:*
Dr. Ling Wang, Obstetrics and Gynecology Hospital, Fudan University, 413 Zhaozhou Road, Shanghai 200011, China.
E-mail: Dr.wangling@fudan.edu.cn

Dr. Hulai Wei, Key Laboratory of Preclinical Study for New Drugs of Gansu Province, School of Basic Medical Sciences, Lanzhou University, 199 Donggang West Road, Lanzhou, 730000 Gansu Province, China.
E-mail: weihulai@lzu.edu.cn

degradation, autophagy is mainly classified into three categories including microautophagy, chaperone-mediated autophagy (CMA) and macroautophagy (*5*). Macroautophagy, referred to autophagy hereinafter, exerts its function through formation of autophagosomes and subsequently being fused with lysosomes, triggering substances being degraded by acid hydrolases. Consequently, the catabolites including amino acids, fatty acids, nucleotides and so on are recycled in cytoplasm to reenter biological energy pathways, ultimately maintaining structure and metabolism of cells (*6*).

It has been reported that multiples of ATG (autophagy-related) proteins are recruited to tightly regulate the occurrence of autophagy, during which LC3 (microtubule- associated protein 1 light-chain 3) plays critical roles in elongation and completion of the autophagosome. In this process, the protein LC3 is cleaved at its C-terminus by Atg4B, resulting in formation of LC3-I. Subsequently, LC3-I conjugates with PE (phosphatidyl ethanolamine) and leads generation of the form of membrane-bound LC3 that called LC3-II. LC3-II is employed to the membrane of the autophagosome and specifically mediates elongation of the autophagosome. Therefore, the ratio of LC3-II to LC3-I will become larger when the quantity of autophagosomes increases (*7*). In addition to the shift of LC3-I to LC3-II, another crucial ATG protein P62 that interacts with ubiquitinated proteins through its UBA domain (ubiquitin-associated domain) and then delivers them to LC3-II *via* another domain LIR (LC3-interacting region) will be finally degraded in the autolysosome, so the level of P62 has a contrary relationship with autophagic activity (*8*).

Over the past few decades, basal autophagy was reported to remove misfolded proteins and damaged organelles to maintain cellular quality and health, involved in many physical processes of cells such as cellular turnover, differentiation and development (*9-11*). Abnormal basal autophagy can lead to various human diseases including cancer, neurodegenerative disorders, autoimmunity disease and inflammation (*12-15*). Autophagy can be induced in response to several stressors including: nutrient deprivation, chemotherapeutics, hypoxia, pathogen infection and endoplasmic reticulum stress (*16-18*). A larger body of research has reported that autophagy which is promoted by chemotherapeutic drugs in cancer cells, is related to drug-resistance of tumor cells (*19-21*). Autophagy is activated by doxorubicin in human colon cancer LoVo cells, and this autophagic activation reduces the sensitivity of cancer cells to doxorubicin (*22*). Enhanced autophagy is a survival mechanism of drug-resistant esophageal cancer cells treated with cisplatin (*23*). In contrast, elemene can reverse the drug resistance of the cisplatin-resistant lung adenocarcinoma cells by promoting autophagy (*24*). To clarify the relationship between autophagy and drug-resistance of AML cells, we tried to compare autophagic activity between K562/ADM cells and ADM-sensitive K562 cells in different environments such as the basic state, starvation and ADM treatment.

2. Materials and Methods

2.1. *Chemicals and antibodies*

ADM was purchased from Kangbao biochemical industry company (Wuhan); HCQ (hydroxychloroquine) was bought from Tokyo Chemical Industry; MTT was obtained from Sigma; newborn bovine serum was from Rongye biotech company (Lanzhou); RPMI 1640 medium from Gibco; anti-P62, anti-LC3, anti-Beclin1 was from Cell Signaling Technology; anti-β-actin was from Biovision; HRP-linked anti-rabbit or anti-mouse IgG antibodies were from Boster biological technology company (Wuhan).

2.2. *Cell lines and culture*

Human ADM-resistant AML cell line (K562/ADM cells) and its parental cell line (K562 cells) were both from Medical experimental center of Lanzhou University. K562/ADM and K562 cells were grown in RPMI 1640 Medium supplied with 10% inactivated newborn bovine serum and 2 mmol/L L-glutamine at 37℃ in a humid atmosphere containing 5% CO_2. The viability of all cultured cells was determined for up to 95% before experiments were performed.

2.3. *Cell proliferation assay (MTT)*

Cells were seeded in 96-well plates at a density of 1×10^5 cells/mL in triplicate and were cultured with ADM at indicated concentrations and times at 37℃. MTT (5 mg/mL, 10 μL) was added to each well and cultured for another 4 h, and then 100 μL of acidifying sodium dodecyl sulfate (10%) was added to dissolve the formazan. 24 hours later, optical density (OD) was measured at 570 nm with a Powerwave X plate reader (Bio-Tek, USA). Cell proliferation inhibition rates were calculated using the following formula: cell proliferation inhibition rate = $[(OD_{control} - OD_{experiment})/OD_{control}] \times 100\%$ (*25*).

2.4. *MDC staining*

MDC has been reported to distinctively mark autophagic vesicles (*26*). Cells were harvested and washed twice with PBS. After resuspending in 1 mL of PBS, cells were stained with 1 μL of MDC stock-solution (50 mmol/L) of which terminal concentration reached 0.05 mmol/L for 30 min at 37℃ in the dark (*27*). Subsequently, cells were gently washed with PBS three times and observed under an IX81 inverted

microscope (Olympus, Japan).

2.5. *Transmission electron microscope detection*

Cells were fixed with glutaraldehyde overnight at 4℃. On the next day, after rinsing with PBS three times each for 5 min, cells were fixed for 1.5 h with osmic acid. Next, cells were rinsed with PBS again and dehydrated in the following steps: 50% alcohol for 10 min, 70% alcohol for 10 min, 90% alcohol for 10 min, 100% alcohol for 10 min, 100% acetone for 10 min twice. Subsequently, cells were embedded in an epoxy resin overnight and then solidified for 12 h at 45℃. Following slicing into sections, cells were stained with uranyl acetate and lead citrate. Finally, the ultrastructure of cells was observed under a JEM1230 transmission electron microscope (JEOL, Japan) (*28*).

2.6. *Real-Time quantitative RT-PCR*

Total RNA was isolated from cells with a Trizol kit following the manufacturer's specifications. Both the concentrations and purity of extracted RNA samples were determined by spectrophotometer. 500 ng of each RNA sample was used to synthesize cDNA with Prime Script RT Master Mix (Takara). Real-time PCR was performed with SYBR Premix Taq II (Takara) and primers. The primers used are as follows: *beclin1* forward: 5'-ACCTCAGCCGAAGACTGAAG-3', *beclin1* reverse: 5'-AACAGCGTTTGTAGTTCTGAC-3'; *β-actin* forward: 5'-TGCTCCTCCTGAGCGCAAGTA-3', *β-actin* reverse: 5'–CCACATCTGCTGGAAGGTGGA-3'. After the procedure was completed, the relative mRNA levels of genes indicated were analyzed by software Roto-Gene6.0 (*29*).

2.7. *Western blotting*

Cells were lysed in RIPA buffer with PMSF (PMSF:RIPA=1:100) for 30 min on ice and then centrifuged for 15 min. Protein concentration of the supernatant was measured using a BCA protein assay kit. Equal amounts of protein from cell extracts were separated by SDS-PAGE (sodium dodecyl sulfate polyacrylamide gel electrophoresis) and transferred onto a PVDF (polyvinylidene fluoride) membrane (*30*). The membrane was incubated with primary antibodies overnight at 4℃ and then with secondary antibodies conjugated with horseradish peroxidase. Finally, the protein level was determined using a chemiluminescent approach in a dark room.

2.8. *Statistical analysis*

All data were statistically analyzed with the student's *t*-test by utilizing SPSS 17.0 software. *P*-value < 0.05 was considered statistically significant.

3. Results

3.1. *ADM inhibits the proliferation of K562 cells greater than K562/ADM cells*

To investigate the sensitivities of K562/ADM and K562 cells to chemotherapeutic drug, we treated these two cell lines with a gradually increased concentration of ADM for different times as indicated. The MTT assay showed that ADM inhibited the growth of K562/ADM and K562 cells to various extents, and ADM-induced cytotoxicity in both cell lines was dose- and time-dependent (Figure1A and 1B). We calculated IC_{50} values of ADM for K562 and K562/ADM cells, which showed that IC_{50} values of ADM for K562 cells for 12 h, 24 h, 48 h were 2.63 ± 0.12, 1.04 ± 0.04, 0.25 ± 0.05 μmol/L respectively and the corresponding values for K562/ADM cells were 54.19 ± 0.87, 46.46 ± 4.36, 15.44 ± 0.81 μmol/L (Figure1C). The degree of ADM-resistance for K562/ADM cells was 20.6~62.9 fold greater when compared with that of K562 cells, suggesting K562/ADM cells have more potential for resistance to ADM than K562 cells.

3.2. *K562/ADM cells show higher basic autophagic activity than K562 cells*

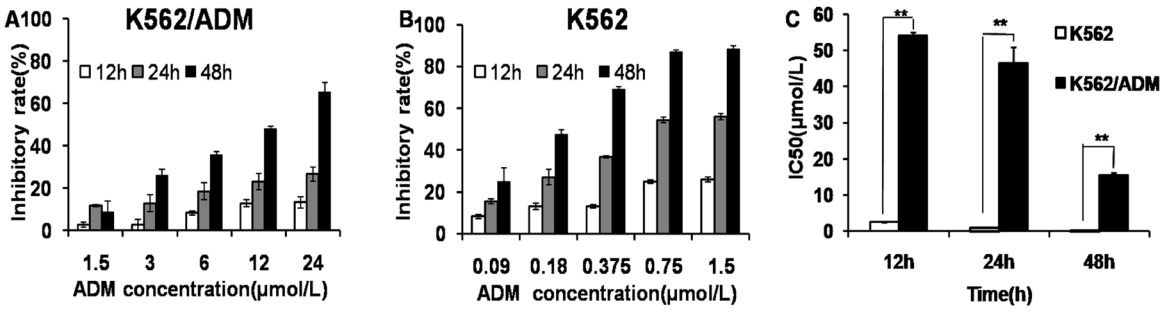

Figure 1. ADM inhibits the proliferation of K562 cells greater than K562/ADM cells. (A) K562/ADM cells were exposed to 1.5, 3, 6, 12 and 24 μmol/L ADM for 12, 24, 48 h, and then MTT assay was performed to detect cell viability; **(B)** K562 cells were treated with 0.09, 0.18, 0.375, 0.75, 1.5 μmol/L ADM for 12, 24, 48h separately, and then MTT assay was performed to determinate cell proliferation; **(C)** IC_{50} values of ADM for K562 and K562/ADM cells. Results are all presented as the mean ± Standard Deviation (SD) of four separate experiments. ***p* < 0.01 versus K562 cells.

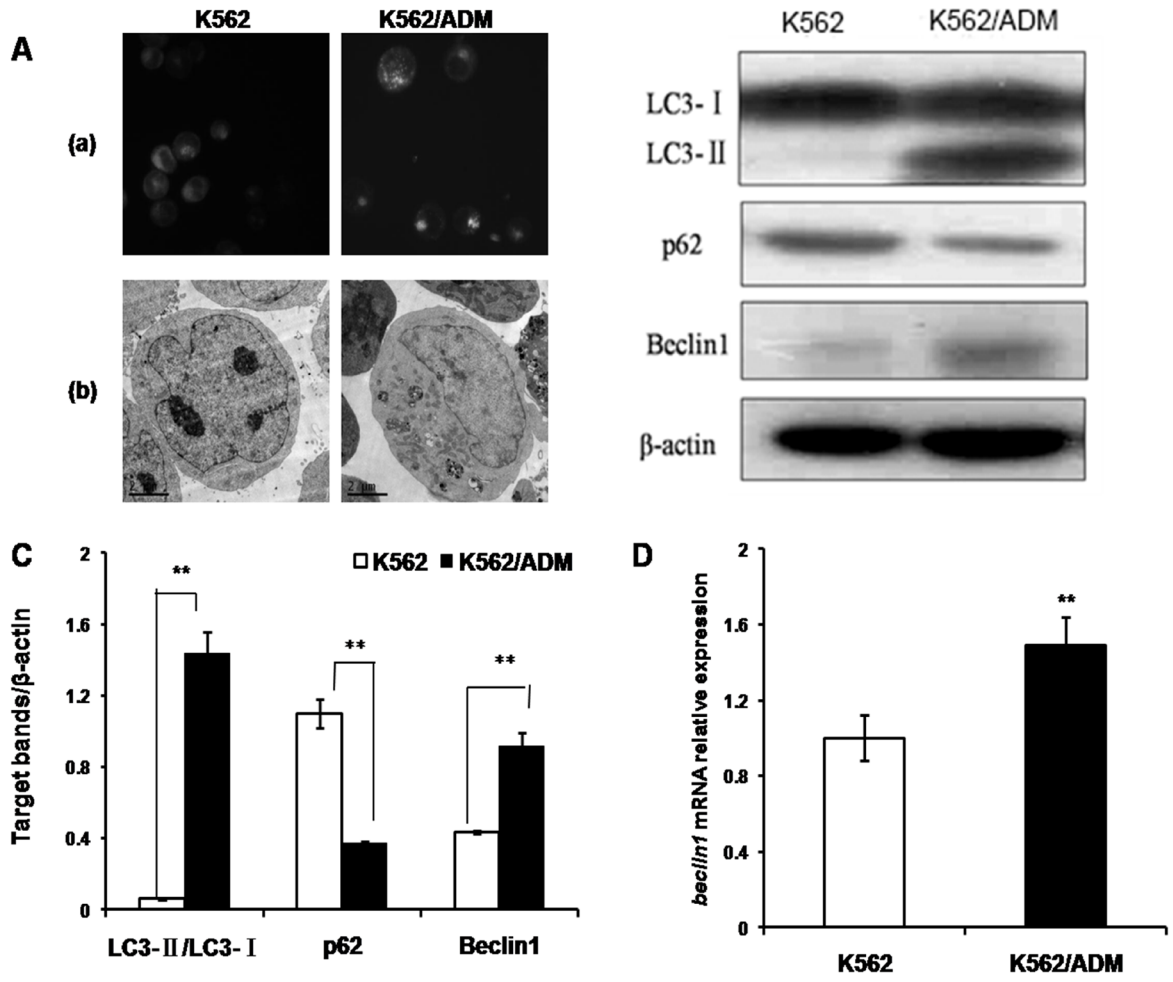

Figure 2. K562/ADM cells show higher basic autophagic activity than K562 cells. (A) Autophagic morphology was observed by fluorescent microscopy followed by MDC staining (×100) (a); Autophagosomes were observed by transmission electron microscope (×8,000) (b); **(B, C)** Expression levels of LC3, P62 and Beclin1 were detected by Western blot; **(D)** Relative expressions of *beclin1* mRNA in two cell lines were analyzed by real-time quantitative RT-PCR. Values are mean ± SD of three separate experiments. $^{**}p < 0.01$ versus K562 cells.

To explore the relationship between autophagy and ADM resistance, we first measured the basic autophagy activities of K562/ADM and K562 cells. After observation of autophagosomes in cells under the fluorescent microscope followed by MDC staining, we found that K562 cells exhibited weak fluorescent intensity in the cytosol, whereas some bright foci could be seen in K562/ADM cells (Figure 2A). A similar result was also found using the transmission electron microscope, a gold standard for determining autophagic activity, which showed more cytosolic contents-packaged autophagic vacuoles in K562/ADM cells when compared with K562 cells (Figure 2A). To further verify the results above, we examined other autophagic indicators such as LC3 and P62/SQSTM1. As shown in Figure 2B and 2C, K562/ADM cells showed a much higher ratio of LC3-II to LC3-I and relatively lower P62 levels when compared with K562 cells, indicating that K562/ADM cells had a higher level of autophagy flux. In addition, *beclin1* is one of the specific genes involved in autophagy regulation. Our results displayed the level of Beclin1, mRNA expression or protein expression, was much higher in K562/ADM cells compared to K562 cells, indicating that Beclin1 might be involved in regulating basic autophagy of these two cell lines (Figure 2C and 2D).

3.3. *Starvation-induced autophagic activity of K562/ADM and K562 cells*

To compare the different autophagic variations between K562/ADM and K562 cells in nutrition depletion, we cultured the cells in serum- and amino acid-free EBSS (Earle's Balanced Salt Solution) for different times. After observing with the fluorescent microscope, we found abundant fluorescent puncta distributed in the cytosol of K562/ADM and K562 cells starved for 1h, which showed stronger fluorescent intensity relative to untreated cells (Figure 3A). A huge number of typical autophagic vesicles were also observed using the transmission electron microscope in the cytosol of starved cells (Figure 3B). Western blot results

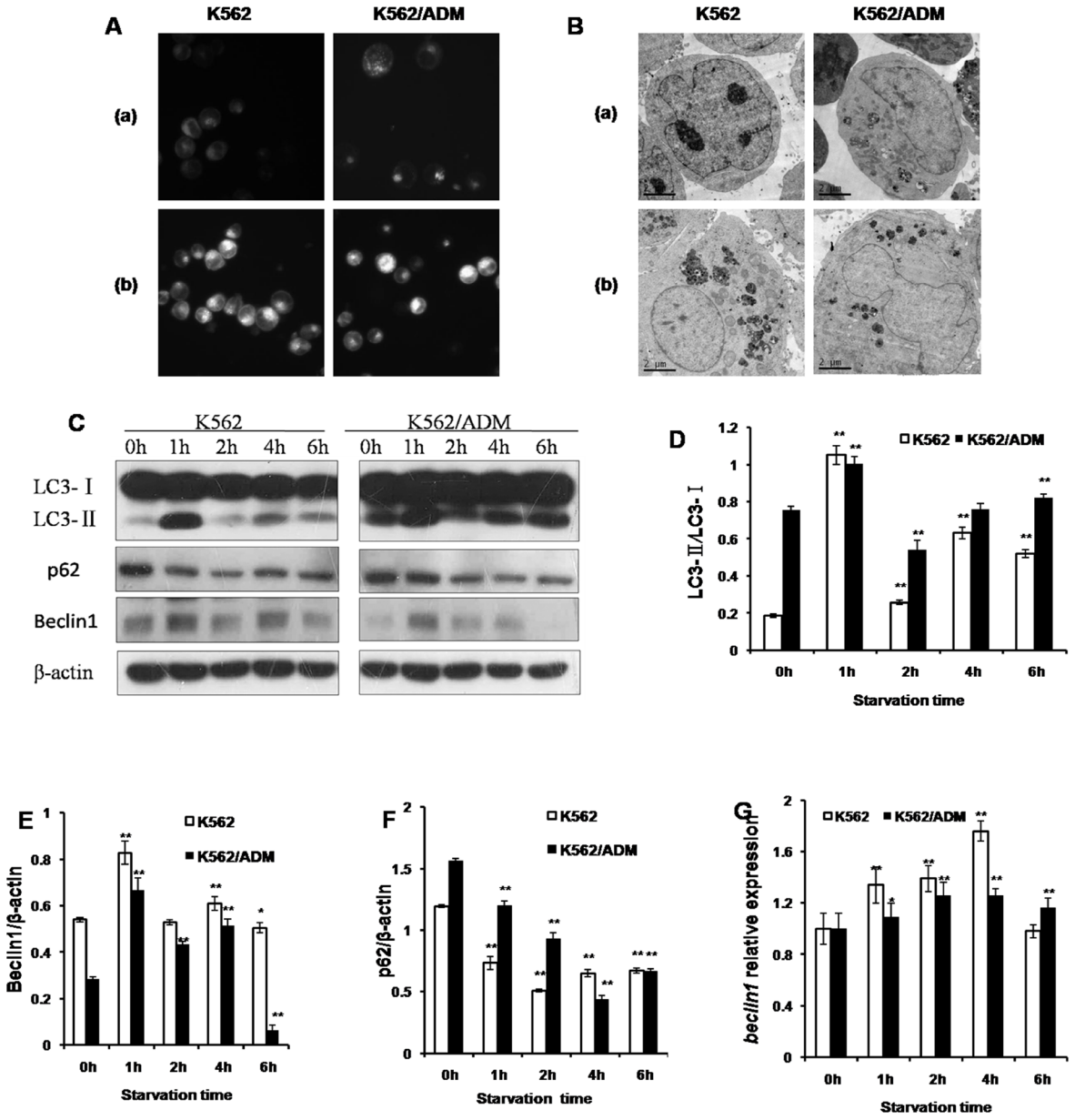

Figure 3. Starvation-induced autophagic activity of K562/ADM and K562 cells. (A) K562/ADM and K562 cells were cultured in EBSS for 0 h (a), 1 h (b), autophagic morphology was observed under a fluorescent microscope (×100); **(B)** Two cell lines were cultivated in EBSS for 0 h (a), 1 h (b), autophagosomes were observed by transmission electron microscopy (×8,000); **(C)** K562/ADM and K562 cells were cultured in EBSS for 0 h,1 h, 2 h, 4 h, 6 h. The levels of LC3, P62 and Beclin1 were determined by Western blot. **(D, E, F)** Densitometric analysis of LC3-II/LC3-I, Beclin1 and P62 normalized to β-actin in K562/ADM and K562 cells starved for 0 h,1 h, 2 h, 4 h, 6 h**; (G)** Relative expressions of *beclin1* mRNA in two cell lines starved for 0 h,1 h, 2 h, 4 h, 6 h were analyzed by real-time quantitative RT-PCR. Values are presented as mean ± SD of three separate experiments. $^{*}p < 0.05$, $^{**}p < 0.01$ *versus* control cells (starvation for 0 h).

described that both the expression of Beclin1 and the ratio of LC3-II to LC3-I reached peak value in 1hour of starvation and then gradually decreased while the degradation of P62 reached peak value after 2~4 hours of starvation. However, according to LC3-II level variation, it was found that autophagic activity of K562/ADM cells always maintained a higher level in contrast with that of K562 cells (Figure 3C-3F). Additionally, the results of RT-PCR indicated *beclin1* mRNA expression was enhanced in two cell lines after starvation (Figure 3G). Taken together, autophagy is induced in K562/ADM and K562 cells in a state of nutrition depletion, however, starvation-induced autophagic activity of K562/ADM cells is significantly stronger than K562 cells.

3.4. ADM potentiates autophagic activity of K562/ADM and K562 cells

To explore the different autophagic appearance in two cell lines with ADM exposure, K562/ADM and K562 cells were treated with 35 μmol/L and 0.75 μmol/L of ADM separately for 12 h or 24 h. Observing through the fluorescent microscope and transmission electron

microscope, ADM enhanced the intensity of fluorescent dots and the amount of autophagic vacuoles in cytosol of both cell lines (Figure 4). The same results were also obtained in cells with exposure to HCQ, a recognized autophagy inhibitor (Figure 4). To investigate whether HCQ can inhibit ADM-induced autophagy, K562/ADM and K562 cells were pre-treated with 16 μmol/L and 4 μmol/L HCQ respectively for 3 h before exposure to ADM. We found HCQ resulted in upregulated intensity of fluorescent dots and increased autophagic vacuoles in K562/ADM and K562 cells with ADM treatment (Figure 4).

It is acknowledged that the accumulation of autophagic vacuoles is attributed either to up-regulated autophagosome generation or to down-regulated autophagosome degradation (*31*). As Figure 5 showed, ADM induced the rise of the LC3-II/LC3-I ratio and Beclin1 expression along with a fall of P62 level, which suggested that ADM promoted autophagy flux and the accumulation of autophagic vacuoles induced by ADM should be attributable to up-regulated autophagosome generation. However, ADM-induced autophagic alteration happened earlier in K562 cells with ADM treatment for 12 h than in K562/ADM cells exposed to ADM for 24 h. In addition, HCQ led to an increased ratio of LC3-II/LC3-I and up-regulated P62 level in

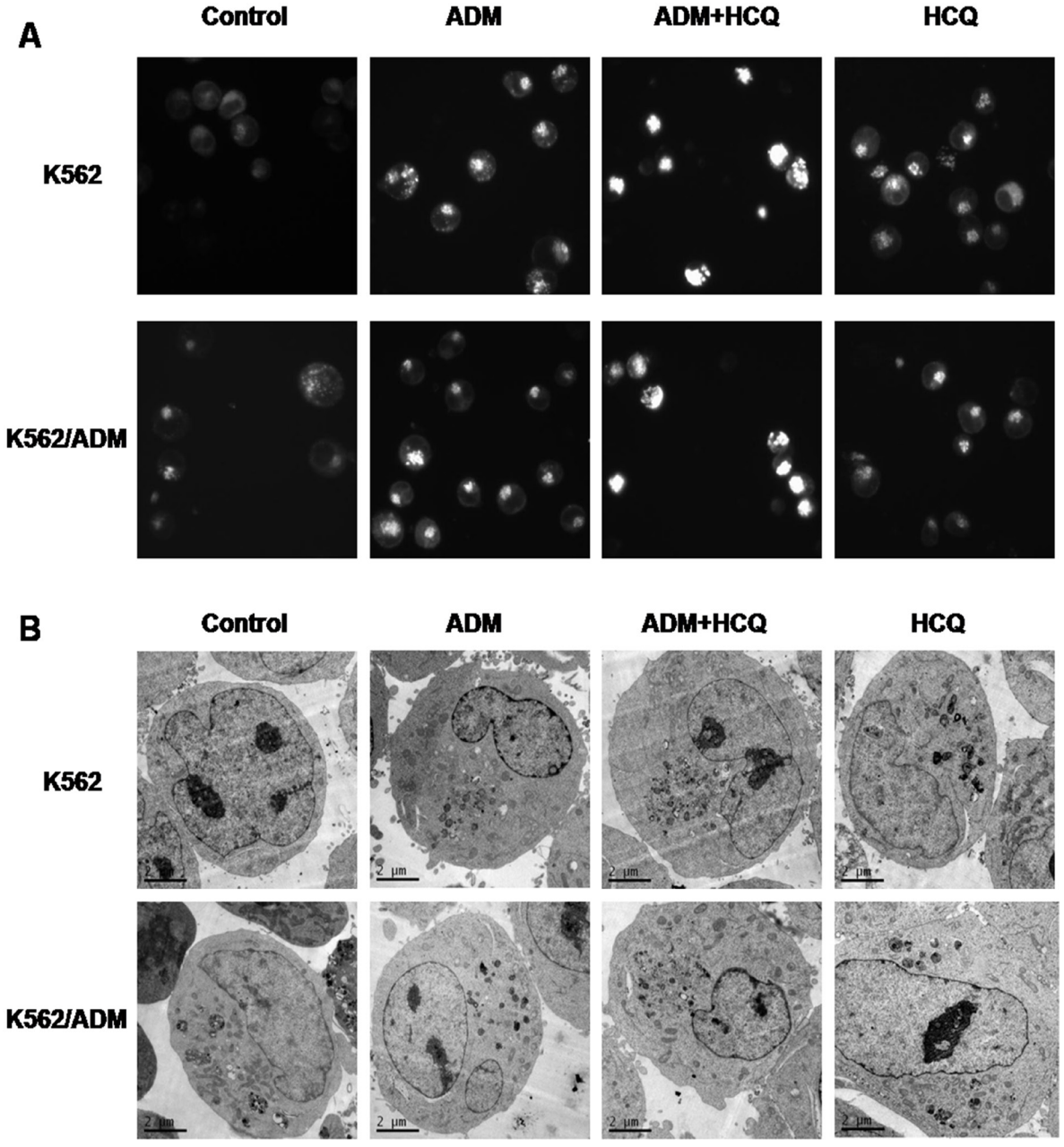

Figure 4. The morphological changes of autophagy in ADM-induced K562 and K562/ADM cells. K562/ADM and K562 cells were respectively treated with 35 and 0.75 μmol/L of ADM alone for 24 h, or 16 and 4 μmol/L of HCQ alone for 12 h, or were pre-treated with HCQ for 3 h before exposure to ADM for 24 h. **(A)** Autophagy morphology was observed under a fluorescent microscope (×100); **(B)** Cellular ultrastructure was observed by transmission electron microscopy (×8,000).

the two cell lines, indicating HCQ hindered autophagy progression and the accumulation of autophagic vesicles induced by HCQ was derived from restrained degradation of autophagy. Furthermore, HCQ increased the level of LC3-II and P62, and had a diminishing effect on Beclin1 level in the case of cells exposed to ADM, implying that HCQ was capable of inhibiting ADM-induced autophagic activity by blocking the degradation of the autophagosome. The relative expression alteration of *beclin1* mRNA detected by RT-PCR was consistent with that analyzed by Western blot.

4. Discussion

Most AML patients are prone to acquire chemotherapy resistance, which remains a troublesome obstacle for

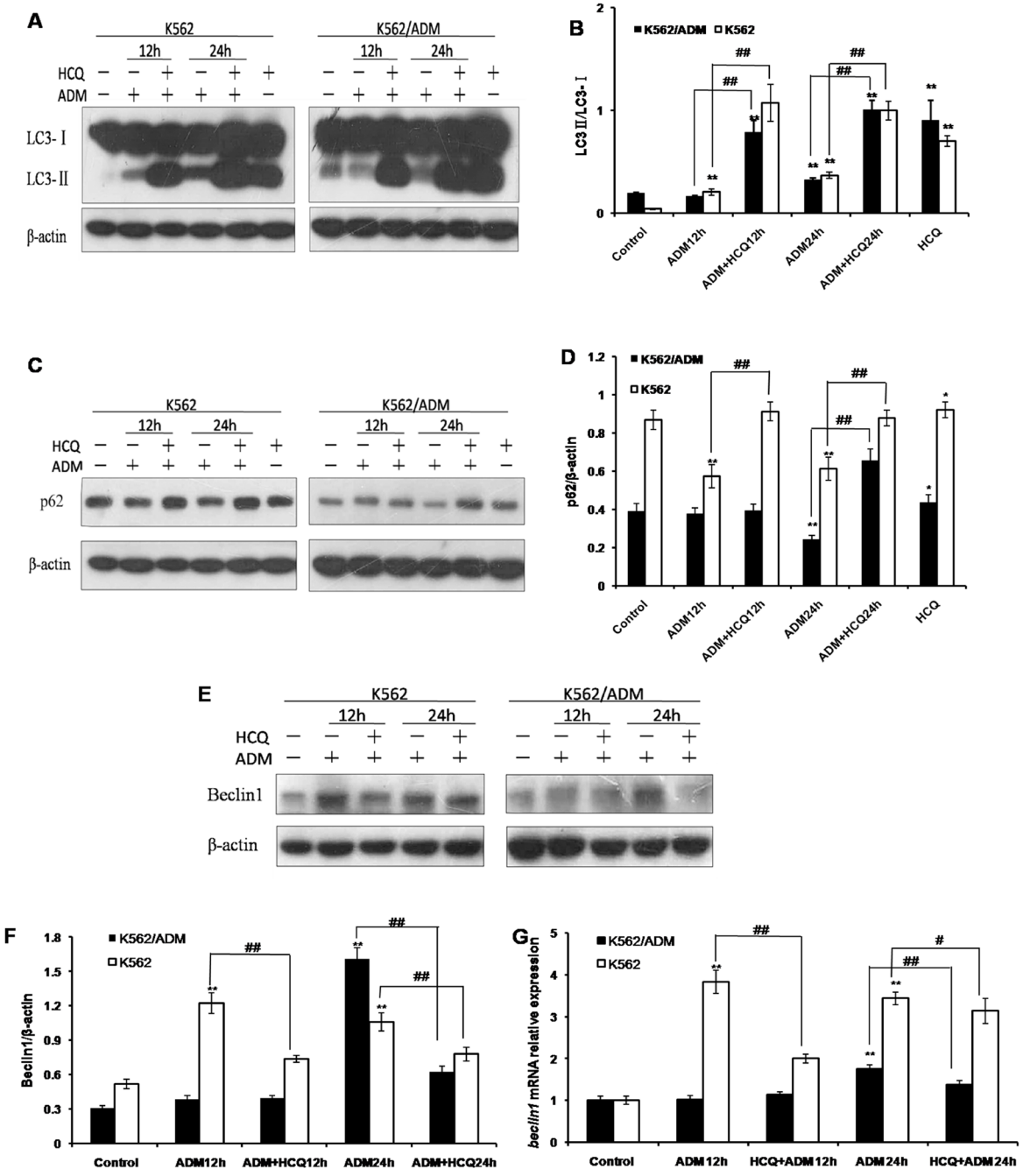

Figure 5. ADM potentiates autophagic activity of K562/ADM and K562 cells. K562/ADM cells were exposed to ADM (35 μmol/L) alone for 12 or 24 h, or treated with HCQ (16 μmol/L) alone for 12 h, or pre-treated with HCQ for 3 h before treatment with ADM for 12 or 24 h. The same procedures were applied to K562 cells with different drugs concentration. In detail, K562 cells were treated with ADM (0.75μmol/L) alone for 12 or 24 h, or HCQ (4 μmol/L) alone for 12 h, or treated with ADM for 12 or 24 h followed by administration of HCQ for 3 h. **(A)** Western blot analysis for translation of LC3-I to LC3-II was performed on lysates from cells treated as above; **(B)** Densitometric analysis of LC3-II/LC3-I normalized to β-actin; **(C)** Expression level of P62 was quantified by Western blot; **(D)** Densitometric analysis of P62 was normalized to β-actin; **(E)** Beclin1 level was monitored by Western blot; **(F)** Densitometric analysis of Beclin1 normalized to β-actin; **(G)** *Beclin1* mRNA relative expression was detected by RT-PCR. Values are mean ± SD of three separate experiments. $^{**}p < 0.01$*versus* untreated cells. $^{\#}p < 0.05$, $^{\#\#}p < 0.01$ *versus* ADM-treated cells.

clinical therapy. Emerging evidence suggests that anti-cancer therapeutic agents can induce autophagy of cancer cells (*32*), which may have a vital effect on drug-resistance. Autophagy inhibition by CQ (chloroquine) significantly enhances the sensitivity of DOX-resistant human acute myelocytic leukemia HL60 cells to DOX (*33*). Heterogeneous nuclear ribonucleoprotein K (hnRNP K) may be associated with the development of ADM resistance in AML by augmenting autophagy (*34*). Inhibition of WAVE1 expression enhances the sensitivity of leukemia cells to chemotherapy by downregulating autophagy (*35*). All this research indicates that autophagy is a mechanism involved in chemotherapy resistance of various leukemia cells. To further elucidate this problem, it is required to analyze the differences of autophagic variation between AML chemoresistant K562/ADM cells and sensitive K562 cells.

K562/ADM cells are a multidrug-resistant cell line acquired by exposing K562 cells to step-wise increasing concentrations of ADM. It is characterized by being resistant not only to ADM, but also to mitoxantrone, homoharringtonine, rubidomycin and etoposide (*36*). K562/ADM cells appear to have sophisticated cross drug-resistance to all these anti-cancer drugs with quite different structures and functions. Our experiments also showed that the IC_{50} of K562/ADM cells was 20.6~62.9 fold greater than that of K562 cells, verifying that K562/ADM cells were highly resistant to ADM-induced proliferation inhibition and apoptosis.

Here, we found that basic autophagy in K562/ADM cells was distinctly higher than that in K562 cells, which could be indicated by more cytosolic contents-packaged autophagic vacuoles, higher Beclin1 expression level and LC3-II/LC3-I ratio, and lower P62 level in K562/ADM cells. Similar results are also obtained in a multiple myeloma cell line, Pan *et al*. (*37*) reported that expression level of LC3-II was higher in DOX-resistant RPMI8226/DOX cells than in DOX-sensitive RPMI8226/S cells. Similarly, compared with K562 cells, there is an increased PI3K/AKT/mTOR signaling and enhanced autophagic activity in imatinib-resistant human chronic myelogenous leukemia K562R cells (*38*).

We further investigated the different autophagic appearance between K562 and K562/ADM cells under serum depletion. A report has described that activation of autophagy is critical for cancer cellular survival under nutrient starvation (*39*). Another report also demonstrates that CD133-positive glioma cells exhibit higher survival under starvation conditions, which depends on induction of autophagy (*40*). Furthermore, autophagy induced by amino acid starvation is accelerated in the multidrug-resistant cells when compared to parental cells, resulting in enhanced cell survival capacity (*41*). Here, we found that starvation-induced autophagic activity of K562/ADM cells was significantly stronger relative to that of K562 cells, which may decipher why K562/ADM cells possess potent resistance to extra stressors. In conclusion, our results showed K562/ADM cells exhibited a higher basic and starvation-induced autophagy, indicating autophagy exerts a vital effect on formation and maintenance of drug-resistance in AML cells.

It is generally accepted that ADM, a canonical anthracycline chemotherapeutic drug, can induce cell death with apoptosis being involved (*42*). More evidence shows that ADM is also capable of inducing autophagy (*43*). Here we found that ADM induced autophagy in both K562/ADM and K562 cells, but the autophagic alteration in K562 cells appeared earlier, which might be attributed to its lower basic autophagic activity. In addition, HCQ suppressed autophagy flux through blocking degradation of autophagosomes. In line with this result, a recent study showed HCQ could inhibit late stage of the autophagy process by hindering lysosomal acidification (*44*). We also found that HCQ inhibited ADM-induced autophagic activity by restraining the degradation of the autophagosome.

Taken together, our findings suggest that autophagy exerts an important effect on formation and maintenance of drug-resistance in AML cells, however, the mechanism is still not clearly defined and is required to be investigated further and more deeply. However, our findings provide some insight into understanding the relationship between autophagy and chemoresistance in AML patients.

Acknowledgements

The present study was supported by the National Natural Science Foundation of China No. 81541025 (to HL Wei), the Fundamental Research Funds for the Central Universities No. lzujbky-2016-174 (to HL Wei) and the Natural Science Fund of Gansu No. 1208RJZA183 (to HL Wei). This work was also supported by the National Natural Science Foundation of China No. 31571196 (to L Wang), the Science and Technology Commission of Shanghai Municipality 2015 YIXUEYINGDAO project No. 15401932200 (to L Wang), the FY2008 JSPS Postdoctoral Fellowship for Foreign Researchers P08471 (to L Wang), the National Natural Science Foundation of China No. 30801502 (to L Wang), the Shanghai Pujiang Program No. 11PJ1401900 (to L Wang), Development Project of Shanghai Peak Disciplines-Integrative Medicine No. 20150407.

References

1. Arber DA, Orazi A, Hasserjian R, Thiele J, Borowitz MJ, Le Beau MM, Bloomfield CD, Cazzola M, Vardiman JW. The 2016 revision to the World Health Organization classification of myeloid neoplasms and acute leukemia. Blood. 2016; 127:2391-2405.

2. Kavanagh S, Murphy T, Law A, Yehudai D, Ho JM, Chan S, Schimmer AD. Emerging therapies for acute myeloid leukemia: Translating biology into the clinic. JCI insight. 2017; 2:e95679. doi: 10.1172/jci.insight.95679.
3. Gao W, Estey E. Moving toward targeted therapies in acute myeloid leukemia. Clin Adv Hematol Oncol. 2015; 13:748-754.
4. Zhi X, Feng W, Rong Y, Liu R. Anatomy of autophagy: From the beginning to the end. Cell Mol Life Sci. 2017. doi: 10.1007/s00018-017-2657-z.
5. Galluzzi L, Baehrecke EH, Ballabio A, et al. Molecular definitions of autophagy and related processes. EMBO J. 2017; 36:1811-1836.
6. Lee YK, Lee JA. Role of the mammalian ATG8/LC3 family in autophagy: Differential and compensatory roles in the spatiotemporal regulation of autophagy. BMB Rep. 2016; 49:424-430.
7. Wild P, McEwan DG, Dikic I. The LC3 interactome at a glance. J Cell Sci. 2014; 127:3-9.
8. Liu WJ, Ye L, Huang WF, Guo LJ, Xu ZG, Wu HL, Yang C, Liu HF. p62 links the autophagy pathway and the ubiqutin-proteasome system upon ubiquitinated protein degradation. Cell Mol Biol Lett. 2016; 21:29.
9. Vescarelli E, Pilloni A, Dominici F, Pontecorvi P, Angeloni A, Polimeni A, Ceccarelli S, Marchese C. Autophagy activation is required for myofibroblast differentiation during healing of oral mucosa. J Clin Periodontol. 2017; 44:1039-1050.
10. Rademacher BL, Matkowskyj KA, Meske LM, Romero A, Sleiman H, Carchman EH. The role of pharmacologic modulation of autophagy on anal cancer development in an HPV mouse model of carcinogenesis. Virology. 2017; 507:82-88.
11. Nguyen-McCarty M, Klein PS. Autophagy is a signature of a signaling network that maintains hematopoietic stem cells. PloS One. 2017; 12:e0177054.
12. Levy JMM, Towers CG, Thorburn A. Targeting autophagy in cancer. Nat Rev Cancer. 2017; 17:528-542.
13. Budini M, Buratti E, Morselli E, Criollo A. Autophagy and its impact on neurodegenerative diseases: New roles for TDP-43 and C9orf72. Front Mol Neurosci. 2017; 10:170.
14. Morandi E, Jagessar SA, t Hart BA, Gran B. EBV infection empowers human B cells for autoimmunity: Role of autophagy and relevance to multiple sclerosis. J Immunol. 2017; 199:435-448.
15. Cosin-Roger J, Simmen S, Melhem H, Atrott K, Frey-Wagner I, Hausmann M, de Valliere C, Spalinger MR, Spielmann P, Wenger RH, Zeitz J, Vavricka SR, Rogler G, Ruiz PA. Hypoxia ameliorates intestinal inflammation through NLRP3/mTOR downregulation and autophagy activation. Nat Commun. 2017; 8:98.
16. Maertin S, Elperin JM, Lotshaw E, Sendler M, Speakman SD, Takakura K, Reicher BM, Mareninova OA, Grippo PJ, Mayerle J, Lerch MM, Gukovskaya AS. Roles of autophagy and metabolism in pancreatic cancer cell adaptation to environmental challenges. Am J Physiol Gastrointest Liver Physiol. 2017; ajpgi.00138.02017. doi: 10.1152/ajpgi.00138.2017.
17. Hu F, Guo XL, Zhang SS, Zhao QD, Li R, Xu Q, Wei LX. Suppression of p53 potentiates chemosensitivity in nutrient-deprived cholangiocarcinoma cells *via* inhibition of autophagy. Oncol Lett. 2017; 14:1959-1966.
18. Zhang W, Wan X, Liu Z, Xiao L, Huang H, Liu X. The emerging role of oxidative stress in regulating autophagy: Applications of cancer therapy. Cell Mol Biol (Noisy-le-grand). 2017; 63:67-76.
19. Pagotto A, Pilotto G, Mazzoldi EL, Nicoletto MO, Frezzini S, Pasto A, Amadori A. Autophagy inhibition reduces chemoresistance and tumorigenic potential of human ovarian cancer stem cells. Cell Death Dis. 2017; 8:e2943.
20. Xu XD, Zhao Y, Zhang M, He RZ, Shi XH, Guo XJ, Shi CJ, Peng F, Wang M, Shen M, Wang X, Li X, Qin RY. Inhibition of autophagy by deguelin sensitizes pancreatic cancer cells to doxorubicin. Int J Mol Sci. 2017; 18:370.
21. Zhang P, Liu X, Li H, Chen Z, Yao X, Jin J, Ma X. TRPC5-induced autophagy promotes drug resistance in breast carcinoma *via* CaMKKβ/AMPKα/mTOR pathway. Sci Rep. 2017; 7:3158.
22. Fang LM, Li B, Guan JJ, Xu HD, Shen GH, Gao QG, Qin ZH. Transcription factor EB is involved in autophagy-mediated chemoresistance to doxorubicin in human cancer cells. Acta Pharmacol Sin. 2017; 38:1305-1316.
23. Cheng CY, Liu JC, Wang JJ, Li YH, Pan J, Zhang YR. Autophagy inhibition increased the anti-tumor effect of cisplatin on drug-resistant esophageal cancer cells. J Biol Regul Homeost Agents. 2017; 31:645-652.
24. Zhou K, Wang L, Cheng R, Liu X, Mao S, Yan Y. Elemene increases autophagic apoptosis and drug sensitivity in human cisplatin (DDP)-resistant lung cancer cell line SPC-A-1/DDP by inducing beclin-1 expression. Oncol Res. 2017. doi: 10.3727/096504017X14954936991990.
25. Li LJ, Li GD, Wei HL, Chen J, Liu YM, Li F, Xie B, Wang B, Li CL. Insulin resistance reduces sensitivity to Cis-platinum and promotes adhesion, migration and invasion in HepG2 cells. Asian Pac J Cancer Prev. 2014; 15:3123-3128.
26. Biederbick A, Kern HF, Elsasser HP. Monodansylcadaverine (MDC) is a specific *in vivo* marker for autophagic vacuoles. Eur J Cell Biol. 1995; 66:3-14.
27. Belounis A, Nyalendo C, Le Gall R, Imbriglio TV, Mahma M, Teira P, Beaunoyer M, Cournoyer S, Haddad E, Vassal G, Sartelet H. Autophagy is associated with chemoresistance in neuroblastoma. BMC Cancer. 2016; 16:891.
28. Li CL, Wei HL, Chen J, Wang B, Xie B, Fan LL, Li LJ. Ebb-and-flow of macroautophagy and chaperone-mediated autophagy in Raji cells induced by starvation and arsenic trioxide. Asian Pac J Cancer Prev. 2014; 15:5715-5719.
29. Cheng J, Chen J, Xie B, Wei HL. Acquired multidrug resistance in human K562/ADM cells is associated with enhanced autophagy. Toxicol Mech Methods. 2013; 23:678-683.
30. Li CL, Wei HL, Chen J, Wang B, Xie B, Fan LL, Li LJ. Arsenic trioxide induces autophagy and antitumor effects in Burkitt's lymphoma Raji cells. Oncol Rep. 2014; 32:1557-1563.
31. Yoshii SR, Mizushima N. Monitoring and measuring autophagy. Int J Mol Sci. 2017; 18: 1865.
32. Fulda S. Autophagy in cancer therapy. Front Oncol. 2017; 7:128.
33. Gao M, Xu Y, Qiu L. Sensitization of multidrug-resistant malignant cells by liposomes co-encapsulating doxorubicin and chloroquine through autophagic inhibition. J Liposome Res. 2017; 27:151-160.
34. Zhang J, Liu X, Lin Y, Li Y, Pan J, Zong S, Li Y, Zhou Y.

HnRNP K contributes to drug resistance in acute myeloid leukemia through the regulation of autophagy. Exp Hematol. 2016; 44:850-856.
35. Zhang Z, Wu B, Chai W, Cao L, Wang Y, Yu Y, Yang L. Knockdown of WAVE1 enhances apoptosis of leukemia cells by downregulating autophagy. Int J Oncol. 2016; 48:2647-2656.
36. Li GY, Liu JZ, Zhang B, Wang LX, Wang CB, Chen SG. Cyclosporine diminishes multidrug resistance in K562/ADM cells and improves complete remission in patients with acute myeloid leukemia. Biomed Pharmacother. 2009; 63:566-570.
37. Pan YZ, Wang X, Bai H, Wang CB, Zhang Q, Xi R. Autophagy in drug resistance of the multiple myeloma cell line RPMI8226 to doxorubicin. Genet Mol Res. 2015; 14:5621-5629.
38. Liu J, Zhang Y, Liu A, Wang J, Li L, Chen X, Gao X, Xue Y, Zhang X, Liu Y. Distinct dasatinib-induced mechanisms of apoptotic response and exosome release in imatinib-resistant human chronic myeloid leukemia cells. Int J Mol Sci. 2016; 17:531.
39. Palorini R, Votta G, Pirola Y, et al. Protein kinase a activation promotes cancer cell resistance to glucose starvation and anoikis. PLoS Genet. 2016; 12:e1005931.
40. Sun H, Zhang M, Cheng K, Li P, Han S, Li R, Su M, Zeng W, Liu J, Guo J, Liu Y, Zhang X, He Q, Shen L. Resistance of glioma cells to nutrient-deprived microenvironment can be enhanced by CD133-mediated autophagy. Oncotarget. 2016; 7:76238-76249.
41. Ding R, Jin S, Pabon K, Scotto KW. A role for ABCG2 beyond drug transport: Regulation of autophagy. Autophagy. 2016; 12:737-751.
42. Zhu C, Yan X, Yu A, Wang Y. Doxycycline synergizes with doxorubicin to inhibit the proliferation of castration-resistant prostate cancer cells. Acta Biochim Biophys Sin (Shanghai). 2017;1-9. doi: 10.1093/abbs/gmx097.
43. Friedhuber AM, Chandolu V, Manchun S, Donkor O, Sriamornsak P, Dass CR. Nucleotropic doxorubicin nanoparticles decrease cancer cell viability, destroy mitochondria, induce autophagy and enhance tumour necrosis. J Pharm Pharmacol. 2015; 67:68-77.
44. Folkerts H, Hilgendorf S, Wierenga ATJ, Jaques J, Mulder AB, Coffer PJ, Schuringa JJ, Vellenga E. Inhibition of autophagy as a treatment strategy for p53 wild-type acute myeloid leukemia. Cell Death Dis. 2017; 8:e2927.

(Received October 13, 2017; Revised October 25, 2017; Accepted November 1, 2017)

Brief Report

DOI: 10.5582/irdr.2017.01065

In vivo quantification of amyloid burden in TTR-related cardiac amyloidosis

Alexander Marco Kollikowski[1,2,§], Florian Kahles[3,§], Svetlana Kintsler[4], Sandra Hamada[3], Sebastian Reith[3], Ruth Knüchel[4], Christoph Röcken[5], Felix Manuel Mottaghy[1,6,*], Nikolaus Marx[3], Mathias Burgmaier[3]

[1] *Department of Nuclear Medicine, University Hospital RWTH Aachen, Aachen, Germany;*
[2] *Department of Neuroradiology, University Hospital of Würzburg, Würzburg, Germany;*
[3] *Department of Internal Medicine I – Cardiology, RWTH Aachen University, Germany;*
[4] *Department of Pathology, University Hospital RWTH Aachen, Aachen, Germany;*
[5] *Institute of Pathology, Christian-Albrechts-University and UKSH Campus, Kiel, Germany;*
[6] *Department of Radiology and Nuclear Medicine, Maastricht University Medical Center (MUMC), Maastricht, The Netherlands.*

Summary **Cardiac transthyretin-related (ATTR) amyloidosis is a severe cardiomyopathy for which therapeutic approaches are currently under development. Because non-invasive imaging techniques such as cardiac magnetic resonance imaging and echocardiography are non-specific, the diagnosis of ATTR amyloidosis is still based on myocardial biopsy. Thus, diagnosis of ATTR amyloidosis is difficult in patients refusing myocardial biopsy. Furthermore, myocardial biopsy does not allow 3D-mapping and quantification of myocardial ATTR amyloid. In this report we describe a ^{99m}Tc-DPD-based molecular imaging technique for non-invasive single-step diagnosis, three-dimensional mapping and semiquantification of cardiac ATTR amyloidosis in a patient with suspected amyloid heart disease who initially rejected myocardial biopsy. This report underlines the clinical value of SPECT-based nuclear medicine imaging to enable non-invasive diagnosis of cardiac ATTR amyloidosis, particularly in patients rejecting biopsy.**

Keywords: Cardiac ATTR amyloidosis, nuclear cardiac imaging, quantification, amyloid burden, myocardial biopsy, cardiac magnetic resonance imaging

1. Introduction

Cardiac transthyretin-related (ATTR) amyloidosis is a rare but severe form of restrictive cardiomyopathy, which is associated with clinical features of heart failure and adverse outcomes (*1*). Currently new promising therapeutic options based on pharmacological stabilization of tetrameric TTR are currently under development for the treatment of hereditary ATTR amyloidosis (*1,2*). However, ATTR amyloidosis is often challenging to diagnose, since non-invasive imaging techniques such as cardiac magnetic resonance imaging and echocardiography are non-specific. Thus, the diagnosis of ATTR amyloidosis is still based on myocardial biopsy, which is associated with a risk of several complications, including cardiac tamponade, myocardial perforation, hematoma, transient right bundle branch block, transient arrhythmias, tricuspid regurgitation, and occult pulmonary embolism (*3*). Moreover, myocardial biopsy does not allow a 3D-mapping and quantification of myocardial ATTR amyloid. Here we describe a ^{99m}Tc-DPD-based molecular imaging technique for non-invasive single-step diagnosis, three-dimensional mapping and semiquantification of cardiac ATTR amyloid in a patient with suspected cardiac amyloidosis who initially rejected myocardial biopsy.

Released online in J-STAGE as advance publication November 27, 2017.

[§]These authors contributed equally to this work.

**Address correspondence to:*
Prof. Dr. Felix Manuel Mottaghy, Department of Nuclear Medicine, University Hospital RWTH Aachen, Pauwelsstr. 30, Aachen 52074, Germany.
E-mail: fmottaghy@ukaachen.de

2. Case Presentation

We report the case of a 76-year-old man who presented in 2016 with progressive dyspnea on exertion (New York Heart Association class III). The patient denied chest pain, syncope or palpitations. Furthermore, he reported a history of progressive sensorimotor polyneuropathy. Relevant coronary artery disease had previously been ruled out using coronary angiography. A 12-lead-ECG showed atrial fibrillation and low voltage (Figure 1A). Echocardiography revealed diastolic dysfunction with cardiac hypertrophy (septum thickness 15 mm) and preserved left ventricular ejection fraction. Consistent with heart failure with preserved ejection fraction (HFpEF), NT-proBNP levels were elevated (4,983 pg/mL). Contrast-enhanced cardiac magnetic resonance imaging (CMR) showed a ubiquitous subendocardial late gadolinium enhancement indicating cardiac storage disease (Figure 1B) and raised the suspicion of cardiac amyloidosis. Additional echocardiographic strain imaging demonstrated inhomogeneous strain patterns with reduced mid and basal myocardial longitudinal strain, whereas apical segments were unaffected (Figure 1C). Laboratory testing for sarcoidosis, hemochromatosis and monoclonal gammopathies proved negative. Because all diagnostic results showed classical - though unspecific - characteristics of cardiac ATTR amyloidosis, we planned myocardial biopsy to confirm the diagnosis. However, the patient rejected myocardial biopsy due to personal reasons.

In light of potential treatment options for ATTR amyloidosis with agents such as diflunisal or tafamidis (*1,2*), we were challenged using a non-invasive technique 1. to confirm the diagnosis of cardiac ATTR amyloidosis and 2. to quantify disease severity and clinical relevance for the patient.

3. Results and Discussion

3.1. *Non-invasive diagnosis of cardiac ATTR amyloidosis*

Gillmore and colleagues reported recently that ^{99m}Technetium-3,3-diphosphono-1,2-propanodicarboxylic acid (^{99m}Tc-DPD) could be used to diagnose cardiac ATTR amyloidosis with excellent sensitivity (> 99%) and high specificity (~86%) (*4*). Although the exact mechanism is not completely understood, ^{99m}Tc-DPD shows highly preferential, potentially calcium-dependent, uptake in myocardial amyloid infiltrations caused by extracellular deposits of destabilized and dissociated TTR-tetramers which form fibrils consisting of misfolded TTR-subunits in a cross β-sheet structure (*1,5*).

In our patient, we performed a dual-phase bone scintigraphy after injection of 705 MBq ^{99m}Tc-DPD using a dual-head system for image acquisition (ECAM, Siemens Healthcare, Erlangen, Germany). Whole body scans were obtained at 5 min and 3 h p.i. revealing inhomogeneous cardiac uptake (Figure 2). Considering the patient's symptoms, clinical history and previous diagnostic steps, the criteria for non-invasive diagnosis of ATTR amyloidosis proposed by Gillmore and colleagues were fulfilled (*4*).

3.2. *Quantification and 3D-mapping of cardiac ATTR amyloidosis*

Quantification of myocardial disease severity is important to determine clinical relevance of disease and treatment success of emerging therapeutic strategies for cardiac ATTR amyloidosis. However, quantification and 3D-mapping of cardiac ATTR amyloidosis using ^{99m}Tc-DPD apart from visual assessment of planar images or heart-to-contralateral ratio is unknown (*5*).

First, we performed 3D-mapping of cardiac amyloid deposits and performed single photon emission computed tomography (SPECT, Symbia, Siemens Healthcare, Erlangen, Germany) 3.5 h p.i., which showed inhomogeneous tracer distribution within the heart with relative tracer absence in the apex, apical and mid-cavitary anterolateral wall, whereas the remaining myocardium revealed avid ^{99m}Tc-DPD uptake (Figure

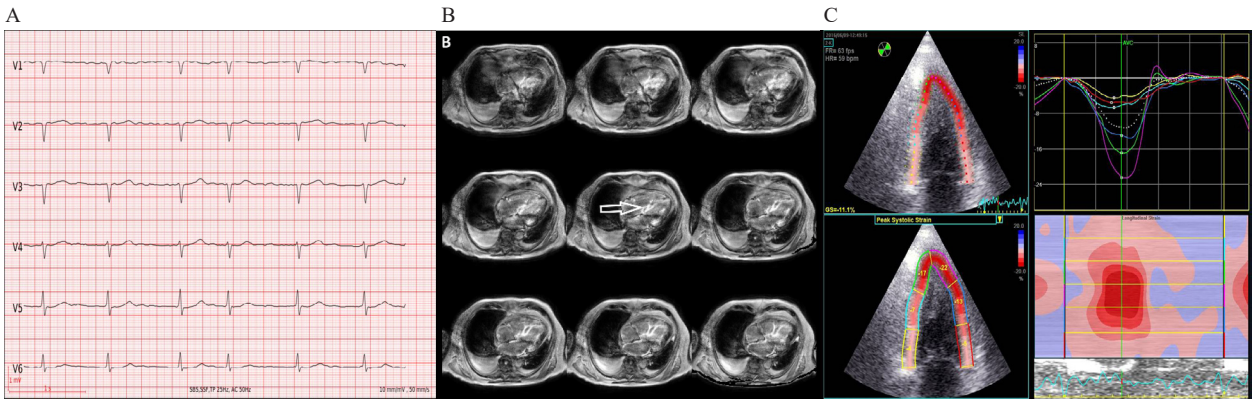

Figure 1. (A), 12 lead ECG revealing atrial fibrillation and low voltage. (B), Late gadolinium enhancement (LGE) Inversion Recovery-Sequence (4-chamber-view), showing subendocardial to diffuse intramyocardial LGE. (C), 2D strain analysis of a 2 chamber-view showing preserved longitudinal strain of the apical LV-segments in contrast to the impaired longitudinal strain of the medial and basal LV-segments ("apical sparing").

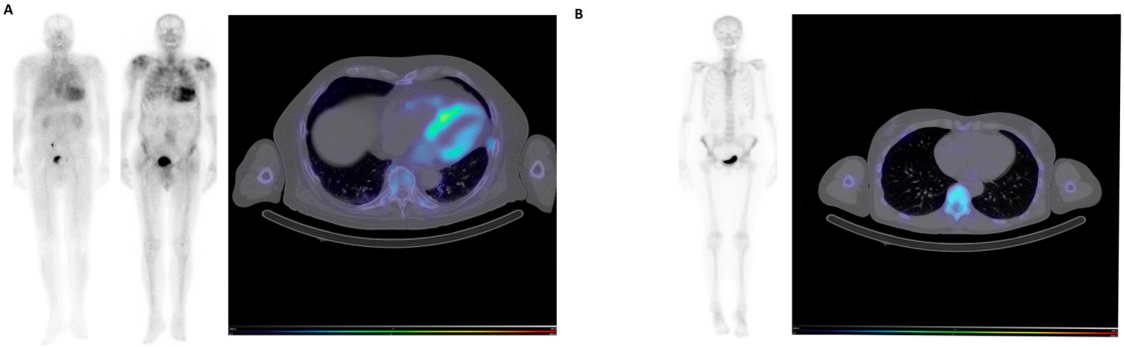

Figure 2. (A), *Left:* Whole body scans 5 min and 3 h p.i. showing inhomogeneous cardiac ^{99m}Tc-DPD retention. *Right section*: Cardiac SPECT/CT 3,5 h p.i. with regionally variable tracer distribution and relative tracer absence in the apex and mid-cavitary anterolateral wall. (B), ^{99m}Tc-DPD scan in a control patient on the same day. Neither analogous planar imaging 3 h p.i. nor SPECT/CT 3,5 h p.i. reveales cardiac tracer uptake.

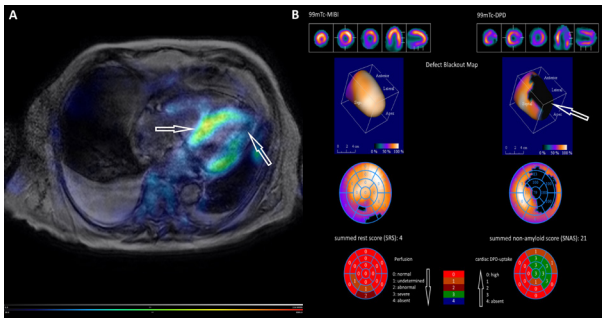

Figure 3. (A), Fusion of SPECT dataset 3,5 h p.i. and CMR (Inversion Recovery-Sequence, 4-chamber-view) in corresponding axial alignment demonstrates congruent ^{99m}Tc-DPD uptake and LGE with unaffected apical segments. (B), Nuclear cardiac imaging using a multi-detector SPECT system. *Left*: ^{99m}Tc-sestamibi scans (cationic complex exclusively characterizing unscathed mitochondria and vital cardiomyocytes), rest-only myocardial perfusion examination. *Upper row*: The summary screen of the main cardiac axes outlines no significant perfusion defects under resting conditions. *Middle*: 3- and 2-dimensional polar mapping. No significantly impaired left ventricular tracer uptake compared to the reference database (^{99m}Tc-sestamibi). Depiction as Defect Blackout Map. *Bottom row*: SRS ("Summed Rest Score"), semiquantitatively reflecting the extent of the perfusion defect (SRS ≤ 4 was regarded as normal). *Right*: ^{99m}Tc-DPD scans 4 h p.i.. Tracer uptake in areas of presumed TTR-deposits. Upper row: The summary screen shows left ventricular ^{99m}Tc-DPD defects in the apex and mid-cavitary anterolateral wall. *Middle*: The 3- and 2-dimensional Defect Blackout Maps show a significantly impaired apical and mid-cavitary anterolateral tracer uptake (reference database ^{99m}Tc-sestamibi), which was regarded as unaffected myocardium. *Bottom row*: SNAS ("Summed Mon-Amyloid Score"), semiquantitatively reflecting the extent of suspected TTR-free myocardium.

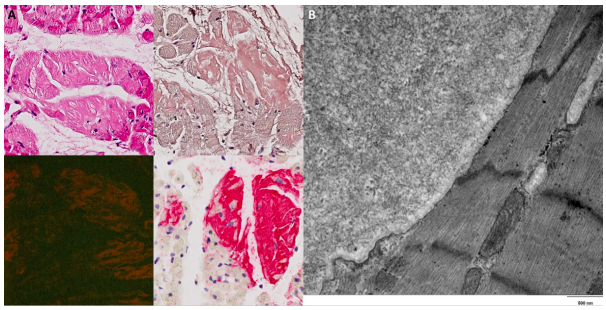

Figure 4. (A), Histology of cardiac biopsy. At the top on the left: eosinophilic deposits, hematoxylin and eosin stain (H&E), ×400 magnification. At the top on the right: acellular amorphic deposits, Congo red stain, ×400 magnification. At the bottom on the left: typical fluorescence signal of amyloid in a Congo red stained section viewed by fluorescence microscopy, ×200 magnification. At the bottom on the right: strong immunostaining of the amyloid deposits with an anti-transthyretin-antibody, ×400 magnification. **(B), Ultrastructural analysis of the cardiac biopsy by electron microscopy reveals the presence of irregular formed fibres.**

2). Then, SPECT and CMR data were merged into one image and both showed identical diseased and healthy segments of the heart (Figure 3A), suggesting that the late gadolinium enhancement observed in CMR could be explained by amyloid deposits.

For direct quantification of cardiac ATTR amyloidosis, we applied a method analogous to the well-established and validated techniques used in myocardial perfusion SPECT (*6*): A multi-detector SPECT system (Discovery NM 530c, GE Healthcare, Chicago, Illinois, USA) optimized for cardiac imaging and photon energy ranges between 40-200keV (^{99m}Tc: 140keV) was utilized to obtain ^{99m}Tc-DPD scans 4 h p.i. (Figure 3B, right section). Additional myocardial perfusion SPECT (7-day time interval) after injection of 388 MBq ^{99m}Tc-sestamibi were used to quantify viable myocardium and revealed no significant perfusion defects under resting conditions (Figure 3B, left section). Semiquantitative analysis of myocardial perfusion and left ventricular amyloid were assessed using polar mapping (Figure 3B, middle), a three- or two-dimensional (voxel- or pixel-based) depiction of the study's normalized cardiac activity counts compared with a reference database (^{99m}Tc-sestamibi) and followed by blacking out regions below a defined threshold of database activity (Defect Blackout Map). For additional semiquantitative scoring of myocardial perfusion defects or amyloid deposits, polar maps comprising 17 segments were generated, each of which was assessed separately with a score between 0 (i.e. no deviation between database and study) and 4 (i.e. significant deviation) (Figure 3B, bottom row). Concerning myocardial perfusion under resting conditions, the total score is referred to as "summed rest score" (SRS),

which, inter alia, reflects areas of myocardial scar tissue (*6*). Finally, to quantify left ventricular ATTR amyloid burden, we propose to introduce a reciprocal "summed non-amyloid score" (SNAS), which presumably reflects the extent of unaffected myocardium. Its theoretical range extends from SNAS = 0, *i.e*. massive ^{99m}Tc-DPD uptake reflecting a homogeneously affected left ventricle, to SNAS = 68, *i.e*. no ^{99m}Tc-DPD uptake and therefore no detectable cardiac ATTR amyloidosis.

3.3. *Myocardial biopsy confirmed imaging diagnosis*

On the basis of these new results, the patient gave informed consent to undertake myocardial biopsy. Ultrastructural analysis by electron microscopy revealed the presence of irregular formed fibrils and large deposits of amyloid were found in Congo red stained tissue sections showing a typical green birefringence under polarized light and a characteristic fluorescence signal in fluorescence microscopy (Figure 4). The amyloid deposits were immunostained with an antibody directed against transthyretin (Figure 4A). No immunostaining was found with antibodies directed against lambda- and kappa light chain (not shown). Later genotyping subclassified wild-type ATTR amyloidosis, as a consequence the patient was referred to a specialized center to assess further treatment options.

4. Conclusion

In this work we describe a ^{99m}Tc-DPD-based molecular imaging approach for non-invasive diagnosis and semiquantification of cardiac ATTR amyloidosis in a patient with suspected cardiac amyloidosis who initially rejected myocardial biopsy. Due to promising new therapy options for hereditary ATTR amyloidosis based on pharmacological stabilization of tetrameric TTR such as diflunisal and tafamidis (*1,2*), imaging is not only crucial for a non-invasive diagnosis and early therapy planning in patients who refuse myocardial biopsy, but also regarding disease monitoring and response to therapy.

Our report stresses the clinical value of ^{99m}Tc-DPD-based nuclear medicine imaging to provide a quick and accurate diagnosis of cardiac ATTR amyloidosis, particularly in patients refusing biopsy. Furthermore, we describe for the first time a widely available SPECT-based technique for single-step diagnosis, three-dimensional mapping and semiquantification of cardiac ATTR amyloidosis. Future studies are warranted to evaluate the suitability of ^{99m}Tc-DPD-based quantification of myocardial ATTR amyloidosis for disease monitoring and its response to medical therapy.

References

1. Ruberg FL, Berk JL. Transthyretin (TTR) cardiac amyloidosis. Circulation. 2012; 126:1286-1300.
2. Maurer MS, Grogan DR, Judge DP, Mundayat R, Packman J, Lombardo I, Quyyumi AA, Aarts J, Falk RH. Tafamidis in transthyretin amyloid cardiomyopathy: Effects on transthyretin stabilization and clinical outcomes. Circ Heart Fail. 2015; 8:519-526.
3. From AM, Maleszewski JJ, Rihal CS. Current status of endomyocardial biopsy. Mayo Clin Proc. 2011; 86:1095-1102.
4. Gillmore JD, Maurer MS, Falk RH, *et al*. Nonbiopsy diagnosis of cardiac transthyretin amyloidosis. Circulation. 2016; 133:2404-2412.
5. Narotsky DL, Castano A, Weinsaft JW, Bokhari S, Maurer MS. Wild-type transthyretin cardiac amyloidosis: Novel insights from advanced imaging. Can J Cardiol. 2016; 32:1166.e1-1166.e10.
6. Verberne HJ, Acampa W, Anagnostopoulos C, *et al*. EANM procedural guidelines for radionuclide myocardial perfusion imaging with SPECT and SPECT/CT: 2015 revision. Eur J Nucl Med Mol Imaging. 2015; 42:1929-1940.

(Received September 28, 2017; Revised November 1, 2017; Accepted November 13, 2017)

Brief Report

DOI: 10.5582/irdr.2017.01068

MTHFR promoter hypermethylation may lead to congenital heart defects in Down syndrome

Ambreen Asim[1], Sarita Agarwal[1,*], Inusha Panigrahi[2], Nazia Saiyed[3], Sonal Bakshi[3]

[1] *Department of Genetics, Sanjay Gandhi Postgraduate Institute of Medical Sciences, Lucknow, India;*
[2] *Department of Pediatrics, PGIMER, Chandigarh, India;*
[3] *Department of Biotechnology, Institute of Science, Nirma University, Ahmedabad, India.*

Summary **Altered global methylation levels revealed LINE-1 methylation in young mothers of Down syndrome (DS) compared to controls suggesting the possibility of impaired DNA methylation causing abnormal segregation of chromosome 21. Methylene Tetrahydrofolate Reductase (MTHFR) is one of the major enzymes of the folate metabolism pathway. MTHFR gene polymorphism has been associated with maternal risk for DS. Studies have revealed that increased MTHFR promoter methylation results in the reduction of MTHFR protein activity further leading to increased risk of various diseases. The aim of this study is to compare the levels of MTHFR promoter methylation in all three study groups. A total of 120 subjects were recruited for the study and was divided into the following three groups: Group I (mothers of DS without Congenital Heart Defects (CHD), *n* = 40); Group II (mothers of DS with CHD, *n* = 40); and Group III (age matched control mothers, *n* = 40). Genomic DNA was isolated from 2 ml peripheral blood and bisulfite treatment was done to convert all unmethylated cytosines into uracil followed by PCR amplification for MTHFR promoter region and Sanger's sequencing. Results showed that there was a two fold increase in methylated promoter region of MTHFR gene in group II compared to other groups. None of the methylation pattern was observed in the control group. MTHFR promoter methylation affects folate metabolism which is known to play a role in chromosomal breakage, abnormal chromosomal segregation and genomic instability and therefore a developmental defect in the form of congenital cardiac anomaly.**

Keywords: Down syndrome, congenital heart defects, MTHFR promoter, sequencing

1. Introduction

Aberrant DNA methylation has been associated with several diseases like cancers (*1,2*), diabetes (*3*) or neurological diseases including Down syndrome (DS) (*4*). DNA methylation leads to the addition of a methyl group at 5' carbon of cytosine, which can bring changes in DNA structure, altering the set patterns of gene expression.

Congenital heart defects (CHD) account for a major portion of life-threatening birth defects. Atrioventricular Septal Defect (AVSD) and Ventricular septal defects (VSD) are common cardiac malformations in DS cases (*5,6*). The relationship between DS and maternal genetic polymorphism in folate/homocysteine metabolism is well established. Folate is essential for various cellular processes viz., synthesis of DNA, RNA, methylation and embryonic developmental processes including the cardiovascular system (*7,8*). Folate deficiency may lead to stunted growth, anemia, weight loss, digestive disorders and behavioral issues. Reports of *in vivo* studies showed a decreased level of folate causes hypomethylation leading to DNA strand breakage and abnormal segregation of chromosomes (*9,10*). Changes in folate metabolism lead to an increase in DNA hypomethylation due to an altered DNA methylation pattern thereby further increasing the risk of chromosome nondisjunction (*11*).

Altered global methylation levels reveal LINE-1 methylation in young mothers of DS thus suggesting

**Address correspondence to:*
Prof. Sarita Agarwal, Department of Genetics, Sanjay Gandhi Postgraduate Institute of Medical Sciences, Lucknow 226014, India.
E-mail: saritasgpgi@gmail.com

the possibility of impaired DNA methylation in mothers of DS children causing abnormal segregation of chromosome 21 (*12*). Also maternal folic acid supplementation has been associated with a decreased risk of congenital heart defects in DS babies (*13*).

The methylenetetrahydrofolate reductase (*MTHFR*) gene is reported to be associated with the risk of CHD in DS. It was also reported that promoter methylation regulates *MTHFR* gene and increased *MTHFR* promoter methylation was seen in DNA isolated from cancer patients, patients with cardiovascular or renal disorders, and placental DNA from women with pre-eclampsia. It was also observed that as the level of promoter methylation in *MTHFR* gene increases, the MTHFR protein activity is reduced, thereby increasing the risk of various diseases (*14,15*). In this study, we investigated *MTHFR* promoter methylation levels in mothers of DS, mothers of DS with CHD and matched healthy control mothers.

2. Materials and Methods

2.1. *Study Subjects*

A total of 120 subjects recruited in the present study included three groups: Group I comprised of mothers of DS without CHD (n = 40); Group II had mothers of DS with CHD (n = 40); and Group III included age-matched control mothers (n = 40). DS subjects were recruited from outpatient clinics of 2 tertiary care institutes in India, after obtaining informed consent. The DS were enrolled in the study after confirmation of karyotype and echocardiography to confirm the presence or absence of AVSD. Quantitative Fluorescent – Polymerase Chain Reaction (PCR) was also done on DNA samples for confirmation of DS using standard protocols. Ethical clearance was from the ethics committee of the Institute where the work was performed. Peripheral blood samples were available from all hundred and twenty women and the age of all the women ranged from 18 to 44 years.

2.2. *Bisulfite treatment and sequencing*

Genomic DNA was isolated from 2 mL peripheral blood using standard Phenol Chloroform method and quantified using Nanodrop spectrophotometer (NanoDrop Thermo Scientific). The EpiTect Bisulfite Kit (Qiagen, Milan, Italy) was used to convert all unmethylated cytosines into uracil. Bisulfite conversion of genomic DNA is divided into 4 steps: denaturation, sulphonation, hydrolic deamination and alkali desulphonation. Double-stranded genomic DNA was first converted into single stranded before the sulphonation step which proceeds with the addition of bisulphite to cytosine. Later hydrolic deamination of the cytosine-bisulphite derivative was done in order to give a uracil-bisulphite derivative. Finally, alkali desulphonation removed the sulphonate group through alkali treatment which finally gave uracil. Bisulphite treatment deaminated cytosine to uracil in single-stranded DNA. PCR amplification finally amplified uracil to thymine and 5' Methyl cytosine residues to cytosine, further distinguishing methylated CpGs from unmethylated CpGs by the presence of a cytosine "C" versus thymine "T" residue after sequencing.

PCR amplification was done for the *MTHFR* promoter region. The CpG islands present in the 5'-untranslated promoter region of *MTHFR*; from + 30 to 184 from the TSS (transcription start site) was studied. This region contains seven CpG islands and the methylation levels of these CpG islands were found to be associated with gene expression levels in human lung cancer cells (*16*).

Table 1 shows the details of PCR reaction and primers including: the sequence of primers used, annealing temperature (Ta), amplicon length, the location of promoter region studied and the number of CpG islands it contained. PCR products were visualised by standard ethidium bromide-agarose gel electrophoresis. PCR purified products were directly sequenced using an ABI 310 Automated Sequencer (ABI, Foster City, CA, USA).

3. Results and Discussion

The age range of the mothers with DS babies was 18-45 years, with median age of 28.5 years. In the DS babies with cardiac defects, the most common cardiac defect was AVSD, comprising 62.5% cases. Other cardiac defects included VSD, atrial septal defects (ASD) and Tetralogy of Fallot (TOF). Mothers of DS with cardiac defects were in Group II for the study.

The sequencing results of bisulfite converted genomic DNA for all three groups showed that there was a two fold increase in methylated promoter region of *MTHFR* gene in group mothers of DS having CHD compared to mothers of DS without CHD. However, no methylation was observed in age matched control mothers group (Figure 1). Figure 2 shows the pictorial representation of CpG island frequencies in all three study groups. CpG island methylation frequencies

Table 1. Sequence of primers, annealing temperature (Ta), amplicon size and number od CpG sites present

S.No.	Primer Sequences	T_a	Amplicon length	CpG sites
1	F: 5'TTTTAATTTTTGTTTGGAGGGTAGT-3' R: 5'AAAAAAACCACTTATCACCAAATTC-3'	55°C	155bp	7

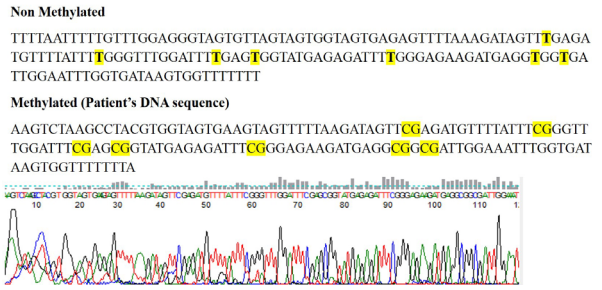

Figure 1. Results of Sanger's sequencing using Bisulfite converted DNA of both non- methylated and methylated (patient's sample). The highlighted text in the non-methylated and methylated sequences shows all seven CpG sites which were methylated in patient's. Given below is the electropherogram of methylated patient's sample.

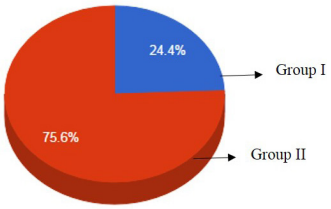

Figure 2. Pictorial representation of CpG island frequencies in all three groups. CpG island methylation frequencies were found to be 24.4% and 75.6% in Group I and II respectively. Note: No methylation was observed in group III.

were found to be 24.4% and 75.6% in Group I and II respectively. No methylation was seen in the control group.

Decreased folate level has been linked to aberrant cell growth, impaired DNA methylation and chromosomal damage (*9,10*). The presence of CHD in DS accounts for 40% to 50% in which AVSD is the most common form of CHD followed by VSD. Thyroid abnormalities are also common in DS patients (*17*). Studies are now focused on why some defects are more common in DS children. The role of epigenetics is considered important in causation of developmental defects.

A case-control study from Spain reported absence of maternal folic acid supplementation was more frequent in DS with atrioventricular septal defects (OR = 1.69, 95% CI = 1.08 - 2.63) or atrial septal defects (OR = 1.69, 95% CI= 1.11 - 2.58) compared to DS without CHD (*18*). Thus, maternal supplementation with folic acid is likely to be associated with reduced risk of CHD in DS. This study revealed a significant difference in methylation profiles in DNA isolated from blood compared to DNA isolated from heart tissues. Further, 22 samples from the heart showed increased methylation in fetuses having DS compared to fetuses having normal karyotypes (*19,20*). The present paper focuses on the presence of CHD due to genetic polymorphism present in the genes of folate metabolism to their occurrence in DS offspring. MTHFR is one of the major enzymes involved in the folate/homocysteine metabolism pathway and MTHFR gene polymorphism has been associated with maternal risk for DS progeny (*21,22,23*). Several congenital complications are reported in an individual with DS. Most of them are affected by maternal carbon metabolism and consequently can lead to epigenetic changes and hence impaired chromosome segregation (*24*). The promoter methylation of a gene is an epigenetic event which leads to reduced expression of genes.

A similar study was conducted by Coppede *et al*. in 2015 (*7*) in Italian mothers of DS along with age-matched controls who conceived before 35 years of age. Authors have investigated MTHFR promoter methylation levels and also searched for correlation between MTHFR promoter methylation and micronucleus frequency and found an increase in the methylation level in mothers of DS when compared to controls (33.3 ± 8.1% *vs*. 28.3 ± 5.8%; $p = 0.001$). The frequency of micronucleated lymphocytes was also found to be higher in mothers of DS group than control mothers (16.1 ± 8.6‰ *vs*. 10.5 ± 4.3‰; $p = 0.0004$) and it correlated with MTHFR promoter methylation levels ($r = 0.33$; $p = 0.006$). The study concluded that MTHFR methylation is likely to contribute to the increased genomic instability observed in DNA isolated from mothers of DS, and could play a role in the risk of birth of a child with DS as well as in the onset of age related diseases in those women. We investigated a CpG island in the *MTHFR* promoter region in three groups (mothers of DS with CHD, mothers of DS without CHD and controls) and the methylation status was found to be elevated in mothers of DS with CHD highlighting the essential role of MTHFR promoter methylation in occurrence of both CHD and DS in women of reproductive age. These studies indicate that MTHFR promoter methylation can be used as a biomarker for screening mothers of DS for the presence of CHD in these populations. However, this is the only study reported in the literature which shows the association of MTHFR promoter methylation with the occurrence of CHD in mothers of DS. Furthermore, these studies can also be conducted in other ethnic groups with a larger sample size to confirm these findings.

In conclusion, MTHFR promoter methylation affects folate metabolism, which is known to play a role in chromosomal breakage, abnormal chromosomal segregation and genomic instability and therefore a developmental defect in the form of congenital cardiac anomaly. The present study thus clearly highlights the association of *MTHFR* promoter hypermethylation in mothers of DS having DS babies with cardiac defects. We reported increased promoter methylation in mothers of DS with CHD when compared to mothers of DS without CHD and healthy control mothers.

Acknowledgements

This research was supported by the Department

of Science and Technology, Ministry of Health, Government of India (DST/Inspire fellowship/2012/499). The study was also supported by Indian Council of Medical Research. We are highly grateful to Sanjay Gandhi Post Graduate Institute of Medical Sciences (SGPGIMS), Lucknow, UP; for providing the infrastructure for research work.

References

1. Heyn H, Esteller M. DNA methylation profiling in the clinic: Applications and challenges. Nat Rev Genet. 2012; 13:679-692.
2. Das PM, Singal R. DNA methylation and cancer. J Clin Oncol. 2004; 22:4632-4642.
3. Fradin D, Le Fur S, Mille C, Naoui N, Groves C, Zelenika D, McCarthy MI, Lathrop M, Bougneres P. Association of the CpG methylation pattern of the proximal insulin gene promoter with type 1 diabetes. PLoS One. 2012; 7:e36278
4. Jin S , Lee YK ,Lim YC, Zheng Z, Lin XM, Ng DP, Holbrook JD, Law HY, Kwek KY, Yeo GS, Ding C. Global DNA hypermethylation in Down syndrome placenta. Plos Genetics. 2013; 9:e1003515.
5. Asim A, Kumar A, Muthuswamy S, Jain S, Agarwal S. Down syndrome: An insight of disease. J Biomed Sci. 2015; 22:41.
6. Hoffman JI, Kaplan S. The incidence of congenital heart disease. J Am Coll Cardiol. 2002; 39:1890-1900.
7. Coppedè F. The genetics of folate metabolism and maternal risk of birth of a child with Down syndrome and associated congenital heart defects. Front Genet. 2015; 25; 6:223.
8. Canfield MA, Collins JS, Botto LD, Williams LJ, Mai CT, Kirby RS, Pearson K, Devine O, Mulinare J, National Birth Defect Preventin Network. Changes in the birth prevalence of selected birth defects after grain fortification with folic acid in the United States: Findings from a multi-state population-based study. Birth Defects Res A Clin Mol Teratol. 2005; 73:679-689.
9. Fenech M. Cytokinesis-block micronucleus assay evolves into a "cytome" assay of chromosomal instability, mitotic dysfunction and cell death. Mutat Res. 2006; 600:58-66.
10. Fenech M. Micronuclei and their association with sperm abnormalities, infertility, pregnancy loss, pre-eclampsia and intra-uterine growth restriction in humans. Mutagenesis. 2011; 26:63-67.
11. James SJ, Pogribna M, Pogribny IP, Melnyk S, Hine RJ, Gibson JB, Yi P, Tafoya DL, Swenson DH, Wilson VL, Gaylor DW. Abnormal folate metabolism and mutation in the methylenetetrahydrofolate reductase gene may be maternal risk factor for Down syndrome. Am J Clin Nutr. 1999; 70:495-501.
12. Bo˘zovi'c IB, Stankovi'c A,˘Zivkovi'c M, Vranekovi'c J, Kapovi'c M, Brajenovi'c-Mili'c B. Altered LINE-1 methylation in mothers of children with Down syndrome. PLoS One. 2015; 10:e0127423.
13. Bean LJ, Allen EG, Tinker SW, Hollis ND, Locke AE, Druschel C, Hobbs CA, Leary'O, Romitti PA, Royle MH,Torfs CP, Dooley KJ, Freeman SB, Sherman SL. Lack of maternal folic acid supplementation is associated with heart defects in Down syndrome: A report from the national Down syndrome project. Birth Defects Res A Clin Mol Teratol. 2011; 91:885-893.
14. Khazamipour N, Noruzinia M, Fatehmanesh P, Keyhanee M, Pujol P. MTHFR promoter hypermethylation in testicular biopsies of patients with non-obstructive azoospermia: The role of epigenetics in male infertility. Hum Reprod. 2009; 24:2361-2364.
15. Wei LK, Sutherland H, Au A, Camilleri E, Haupt LM, Gan SH, Griffiths LR. Apotential epigenetic marker mediating serum folate and vitamin B12 levels contributes to the risk of ischemic stroke. Biomed Res Int. 2015; 167976.
16. Botezatu A, Socolov D, Iancu IV, Huica I, Plesa A, Ungureanu C Anton G. Methylenetetrahydrofolate reductase (MTHFR) polymorphisms and promoter methylation in cervical oncogenic lesions and cancer. J Cell Mol Med. 2013; 17:543-549.
17. Dayal D, Jain P, Panigrahi I, Bhattacharya A, Sachdeva N. Thyroid dysfunction in children with Down syndrome. Indian Pediatr. 2014; 51:751-752.
18. Serra-Juhé C, Cuscó I, Homs A, Flores R, Torán N, Pérez-Jurado LA. DNA methylation abnormalities in congenital heart disease. Epigenetics. 2015; 10:167-177.
19. Guéant JL, Caillerez-Fofou M, Battaglia-Hsu S, Alberto JM, Freund JN, Dulluc I, Adjalla C, MAurya F, Merle C, Nicolas JP, Namour F, Daval JL. Molecular and cellular effects of vitamin B12 in brain, myocardium and liver through its role as co-factor of methionine synthase. Biochimie. 2013; 95:1033-1040.
20. Rotondo JC, Bosi S, Bazzan E, Di Domenico M, De Mattei M, Selvatici R, Patella A, Marci R, Toqnon M, martini F.Methylenetetrahydrofolate reductase gene promoter hypermethylation in semen samples of infertile couples correlates with recurrent spontaneous abortion. Hum Reprod. 2012; 27:3632-3638.
21. Wu W, Shen O, Qin Y, Niu X, Lu C, Xia Y, Song L, Wang X. Idiopathic male infertility is strongly associated with aberrant promoter methylation of methylenetetrahydrofolate reductase (MTHFR). PLoS One. 2010; 5:e13884.
22. Vaissière T, Hung RJ, Zaridze D, Moukeria A, Cuenin C, Fasolo V,Ferro G, paliwal A, Hainaut P, Brennan P, Tost J, Boffetta P, Herceq Z. Quantitative analysis of DNA methylation profiles in lung cancer identifies aberrant DNA methylation of specific genes and its association with gender and cancer risk factors. Cancer Res. 2009; 69:243-252.
23. Obeid R. The metabolic burden of methyl donor deficiency with focus on the betaine homocysteine methyltransferase pathway. Nutrients. 2013; 5:3481-3495.
24. Blom HJ, Smulders Y. Overview of homocysteine and folate metabolism: With special references to cardiovascular disease and neural tube defects. J Inherit Metab Dis. 2011; 34:75-81.

(Received October 13, 2017; Revised November 21, 2017; Accepted November 23, 2017)

Brief Report

DOI: 10.5582/irdr.2017.01037

Steroid-resistant nephrotic syndrome caused by co-inheritance of mutations at *NPHS1* and *ADCK4* genes in two Chinese siblings

Hongwen Zhang, Fang Wang, Xiaoyu Liu, Xuhui Zhong, Yong Yao, Huijie Xiao*

Department of Pediatric, Peking University First Hospital, Beijing, China;

Summary **Hereditary nephrotic syndrome often presents with steroid-resistance and onset within the first year of life. Mutations in genes highly expressed in podocytes have been found in two thirds of these patients, especially *NPHS1* and *NPHS2* among at least 29 genetic causes that have been discovered. We reported two siblings with steroid-resistant nephrotic syndrome caused by co-inheritance of mutations at *NPHS1* (c.1339G>A, p.E447K) and *ACDK4* (c.748G>C, p.D250H) genes. The siblings presented with steroid-resistant nephrotic syndrome and pathological lesions of focal segmental glomerulosclerosis (FSGS), while the elder sister also developed hypertension, renal failure and cardiac dysfunction.**

Keywords: Steroid-resistant nephrotic syndrome, *NPHS1*, *ADCK4*, China

1. Introduction

Nephrotic syndrome is the most common glomerular disease encountered during childhood. It is characterised by significant proteinuria (early morning urine protein with creatinine ratio greater than 200 mg/mmol) leading to hypoalbuminaemia (plasma albumin of less than 25 g/L). Following the reduction in circulating proteins there is a drop in plasma oncotic pressure which manifests as generalised edema. The clinical triad of edema, nephrotic range proteinuria and hypoalbuminaemia defines nephrotic syndrome. This triad is typically accompanied by dyslipidaemia with elevated plasma cholesterol and triglycerides (*1*).

Nephrotic syndrome can be classified by the etiology into primary (hereditary), secondary and idiopathic one. Hereditary nephrotic syndrome often presents with steroid-resistance and onset within the first year of life, sometimes beginning at late childhood or even adulthood. Mutations in genes highly expressed in podocytes have been found in two thirds of these patients, especially *NPHS1*, *NPHS2*, *WT1*, *LAMB2* and *ADCK4* among the discovered at least 29 genetic causes (*2-7*).

Released online in J-STAGE as advance publication November 27, 2017.

**Address correspondence to:*
Dr. Huijie Xiao, Department of Pediatric, Peking University First Hospital, No.1 Xi An Men Da Jie, Beijing 100034, China.
E-mail: huijiexiao2@hotmail.com

We reported here steroid-resistant nephrotic syndrome caused by co-inheritance of mutations at *NPHS1* and *ACDK4* genes in two Chinese siblings.

2. Materials and Methods

2.1. *Participants*

This work was carried out with human research ethics approval from the Peking University First Hospital, and it followed the guidelines of the 2000 Declaration of Helsinki and the Declaration of Istanbul 2008. All patients and their family members gave their consent for inclusion in this study.

2.2. *Methods*

Genetic analysis was performed in the genetics laboratories of MyGenostics biotechnology companies in China, using "the hereditary nephrotic syndrome panel" which includes *NPHS1*, *NPHS2*, *ADCK3*, *ADCK4*, *PLCE1*, *WT1*, *CD2AP*, *ACTN4*, *TRPC6*, *INF2*, *LMX1B*, *LAMB2*, *GLA*, *ITGB4*, *SCARB2*, *COQ2*, *COQ4*, *COQ9*, *PDSS2*, *MTTL1*, *CRB2*, *MIF*, *APOL1*, and *SMARCAL1* (*8,9*). In order to exclude Alport syndrome, *COL4A3*, C*OL4A4*, and *COL4A5* gene were also analyzed.

Genomic DNA was isolated from peripheral blood of the siblings and their parents using the salting-out method. Target sequences of exons and their flanking

sequences about 50 bp were captured using Agilent probes and sequenced using a NGS sequencer Genome Analyser IIx (GAIIx, Illumina) and Illumina/Solexa platforms. The expected segregation of putative mutations was confirmed in families, whenever possible, and their absence was confirmed in SNPs databases of common benign variants (*http://exac.broadinstitute.org/*, *http://www.1000genomes.org/*, *http://snp.ims.u-tokyo.ac.jp* and *http://www.ncbi.nlm.nih.gov/projects/SNP/*). Human Splicing Finder (*http://www.umd.be/HSF/*) and Mutation tasting (*http://mutationtaster.org/*) were used for analysis on splicing mutation and other mutations, respectively. If a novel mutation was found, 100 normal Chinese controls would be examined directly using PCR amplification and sequencing techniques.

2.3. *Case presentation*

Case 1: An 11-year-old girl (elder sister) was hospitalized to our hospital on October 11, 2013 with the complaint of edema and proteinuria for 22 months, dyspnea and weakness for 8 months. She was found with edema 22 months ago, which wasn't taken seriously. Dyspnea and weakness appeared 8 months ago. Laboratory tests in local hospital showed anemia (hemoglobin 77.3 g/L), abnormal renal function (Scr 927 μmol/L, BUN 23 mol/L), proteinuria (174 mg/kg/24h) and hypoalbuminemia (25 g/L). Renal biopsy yielded 33 glomeruli under light microscopy, which included 4 globally sclerotic glomeruli, the others showed mesengial hypercellularity and matrix hyperplasia with 6 focal segmental sclerosis, tubular epithelia vacuolar and granular degeneration without atrophic tubules and interstitial fibrosis. Immunohistochemical studies showed moderate granular C3 and IgM staining of the basal membranes and mesangium. Electron microscopy revealed glomerular basement membrane (GBM) to be not abnormal; no electron-dense deposits were identified within the mesangial and GBM; mesangial hypercellularity and matrix increase combined with sclerosis were present. She was given hemodialysis and maintenance therapy. Her anuria lasted for three months, and she came to our hospital for further diagnosis and treatment.

There was no abnormal birth and past medical history, but a consanguineous family history of father and mother being first cousins.

At admission, her blood pressure was high (140/90 mmHg). Her height was 140 cm, weight was 30 kg and pulse was 120 beats per minute. Physical examination showed cardiac dilatation with a grade 2 precordial systolic murmur, hepatomegaly and splenomegaly (6 and 5 cm below rib cage, respectively). No neurodevelopmental and ophthalmologic deficits were observed. Laboratory tests in our hospital revealed hemoglobin to be 90 g/L, Scr 739 μmol/L and BUN 22. 2 mol/L; type B natriuretic peptide was 4982 pg/mL. Her liver function was normal. There was no evidence of virus infection such as Epstein-Barr virus, cytomegalovirus or hepatitis virus. Autoimmune profile was within normal range including compliments, anti-nuclear antibody, anti-double-stranded DNA antibody, and anti-neutrophil cytoplasmic antibodies. Ultra-sonography and MRI showed atrophy of renal bodies (6.0 × 2.5 *vs*. 6.0 × 2.2 cm), the border of cortex and medulla was not clear but without polycystic lesions. No cysts were found in liver and pancreas. Echocardiography showed left ventricular enlargement and hypertrophy, with a decreased ejection fraction (EF) value of 10 percent.

Because their parents were consanguineous and her litter brother (see case 2) also had steroid-resistant nephrotic syndrome, hereditary nephrotic syndrome was suspected.

Case 2: A 2-year and-7-month-old boy (litter brother) was hospitalized to our hospital on November 07, 2013 with a complaint of edema and proteinuria for 7 months. Laboratory tests in the local hospital showed proteinuria (189 mg/kg/24h), hypoalbuminaemia (22.5 g/L) hypercholesterolemia (6.12 mmol/L) and microscopic hematuria (RBC 10~30/HP). His renal function was abnormal (Scr 28 μmol/L and BUN 2.6 mol/L). He was treated for nephrotic syndrome with full dose of prednisone for 8 weeks without response. The subsequent courses of cyclophosphamide pulse therapy (total 150mg/kg) proved futile. He came to our hospital together with his elder sister for further diagnosis and treatment.

There was no abnormal birth and past medical history, but a consanguineous family history of father and mother being first cousins.

At admission, his blood pressure was normal (95/65 mmHg). His height and weight were normal. Physical examination showed no positive signs. No neurodevelopmental and ophthalmologic deficits were observed. Laboratory tests in our hospital revealed heavy proteinuria (158 mg/kg/24h); urine microalbumin was 2290 while α1-microglobin was 18.6 mg/L. Albuminaemia (23.8 g/L) and cholesterolemia (8.45 mmol/L) were also shown positive. Scr was 28 μmol/L, BUN was 3.1 mol/L and hemoglobin was 140 g/L. There was no evidence of virus infection such as Epstein-Barr virus, cytomegalovirus or hepatitis virus. Autoimmune profile was within normal range including compliments, anti-nuclear antibody, anti-double-stranded DNA antibody, and anti-neutrophil cytoplasmic antibodies. Ultra-sonography and MRI showed enlarged renal bodies (7.5 × 3.2 *vs*. 7.3 × 3.0 cm), the border of cortex and medulla was not clear, with enhanced echo and without polycystic lesions. No cysts were found in liver and pancreas. Brain MRI showed no abnormal findings. Echocardiography showed normal heart function with an EF value of 69 percent. Renal biopsy yielded 46 glomeruli under

Table 1. Genetic analysis results of the families

Gene	Case 1	Case 2	Father	Mother
NPHS1	c.1339G>A (p.E447K), Hom*	c.1339G>A (p.E447K) Hom	c.1339G>A (p.E447K) Het*	c.1339G>A (p.E447K) Het
ADCK4	c.748G>C (p.D250H) Hom	c.748G>C (p.D250H) Hom	c.748G>C (p.D250H) Het	c.748G>C (p.D250H) Het

*: Hom: homozygous; Het: heterozygous.

light microscopy, which included 3 globally sclerotic glomeruli, the others showed mesengial hypercellularity and matrix hyperplasia with 5 focal segmental sclerosis, tubular epithelia vacuolar and granular degeneration with interstitial fibrosis. Immunohistochemical studies showed moderate granular C3 (1+ ~ 2+) staining of the mesangium. Electron microscopy revealed irregular thickening and segmental layering of the glomerular basement membrane, segmental fusion of the epithelial foot process; no electron-dense deposits were identified; mesangial hypercellularity and matrix increase combined with sclerosis were present.

Because their parents were consanguineous and his elder sister (see case 1) also had steroid-resistant nephrotic syndrome, hereditary nephrotic syndrome was suspected.

3. Results and Discussion

Genetic analysis results showed that both of the siblings carried a homozygous mutation in exon 11 c.1339G>A (p.E447K) in the *NPHS1* gene and a homozygous mutation in exon 9 c.748G>C (p.D250H) in the *ADCK4* gene. Their father and mother carried the same heterozygous mutations as the siblings. The parents showed no proteinuria, hematuria, and their renal function was normal. No variations were found on *NPHS2*, *WT1*, *COL4A3*, *COL4A4* and other associated genes. See Table 1.

The p.E447K mutation of *NPHS1* was found in the SNPs databases rs28939695, A = 0.0070/35 and 0.002898/347 in 1000Genomes and ExAX, respectively. Mutation tasting analysis showed amino acid sequence changed heterozygously in TGP or ExAC, known disease mutation at this position (HGMD CM004008), protein features might be affected, known disease mutation could be pathogenic. And it was not found in 100 normal Chinese controls.

The p.D250H mutation of ADCK4 was found 3 in ExAX (19-41209497-C-T, A = 2.514e-05) but not in 1000Genomes. Mutation tasting analysis showed that amino acid sequence was changed, protein features might be affected. And also it was not found in 100 normal Chinese controls.

The elder sister was changed from hemodialysis to peritoneal dialysis, given metoprolol tartrate, losartan potassium, coenzyme Q10 synthetic and maintenance therapy. With a follow-up of 24 months, her renal function remained stable (Scr 368 ~ 453 μmol/L, BUN 12.5 ~ 18.8 mol/L) and blood pressure was normal (100 ~ 120/75 ~ 90 mmHg) while her heart function showed no improvement (EF value of 15 ~ 25 percent).

The litter brother was treated with prednisone and tacrolimus for 6 months, his proteinuria variated from 86 to 136 mg/kg/24h. Prednisone and tacrolimus were withdrawn after the genetic diagnosis, he was also given coenzyme Q10 synthetic and maintenance therapy. With a follow up of 24 months, his renal function showed a slight increase (Scr 45 ~ 56 μmol/L, BUN 6.8 ~ 11.5 mol/L), blood pressure remained normal (90 ~ 115/60~85 mmHg), proteinuria variated between 86~136 mg/kg/24h, heart functionwas normal (EF value of 62 ~ 71 percent).

Nephrotic syndrome (NS) is a clinicopathological entity characterized by proteinuria, hypoalbuminemia, peripheral edema, and hyperlipidemia. It is the most common cause of glomerular disease in children and adults. Classically, 80% of cases in the pediatric age group are steroid sensitive nephrotic syndrome (SSNS), while the remaining 20% are called steroid-resistant nephrotic syndrome (SRNS). SRNS is characterized by a rapid progression to end-stage kidney disease (ESKD) with apathological lesion of focal and segmental glomerulosclerosis (FSGS), and it is the most common glomerular cause of ESKD (*10*). Inherited structural defects of the glomerular filtration barrier are responsible for a large proportion of SRNS cases (*2-7*). Classically, mutations in the *NPHS1* and *NPHS2* genes have been distinguished by their implications in familial congenital (onset at birth to 3 month) and in childhood-onset (later than 3 month) cases, respectively (*5,11*). Furthermore, it has recently been shown that mutations in *NPHS1* also account for a nonnegligible proportion of infantile, childhood and adult-onset SRNS cases (*12-14*). *ADCK4* gene, which located on chromosome 19q13.2 and encodes the aarF domain containing kinase 4, is now well-known as a single-gene cause of SRNS (*15-17*).

However, there was no report on SRNS caused by co-inheritance of mutations of *NPHS1* and *ACDK4* genes.

Our two siblings both presented with SRNS and pathological lesions of focal segmental glomerulosclerosis (FSGS), the elder sister also had hypertension, renal failure and cardiac dysfunction. They were from a consanguineous family. Genetic analysis showed that both of the siblings carried a homozygous mutation c.1339G>A (p. E447K) in the *NPHS1* gene and a homozygous mutation c.748G>C (p. D250H) in the *ADCK4* gene. Their father and mother carried the same

mutations heterozygously as the siblings but without any abnormal manifestations.

Both of the mutations are analyzed by Mutation tasting to be disease-causing. The E447K mutation of *NPHS1* had been reported previously in congenital nephrotic syndrome (CNS), which is within motif Ig5 and is unlikely to affect the function of nephrin because both glutamic acid and lysine are hydrophilic (*18*). However, the onset ages of the siblings are 9-year and 2-year old respectively, they are childhood and infantile nephrotic syndrome but not CNS. The onset ages of SRNS caused by *ADCK4* mutation are generally late that range from 7 ~ 21 years old when patients develope ESRD to 7 ~ 23 years old when they were found with a renal pathology of FSGS (*16*). ADCK4 is thought to be an important differential diagnosis to consider in case of adolescent-onset multidrug-resistant proteinuria with FSGS on biopsy (*15*). We are not sure which mutation is the main genetic cause of our SRNS siblings although their pathologic results are both FSGS.

There are reports on digenic inheritance of *NPHS1* and *NPHS2* mutations in congenital FSGS (*19*), *TRPC6* and *NPHS1* mutations in FSGS (*20*), respectively. We confirm an overlap in the *NPHS1/ADCK4* mutation spectrum with a unique characterization which results in a second hit and appears to modify the phenotype. This may result from an epistatic gene interaction, and provides a rare example of multiple allelic hits being able to modify an autosomal recessive disease phenotype in humans. The elder sister showed ESRD and especially severe heart function failure, besides relating to ESKD and hypertension itself, which might be explained by the D250H in *ADCK4* gene. Our findings provide the first evidence for a functional inter-relationship between *NPHS1* and *ADCK4* in human nephrotic disease, thus underscoring their critical role in the regulation of glomerular filtration (*19*).

Coenzyme Q10 (CoQ10) is an essential component of eukaryotic cells and is involved in crucial biochemical reactions such as the production of ATP in the mitochondrial respiratory chain, the biosynthesis of pyrimidines, and the modulation of apoptosis. CoQ10 requires at least 13 genes for its biosynthesis (*21*). Mutations in these genes cause primary CoQ10 deficiency, a clinically and genetically heterogeneous disorder. To date mutations in 8 genes (*PDSS1*, *PDSS2*, *COQ2*, *COQ4*, *COQ6*, *ADCK3*, *ADCK4*, and *COQ9*) have been associated with CoQ10 deficiency presenting with a wide variety of clinical manifestations. Onset can be virtually at any age, although pediatric forms are more common. Symptoms include those typical of respiratory chain disorders (encephalomyopathy, ataxia, lactic acidosis, deafness, retinitis pigmentosa, hypertrophic cardiomyopathy), but some (such as steroid-resistant nephrotic syndrome) are peculiar to this condition (*22*).

Primary CoQ10 deficiency is caused by mutations in *COQ* genes, while secondary deficiencies are related to defects in genes not directly involved in CoQ10 biosynthesis, or to non-genetic factors such as fibromyalgia. The peculiarity of CoQ10 deficiency among mitochondrial disorders is that patients respond well to oral supplementation with CoQ10, making this the only currently treatable mitochondrial disorder. High-dose oral CoQ10 supplementation can stop the progression of the encephalopathy (*23*) and also of the renal manifestations in patients with *COQ2* (*24*), *COQ6* (*25*) and *ADCK4* (*16*) mutations. However, oral CoQ10 supplementation showed no response on heart function in our elder sister, maybe because it was too late for her disease course. It is known that oral CoQ10 supplementation treatment should start as early as possible in the course of the disease, because, although it is possible to stop the progression of the disease, once damage in critical organs such as heart or kidney is established, only minimal recovery is possible (*24*). It needs further follow up to observe whether oral CoQ10 supplementation could delay or prevent ESRD and heart problem in our litter brother. It was a pity that we could not detect the levels of CoQ10 in our two cases.

In conclusion, we were the first to report two childhood SRNS cases with FSGS caused by co-inheritance of mutations at *NPHS1* and *ACDK4* genes in China, one case also developed ESRD and presented with especially severe heart function failure. Our findings provide the first evidence for a phenotype inter-relationship between *NPHS1* and *ADCK4* in human nephrotic disease.

References

1. Andolino TP, Reid-Adam J. Nephrotic syndrome. Pediatr Rev. 2015; 36:117-125; quiz 126, 129.
2. Hinkes BG, Mucha B, Vlangos CN, Gbadegesin R, Liu J, Hasselbacher K, Hangan D, Ozaltin F, Zenker M, Hildebrandt F; Arbeitsgemeinschaft für Paediatrische Nephrologie Study Group. Nephrotic syndrome in the first year of life: Two thirds of cases are caused by mutations in 4 genes (*NPHS1*, *NPHS2*, *WT1*, and *LAMB2*). Pediatrics. 2007; 119:e907-919.
3. Sako M, Nakanishi K, Obana M, Yata N, Hoshii S, Takahashi S, Wada N, Takahashi Y, Kaku Y, Satomura K, Ikeda M, Honda M, Iijima K, Yoshikawa N. Analysis of *NPHS1*, *NPHS2*, *ACTN4*, and *WT1* in Japanese patients with congenital nephrotic syndrome. Kidney Int. 2005; 67:1248-1255.
4. Tory K, Menyhard DK, Woerner S, Nevo F, Gribouval O, Kerti A, Straner P, Arrondel C, Huynh Cong E, Tulassay T, Mollet G, Perczel A, Antignac C. Mutation-dependent recessive inheritance of *NPHS2*-associated steroid-resistant nephrotic syndrome. Nat Genet. 2014; 46:299-304.
5. Bouchireb K, Boyer O, Gribouval O, *et al*. *NPHS2* mutations in steroid-resistant nephrotic syndrome: A mutation update and the associated phenotypic spectrum. Hum Mutat. 2014; 35:178-186.
6. Abid A, Khaliq S, Shahid S, Lanewala A, Mubarak M,

Hashmi S, Kazi J, Masood T, Hafeez F, Naqvi SA, Rizvi SA, Mehdi SQ. A spectrum of novel *NPHS1* and *NPHS2* gene mutations in pediatric nephrotic syndrome patients from Pakistan. Gene. 2012; 502:133-137.
7. Hall G, Gbadegesin RA. Translating genetic findings in hereditary nephrotic syndrome: The missing loops. Am J Physiol Renal Physiol. 2015; 309:F24-28.
8. Benoit G, Machuca E, Antignac C. Hereditary nephrotic syndrome: A systematic approach for genetic testing and a review of associated podocyte gene mutations. Pediatr Nephrol. 2010; 25:1621-1632.
9. Lovric S, Ashraf S, Tan W, Hildebrandt F. Genetic testing in steroid-resistant nephrotic syndrome: When and how? Nephrol Dial Transplant. 2016; 31:1802-1813.
10. Gbadegesin R, Lavin P, Foreman J, Winn M. Pathogenesis and therapy of focal segmental glomerulosclerosis: An update. Pediatr Nephrol. 2011; 26:1001-1015.
11. Schoeb DS, Chernin G, Heeringa SF, *et al*. Nineteen novel *NPHS1* mutations in a worldwide cohort of patients with congenital nephrotic syndrome (CNS). Nephrol Dial Transplant. 2010; 25:2970-2976.
12. Philippe A, Nevo F, Esquivel EL, *et al*. Nephrin mutations can cause childhood-onset steroid-resistant nephrotic syndrome. J Am Soc Nephrol. 2008; 19:1871-1878.
13. Machuca E, Hummel A, Nevo F, Dantal J, Martinez F, Al-Sabban E, Baudouin V, Abel L, Grunfeld JP, Antignac C. Clinical and epidemiological assessment of steroid-resistant nephrotic syndrome associated with the *NPHS2* R229Q variant. Kidney Int. 2009; 75:727-735.
14. Santin S, Garcia-Maset R, Ruiz P, *et al*. Nephrin mutations cause childhood- and adult-onset focal segmental glomerulosclerosis. Kidney Int. 2009; 76:1268-1276.
15. Korkmaz E, Lipska-Zietkiewicz BS, Boyer O, *et al*. *ADCK4*-Associated Glomerulopathy Causes Adolescence-Onset FSGS. J Am Soc Nephrol. 2016; 27:63-68.
16. Ashraf S, Gee HY, Woerner S, *et al*. *ADCK4* mutations promote steroid-resistant nephrotic syndrome through CoQ10 biosynthesis disruption. J Clin Invest. 2013; 123:5179-5189.
17. Malaga-Dieguez L, Susztak K. *ADCK4* "reenergizes" nephrotic syndrome. J Clin Invest. 2013; 123:4996-4999.
18. Aya K, Tanaka H, Seino Y. Novel mutation in the nephrin gene of a Japanese patient with congenital nephrotic syndrome of the Finnish type. Kidney Int. 2000; 57:401-404.
19. Koziell A, Grech V, Hussain S, Lee G, Lenkkeri U, Tryggvason K, Scambler P. Genotype/phenotype correlations of *NPHS1* and *NPHS2* mutations in nephrotic syndrome advocate a functional inter-relationship in glomerular filtration. Hum Mol Genet. 2002; 11:379-388.
20. Sun ZJ, Ng KH, Liao P, Zhang Y, Ng JL, Liu ID, Tan PH, Chong SS, Chan YH, Liu J, Davila S, Heng CK, Jordan SC, Soong TW, Yap HK. Genetic Interactions Between TRPC6 and NPHS1 Variants Affect Posttransplant Risk of Recurrent Focal Segmental Glomerulosclerosis. Am J Transplant. 2015; 15:3229-3238.
21. Doimo M, Desbats MA, Cerqua C, Cassina M, Trevisson E, Salviati L. Genetics of coenzyme q10 deficiency. Mol Syndromol. 2014; 5:156-162.
22. Trevisson E, DiMauro S, Navas P, Salviati L. Coenzyme Q deficiency in muscle. Curr Opin Neurol. 2011; 24:449-456.
23. Salviati L, Sacconi S, Murer L, Zacchello G, Franceschini L, Laverda AM, Basso G, Quinzii C, Angelini C, Hirano M, Naini AB, Navas P, DiMauro S, Montini G. Infantile encephalomyopathy and nephropathy with CoQ10 deficiency: A CoQ10-responsive condition. Neurology. 2005; 65:606-608.
24. Montini G, Malaventura C, Salviati L. Early coenzyme Q10 supplementation in primary coenzyme Q10 deficiency. N Engl J Med. 2008; 358:2849-2850.
25. Heeringa SF, Chernin G, Chaki M, *et al*. *COQ6* mutations in human patients produce nephrotic syndrome with sensorineural deafness. J Clin Invest. 2011; 121:2013-2024.

(Received July 2, 2017; Revised November 12, 2017; Accepted November 15, 2017)

Case Report

DOI: 10.5582/irdr.2017.01060

Inflammatory fibroid polyp of the gastric antrum presenting as hypovolemic shock: Case report and literature review

Kyle D. Klingbeil[1,*], Alexandra Balaban[1], Raymond M. Fertig[1], A. Caresse Gamret[1], Yuna Gong[2], Carolyn Torres[3], Shevonne S. Satahoo[1]

[1] *University of Miami, Miller School of Medicine, Miami, FL, USA;*
[2] *Oak Hill Hospital, Graduate Medical Education, Department of Internal Medicine, Miami, FL, USA;*
[3] *University of Pennsylvania, College of Liberal and Professional Studies, Philadelphia, PA, USA.*

Summary **Inflammatory fibroid polyps (IFP) are an extremely rare entity that arise within the submucosa of the gastrointestinal tract, and represent less than 0.1% of all gastric polyps. They are most commonly localized to the gastric antrum, small intestines and recto-sigmoid colon. IFPs are most commonly found incidentally upon endoscopic evaluation in the absence of symptoms. Presenting symptoms depend on the location of the tumor, although polyps located in the stomach most commonly present with epigastric pain and early satiety. Classic histologic features include perivascular onion skinning of spindle cells with an abundance of eosinophilic infiltration. The prompt diagnosis and management of IFP is essential due to its underlying risk for intussusception, outlet obstruction and acute hemorrhage. In addition, recent evidence has shown that IFP is driven by an activating mutation in the platelet derived growth factor receptor alpha (*PDGFRA*) gene, suggesting a neoplastic etiology. Herein, we discuss a case of a 65-year-old woman with an inflammatory fibroid polyp of the gastric antrum who initially presented with early hypovolemic shock and melena. Diagnosis was made by endoscopic visualization, biopsy and immunohistochemical analysis.**

Keywords: Inflammatory fibroid polyp, vanek tumor, gastric polyp, platelet derived growth factor receptor alpha, benign neoplasms of the gastrointestinal tract

1. Introduction

Inflammatory fibroid polyps (IFP) are an extremely rare entity that arise within the gastrointestinal tract, and represent less than 0.1% of all gastric polyps (*1*). These lesions most commonly affect older adults, especially those localizing to the gastric antrum. In children, IFPs more commonly occur in the small intestines and present as intussusception (*2*). IFPs arise from the submucosa and penetrate through the lamina propria leading to bulging of the mucosal layer. Rarely, they can ulcerate through the mucosa causing hemorrhage, leading to progressive blood loss and symptoms related to hypovolemic shock. Herein, we discuss a case of an adult woman who initially presented with a recent history of orthostatic hypotension and melena who was found to have an IFP of the gastric antrum evaluated by endoscopic visualization, biopsy and immunohistochemical analysis. A discussion involving the pathological characterization and management of IFP, followed by a brief review of the literature, is included in this article.

2. Case Report

A 65-year-old Puerto Rican woman with a past medical history of hypertension and asthma first presented to the emergency department with a one-day history of lightheadedness and a recent fall at home. The patient endorsed feeling generally unwell for several days, associated with two weeks of diarrhea, and was recovering with bed rest at home. On the day of presentation, while attempting to stand up from bed,

Released online in J-STAGE as advance publication November 15, 2017.

**Address correspondence to:*
Dr. Kyle D. Klingbeil, University of Miami Miller School of Medicine, 1600 NW 10th Ave #1140, Miami, Florida 33136, USA.
E-mail: kdk24@med.miami.edu

the patient immediately felt dizzy and eventually lost consciousness. She awoke on the floor, denying convulsive limb movements, tongue biting, or post-event confusion, and came to the hospital for further evaluation.

The patient was initially found to be hypotensive and tachycardic. While taking a urine sample, the patient noticed black, tarry stools. She denied any abdominal pain, nausea, vomiting, dysphagia, early satiety or use of iron supplementation. The patient denied having an upper endoscopy or colonoscopy in the past and was not currently taking anticoagulation or antiplatelet therapy. Family history was significant for a maternal grandmother and niece with stomach cancer. Physical examination revealed dry mucous membranes, reduced skin turgor and guaiac positive stool. Initial laboratory studies revealed a hemoglobin of 8.3 mg/dL and mean corpuscular volume of 91.6 fL with normal electrolytes and kidney function.

The patient was admitted to the hospital and given aggressive intravenous (IV) fluid resuscitation. A chest radiograph and computed tomography (CT) scan of the head were both negative for acute changes. CT abdomen/pelvis revealed an antral mass, measuring 1.82 × 2.08 cm in greatest diameter, protruding within the gastric lumen with associated sub-centimeter perigastric lymph nodes (Figure 1). No other sources of acute hemorrhage were identified. Upper endoscopy revealed a 3 cm ulcerated, semi-sessile mass in the gastric antrum with evidence of recent hemorrhage (Figure 2). An endoscopic ultrasound of the antral mass showed it to be derived from the submucosa and extending through the mucosa, with no evidence of invasion to surrounding organs. A repeat upper endoscopy was completed for tumor resection using a snare technique.

Pathological evaluation showed a nodular proliferation of bland spindle cells, small vessels, and an eosinophil-rich inflammatory infiltrate localized primarily to the submucosa with extension into the mucosa of the gastric antrum (Figure 3A-D). Immunohistochemistry analysis revealed positive staining for CD34 and negative staining for CD117, supporting the diagnosis of an inflammatory fibroid polyp. The patient tolerated the procedure and recovered without complications. Upon two-week follow-up evaluation, the patient's symptoms had resolved completely. An outpatient colonoscopy revealed no abnormalities.

3. Discussion

The inflammatory fibroid polyp, also known as a Vanek tumor/polyp, was first reported in 1949 by Vanek (*3*). The term inflammatory fibroid polyp was first proposed in 1953 by Helwig and Ranier (*4*). As a result, IFP has now been defined as a benign lesion of the GI tract derived from the submucosa. It is characterized pathologically by the presence of CD34 staining spindle cells, a prominent network of blood vessels, fibromyxoid stroma and an inflammatory infiltrate, typically dominated by eosinophils. Perivascular spindle cell "onion skinning" is present in about half of the lesions (*5,6*).

IFP must be differentiated from other benign and malignant spindle cell lesions including gastrointestinal stromal tumor (GIST), leiomyoma, leiomyosarcoma, schwannoma, and inflammatory myofibroblastic tumors (*6,7*). Definite diagnosis is made by immunohistochemical analysis. IFPs are most commonly positive for vimentin and CD34, and negative for S100, CD117 and desmin (*5,7,8*). The most common site of IFP was first reported at the gastric antrum (70%) followed by the small intestines (20%) in 1986 (*9*). However, the largest series of IFP to date (83 specimens) found the most commonly involved site to be the large intestines (37%), followed by the gastric antrum (23%) and small intestines (20%) (*5*).

The true pathogenesis of IFP is currently unknown. Historically, the etiology was thought to be the result of

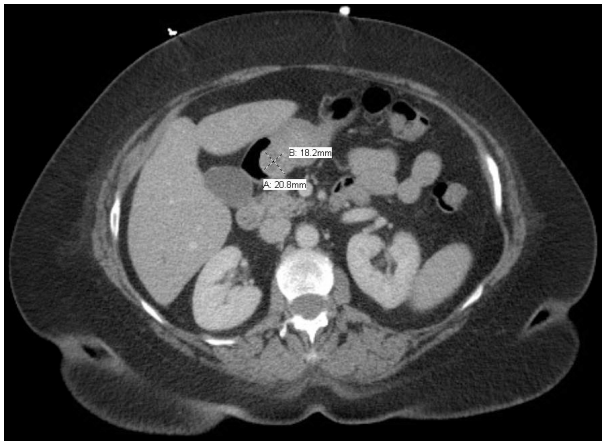

Figure 1. CT Abdomen with IV Contrast depicting a 1.82 × 2.08 cm mass of the antrum of the stomach. There are small subcentimeter perigastric nodes identified.

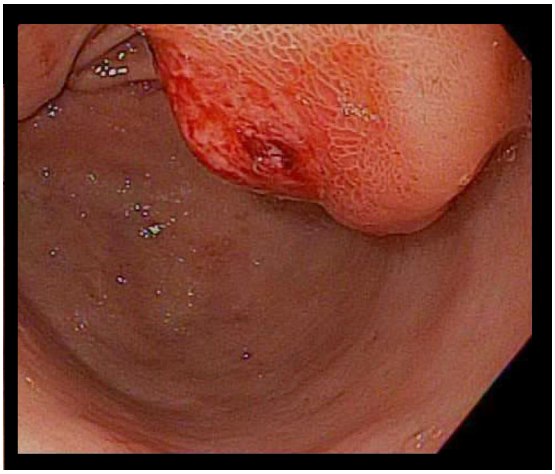

Figure 2. Upper endoscopy identifying a 3 cm large, submucosal, ulcerated, semi-sessile mass located in the gastric antrum.

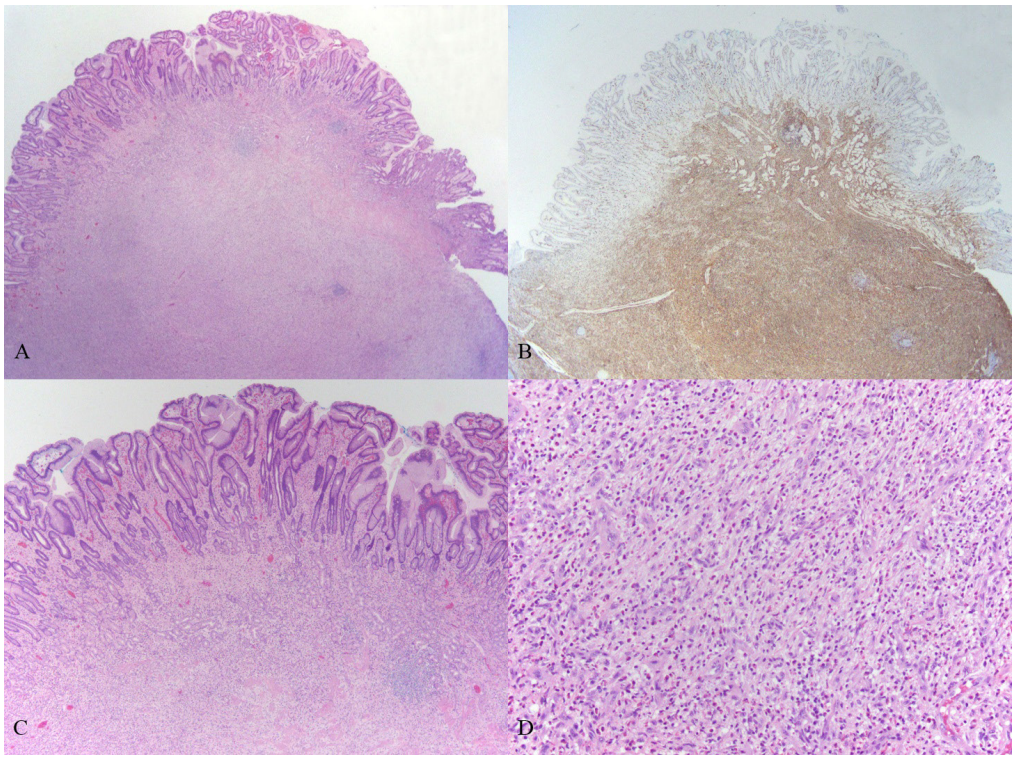

Figure 3: Pathological examination of case. (A), Low-power image of the inflammatory fibroid polyp showing a predominantly submucosal, nodular proliferation with extension into the mucosa (H&E, 20×); **(B)**, Immunohistochemical stain for CD34 shows characteristic diffuse positivity in the lesional cells (20×); **(C)**, Higher power image of the lesion infiltrating into and effacing mucosal architecture (H&E, 40×); **(D)**, High-power image showing the primary constituents of the lesion: bland spindled cells, small vessels, and eosinophil-rich mixed inflammatory infiltrate (H&E, 200×).

an inflammatory response to an underlying granuloma. The development of a submucosal granuloma is often associated with an irritating stimulus (*e.g.* trauma, tuberculosis, *helicobacter pylori*, Crohn disease, sarcoidosis) (*10*). However, IFP has been showed to occur more frequently in patients with a family history of gastrointestinal polyps (*11*). More recently, in the first genetic study involving IFP, activating mutations in the platelet-derived growth factor receptor alpha (*PDGFRA*) gene were present in 70% of cases (*12*). This evidence suggests instead that IFP may represent a true neoplastic lesion driven by activating mutations in *PDGFRA*. However, no evidence of invasive growth or aggressive metastatic spread has been reported to our knowledge.

The therapeutic strategy of IFP can be viewed similar to that of other benign gastrointestinal polyps. More than 90% of gastrointestinal polyps discovered by routine endoscopic evaluation are present in asymptomatic patients and have no malignant potential (*13*). However, these polyps cannot be distinguished from those that require further intervention by gross examination alone. Therefore, histological analysis is always indicated in determining the polyp type and presence of underlying dysplasia (*14*). Additional diagnostic modalities including immunohistochemistry staining, tandem biopsies, and endoscopic ultrasound (EUS) may also be necessary to correctly identify the polyp type (*13*).

Once the diagnosis of IFP is made, the decision to resect the polyp should be based on both the clinical presentation of the patient and the expertise of the gastroenterologist. Patients presenting with early satiety, chronic epigastric pain, or obstruction should undergo resection. Those who present with an acutely bleeding polyp should be treated swiftly by localizing the lesion and achieving adequate hemostasis. Once the patient is stabilized, eventual polyp resection is suggested to avoid similar adverse events in the future. Following IFP resection, pathological analysis should be initiated to confirm the diagnosis and rule out any potential for malignancy. Finally, because IFPs have no documented malignant potential, routine endoscopic follow-up is not recommended for both post-operative and asymptomatic patients (*13*).

A MEDLINE review of the literature published from 2000-2017 was conducted using the search terms "(Stomach neoplasms [MeSH Terms]) AND inflammatory fibroid polyp" to evaluate the characteristics of IFPs localized to the stomach. A total of 37 cases were identified (Table 1), with ages ranging from 19-93 year-old, averaging 64.3, including 19 women (51.4%) and 18 men (48.6%) (*8,15-37*). The gastric antrum was the most commonly involved site, n = 22 (59.5%), followed by the pyloric and pre-pyloric area, n = 5 (13.5%), gastric cardia, n = 2 (5.4%), gastric body,

Table 1. Review of inflammatory fibroid polyp cases

Reference, Year, (Ref.)	Age, Gender	Location	Largest diameter (cm)	Gross Appearance	Presenting Symptoms	Associated Findings	Treatment
Shalom, 2000 (*31*)	57, F	Antrum	5.5 × 3	Polypoid, two ulcers	Epigastric pain	H. Pylori +	Antrectomy with truncal vagotomy
Daum, 2003 (*8*)	45-93, M (9) F (5)	Antrum (9) Stomach NOS (5)	0.4 – 5.0	(9) surface erosions or ulcerations	N/A	H. pylori + (2)	N/A
Fuke, 2003 (*19*)	46, F	Antrum	2 × 1.3 × 1.2	Polypoid	Asymptomatic	Anemia	Endoscopic polypectomy
Hirasaki, 2003 (*21*)	66, M	Antrum	0.9 × 0.6	Protruding lesion	Found incidentally	Gastric adenocarcinoma close to IFP, H. pylori +	Endoscopic polypectomy
Nishiyama, 2003 (*26*)	70, F	Antrum	N/A	Broad based pyramidal with ulceration at apex	Found incidentally	Gastric adenocarcinoma, H. pylori +, anemia	Endoscopic polypectomy
Shigeno, 2003 (*32*)	74, F	Body	6.2 × 3.1	Pedunculated with ulcer	Melena, pallor, tachycardia	Anemia	Endoscopic polypectomy
Aydin, 2004 (*15*)	71, F	Antrum	0.2	Broad based polypoid with normal mucosa	Dyspepsia	N/A	Endoscopic polypectomy
Matsuhashi, 2004 (*23*)	43, F	Pre-pyloric	2.0	Elevated lesion with central reddish depression	N/A	H. pylori +	Regressed with H pylori eradication
Zinkiewicz, 2004 (*37*)	48, M	Cardia	0.25 × 0.39	Polypoid with central ulcer with necrotic tissue	Dysphagia, epigastric pain	Recurred after endoscopic excision one year ago	Proximal gastrectomy, local lymphadenectomy
Hirasaki, 2005 (*22*)	61, M	Pyloric	0.2	Protruding lesion	Found during yearly checkup on radiograph	H. pylori +	ESD
Paikos, 2007 (*27*)	65, F	Pre-pyloric	3.0 × 5.0	Polypoid	Epigastric f with projectile vomiting	Tumor was obstructing duodenal bulb	Endoscopic polypectomy
Bhatti, 2008 (*16*)	60, M	Antrum	N/A	N/A	Abdominal pain, tachycardia, epigastric tenderness	Perforated viscus	Billroth II gastrectomy
Ramachandra, 2008 (*28*)	50, M	Cardia	5	Polypoid with small ulcer	Epigastric pain	N/A	Laparoscopic transgastric excision
Tanaka, 2008 (*33*)	73, F	Antrum	0.1 × 0.2	Pedunculated	Presented for Anemia evaluation	N/A	Endoscopic polypectomy
Yen, 2010 (*36*)	61, F	Stomach NOS	1.0	N/A	Found incidentally EGD	N/A	Endoscopic submucosal dissection
Saritas, 2011 (*30*)	60, F	Antrum	6 × 4	Pendunculated mass	Epigastric pain and vomiting	Anemia	Endoscopic polypectomy
Woodward, 2011 (*34*)	64, F	Antrum	1 × 1 × 0.8	Pedunculated round polyp	Chest discomfort	History of GERD	N/A
Yamashita, 2011 (*35*)	73, M	Antrum	N/A	Smooth, flat elevation, with ulceration	Found incidentally on EGD	N/A	N/A
Ergun, 2012 (*18*)	51, F	Antrum	3	Polypoid	Epigastric pain and weight loss	N/A	Endoscopic polypectomy
Mucientes, 2012 (*25*)	69, M	Antrum	0.9	Polypoid	Epigastric pain	Superficial early gastric carcinoma in submucosa	Subtotal gastrectomy
Rossi, 2012 (*29*)	71, F	Pre pyloric	6	Rounded with central ulcer	Anorexia, nausea, early satiety	N/A	Gastric resection with Roux-en-Y reconstruction
He, 2013 (*20*)	19, M	Pre-pyloric	6	Sessile	Anemia and hyperpyrecia	N/A	Partial gastrectomy
Mitsui, 2015 (*24*)	60, M	Antrum	0.15	Pedunculated with erosion	Found on EGD	H pylori positive	Partial gastrectomy
Bilgin, 2016 (*17*)	65, F	Stomach NOS	N/A	Pedunculated tumor	Post prandial abdominal pain, projectile vomiting	Increased 18F-FDG uptake, gastric outlet obstruction	Total resection

EGD, esophagogastroduodenoscopy; ESD, endoscopic submucosal dissection; F, female; H, Pylori +, Helicobacter Pylori Positive; M, Male; N/A, not available; NOS, not otherwise specified.

n = 1 (2.7%), and the stomach not otherwise specified, *n* = 7 (18.9%). Gross morphology, when available, was most commonly described as polypoid or pedunculated, *n* = 14 (66.7%), followed by sessile, protruding, or rounded, *n* = 7 (33.3%). Associated ulceration or erosion of the tumor was often present, *n* = 18 (48.6%). Tumor size ranged from 0.15 to 6.2 cm in greatest diameter, with an average of 2.33 cm. Helicobacter pylori testing was positive in seven cases (18.9%). The most common presenting symptom was epigastric pain, *n* = 7 (18.9%) followed by anemia, *n* = 6 (16.2%). The most common treatment modality was endoscopic polypectomy, *n* = 10 (47.6%), followed by surgical gastrectomy, *n* = 9 (42.9%), and endoscopic submucosal dissection (ESD) (4.8%). One case regressed after helicobacter pylori eradication. Complications were rarely reported, with three cases (8.1%) developing gastric adenocarcinoma in close proximity to the IFP and two cases resulting in gastric outlet obstruction (5.4%). Only one polyp (2.7%) was described as having recurred after treatment.

4. Conclusion

The case herein represents a rare entity leading to the common presentation of an acute upper gastrointestinal hemorrhage. IFP remains one of the rarest benign tumors of the gastrointestinal tract, and appears most commonly in the gastric antrum and the rectosigmoid colon. Its pathogenesis is not completely understood. However, it is now widely viewed as a *PDGFRA*-driven benign neoplasm. Patients rarely present with symptoms, but may endorse epigastric pain, early satiety or symptoms related to obstruction. Diagnosis is made primarily with endoscopic biopsy, however additional studies including immunohistochemistry analysis may be required. Therapeutic management is based on the patient's clinical presentation and the expertise of the procedural team. Resection is generally recommended for symptomatic patients and for bleeding IFP lesions. Routine endoscopic evaluation is not indicated due to the lack of evidence for malignant transformation and recurrence.

References

1. Roseau G, Ducreux M, Molas G, Ponsot P, Amouyal P, Palazzo L, Amouyal G, Paolaggi JA. [Epithelial gastric polyps in a series of 13000 gastroscopies]. Presse Med. 1990; 19:650-654. (in French)
2. Huss S, Wardelmann E, Goltz D, Binot E, Hartmann W, Merkelbach-Bruse S, Buttner R, Schildhaus HU. Activating *PDGFRA* mutations in inflammatory fibroid polyps occur in exons 12, 14 and 18 and are associated with tumour localization. Histopathology. 2012; 61:59-68.
3. Vanek J. Gastric submucosal granuloma with eosinophilic infiltration. Am J Pathol. 1949; 25:397-411.
4. Helwig EB, Ranier A. Inflammatory fibroid polyps of the stomach. Surg Gynecol Obstet. 1953; 96:335-367.
5. Liu TC, Lin MT, Montgomery EA, Singhi AD. Inflammatory fibroid polyps of the gastrointestinal tract: Spectrum of clinical, morphologic, and immunohistochemistry features. Am J Surg Pathol. 2013; 37:586-592.
6. Makhlouf HR, Sobin LH. Inflammatory myofibroblastic tumors (inflammatory pseudotumors) of the gastrointestinal tract: How closely are they related to inflammatory fibroid polyps? Hum Pathol. 2002; 33:307-315.
7. Ozolek JA, Sasatomi E, Swalsky PA, Rao U, Krasinskas A, Finkelstein SD. Inflammatory fibroid polyps of the gastrointestinal tract: Clinical, pathologic, and molecular characteristics. Appl Immunohistochem Mol Morphol. 2004; 12:59-66.
8. Daum O, Hes O, Vanecek T, Benes Z, Sima R, Zamecnik M, Mukensnabl P, Hadravska S, Curik R, Michal M. Vanek's tumor (inflammatory fibroid polyp). Report of 18 cases and comparison with three cases of original Vanek's series. Ann Diagn Pathol. 2003; 7:337-347.
9. Blackshaw AJ, Levison DA. Eosinophilic infiltrates of the gastrointestinal tract. J Clin Pathol. 1986; 39:1-7.
10. Calderon MG, Caivano VC, Bagnaresi S, Jr, de Oliveira Lira JO, Raimundo RD, de Abreu LC, Correa JA. A unique case of inflammatory fibroid polyp in the duodenum of a female adolescent: Case report and literature review. Medicine (Baltimore). 2017; 96:e6131.
11. Allibone RO, Nanson JK, Anthony PP. Multiple and recurrent inflammatory fibroid polyps in a Devon family ('Devon polyposis syndrome'): An update. Gut. 1992; 33:1004-1005.
12. Schildhaus HU, Cavlar T, Binot E, Buttner R, Wardelmann E, Merkelbach-Bruse S. Inflammatory fibroid polyps harbour mutations in the platelet-derived growth factor receptor alpha (*PDGFRA*) gene. J Pathol. 2008; 216:176-182.
13. Islam RS, Patel NC, Lam-Himlin D, Nguyen CC. Gastric polyps: A review of clinical, endoscopic, and histopathologic features and management decisions. Gastroenterol Hepatol (N Y). 2013; 9:640-651.
14. Park DY, Lauwers GY. Gastric polyps: Classification and management. Arch Pathol Lab Med. 2008; 132:633-640.
15. Aydin A, Tekin F, Gunsar F, Tuncyurek M. Gastric inflammatory fibroid polyp. Gastrointest Endosc. 2004; 60:802-803.
16. Bhatti I, Melhado R, Leeder P, Semeraro D, Tierney G. Clinical challenges and images in GI. Image 3: Inflammatory fibroid polyp. Gastroenterology. 2008; 135:1465, 1808.
17. Bilgin SS, Bilgin M, Savas R, Erdogan EB. Inflammatory fibroid polyp of the stomach mimics malignancy on 18F FDG PET/CT imaging. Clin Nucl Med. 2016; 41:712-713.
18. Ergun M, Zengin N, Kayacetin E. Loop observe and snare technique for endoscopic resection of a gastric inflammatory fibroid polyp. Endoscopy. 2012; 44 Suppl 2 UCTN:E86-87.
19. Fuke H, Hashimoto A, Shimizu A, Yoshimura H, Nakano T, Shiraki K. Computed tomographic image of an inflammatory fibroid polyp of the stomach. Clin Imaging. 2003; 27:400-402.
20. He HY, Shen ZB, Fang Y, Sun YH, Qin XY. Bleeding and hyperpyrexia in an adult with gastric inflammatory fibroid polyp. Chin Med J (Engl). 2013; 126:2594.

21. Hirasaki S, Endo H, Nishina T, Masumoto T, Tanimizu M, Hyodo I. Gastric cancer concomitant with inflammatory fibroid polyp treated with endoscopic mucosal resection using an insulation-tip diathermic knife. Intern Med. 2003; 42:259-262.
22. Hirasaki S, Tanimizu M, Tsubouchi E, Nasu J, Masumoto T. Gastritis cystica polyposa concomitant with gastric inflammatory fibroid polyp occurring in an unoperated stomach. Intern Med. 2005; 44:46-49.
23. Matsuhashi N, Nakajima A, Nomura S, Kaminishi M. Inflammatory fibroid polyps of the stomach and Helicobacter pylori. J Gastroenterol Hepatol. 2004; 19:346-347.
24. Mitsui Y, Kagemoto K, Itagaki T, Inoue S, Naruse K, Muguruma N, Takayama T. Gastric inflammatory fibroid polyp morphologically changed by Helicobacter pylori eradication. Clin J Gastroenterol. 2015; 8:77-81.
25. Mucientes P, Mucientes F, Klaassen R. Inflammatory fibroid polyp associated with early gastric carcinoma: A case report. Ann Diagn Pathol. 2012; 16:148-151.
26. Nishiyama Y, Koyama S, Andoh A, Kishi Y, Yoshikawa K, Ishizuka I, Yokono T, Fujiyama Y. Gastric inflammatory fibroid polyp treated with Helicobacter pylori eradication therapy. Intern Med. 2003; 42:263-267.
27. Paikos D, Moschos J, Tzilves D, Koulaouzidis A, Kouklakis G, Patakiouta F, Kontodimou K, Tarpagos A, Katsos I. Inflammatory fibroid polyp or Vanek's tumour. Dig Surg. 2007; 24:231-233.
28. Ramachandra S, Lapsia S, Latifaj B, Ghai S. A rare cause of anaemia (2008: 3b). Eur Radiol. 2008; 18:1300-1302.
29. Rossi P, Montuori M, Balassone V, Ricciardi E, Anemona L, Manzelli A, Petrella G. Inflammatory fibroid polyp. A case report and review of the literature. Ann Ital Chir. 2012; 83:347-351.
30. Saritas U, Ustundag Y, Gedikoglu G. Successful endoscopic treatment of huge gastric inflammatory fibroid polyp. Turk J Gastroenterol. 2011; 22:224-226.
31. Shalom A, Wasserman I, Segal M, Orda R. Inflammatory fibroid polyp and Helicobacter pylori. Aetiology or coincidence? Eur J Surg. 2000; 166:54-57.
32. Shigeno T, Fujimori K, Nakatsuji Y, Kaneko Y, Maejima T. Gastric inflammatory fibroid polyp manifesting massive bleeding and marked morphological changes for a short period. J Gastroenterol. 2003; 38:611-612.
33. Tanaka K, Toyoda H, Imoto I, Hamada Y, Aoki M, Kosaka R, Noda T, Takei Y. Anemia caused by a gastric inflammatory fibroid polyp. Gastrointest Endosc. 2008; 67:345-346.
34. Woodward K, Gangarosa LM, Hunt HV. Gastric inflammatory fibroid polyp. Indian J Pathol Microbiol. 2011; 54:622-623.
35. Yamashita K, Arimura Y, Tanuma T, Endo T, Hasegawa T, Shinomura Y. Pattern of growth of a gastric inflammatory fibroid polyp with *PDGFRA* overexpression. Endoscopy. 2011; 43 Suppl 2 UCTN:E171-172.
36. Yen HH, Chen CJ. Education and Imaging. Gastrointestinal: Endoscopic submucosal dissection for gastric inflammatory fibroid polyp. J Gastroenterol Hepatol. 2010; 25:1465.
37. Zinkiewicz K, Zgodzinski W, Dabrowski A, Szumilo J, Cwik G, Wallner G. Recurrent inflammatory fibroid polyp of cardia: A case report. World J Gastroenterol. 2004; 10:767-768.

(Received September 3, 2017; Revised October 27, 2017; Accepted November 3, 2017)

Case Report

DOI: 10.5582/irdr.2017.01063

Disseminated mucormycosis: A sinister cause of neutropenic fever syndrome

Ghazal Tansir[1], Neha Rastogi[2], Prashant Ramteke[3], Prabhat Kumar[1,*], Manish Soneja[1], Ashutosh Biswas[1], Sanchit Kumar[1], Pankaj Jorwal[1], Upendra Baitha[1]

[1] *Department of Medicine, All India Institute of Medical Science, New Delhi, India;*
[2] *Division of Infectious Disease, Department of Medicine and Microbiology. All India Institute of Medical Science, New Delhi, India;*
[3] *Department of Pathology, All India Institute of Medical Science, New Delhi, India.*

Summary **A 15 year old girl presented with complaints of prolonged fever and recurrent episodes of hemoptysis. Initial investigation showed pancytopenia and radiological imaging was suggestive of necrotizing pneumonia. Subsequently, mucor was isolated from bronchoalveolar lavage fluid, but even on appropriate medications her condition kept deteriorating. She had multiple bouts of hemoptysis and a repeat imaging of chest showed dissemination of mucormycosis to pulmonary vein and heart. Bone marrow biopsy identified acute lymphoblastic leukemia (ALL) as the cause of pancytopenia. She was planned for bronchial artery embolization and chemotherapy for ALL, but consent was not given and she left our institute against medical advice. Our case highlights the importance of keeping a high index of suspicion for disseminated mucormycosis in neutropenic patients, as any delay in diagnosis and treatment could have grave consequences.**

Keywords: Cardiac mucormycosis, acute lymphoblastic leukemia, galactomannan

1. Introduction

Fever in neutropenic patient is a medical emergency and warrants extensive evaluation and appropriate management. The risk of infection increases with severity and duration of neutropenia (*1*). Bacterial infections are the most common cause of neutropenic fever. Fungal infection often complicates these individuals and can have myriad presentations. Most of these invasive fungal infections are caused by Candida and Aspergillus spp. Mucormycosis is a rare infection in neutropenic patients and carries a grave prognosis (*2*).

Mucorales are responsible for life threatening mucormycosis infection in the immunocompromised. Increasing incidence of this infection has recently been observed in the immunocompromised population. This includes patients with uncontrolled diabetes especially in ketoacidosis, on prolonged steroid or broad spectrum antibiotic therapy, on voriconazole prophylaxis, hematological malignancies, hematopoietic stem cell transplants, burns and penetrating trauma. The aggressive, angio-invasive nature of the disease, coupled with weakened host defenses is responsible for its devastative consequences (*3*). There has been an increase in the incidence of mucormycosis in recent times, yet it still largely remains under-diagnosed. Disseminated mucormycosis is the least common type and mostly begins in lung and then disseminates to other sites. Dissemination of pulmonary mucormycosis to heart is unusual and diagnosis is often made on autopsy, antemortem diagnosis of this entity is very rare and only three such cases have been reported so far (*4-6*). We present a rare case of disseminated mucormycosis having pulmonary and cardiac involvement in a young girl with previously undiagnosed hematological malignancy.

2. Case Report

A 15 year old girl presented in medical emergency of our institute on 26th July 2017, with a five month history of continuous, low grade fever with early satiety and easy fatigability, productive cough for one month which

Released online in J-STAGE as advance publication November 14, 2017.

**Address correspondence to:*
Dr. Prabhat Kumar, Department of Medicine, 3rd floor, Teaching Block, All India Institute of Medical Science, New Delhi 110029, India.
E-mail: drkumar.prabhat@gmail.com

was associated with recurrent episodes of epistaxis and hemoptysis. She was treated at a local hospital and found to have pancytopenia and pneumonia. She was managed with blood transfusions along with antibiotics and referred to our institute for further management.

On examination, she had tachycardia and tachypnea, with pallor and significant submandibular lymphadenopathy. There was bronchial breath sounds with crepitations over the left infrascapular and infraaxillary regions of the chest. Preliminary investigations revealed pancytopenia with hemoglobin - 5.6 gm/dL, total leucocyte count (TLC) - 1,400/cu mm, platelets – 45,000/cu mm and an absolute neutrophil count of 980/cu mm. Her peripheral smear was suggestive of pancytopenia with normocytic normochromic anemia. Serum Vitamin B12, folate and Lactate Dehydrogenase (LDH) levels were normal.

Chest X Ray showed heterogeneous opacity over left middle and lower zone with blunting of left costophrenic angle (Figure 1). A Contrast Enhanced Computed Tomography (CECT) of chest revealed necrotizing pneumonia with organized empyema in the left lung. 2D Echocardiography was suggestive of mild pericardial effusion and all cardiac chambers were normal. Her blood, urine and sputum cultures were sterile. Sputum examination didn't show any acid fast bacilli and cartridge based nucleic acid amplification test (GeneXpert) for mycobacterium tuberculosis (MTB) was negative. Serum procalcitonin level was normal and serum galactomannan was not detected. The patient was empirically started on intravenous antibiotics (piperacillin-tazobactam with teicoplanin) and liposomal Amphotericin B (5 mg/kg/day).

Gradually she responded to treatment with improvement in fever and hematological profile. On day 6, her hemoglobin was 8.1 gm/dL, TLC was 2,000/cu

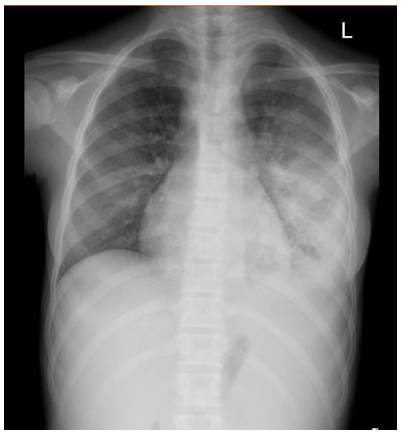

Figure 1. Chest X ray showing left middle and lower zone opacity with blunted left costophrenic angle.

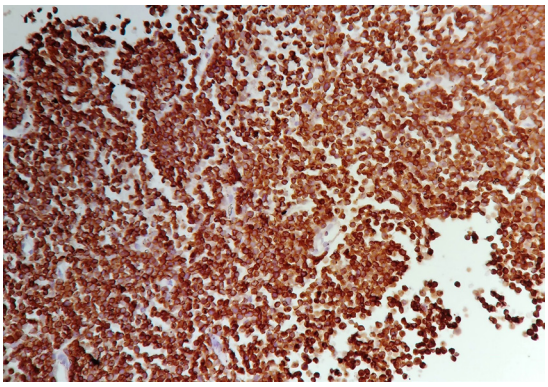

Figure 2. Immunohistochemistry slide (10×) with CD20 positive sheets of immature B-lymphocytes.

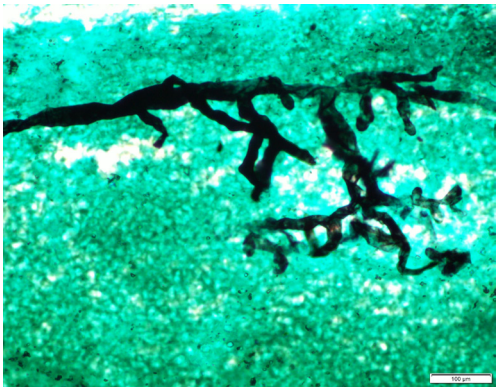

Figure 3. Silver methenamine staining (40×) showing aseptate broad fungal hyphae with wide angle branching suggestive of mucormycosis.

Figure 4. CECT Chest showing left lung necrotizing pneumonia.

Figure 5. CECT Chest with absence of contrast filling in left pulmonary vein (1) and left atrium (2) suggestive of thrombosis.

mm and platelet count was 63,000/cu mm. Review chest ultrasound revealed an organized empyema with non-drainable contents. Hence, a bronchoalveolar lavage (BAL) was performed. Bone marrow aspiration and biopsy were also performed. While we waited the BAL and bone marrow reports, her blood flow cytometry suggested presence of atypical lymphoid cells. Subsequently, her bone marrow biopsy revealed the presence of sheets of immature cells immunopositive for CD20 and terminal deoxynucleotidyl transferase (TdT) clinching the diagnosis of B-cell Acute Lymphoblastic Leukemia (Figure 2). BAL showed acute inflammatory exudate with aseptate broad fungal hyphae with wide angle branching consistent with mucormycosis (Figure 3). BAL was negative for acid-fast bacilli, GeneXpert MTB and galactomannan.

By day 15, the patient began to run fever again and experienced multiple episodes of hemoptysis. So, a repeat CECT chest was carried out urgently. This time, there was a large necrotizing pneumonia in the left lung along with intraluminal extension of the mass into the left pulmonary vein until the left atrium. The inferior pulmonary vein was also encased by the mass (Figure 4 and Figure 5). 2D Echocardiography showed a left atrial thrombus of (9 × 7 mm) entering through the left inferior pulmonary vein, suggestive of intracardiac mucormycosis. Addition of caspofungin for combination therapy and surgical intervention was planned for the patient. However her family did not consent for further treatment and left our hospital against medical advice on 13th August 2017.

3. Discussion

Mucormycosis is an uncommon, life-threatening infection caused by ubiquitous fungi of the group Mucorales. The vast spectrum of mucormycosis depends on the underlying condition. The infection can be of rhino-orbito-cerebral, pulmonary, gastrointestinal, cutaneous, renal and disseminated types. Mucormycosis is said to be disseminated when it involves two or more noncontiguous sites. Overall, rhino-orbito-cerebral involvement is most common (48%) with diabetics predominantly harboring the condition (*7*). Pulmonary mucormycosis is found in 17% of cases, most commonly in patients with hematological diseases. Disseminated disease forms the least common type (5%) and mostly begins with pulmonary mucormycosis (*8*). The most common site of dissemination is cerebral with involvement also being reported in spleen, heart, kidney and other organs. The vasculotropic nature of the infection leads to angioinvasion and widespread tissue necrosis contributing to the fatality of disease. Indeed, pulmonary mucormycosis has a mortality of 76% that increases to more than 90% with dissemination (*9*).

Patients of hematological disorders are especially susceptible to mucormycosis due to effects of chemotherapeutic drugs and the underlying cytopenias. Acute leukemia is the most common hematological disorder (78%), followed by lymphomas, myelodysplastic syndrome, multiple myeloma and aplastic anemia (*10*). Studies have found mucormycosis to be the third most common fungal infection in hematological malignancies after *Aspergillus* and *Candida*, with a share of 13% (*11*). And though the prevalence of mucormycosis in hematological malignancies is reported as 4.29 per 100 patients, it is probably an underestimation because this disease remains under-diagnosed (*12*). There is no specific biomarker and cultures may be negative. Moreover, thrombocytopenia in hematological diseases may preclude extraction of tissue specimens for diagnosis. Therefore, the disease is usually diagnosed at a much later stage, or even post-mortem in almost 85% patients (*13*).

Pulmonary infection can present as a non-resolving pneumonia, cavitation, air-crescent sign, halo sign, reverse halo sign, pulmonary mass, nodules, bronchopulmonary fistulae, pleural effusions or lymphadenopathy (*14*). The radiographic picture is not different from that of aspergillosis, and hence may lead to voriconazole use, which can be detrimental. This infection has a predilection for invasion into adjacent structures and vessels, which becomes the basis for cardiac involvement with pulmonary mucormycosis. Cardiac mucormycosis has not been extensively reported in the medical literature and most cases are diagnosed on autopsy (*15*). The hallmark of infection is presence of septic fungal thrombosis containing non-branching aseptate hyphae enmeshed with fibrin and leucocytes. These thrombi can invade the myocardium or endocardium causing infarctions by blockage of small myocardial blood vessels. Acute myocardial infarction has also been reported due to blockage of major epicardial arteries. There may be endocarditis, myocarditis and pericarditis (*16*). Left atrium and ventricle are the most common cardiac chambers affected with mural mycotic thrombi. To the best of our knowledge, there are only three case reports of pulmonary antemortem diagnosis with cardiac mucormycosis. Hence, this case of pulmonary mucormycosis invading to heart and diagnosed antemortem, is unique.

Amphotericin B has been used for medical treatment of mucormycosis, with its liposomal form preferred due to less toxicity. Newer drugs have been introduced namely: posaconazole, isuvaconzole and echinocandins. While posaconazole has shown promising outcomes, Amphotericin B remains the first-line drug with posaconazole used as a salvage therapy (*17*). However, it has been proven that management of mucormycosis is multi-modal with surgical management and treatment of the underlying condition as important in antifungal therapy.

Our patient had a unique presentation with a newly diagnosed ALL, which came to light due to

disseminated fungal pneumonia. Although we kept a high index of suspicion from the outset and gave her Liposomal Amphotericin B, the disease progressed. This emphasizes the superiority of multi-pronged management, comprised of both medical and surgical approaches.

In conclusion, disseminated mucormycosis is a rare entity that warrants early diagnosis and aggressive management. With an increase in the immunocompromised population, the incidence of mucormycosis is expected to rise in the future. A high index of suspicion is necessary as the diagnosis of mucormycosis can be elusive. Medical management, surgical therapy and treatment of the underlying disease all go hand-in-hand for management of these patients.

References

1. Keng MK, Sekeres MA. Febrile neutropenia in hematologic malignancies. Curr Hematol Malig Rep. 2013; 8:370-378.
2. Kauffman CA, Malani AN. Zygomycosis: An emerging fungal infection with new options for management. Curr Infect Dis Rep. 2007; 9:435-440.
3. Katragkou A, Walsh TJ, Roilides E. Why is mucormycosis more difficult to cure than more common mycoses? Clin Microbiol Infect. 2014; 20:74-81.
4. Mititelu R, Bourassa-Blanchette S, Sharma K, Roth V. Angioinvasive mucormycosis and paradoxical stroke: A case report. JMM Case Rep. 2016; 3:e005048.
5. Gubarev N, Separovic J, Gasparovic V, Jelic I. Successful treatment of Mucormycosis endocarditis complicated by pulmonary involvement. Thorac Cardiovasc Surg 2007; 55:257-258.
6. Muqeetadnan M, Rahman A, Amer S, Nusrat S, Hassan S, Hashmi S. Pulmonary mucormycosis: An emerging infection. Case Rep Pulmonol. 2012; 2012:120809.
7. Chakrabarti A, Chatterjee SS, Das A, Panda N, Shivprakash MR, Kaur A, Varma SC, Singhi S, Bhansali A, Sakhuja V. Invasive zygomycosis in India: Experience in a tertiary care hospital. Postgrad Med J. 2009; 85:573-581.
8. Petrikkos G, Skiada A, Lortholary O, Roilides E, Walsh TJ, Kontoyiannis DP. Epidemiology and clinical manifestations of mucormycosis. Clin Infect Dis. 2012; 54:S23-S34.
9. Gleissner B, Schilling A, Anagnostopolous I, Siehl I, Thiel E. Improved outcome of zygomycosis in patients with hematological disease? Leuk Lymphoma. 2004; 45:1351-1360.
10. Hsu LY, Lee DG, Yeh SP, Bhurani D, Khanh BQ, Low CY, Norasetthada L, Chan T, Kwong YL, Vaid AK, Alejandria I, Mendoza M, Chen CY, Johnson A, Tan TY. Epidemiology of invasive fungal diseases among patients with hematological disorders in the Asia-Pacific: A prospective observational study. Clin Microbiol Infect. 2015; 21:594.e7-11.
11. Atkinson JB, Connor DH, Robinowitz M, McAllister HA, Virmani R. Cardiac fungal infections: Review of autopsy findings in 60 patients. Hum Pathol. 1984; 15:935-942.
12. Noorifard M, Sekhavati E, Jalaei Khoo H, Hazraty I, Tabrizi R. Epidemiology and clinical manifestations of fungal infection related to mucormycosis in hematological malignancies. J Med Life. 2015; 8:32-37.
13. Kontoyiannis DP, Wessel VC, Bodey GP, Rolston KV. Zygomycosis in the 1990s in a tertiary care cancer center. Clin Infect Dis. 2000; 30:851-856.
14. McAdams HP, Rosado de Christenson M, Strollo DC, Patz EF Jr. Pulmonary mucormycosis: Radiologic findings in 32 cases. AJR Am J Roentgenol. 1997; 168:1541-1548.
15. Virmani R, Connor DH, McAllister HA. Cardiac mucormycosis: A report of five patients and review of 14 previously reported cases. Am J Clin Pathol. 1982; 78:42-47.
16. Jackman JD Jr, Simonsen RL. The clinical manifestations of cardiac mucormycosis. Chest. 1992; 101:1733-1736.
17. van Burik JA, Hare RS, Solomon HF, Corrado ML, Kontoyiannis DP. Posaconazole is effective as salvage therapy in zygomycosis: A retrospective summary of 91 cases. Clin Infect Dis. 2006; 42:e61-e65.

(Received September 18, 2017; Revised October 17, 2017; Accepted October 24, 2017)

Case Report

DOI: 10.5582/irdr.2017.01071

Expanded dengue syndrome in secondary dengue infection: A case of biopsy proven rhabdomyolysis induced acute kidney injury with intracranial and intraorbital bleeds

Ghazal Tansir, Chhavi Gupta, Shubham Mehta, Prabhat Kumar*, Manish Soneja, Ashutosh Biswas

Department of Medicine, All India Institute of Medical Science, New Delhi, India.

Summary **Dengue fever is endemic in the Indian subcontinent and can have myriad presentations. The term expanded dengue syndrome (EDS) is used for atypical manifestations in dengue fever. We present a rare case of EDS in a patient with secondary dengue infection who developed rhabdomyolysis induced acute kidney injury (RAKI) along with intracranial and intraorbital bleeds. Patient was successfully managed in our institute and was discharged in stable condition. To the best of our knowledge, this is the only reported case of simultaneous occurrence of these complications in a dengue patient. This case is being presented to make clinicians aware of the spectrum of dengue infection.**

Keywords: Acute tubular necrosis, acute febrile illness, choroidal hematoma

1. Introduction

Dengue is one of the most important arthropod-borne viral diseases. More than 50 million people residing in tropical areas are infected with dengue every year and its incidence has increased 30 times in the last 50 years (*1*). The dengue virus is an RNA virus from the genus Flavivirus transmitted *via* the bite of female *Aedes aegypti* mosquitoes. There are four virus serotypes, designated as DENV-1, DENV-2, DENV-3 and DENV-4. Infection with any one serotype confers lifelong immunity to that virus serotype and only partial cross immunity to other serotypes. However, secondary infection with another serotype or multiple infections with different serotypes can lead to a severe form of disease (*2*).

The clinical presentation of dengue has varied patterns ranging from asymptomatic infection, to severe bleeding, hemodynamic instability and even death. While fever, headache, malaise, bleeding manifestations, shock and hemoconcentration are known manifestations of the disease, certain atypical conditions have also been reported, which are now known as expanded dengue syndrome (*3*). Rhabdomyolysis induced acute kidney injury (RAKI) is one such atypical manifestation of dengue infection which is rarely seen and a single biopsy proven case has been reported so far (*4*). Similarly intracranial and intraorbital bleeds in dengue infection are very unusual (*5,6*). Expanded dengue syndrome (EDS) cases are underreported and pose a serious challenge for the treating physician.

2. Case Report

A 35 year old male patient with no prior comorbidities presented in emergency department in September 2017 with complaints of shortness of breath and reduced urine output for 6 days which was associated with hematuria, myalgia and rash over extremities. He also had swelling of right eye for the last 2 days that was associated with diminution of vision. These symptoms were preceded by fever of 6 days duration that subsided after taking antipyretics. He also gave history of dengue fever two years back for which he was admitted to a hospital for two days and had recovered completely. On examination, he was afebrile, blood pressure was 160/90 mm Hg, pulse rate- 110/min, respiratory rate-

**Address correspondence to:*
Dr. Prabhat Kumar, Department of Medicine, 3rd floor, Teaching Block, All India Institute of Medical Science, New Delhi 110029, India.
E-mail: drkumar.prabhat@gmail.com

Figure 1. Conjunctival suffusion with eyelid edema of the right eye.

Figure 2. Axial NCCT of orbits showing expansion of the right posterior segment with hyperdense hematoma over the choroid (arrow).

Figure 3. NCCT head showing right frontal hematoma (3.5 × 8.0 mm) with perilesional edema.

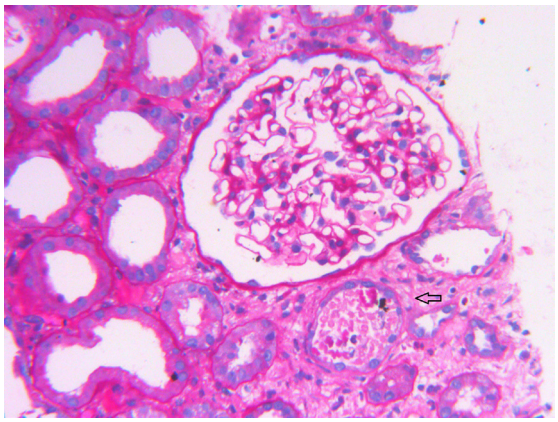

Figure 4. Renal biopsy showing normal glomerulus, dilated proximal tubules with tubular epithelial cell swelling and necrosis. Some of the tubules contain proteinaceous substances (arrow).

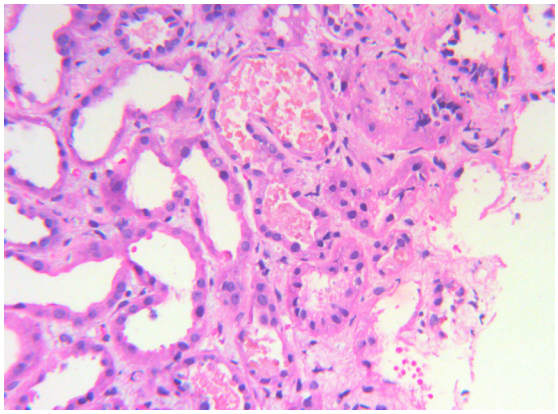

Figure 5. PAS stain highlights thinning and loss of PAS positive brush border.

30/min and had oxygen saturation of 90% on room air. There was conjunctival suffusion and eyelid edema with impaired vision in the right eye (Figure 1). There were fine basal crepitations over the chest and ascites was present. He had no focal neurological deficit at the time of admission. A suspicion of dengue was kept and following investigation were done immediately.

Hemogram showed hemoglobin: 9 gm/dL, total leucocyte count (TLC): 7,000/cu mm, platelet count: 29,000/cu mm. Renal and liver parameters were grossly deranged, urea/creatinine:130/9.5 mg/dL, total bilirubin: 3 mg/dL, aspartate transaminase/alanine transaminase (AST/ALT): 16,280 / 5,982 U/L. Urine examination showed gross proteinuria and > 100 RBCs/hpf without any casts or dysmorphic RBCs. Arterial blood gas analysis (ABG) showed severe metabolic acidosis. Serum electrolytes and coagulation profile were normal. Serum creatine phosphokinase (CPK) was 6,400 U/L (Normal: 20-200) and lactate dehydrogenase (LDH) was 10,240 IU/L (Normal: 100-400). Ultrasound abdomen showed gall bladder wall edema with moderate ascites and normal kidneys. Dengue serology was positive for both IgM and IgG in high

Table 1. Summary of patients with dengue associated rhabdomyolysis induced acute kidney injury

Ref.	Age, Sex	Diagnosis	Treatment	Duration of hospital stay	Outcome
Gunasekera *et al*. 2000 (*16*)	28 yr, F	Dengue with RAKI	Forced alkaline diuresis, hydration Antibiotics,	NA	Recovered
Karakus *et al*. 2007 (*17*)	66 yr, M	Dengue with RAKI, pneumonia, septic shock and respiratory failure	Mechanical ventilation, ionotropes	47 days	Death
Acharya *et al*. 2010 (*18*)	40 yr, M	Dengue myositis, RAKI with respiratory failure	Mechanical ventilation	NA	Recovered
Wijesinghe *et al*. 2013 (*19*)	42 yr, M	Dengue with RAKI	Hemodialysis, forced alkaline diuresis	9 days	Recovered
Sunderlingam *et al*. 2013 (*20*)	17 yr, M	Dengue, RAKI, MRSA infection with refractory shock	Antibiotics, ionotropes and hydration	NA	Death
Jha R *et al*. 2013 (*21*)	21 yr, M	Dengue with RAKI	Hemodialysis	9 days	Recovered
Repizo *et al*. 2014 (*4*)	28 yr, M	Dengue with biopsy proven RAKI	Hemodialysis	21 days	Recovered
Siriyakorn N *et al*. 2015 (*22*)	17 yr, M	Dengue, RAKI, severe hepatitis and coagulopathy	Hemodialysis, Mechanical ventilation	12 days	Death
Mishra A *et al*. 2015 (*23*)	21 yr, M	Dengue with RAKI	Hydration, forced alkaline diuresis	9 days	Recovered
Present case	35 yr, M	Dengue, biopsy proven RAKI, intracerebral and intraorbital bleed	Hemodialysis, antibiotics	30 days	Recovered

yr: years, M: Male, F: Female, RAKI: Rhabdomyolysis induced acute kidney injury.

titres, confirming our diagnosis of secondary dengue infection. Other relevant tests for malaria, leptospirosis and rickettsial infections were negative. Chest X ray and ECG was normal. A possibility of dengue associated RAKI was kept, however urinary myoglobin levels couldn't be done because of its unavailability in our institute.

He was given broad spectrum antibiotics and was transfused with multiple random donor platelet concentrates. He also received alternate-day dialysis for RAKI. Ophthalmologist's opinion was taken for right eye swelling and an ultrasound B-scan showed a choroidal hematoma measuring 15 × 10 mm. This was confirmed on non-contrast computed tomography (NCCT) of the orbit (Figure 2). He was also given topical antibiotics for orbital cellulitis. On the seventh day of admission he noticed weakness of left lower limb. NCCT head showed an intracranial bleed in the right frontal region with minimal perilesional edema (Figure 3). This was conservatively managed and his power gradually improved. Subsequent reports showed normalization of platelet count, liver enzymes, CPK and LDH levels in the next two weeks. However, there was minimal improvement in renal function rendering the patient oliguric and dialysis-dependent for a long time. The unusually slow renal recovery prompted us to carry out a renal biopsy. Biopsy showed normal glomeruli, dilated proximal tubules with tubular epithelial cell swelling and necrosis along with deposition of proteinaceous granular substances (Figure 4 and Figure 5). Hence, rhabdomyolysis induced acute tubular necrosis was proven histopathologically. He received a total of 12 cycles of hemodialysis, following which his urine output improved and renal function tests normalized. He was discharged after a month-long stay in October 2017.

3. Discussion

India has the largest number of dengue cases, with about 33 million apparent and another 100 million asymptomatic infections occurring annually. It is a well known fact that primary or first infection in nonimmune person usually causes inapparent or mild infection. However, subsequent dengue infection by a different serotype causes more severe illness. Although pathogenesis is not well-defined, the antibody dependent enhancement effect, cross-reactive T cells and shift from Th1 to Th2 pathway leads to a cytokine storm, which is possibly responsible for severe illness during secondary infection (*7,8*).

EDS is a terminology introduced by the WHO in 2012 to encompass the unusual manifestations of dengue involving severe damage to the liver, heart,

kidneys or brain. They may be related to underlying co-morbidities, associated co-infections or prolonged shock. Certain high-risk groups such as pregnant, infants, geriatric group, patients with coronary artery disease, hemoglobinopathies and immunocompromised individuals are particularly susceptible to developing EDS. As clinicians, we must be aware of these atypical features so that we can suspect dengue early, especially during ongoing epidemics.

Dengue has been associated with multiple patterns of renal involvement. These include proteinuria, glomerulonephritis, IgA nephropathy, hemolytic uremic syndrome and acute tubular necrosis (*9*). Despite the multitude of patterns of involvement, acute kidney injury (AKI) remains a poorly studied area in dengue infection. Various studies have found the prevalence of AKI in dengue to be between 1-13% (*10-12*). The mechanisms proposed for this affliction of the kidneys include direct viral action on renal tissue, hypoperfusion secondary to shock, and rhabdomyolysis.

Rhabdomyolysis is characterized by muscle necrosis leading to release of muscle enzymes like creatine phosphokinase, lactate dehydogenase, aldolase and myoglobin in the systemic circulation. It has been described in a few case reports among dengue patients (*13*). These patients present with severe myalgias and have high levels of muscle enzymes, most often in thousands. It is caused by either a direct viral or toxin-mediated effect on myocytes and is associated with renal failure in 57% of cases. Deposition of myoglobin in the tubules leading to direct or ischemic tubular injury, tubular obstruction or intrarenal vasoconstriction, are responsible for the renal failure. Although not traditionally believed to be associated with myositis, dengue virus is being recognized now as a cause. Studies have found histopathological changes of myositis even in dengue patients devoid of muscular symptoms (*14,15*). Renal tubular injury caused by rhabdomyolysis has been scarcely reported among dengue patients. To the best of our knowledge nine such cases have been reported, with only a single biopsy-proven case (Table 1) (*4,16-23*). Three out of the nine patients died, proves the seriousness of this condition (*17,20,22*). Treatment includes hydration with normal saline and forced alkaline diuresis with sodium bicarbonate to maintain adequate urine output. However, in oliguric AKI intravenous fluids should be judiciously used and hemodialysis should be commenced as soon as possible. Four out of these nine patients required dialysis for deteriorating AKI. Apart from AKI, other complications of rhabdomyolysis include compartment syndrome, arrhythmias, disseminated intravascular coagulation (DIC), hepatic dysfunction and metabolic acidosis (*24*). Any delay in diagnosis and treatment of these complications can be detrimental. In the present case too, the patient developed oliguric renal failure along with hepatitis as a complication of rhabdomyolysis for which he received several sessions of hemodialysis.

Along with renal involvement, our patient also had intracranial and ophthalmic complications. Neurological manifestations have been described in dengue fever, with encephalitis being the most common. The pathogenesis has been postulated to be due to direct viral invasion, increased capillary permeability, capillary hemorrhage, DIC, dyselectrolytemias and fulminant hepatic failure. Intracranial hemorrhage in dengue patients is an unusual entity with a study finding only 3% of cases of dengue encephalopathy attributable to it (*5*).

Ophthalmic complications in dengue has recently been recognized and reported more often. Studies have found 60% dengue patients to have ocular complications with subconjunctival hemorrhage being most common. Posterior segment involvement is reported too, with macular edema, vascular occlusion, vitreous hemorrhage, optic neuropathy, chorioretinitis, retinal hemorrhages and cotton wool spots (*6*). Our patient had both orbital cellulitis and choroidal hematoma with loss of vision that was opined to be irreversible by the ophthalmologists. This patient is an example of the complicated turn of events that dengue fever can have.

In conclusion, in a dengue patient with AKI, CPK and LDH levels should be always screened to look for rhabdomyolysis, as early diagnosis and treatment can have a favorable outcome. A thorough neurological examination should be carried out in such critical patients and even subtle signs should be evaluated appropriately. Managing dengue infection can be challenging for treating physician if patient develops EDS, which carries an unfavorable prognosis.

References

1. World Health Organization (WHO). Dengue: Guidelines for Diagnosis, Treatment, Prevention and Control: New Edition. WHO:Geneva, Switzerland, 2009.
2. Ranjit S, Kissoon N. Dengue hemorrhagic fever and shock syndromes. Pediatr Crit Care Med. 2011; 12:90-100.
3. Kadam DB, Salvi S, Chandanwale A. Expanded dengue. J Assoc Physicians India. 2016; 64:59-63.
4. Repizo LP, Malheiros DM, Yu L, Barros RT, Burdmann EA. Biopsy proven acute tubular necrosis due to rhabdomyolysis in a dengue fever patient: A case report and review of literature. Rev Inst Med Trop Sao Paulo. 2014; 56:85-88.
5. Murthy JM. Neurological complications of dengue infection. Neurol India. 2010; 58:581-584.
6. Sujatha R, Nousheen S, Nazlin A, Prakash S. Ocular manifestations of dengue fever. Int J Med Sci Public Health. 2015; 4:690-693.
7. Kurane I, Ennis FE. Immunity and immunopathology in dengue virus infections. Semin Immunol 1992; 4:121-127.
8. Chaturvedi UC. Shift to Th2 cytokine response in dengue

haemorrhagic fever. Indian J Med Res. 2009; 129:1-3.
9. Lizarraga KJ, Nayer A. Dengue-associated kidney disease. J Nephropathol. 2014; 3:57-62.
10. Laoprasopwattana K, Pruekprasert P, Dissaneewate P, Geater A, Vachvanichsanong P. Outcome of dengue hemorrhagic fever-caused acute kidney injury in Thai children. J Pediatr. 2010; 157:303-309.
11. Lee IK, Liu JW, Yang KD. Clinical characteristics, risk factors, and outcomes in adults experiencing dengue hemorrhagic fever complicated with acute renal failure. Am J Trop Med Hyg. 2009;80:651-655.
12. Khalil MA, Sarwar S, Chaudry MA Maqbool B, Khalil Z, Tan J, Yaqub S, Hussain SA. Acute kidney injury in dengue virus infection. Clin Kidney J. 2012; 5:390-394.
13. Sargeant T, Harris T, Wilks R, Barned S, Galloway-Blake K, Ferguson T. Rhabdomyolysis and dengue Fever: A case report and literature review. Case Rep Med. 2013; 2013:101058.
14. Malheiros SM, Oliveira AS, Schmidt B, Lima JG, Gabbai AA. Dengue. Muscle biopsy findings in 15 patients. Arq Neuropsiquiatr. 1993; 51:159-164.
15. Said SM, Elsaeed KM, Alyan Z. Benign acute myositis in association with acute dengue viruses' infections. Egypt J Neurol Psychiatr Neurosurg. 2008; 45:193-200.
16. Gunasekera HH, Adikaram AV, Herath CA, Samarasinghe HH. Myoglobinuric acute renal failure following dengue viral infection. Ceylon Med J. 2000; 45:181.
17. Karakus A, Banga N, Voorn GP, Meinders AJ. Dengue shock syndrome and rhabdomyolysis. Neth J Med. 2007; 65:78-81.
18. Acharya S, Shukla S, Mahajan SN, Diwan SK. Acute dengue myositis with rhabdomyolysis and acute renal failure. Ann Indian Acad Neurol. 2010; 13:221-222.
19. Wijesinghe A, Gnanapragash N, Ranasinghe G, Ragunathan MK. Acute renal failure due to rhabdomyolysis following dengue viral infection: A case report. J Med Case Rep. 2013; 26; 7:195.
20. Sunderalingam V, Kanapathipillai T, Edirisinghe PA, Dassanayake KM, Premawansa IH. Dengue viral myositis complicated with rhabdomyolysis and superinfection of methicillin-resistant staphylococcus aureus. Case Rep Infect Dis. 2013; 2013:194205.
21. Jha R, Gude D, Chennamsetty S. Non-hemorrhagic dengue fever with rhabdomyolysis. Saudi J Kidney Dis Transpl. 2013; 24:1207-1209.
22. Siriyakorn N, Insiripong S. Fatal rhabdomyolysis in dengue hemorrhagic fever: A case report. Southeast Asian J Trop Med Public Health. 2015; 46 Suppl 1:149-152.
23. Mishra A, Singh VK, Nanda S. Rhabdomyolysis and acute kidney injury in dengue fever. BMJ Case Rep. 2015; 2015. pii: bcr2014209074.
24. Khan FY. Rhabdomyolysis: A review of the literature. Neth J Med. 2009; 67:272-283.

(Received October 21, 2017; Revised November 17, 2017; Accepted November 20, 2017)

Communication

DOI: 10.5582/irdr.2017.01070

An up-date on epigenetic and molecular markers in testicular germ cell tumors

Paolo Chieffi*

Dipartimento di Psicologia, Università della Campania, Caserta, Italy.

Summary **Testicular germ cell tumor (TGCT) is the most common solid malignancy occurring in young men between 20 and 34 years of age, and its incidence has increased significantly over the last decades. Clinically several types of immunohistochemical markers are useful and sensitive. These new biomarkers are genes expressed in primordial germ cells/gonocytes and embryonic pluripotency-related cells but not in normal adult germ cells and they include OCT3/4, HMGA1 and 2, NANOG, SOX2, and LIN28. Gene expression in TGCT is regulated, at least in part, by DNA and histone modifications, and the epigenetic profile of these tumours is characterised by genome-wide demethylation. There are different epigenetic modifications in TGCT subtypes that reflect the normal developmental switch in primordial germ cells from an under to normally methylated genome.**

Keywords: Testicular germ cells tumors, seminomas, epigenetic, GPR30, PATZ1, HMGA

Testicular germ cell tumor (TGCT) is the most common neoplasia that occurs in males between 20-40 years old and it accounts for approximately 1-1.5% of all cancers in men (*1,2*). The incidence rate and mortality change considerably in different geographical areas: the rates are highest in Northern and Western Europe, Northern America and Australia, while lowest rates have been found in South Europe, Central America and, at last, in Asia and Africa (*3*). Over the last decades, the incidence of TC in western countries has been increasing, maybe because of an increased exposure to etiologic factors (*4*). Genetic and environmental factors play an important role in the genesis and development of TGCT; in fact, several genes are implicated in its pathogenesis (*5*) and different environmental factors have been investigated. In the environmental agents there are pesticides and non-steroidal estrogens, such as diethylstilbestrol (DES) (*6,7*). There is an association between increased TC risk and maternal smoking during pregnancy, adult height, body mass index, diet rich in cheese are other factors correlated to TGCT development (*8*). However, the biological mechanisms involved in TGCT development are poorly known. Among the risk factors correlated to the onset of disease we can remember: age, cryptorchidism, family history of TGCT, Klinefelter's syndrome, congenital abnormalities and infertility (*2,3*). Young age represents one of the most frequent factors of TGCT occurrence (*3*).

The World Health Organization (WHO) recapitulates the classical histological entities of testicular cancers, but now divides the tumours of adult men into two main groups: those that are derived from germ cell neoplasia *in situ* (GCNIS): seminoma and nonseminoma (NSE), and a spermatocytic tumor, which is a histotype not associated with GCNIS. In NSE are included choriocarcinoma, embryonal carcinoma, teratoma and yolk sac tumors. Testicular germ cell tumors may arise from a non-invasive form of disease named carcinoma *in situ* (CIS): under the microscope these cells appear abnormal although they have not yet spread outside the walls of the seminiferous tubules. CIS doesn't always degenerate in invasive cancer but it's very difficult to discover it because it often doesn't involve side effects; a good way to diagnose CIS is to have a biopsy. According to its evolution, three stages of the disease can be distinguished: stage I (the tumor is circumscribed by the testicle), stage II (the tumor has spread to the lymph nodes of the abdomen) and stage III (the tumor has spread to the lymph nodes also with distant metastases in organs such as lungs and liver) (*9*).

Compared to the latest classification of urinary tract

Released online in J-STAGE as advance publication November 21, 2017.

**Address correspondence to:*
Dr. Paolo Chieffi, Dipartimento di Psicologia, Viale Ellittico, 31 81100 Caserta, Italy.
E-mail: paolo.chieffi@unicampania.it

and male genital organs in the WHO, there have been updates in 2016 that reflect the different behaviour, pathogenesis and tumour biology of similar histological patterns occurring in different contexts. In particular, GCNIS has been used as a new name for the precursor lesion (*9*). TGCT is a developmental disease of germ cell differentiation, and almost all TGCTs are derived from dysfunctional fetal germ cells. The characterization of gene expression profile in seminoma may be useful not only to improve our knowledge on their relation with oncogenesis, but also to better understand the role of PGCs (*10-13*).

NSE tumors are usually treated with surgery and chemotherapy, with different cure rates depending on the stage of the disease. The cure rate reaches up to 99% in the early stages of NSE tumors, although in advanced disease stages decreases from 90% in patients with good prognostic category to 50% in patients with poor prognostic features (*10-13*).

The fast progression and the rapid growth of postpuberal TGCTs cause early lymph node metastases and/or distant metastases. In fact, about 25% of patients with seminoma and up to 60% of those with NSE suffer from metastatic disease (*10-13*), and the therapeutic treatments are often ineffective. Thus, despite the general success of postpuberal TGCTs treatment, 10-20% of patients diagnosed with metastatic disease will not achieve a durable and complete remission after initial treatment, either due to incomplete response or a tumor relapse.

There are several types of markers for testicular TGCTs: serum tumor markers and immunohistochemical markers. Clinically useful immunohistochemical markers for TGCT are genes expressed in primordial germ cells (PGCs)/gonocytes and embryonic pluripotency-related cells but not in normal adult germ cells. They are OCT3/4, NANOG, SOX2, REX1, AP-2γ (TFAP2C) and LIN28. Moreover, HMGA1 and HMGA2 represent valuable diagnostic markers as they are differently expressed depending upon the states of differentiation of TGCTs (*15-25*). A nuclear transcriptional repressor PATZ1 interacting protein RNF4 suggests an impaired function when it is delocalized in the cytoplasm in human seminomas; it has been shown that both PATZ1 and HMGA1 cytoplasmic delocalization associates with estrogen receptor β (ER β) down-regulation in human seminomas (*15-24*). More recently, it has been demonstrated that the down regulation of ERβ associates with GPR30 over-expression both in human CIS and seminomas; in addition, it has been shown that 17β-estradiol induces the ERK1/2 activation through GPR30 (*25,26*). Many studies are devoted to design selective GPR30 inhibitors to block neoplastic germ cells with a high proliferative rate, representing a novel therapeutic strategy for the treatment of TGCTs (*25,26*).

The kinase Aurora-B is another valuable marker able to discriminate among the different tumor histotypes; in fact, it is detected in IGCNU, seminomas and embryonal carcinomas, but not in teratomas and YST. Pharmacological inhibition of Aurora B significantly decreases the cell growth in testicular GC1 and TCam2 cell lines (*26-29*).

During recent years the epigenetic factors have been found to be extremely important in the development of cancer. Indeed, nuclear morphologies are often pleiotropic across a single tumor, reflecting the heterogeneous nature of cancer. These modifications and changes of nuclear structure are key features distinguishing cancer cells from their normal counterparts. Altered nuclear morphology also reflects broad changes in genome positioning and epigenetic changes, which occur during transformation. In particular, in cancer the tight regulation of DNA methylation and the distribution of methyl-cytosine change. Commonly, the heavy methylation in the bulk chromatin is reduced, while the normally unmethylated CpG islands become hypermethylated (*30,31*). In testicular GCTs it is important to evaluate DNA methylation in the context of the PGCs from which the tumors arise because PGCs are at a developmental stage where their genomes are highly under-methylated (*30,31*). Several studies have demonstrated minimal or no methylation in seminomas, and hypermethylation in specific gene promoters of NSE, especially in highly differentiated NSE, suggesting that the degree of cell differentiation may be related to the genome methylation status (*30,31*). CIS cells as PGCs and gonocytes, express transcription factors associated with embryonic stem cell pluripotency, such as POU5F1/OCT-3/4, NANOG, T1A-2, MYCL1, GDF3, LIN28-A, DPPA4, DPPA5, KIT and AP-2γ. Genome-wide gene expression profiling revealed specific embryonic stem cell-like features of testicular CIS (*30-32*). The epigenetic pattern of CIS is associated with an open and permissive chromatin structure based on expression pattern of genes and transcription factors.

A new dawn is arising in the scenario of TGCT diagnostic and prognostic classification based upon the use of epigenetic molecular markers.

References

1. Oosterhuis, JW, Looijenga LH. Testicular germ-cell tumours in a broader perspective. Nat Rev Cancer. 2005; 5:210-222.
2. Chieffi P, Franco R, Portella G. Molecular and cell biology of testicular germ cell tumors. Int Rev Cell Mol Biol. 2009; 278:277-308.
3. Chieffi P, Chieffi S, Franco R, Sinisi AA. Recent advances in the biology of germ cell tumors: Implications for the diagnosis and treatment. J Endocrinol Invest. 2012; 35:1015-1020.
4. Chieffi P, Chieffi S. Molecular biomarkers as potential targets for therapeutic strategies in human testicular germ cell tumours: An overview. J Cell Physiol. 2013; 228:1641-1646.
5. Picascia A, Stanzione R, Chieffi P, Kisslinger A, Dikic

I, Tramontano D. Proline-rich tyrosine kinase 2 regulates proliferation and differentiation of prostate cells. Mol Cell Endocrinol. 2002; 186:81-87.
6. Dieckmann KP, Hartmann JT, Classen J, Lüdde R, Diederichs M, Pichlmeier U. Tallness is associated with risk of testicular cancer: Evidence for the nutrition hypothesis. Br J Cancer. 2008, 99: 1517-1521.
7. Dieckmann KP, Hartmann JT, Classen J, Diederichs M, Pichlmeier U. Is increased body mass index associated with the incidence of testicular germ cell cancer? J Cancer Res.Clin Oncol. 2009; 135:731-738.
8. McGlynn KA, Quraishi SM, Graubard BI, Weber JP, Rubertone MV, Erickson RL. Persistent organochlorine pesticides and risk of testicular germ cell tumors. J Natl Cancer Inst. 2008; 100:663-671.
9. Moch H, Cubilla AL, Humphrey PA, Reuter VE, Ulbright TM. The 2016 WHO Classification of Tumours of the Urinary System and Male Genital Organs-Part A: Renal, Penile, and Testicular Tumours. Eur Uro. 2016; 70:93-105.
10. Chieffi P, Chieffi S. An up-date on newly discovered immunohistochemical biomarkers for the diagnosis of human testicular germ cell tumors. Histol Histopathol. 2014; 29:999-1006.
11. Chieffi P. Potential new anticancer molecular targets for the treatment of human testicular seminomas. Mini Rev Med Chem. 2011, 11:1075-1081.
12. Chieffi P. Molecular targets for the treatment of testicular germ cell tumors. Mini Rev Med Chem. 2007; 7:755-759.
13. Chieffi P. Recent advances in molecular and cell biology of testicular germ-cell tumors. Int Rev Cell Mol Biol. 2014; 312:79-100.
14. Lutke Holzik MF, Rapley EA, Hoekstra HJ, Sleijfer DT, Nolte IM, Sijmons RH. Genetic predisposition to testicular germ-cell tumours. Lancet Oncol. 2004; 5:363-371.
15. Chieffi P, Battista S, Barchi M, Di Agostino S, Pierantoni G, Fedele M, Chiariotti L, Tramontano D, Fusco A. HMGA1 and HMGA2 protein expression in mouse spermatogenesis. Oncogene. 2002; 21:3644-3650.
16. Franco R, Esposito F, Fedele M, Liguori G, Pierantoni G, Botti G, Tramontano D, Fusco A, Chieffi P. Detection of high mobility group proteins A1 and A2 represents a valid diagnostic marker in post-puberal testicular germ cell tumours. J Pathol. 2008; 214:58-64.
17. Pero R, Lembo F, Di Vizio D, Boccia A, Chieffi P, Fedele M, Pierantoni MG, Rossi P, Iuliano R, Santoro M, Viglietto G, Bruni CB, Fusco A, Chiariotti L. RNF4 is a growth inhibitor expressed in germ cells and lost in human testicular tumours. Am J Pathol. 2001; 159:1225-1230.
18. Pero R, Lembo F, Chieffi P, Del Pozzo G, Fedele M, Fusco A, Bruni CB, Chiariotti L. Translational regulation of a novel testis-specific RNF4 transcript. Mol Reprod Dev. 2003; 66:1-7.
19. Fedele M, Franco R, Salvatore G, Paronetto MP, Barbagallo F, Pero R, Chiariotti L, Sette C, Tramontano D, Chieffi G, Fusco A, Chieffi P. PATZ1 gene has a critical role in the spermatogenesis and testicular tumours. J Pathol. 2008; 215:39-47.
20. Esposito F, Boscia F, Franco R, Tornincasa M, Fusco A, Kitazawa S, Looijenga LH, Chieffi P. Down-regulation of estrogen receptor-β associates with transcriptional coregulator PATZ1 delocalization in human testicular seminomas. J Pathol. 2011; 224:110-120.
21. Esposito F, Boscia F, Gigantino V, Tornincasa M, Fusco A, Franco R, Chieffi P. The high-mobility group A1-oestrogen receptor β nuclear interaction is impaired in human testicular seminomas. J Cell Physiol. 2012; 227:3749-3755.
22. Barbagallo F, Paronetto MP, Franco R, Chieffi P, Dolci S, Fry AM, Geremia R, Sette C. Increased expression and nuclear localization of the centrosomal kinase Nek2 in human testicular seminomas. J Pathol. 2009; 217:431-441.
23. Vicini E, Loiarro M, Di Agostino S, Corallini S, Capolunghi F, Carsetti R, Chieffi P, Geremia R, Stefanini M, Sette C. 17-β-estradiol elicits genomic and non-genomic responses in mouse male germ cells. J Cell Physiol. 2006; 206:238-245.
24. Franco R, Boscia F, Gigantino V, Marra L, Esposito F, Ferrara D, Pariante P, Botti G, Caraglia M, Minucci S, Chieffi P. GPR30 is over-expressed in post-puberal testicular germ cell tumors. Cancer Biol Ther. 2011; 11:609-613.
25. Boscia F, Passaro C, Gigantino V, Perdonà S, Franco R, Portella G, Chieffi S,Chieffi P. High levels of GPR30 protein in human testicular carcinoma *in situ* and seminomas correlate with low levels of estrogen receptor-beta and indicate a switch in estrogen responsiveness. J Cell Physiol. 2015; 230:1290-1297.
26. Chieffi P, Troncone G, Caleo A, Libertini S, Linardopoulos S, Tramontano D, Portella G. Aurora B expression in normal testis and seminomas. J Endocrinol. 2004; 181:263-270.
27. Esposito F, Libertini S, Franco R, Abagnale A, Marra L, Portella G, Chieffi P. Aurora B expression in post-puberal testicular germ cell tumours. J Cell Physiol. 2009; 221:435-439.
28. Portella G, Passaro C, Chieffi P. Aurora B: A new prognostic marker and therapeutic target in cancer. Curr Med Chem. 2011; 18:482-496.
29. Chieffi P, Boscia F. New discovered molecular markers as promising therapeutic targets in germ cell tumors. Exp Opin Orphan Drugs. 2015; 3:1021-1030.
30. Looijenga LH, Gillis AJ, van Gurp RJ, Verkerk AJ, Oosterhuis JW. X inactivation in human testicular tumors. XIST expression and androgen receptor methylation status. Am J Pathol. 1997; 151:581-590.
31. Smiraglia DJ, Szymanska J, Kraggerud SM, Lothe RA, Peltomäki P, Plass C. Distinct epigenetic phenotypes in seminomatous and nonseminomatous testicular germ cell tumors. Oncogene. 2002; 21:3909-3916.
32. Boccellino M, Vanacore D, Zappavigna S, *et al*. Testicular cancer from diagnosis to epigenetic factors. Oncotarget. 2017; *https://doi.org/10.18632/oncotarget.20992*

(Received October 19, 2017; Revised November 11, 2017; Accepted November 14, 2017)

IRDR
Intractable & Rare Diseases Research

Guide for Authors

1. Scope of Articles

Intractable & Rare Diseases Research is an international peer-reviewed journal. Intractable & Rare Diseases Research devotes to publishing the latest and most significant research in intractable and rare diseases. Articles cover all aspects of intractable and rare diseases research such as molecular biology, genetics, clinical diagnosis, prevention and treatment, epidemiology, health economics, health management, medical care system, and social science in order to encourage cooperation and exchange among scientists and clinical researchers.

2. Submission Types

Original Articles should be well-documented, novel, and significant to the field as a whole. An Original Article should be arranged into the following sections: Title page, Abstract, Introduction, Materials and Methods, Results, Discussion, Acknowledgments, and References. Original articles should not exceed 5,000 words in length (excluding references) and should be limited to a maximum of 50 references. Articles may contain a maximum of 10 figures and/or tables.

Brief Reports definitively documenting either experimental results or informative clinical observations will be considered for publication in this category. Brief Reports are not intended for publication of incomplete or preliminary findings. Brief Reports should not exceed 3,000 words in length (excluding references) and should be limited to a maximum of 4 figures and/or tables and 30 references. A Brief Report contains the same sections as an Original Article, but the Results and Discussion sections should be combined.

Reviews should present a full and up-to-date account of recent developments within an area of research. Normally, reviews should not exceed 8,000 words in length (excluding references) and should be limited to a maximum of 100 references. Mini reviews are also accepted.

Policy Forum articles discuss research and policy issues in areas related to life science such as public health, the medical care system, and social science and may address governmental issues at district, national, and international levels of discourse. Policy Forum articles should not exceed 2,000 words in length (excluding references).

Case Reports should be detailed reports of the symptoms, signs, diagnosis, treatment, and follow-up of an individual patient. Case reports may contain a demographic profile of the patient but usually describe an unusual or novel occurrence. Unreported or unusual side effects or adverse interactions involving medications will also be considered. Case Reports should not exceed 3,000 words in length (excluding references).

News articles should report the latest events in health sciences and medical research from around the world. News should not exceed 500 words in length.

Letters should present considered opinions in response to articles published in Intractable & Rare Diseases Research in the last 6 months or issues of general interest. Letters should not exceed 800 words in length and may contain a maximum of 10 references.

3. Editorial Policies

Ethics: Intractable & Rare Diseases Research requires that authors of reports of investigations in humans or animals indicate that those studies were formally approved by a relevant ethics committee or review board.

Conflict of Interest: All authors are required to disclose any actual or potential conflict of interest including financial interests or relationships with other people or organizations that might raise questions of bias in the work reported. If no conflict of interest exists for each author, please state "There is no conflict of interest to disclose".

Submission Declaration: When a manuscript is considered for submission to Intractable & Rare Diseases Research, the authors should confirm that 1) no part of this manuscript is currently under consideration for publication elsewhere; 2) this manuscript does not contain the same information in whole or in part as manuscripts that have been published, accepted, or are under review elsewhere, except in the form of an abstract, a letter to the editor, or part of a published lecture or academic thesis; 3) authorization for publication has been obtained from the authors' employer or institution; and 4) all contributing authors have agreed to submit this manuscript.

Cover Letter: The manuscript must be accompanied by a cover letter signed by the corresponding author on behalf of all authors. The letter should indicate the basic findings of the work and their significance. The letter should also include a statement affirming that all authors concur with the submission and that the material submitted for publication has not been published previously or is not under consideration for publication elsewhere. The cover letter should be submitted in PDF format. For example of Cover Letter, please visit http://www.irdrjournal.com/downcentre.php (Download Centre).

Copyright: A signed JOURNAL PUBLISHING AGREEMENT (JPA) form must be provided by post, fax, or as a scanned file before acceptance of the article. Only forms with a hand-written signature are accepted. This copyright will ensure the widest possible dissemination of information. A form facilitating transfer of copyright can be downloaded by clicking the appropriate link and can be returned to the e-mail address or fax number noted on the form (Please visit Download Centre). Please note that your manuscript will not proceed to the next step in publication until the JPA Form is received. In addition, if excerpts from other copyrighted works are included, the author(s) must obtain written permission from the copyright owners and credit the source(s) in the article.

Suggested Reviewers: A list of up to 3 reviewers who are qualified to assess the scientific merit of the study is welcomed. Reviewer information including names, affiliations, addresses, and e-mail should be provided at the same time the manuscript is submitted online. Please do not suggest reviewers with known conflicts of interest, including participants or anyone with a stake in the proposed research; anyone from the same institution; former students, advisors, or research collaborators (within the last three years); or close personal contacts. Please note that the Editor-in-Chief may accept one or more of the proposed reviewers or may request a review by other qualified persons.

Language Editing: Manuscripts prepared by authors whose native language is not English should have their work proofread by a native English speaker before submission. If not, this might delay the publication of your manuscript in Intractable & Rare Diseases Research.

The Editing Support Organization can provide English proofreading, Japanese-English translation, and Chinese-English translation services to authors who want to publish in Intractable & Rare Diseases Research and need assistance before submitting a manuscript. Authors can visit this organization directly at http://www.iacmhr.com/iac-eso/support.php?lang=en. IAC-ESO was established to facilitate manuscript preparation by researchers whose native language is not English and to help edit works intended for international academic journals.

4. Manuscript Preparation

Manuscripts should be written in clear, grammatically correct English and submitted as a Microsoft Word file in a single-column format. Manuscripts must be paginated and typed in 12-point Times New Roman font with 24-point line spacing. Please do not embed figures in the text. Abbreviations should be used as little as possible and should be explained at first mention unless the term is a well-known abbreviation (*e.g.* DNA). Single words should not be abbreviated.

Title page: The title page must include 1) the title of the paper (Please note the title should be short, informative, and contain the major key words); 2) full name(s) and affiliation(s) of the author(s), 3) abbreviated names of the author(s), 4) full name, mailing address, telephone/fax numbers, and e-mail address of the corresponding author; and 5) conflicts of interest (if you have an actual or potential conflict of interest to disclose, it must be included as a footnote on the title page of the

manuscript; if no conflict of interest exists for each author, please state "There is no conflict of interest to disclose"). Please visit Download Centre and refer to the title page of the manuscript sample.

Abstract: The abstract should briefly state the purpose of the study, methods, main findings, and conclusions. For article types including Original Article, Brief Report, Review, Policy Forum, and Case Report, a one-paragraph abstract consisting of no more than 250 words must be included in the manuscript. For News and Letters, a brief summary of main content in 150 words or fewer should be included in the manuscript. Abbreviations must be kept to a minimum and non-standard abbreviations explained in brackets at first mention. References should be avoided in the abstract. Key words or phrases that do not occur in the title should be included in the Abstract page.

Introduction: The introduction should be a concise statement of the basis for the study and its scientific context.

Materials and Methods: The description should be brief but with sufficient detail to enable others to reproduce the experiments. Procedures that have been published previously should not be described in detail but appropriate references should simply be cited. Only new and significant modifications of previously published procedures require complete description. Names of products and manufacturers with their locations (city and state/country) should be given and sources of animals and cell lines should always be indicated. All clinical investigations must have been conducted in accordance with Declaration of Helsinki principles. All human and animal studies must have been approved by the appropriate institutional review board(s) and a specific declaration of approval must be made within this section.

Results: The description of the experimental results should be succinct but in sufficient detail to allow the experiments to be analyzed and interpreted by an independent reader. If necessary, subheadings may be used for an orderly presentation. All figures and tables must be referred to in the text.

Discussion: The data should be interpreted concisely without repeating material already presented in the Results section. Speculation is permissible, but it must be well-founded, and discussion of the wider implications of the findings is encouraged. Conclusions derived from the study should be included in this section.

Acknowledgments: All funding sources should be credited in the Acknowledgments section. In addition, people who contributed to the work but who do not meet the criteria for authors should be listed along with their contributions.

References: References should be numbered in the order in which they appear in the text. Citing of unpublished results, personal communications, conference abstracts, and theses in the reference list is not recommended but these sources may be mentioned in the text. In the reference list, cite the names of all authors when there are fifteen or fewer authors; if there are sixteen or more authors, list the first three followed by *et al*. Names of journals should be abbreviated in the style used in PubMed. Authors are responsible for the accuracy of the references. Examples are given below:

Example 1 (Sample journal reference):
Inagaki Y, Tang W, Zhang L, Du GH, Xu WF, Kokudo N. Novel aminopeptidase N (APN/CD13) inhibitor 24F can suppress invasion of hepatocellular carcinoma cells as well as angiogenesis. Biosci Trends. 2010; 4:56-60.

Example 2 (Sample journal reference with more than 15 authors):
Darby S, Hill D, Auvinen A, *et al*. Radon in homes and risk of lung cancer: Collaborative analysis of individual data from 13 European case-control studies. BMJ. 2005; 330:223.

Example 3 (Sample book reference):
Shalev AY. Post-traumatic stress disorder: Diagnosis, history and life course. In: Post-traumatic Stress Disorder, Diagnosis, Management and Treatment (Nutt DJ, Davidson JR, Zohar J, eds.). Martin Dunitz, London, UK, 2000; pp. 1-15.

Example 4 (Sample web page reference):
World Health Organization. The World Health Report 2008 – primary health care: Now more than ever. *http://www.who.int/whr/2008/whr08_en.pdf* (accessed September 23, 2010).

Tables: All tables should be prepared in Microsoft Word or Excel and should be arranged at the end of the manuscript after the References section. Please note that tables should not in image format. All tables should have a concise title and should be numbered consecutively with Arabic numerals. If necessary, additional information should be given below the table.

Figure Legend: The figure legend should be typed on a separate page of the main manuscript and should include a short title and explanation. The legend should be concise but comprehensive and should be understood without referring to the text. Symbols used in figures must be explained.

Figure Preparation: All figures should be clear and cited in numerical order in the text. Figures must fit a one- or two-column format on the journal page: 8.3 cm (3.3 in.) wide for a single column, 17.3 cm (6.8 in.) wide for a double column; maximum height: 24.0 cm (9.5 in.). Please make sure that artwork files are in an acceptable format (TIFF or JPEG) at minimum resolution (600 dpi for illustrations, graphs, and annotated artwork, and 300 dpi for micrographs and photographs). Please provide all figures as separate files. Please note that low-resolution images are one of the leading causes of article resubmission and schedule delays. All color figures will be reproduced in full color in the online edition of the journal at no cost to authors.

Units and Symbols: Units and symbols conforming to the International System of Units (SI) should be used for physicochemical quantities. Solidus notation (*e.g.* mg/kg, mg/mL, mol/mm^2/min) should be used. Please refer to the SI Guide www.bipm.org/en/si/ for standard units.

Supplemental data: Supplemental data might be useful for supporting and enhancing your scientific research and Intractable & Rare Diseases Research accepts the submission of these materials which will be only published online alongside the electronic version of your article. Supplemental files (figures, tables, and other text materials) should be prepared according to the above guidelines, numbered in Arabic numerals (*e.g.*, Figure S1, Figure S2, and Table S1, Table S2) and referred to in the text. All figures and tables should have titles and legends. All figure legends, tables and supplemental text materials should be placed at the end of the paper. Please note all of these supplemental data should be provided at the time of initial submission and note that the editors reserve the right to limit the size and length of Supplemental Data.

5. Submission Checklist

The Submission Checklist will be useful during the final checking of a manuscript prior to sending it to Intractable & Rare Diseases Research for review. Please visit Download Centre and download the Submission Checklist file.

6. Online submission

Manuscripts should be submitted to Intractable & Rare Diseases Research online at http://www.irdrjournal.com. The manuscript file should be smaller than 5 MB in size. If for any reason you are unable to submit a file online, please contact the Editorial Office by e-mail at office@irdrjournal.com

7. Accepted manuscripts

Proofs: Galley proofs in PDF format will be sent to the corresponding author *via* e-mail. Corrections must be returned to the editor (office@irdrjournal.com) within 3 working days.

Offprints: Authors will be provided with electronic offprints of their article. Paper offprints can be ordered at prices quoted on the order form that accompanies the proofs.

Page Charge: No page charges will be levied to authord for the publication of their article except for reprints.

(As of February 2013)

Editorial and Head Office:

Pearl City Koishikawa 603
2-4-5 Kasuga, Bunkyo-ku
Tokyo 112-0003, Japan
Tel: +81-3-5840-9968
Fax: +81-3-5840-9969
E-mail: office@irdrjournal.com

IRDR
Intractable & Rare Diseases Research

JOURNAL PUBLISHING AGREEMENT (JPA)

Manuscript No.:

Title:

Corresponding Author:

The International Advancement Center for Medicine & Health Research Co., Ltd. (IACMHR Co., Ltd.) is pleased to accept the above article for publication in Intractable & Rare Diseases Research. The International Research and Cooperation Association for Bio & Socio-Sciences Advancement (IRCA-BSSA) reserves all rights to the published article. Your written acceptance of this JOURNAL PUBLISHING AGREEMENT is required before the article can be published. Please read this form carefully and sign it if you agree to its terms. The signed JOURNAL PUBLISHING AGREEMENT should be sent to the Intractable & Rare Diseases Research office (Pearl City Koishikawa 603, 2-4-5 Kasuga, Bunkyo-ku, Tokyo 112-0003, Japan; E-mail: office@irdrjournal.com; Tel: +81-3-5840-9968; Fax: +81-3-5840-9969).

1. Authorship Criteria

As the corresponding author, I certify on behalf of all of the authors that:

1) The article is an original work and does not involve fraud, fabrication, or plagiarism.
2) The article has not been published previously and is not currently under consideration for publication elsewhere. If accepted by Intractable & Rare Diseases Research, the article will not be submitted for publication to any other journal.
3) The article contains no libelous or other unlawful statements and does not contain any materials that infringes upon individual privacy or proprietary rights or any statutory copyright.
4) I have obtained written permission from copyright owners for any excerpts from copyrighted works that are included and have credited the sources in my article.
5) All authors have made significant contributions to the study including the conception and design of this work, the analysis of the data, and the writing of the manuscript.
6) All authors have reviewed this manuscript and take responsibility for its content and approve its publication.
7) I have informed all of the authors of the terms of this publishing agreement and I am signing on their behalf as their agent.

2. Copyright Transfer Agreement

I hereby assign and transfer to IACMHR Co., Ltd. all exclusive rights of copyright ownership to the above work in the journal Intractable & Rare Diseases Research, including but not limited to the right 1) to publish, republish, derivate, distribute, transmit, sell, and otherwise use the work and other related material worldwide, in whole or in part, in all languages, in electronic, printed, or any other forms of media now known or hereafter developed and the right 2) to authorize or license third parties to do any of the above.

I understand that these exclusive rights will become the property of IACMHR Co., Ltd., from the date the article is accepted for publication in the journal Intractable & Rare Diseases Research. I also understand that IACMHR Co., Ltd. as a copyright owner has sole authority to license and permit reproductions of the article.

I understand that except for copyright, other proprietary rights related to the Work (*e.g.* patent or other rights to any process or procedure) shall be retained by the authors. To reproduce any text, figures, tables, or illustrations from this Work in future works of their own, the authors must obtain written permission from IACMHR Co., Ltd.; such permission cannot be unreasonably withheld by IACMHR Co., Ltd.

3. Conflict of Interest Disclosure

I confirm that all funding sources supporting the work and all institutions or people who contributed to the work but who do not meet the criteria for authors are acknowledged. I also confirm that all commercial affiliations, stock ownership, equity interests, or patent-licensing arrangements that could be considered to pose a financial conflict of interest in connection with the article have been disclosed.

Corresponding Author's Name (Signature):

Date: